

NASA/TM—2016-219433



Composites for Exploration Upper Stage

*J.C. Fikes, J.R. Jackson, S.W. Richardson, and A.D. Thomas
Marshall Space Flight Center, Huntsville, Alabama*

*T.O. Mann
Langley Research Center, Hampton, Virginia*

*S.G. Miller
Glenn Research Center, Cleveland, Ohio*

The NASA STI Program...in Profile

Since its founding, NASA has been dedicated to the advancement of aeronautics and space science. The NASA Scientific and Technical Information (STI) Program Office plays a key part in helping NASA maintain this important role.

The NASA STI Program Office is operated by Langley Research Center, the lead center for NASA's scientific and technical information. The NASA STI Program Office provides access to the NASA STI Database, the largest collection of aeronautical and space science STI in the world. The Program Office is also NASA's institutional mechanism for disseminating the results of its research and development activities. These results are published by NASA in the NASA STI Report Series, which includes the following report types:

- **TECHNICAL PUBLICATION.** Reports of completed research or a major significant phase of research that present the results of NASA programs and include extensive data or theoretical analysis. Includes compilations of significant scientific and technical data and information deemed to be of continuing reference value. NASA's counterpart of peer-reviewed formal professional papers but has less stringent limitations on manuscript length and extent of graphic presentations.
- **TECHNICAL MEMORANDUM.** Scientific and technical findings that are preliminary or of specialized interest, e.g., quick release reports, working papers, and bibliographies that contain minimal annotation. Does not contain extensive analysis.
- **CONTRACTOR REPORT.** Scientific and technical findings by NASA-sponsored contractors and grantees.

- **CONFERENCE PUBLICATION.** Collected papers from scientific and technical conferences, symposia, seminars, or other meetings sponsored or cosponsored by NASA.
- **SPECIAL PUBLICATION.** Scientific, technical, or historical information from NASA programs, projects, and mission, often concerned with subjects having substantial public interest.
- **TECHNICAL TRANSLATION.** English-language translations of foreign scientific and technical material pertinent to NASA's mission.

Specialized services that complement the STI Program Office's diverse offerings include creating custom thesauri, building customized databases, organizing and publishing research results...even providing videos.

For more information about the NASA STI Program Office, see the following:

- Access the NASA STI program home page at <<http://www.sti.nasa.gov>>
- E-mail your question via the Internet to <help@sti.nasa.gov>
- Phone the NASA STI Help Desk at 757-864-9658
- Write to:
NASA STI Information Desk
Mail Stop 148
NASA Langley Research Center
Hampton, VA 23681-2199, USA

NASA/TM—2016-219433



Composites for Exploration Upper Stage

*J.C. Fikes, J.R. Jackson, S.W. Richardson, and A.D. Thomas
Marshall Space Flight Center, Huntsville, Alabama*

*T.O. Mann
Langley Research Center, Hampton, Virginia*

*S.G. Miller
Glenn Research Center, Cleveland, Ohio*

National Aeronautics and
Space Administration

Marshall Space Flight Center • Huntsville, Alabama 35812

December 2016

Acknowledgments

The following personnel are acknowledged for their valuable contribution to actively running the Program Management office for this project:

NASA Marshall Space Flight Center (MSFC):

John Vickers, Project Manager
John Fikes, Deputy Project Manager
Justin Jackson, Project Lead Engineer
Robert Gower, Scheduler
Frank Ledbetter, Project Technical Support & Risk Management
Lynn Machamer, Project Coordinator
Dana Solomon, Budget Analyst
Ruth Conrad, Safety & Mission Assurance
Deborah Cran, Chief Engineer
Stephen Richardson, Analysis and Design Lead
Allyson Thomas, Analysis and Design Co-Lead
Larry Pelham, Manufacturing Lead
Erika Alvarez, Chief Engineer
NASA Glenn Research Center (GRC):
Sandi Miller, Materials Lead
NASA Langley Research Center (LaRC):
Troy Mann, Joint Structures Lead, Analysis Co-Lead

The authors also acknowledge the following personnel for significant contributions to this project:

GRC:

Bob Allen, Structural Analysis
Eric Baker, Structural Analysis
Brett Bednarcyk, Structural Analysis
Bill Brown, Panel Testing
Chris Burke, Panel Testing
Cameron C. Cunningham, Analysis and Design
Mike Doherty, Project Lead
Paula Heimann, Panel Fabrication
Dan Kosareo, Design & Analysis
Ted Kovacevich, Structural Analysis
Tom Krivanek, Analysis and Design Lead
Brad Lerch, Test & Evaluation Lead
Linda McCorkle, Panel Inspection
Dutch Myers, Structural Analysis

GRC:

Noel Nemeth, Structural Analysis
Abigail Rodriguez, Safety and Mission Assurance Lead
Dan Scheiman, Panel Inspection
Kenneth Smith, Panel Testing
John Thesken, Structural Analysis
Tiffany Williams, Panel Fabrication
Goddard Space Flight Center:
Babak Farrokh, Structural Analysis
Kenneth Segal, Structural Design, Manufacturing

LaRC:

Darrell Branscome, Subject Matter Expert
Andrew Bergan, Structural Analysis
Eric Burke, Non-Destructive Evaluation
Patrick A. Cosgrove, Project Lead
Mark Hillburger, Subject Matter Expert
Kay Little, Program Analyst
Zoran Martinovic, Structural Analysis
Joe McKenny, Structural Design, ISAAC Support
Thuan Nguyen, ISAAC Programming
Sverrir "Sev" Rosario, Structural Analysis
Arunkumar Satyanarayana, Structural Analysis
Jamie Shiflett, Structural Design
David Sleight, Structural Analysis
Brian Stewart, ISAAC Integration Manager
Chauncey Wu, ISAAC Lead

MSFC:

Lauren Badia	John (Andy) Smith
John Bausano	Todd Swearingen
Zenia Garcia	Norris Vaughn
William (Chad) Hastings	Stephen Wess
Alan Nettles	Rob Wingate
Dawn R. Phillips	Greg Zelinsky

NASA also acknowledges the following personnel from our major suppliers for their valuable contributions to this project:

Janicki Industries
Cytel Industries
Southern Research Institute (SRI)
NCAM

Available from:

NASA STI Information Desk
Mail Stop 148
NASA Langley Research Center
Hampton, VA 23681-2199, USA
757-864-9658

This report is also available in electronic form at
<<http://www.sti.nasa.gov>>

PREFACE

This Technical Memorandum documents the work accomplished by the NASA Composites for Exploration Upper Stage team from when the project received authority to proceed to systems requirements review (KDP-A) on June 6, 2014, to when the project received a cancellation notice from the Technology Demonstration Missions program office on February 4, 2016. The project was discontinued due to the FY 2016 NASA Appropriations Bill impacts to the Space Technology Mission Directorate budget. The initial project scope was to develop, build, and test two 8.4-m composite structures (forward and aft skirts) applicable to the Exploration Upper Stage for the Space Launch System vehicle. This technology project would mature the dry structure composite technologies to a Technology Readiness Level 6 at the 8.4-m-diameter scale. The project went through numerous scope trade studies, including applications to the Universal Stage Adapter as well as technology development accomplishments in the areas of materials, joints, design and manufacturing.

EXECUTIVE SUMMARY

The Composites for Exploration Upper Stage (CEUS) was a 3-year, level III project within the Technology Demonstration Missions program of the NASA Space Technology Mission Directorate. Studies have shown that composites provide important programmatic enhancements, including reduced weight to increase capability and accelerated expansion of exploration and science mission objectives. The CEUS project was focused on technologies that best advanced innovation, infusion, and broad applications for the inclusion of composites on future large human-rated launch vehicles and spacecraft. The benefits included near- and far-term opportunities for infusion (NASA, industry/commercial, Department of Defense), demonstrated critical technologies and technically implementable evolvable innovations, and sustained Agency experience.

The initial scope of the project was to advance technologies for large composite structures applicable to the Space Launch System (SLS) Exploration Upper Stage (EUS) by focusing on the affordability and technical performance of the EUS forward and aft skirts. The project was tasked to develop and demonstrate critical composite technologies with a focus on full-scale materials, design, manufacturing, and test using NASA in-house capabilities. This would have demonstrated a major advancement in confidence and matured the large-scale composite technology to a Technology Readiness Level 6. This project would, therefore, have bridged the gap for providing composite application to SLS upgrades, enabling future exploration missions.

TABLE OF CONTENTS

1. PROJECT OVERVIEW	1
1.1 Management Approach	3
1.2 Risk Management	4
1.3 Lessons Learned	6
2. MATERIALS	14
2.1 Selection and Preexisting Data	14
2.2 Prepreg Procurement Specification	15
2.3 Storage and Handling	15
2.4 Film Adhesive Out-Time Study	15
2.5 Equivalency Tests	16
2.6 Safety and Mission Assurance	27
2.7 Computational/Model Based Material	28
2.8 Digimat Test Simulation	32
3. DESIGN	37
3.1 Composites for Exploration Upper Stage Skirt Design	37
3.2 Wall Construction Trade Study.....	38
3.3 Design Requirements for Structural Test Article.....	42
3.4 Development of the Skirt Structural Test Article Layout	43
3.5 Evaluation of Model Based Design Tools.....	46
3.6 Composite Universal Stage Adapter	51
3.7 Structural Test Article.....	52
3.8 Pathfinder Design Effort.....	56
4. JOINTS AND ANALYSIS OVERVIEW	58
4.1 Composites for Exploration Upper Stage Skirt Activities	58
4.2 Composites for Exploration Upper Stage Universal Stage Adapter Activities	72
5. MANUFACTURING	91
5.1 Tooling Development	91
5.2 Composites for Exploration Upper Stage Tooling Requirements	92
5.3 Assembly Concept	96
5.4 Automated Fiber Placement Trials	98
5.5 Curing	105

TABLE OF CONTENTS (Continued)

6. TEST	117
7. SUMMARY	120
APPENDIX A—LESSONS LEARNED	121
APPENDIX B—MATERIALS	126
B.1 8552 IM7 Unidirectional Prepeg Reports	127
APPENDIX C—TECHNOLOGY READINESS LEVEL ASSESSMENT	237
APPENDIX D—DESIGN DATA SHEETS AND DRAWINGS	239
APPENDIX E—MANUFACTURING	256
REFERENCES	266

LIST OF FIGURES

1.	Project evaluation: (a) Scope options and (b) USA risk reduction evaluation	3
2.	Project organization structure	4
3.	Core and adhesive failure within the coupons fabricated from 20-day–aged film adhesive	16
4.	Recommended bagging sequence	17
5.	LaRC ISAAC system	18
6.	Equivalency panel fabrication at LaRC	19
7.	Panel layups tested on CGtech VCP	19
8.	CGTech VERICUT tested virtually	20
9.	C-scan images of the 16-ply panels fabricated for (a) UNT, (b) UNC, and (c) OHT tests	20
10.	Photomicrographs of GRC panels: (a) 24 ply and (b) 36 ply, LaRC panels: (c) 24 ply and (d) 36 ply, and MSFC panels: (e) 24 ply and (f) 36 ply	21
11.	Digimat platform and available modulus a GSFC	29
12.	Design and material property computation of a unitape material	30
13.	A 3D woven RVE creation and corresponding FE mesh	31
14.	FEA results and property extraction for a 3D woven RVE	31
15.	Test matrix definition	32
16.	Test variability definition	33
17.	Simulation and allowable computation	34
18.	Digimat software verification approach	35

LIST OF FIGURES (Continued)

19.	RVE: (a) With 60% FV and (b) with 60% FV and 7% void content	36
20.	Early concept of a cryogenic Upper Stage for the SLS	37
21.	Composites for Upper Exploration Stage CEUS-TRADE-001	39
22.	DDS for the forward skirt STA	43
23.	Forward skirt STA layout.....	45
24.	Forward skirt STA layout second angle	45
25.	CREO model of tool surface	47
26.	Fibersim is used to generate plies	47
27.	Fibersim generated 3D cross section of laminate showing interleaved plies.....	48
28.	Fibersim has a ply sequence editor that allows the designer to easily edit the ply sequence	48
29.	CGTech VERICUT VCPe with imported Creo model and Fibersim ply data.....	49
30.	CGTech VCS manufacturing simulation	50
31.	CGTech VERICUT VCPe-generated course data for AFP (reinforcement ply)	50
32.	CUSA2 STA traded assembly options	51
33.	Interface definition for the STA assembly fixture (sheet 1)	53
34.	Interface definition for the STA assembly fixture (sheet 2)	53
35.	Layout drawing for the STA (sheet 1)	54
36.	Layout drawing for the STA (sheet 2)	55
37.	Layout drawing for the STA (sheet 3)	55
38.	Pathfinder conceptual model	56
39.	OML trade study considerations: (a) Two-part cone and cylinder and (b) alternate geometries	57

LIST OF FIGURES (Continued)

40.	Aft skirt sizing model	59
41.	Joint interface details	59
42.	Configuration used for analysis of the critical size of kissing bonds at the facesheet-core interface	63
43.	Typical mesh used for the critical disband size analysis: (a) Front and (b) side	64
44.	Boundary conditions for the critical disband size analysis	65
45.	Typical first mode of eigenvalue buckling analysis	66
46.	Damage, load-displacement response, and out-of-plane deformation predicted using cohesive elements: (a) Damage propagation, (b) load displacement response, and (c) u_z (in)	67
47.	Damage, load-displacement response, and out-of-plane deformation predicted using VCCT: (a) Damage propagation, (b) load displacement response, and (c) u_z (in)	67
48.	Critical disbond size	69
49.	Schematic of the ELC	70
50.	Wide-area, vacuum-assisted disbond inspection method	71
51.	Detectable size for vacuum-assisted disbond inspection	71
52.	USA options	72
53.	Analysis model for USA initial design concept	73
54.	USA: (a) Baseline geometry and (b) representative buckling results	74
55.	STA model with typical buckling eigenmode response	76
56.	STA core depth study results	77
57.	Simulator capability memorandum	78
58.	Full stack model—assembly of STA, simulators, loading rings, and load jacks	79

LIST OF FIGURES (Continued)

59.	Load versus displacement curve and radial deformation contours in stack	79
60.	Radial deformations in LH ₂ simulator: (a) Just before buckling and (b) at the end of the analysis	80
61.	Axial displacement of load jacks (in inches)	80
62.	Load versus displacement curve and radial deformation contours in stack	81
63.	Radial deformation contours in the STA: (a) Just before buckling and (b) just after buckling	81
64.	Strain contours in LH ₂ simulator: (a) Just before buckling and (b) just after buckling	82
65.	Displacement and load configurations (in inches)	82
66.	Load versus displacement curve and radial deformation contours in stack	83
67.	Radial deformation contours in the STA: (a) Just before buckling and (b) just after buckling	83
68.	Nodal imperfections applied to the STA	84
69.	Load deflection curve of transient dynamic nonlinear analysis	85
70.	Radial deformation of perfect STA model: (a) At buckling load and (b) at last load increment in the transient dynamic analysis	85
71.	Radial deformation of STA model with imperfections: (a) At buckling load and (b) at last load increment in the transient dynamic analysis	86
72.	Buckling and EWC FEMs with end-fitting details	88
73.	Buckling performance: (a) 4.5 pcf and (b) 3.1 pcf core models	89
74.	Facesheet failure indices at buckling	90
75.	CEUS tooling design concept	92
76.	CEUS final tool	94
77.	CEUS metrology (dimensions are in mm)	94

LIST OF FIGURES (Continued)

78.	CEUS tool installed in MSFC AFP cell	95
79.	CEUS tool AFP trials	95
80.	Assembly fixture concept and finished CEUS	98
81.	Debulk vacuum bag schematic	99
82.	AFP of first skin	100
83.	Film adhesive installed on first composite skin	100
84.	Honeycomb core cell irregular shapes	101
85.	Foaming core splice installation	101
86.	Paste core splice adhesive injection	102
87.	Second film adhesive layer with overlap	103
88.	View of honeycomb core after fiber placement of top skin, showing no damage	103
89.	AFP of second skin onto surface of honeycomb core	104
90.	Autoclave cure vacuum bag	104
91.	Part loaded into autoclave	105
92.	Voids	107
93.	Tan delta peak at various 285 °F hold times	109
94.	Ramp rate of 2 °F/min with 30-min, 285 °F hold time	110
95.	Ramp rate of 5 °F/min with 30-min, 285 °F/min to cure temperature	111
96.	Micrograph of 8552-1 DDS/TGDDM resin (darker section) deforming the Cytec FM-300 film adhesive (lighter section) at core interface	112
97.	Loss and storage modulus values of FM300-3	113

LIST OF FIGURES (Continued)

98.	Combining the results of the FM300-2 film adhesive and 8552-1	114
99.	Clean cross section using developed cure cycle	115
100.	Typical profile of porosity using developed cure cycle	115
101.	Example of void most likely caused from air entrainment	115
102.	Example of digital image correlation data: (a) Superimposed on a barrel that has been painted with a high contrast speckle pattern compared to (b) an analytical model of predicted displacement	117
103.	Test configuration in test stand 4699	118
104.	Progress made in composite technologies	120

LIST OF TABLES

1.	Level 1 requirements for CEUS-1 through CEUS-7	2
2.	Open moderate risks at project termination	5
3.	Historic lessons learned March 2015	7
4.	Ares I Interstage mapping to MSFC-RQMT-3479	9
5.	Ares I First Stage frustum mapping to MSFC-RQMT-3479	10
6.	Space Shuttle ET Fwd GH ₂ Press Line Fairing mapping to MSFC-RQMT-3479	10
7.	Space Shuttle ET Intertank Access Door mapping to MSFC-RQMT-3479	11
8.	Space Shuttle ET composite nose cone mapping to MSFC-RQMT-3479	12
9.	Space Shuttle FWC mapping to MSFC-RQMT-3479	12
10.	HST SLIC mapping to MSFC-RQMT-3479	13
11.	Orion MPCV mapping to MSFC-RQMT-3479	13
12.	Test matrix	22
13.	Lamina tensile strength and modulus data	24
14.	Unnotched tensile strength and modulus data	24
15.	Unnotched compression strength and modulus data	25
16.	Laminate short beam shear data	25
17.	Open-hole tension data	26
18.	Open-hole compression data	26
19.	OHT data	40

LIST OF TABLES (Continued)

20.	OHC data.....	41
21.	Wall construction trade study mass results	60
22.	Buckling trade study results	75
23.	Summary of buckling load line load and principal strain	84
24.	Summary of buckling load sensitivity to geometric imperfections study	86
25.	Lightweight core validation test plan	87
26.	Predicted loads and end-shortening: Core trade study.....	89
27.	Fiber (IM7) test matrix	126
28.	Matrix (8552-1 neat resin) test matrix.....	126
29.	IM7/8552-1 lamina/laminate test matrix.....	126
30.	Assessment of TRL/MRL of 8.4-m-diameter composite technologies.....	237
31.	Assessment of composite technologies versus perceived impediments.....	238

LIST OF ACRONYMS, SYMBOLS, AND ABBREVIATIONS

AFP	automated fiber placement
Al	aluminum
ANOVA	analysis of variance
ASTM	American Society of Testing and Materials
CAD	computer-aided design
CE	chief engineer
CEUS	Composite Exploration Upper Stage
CMM	coordinate measuring machine
CPT	cured ply thickness
CUSA	composite for the universal stage adapter
CV	coefficient of variation
DDS	design data sheet
DDT&E	design, development, test, and evaluation
DSC	Differential Scanning Calorimetry (test)
DTA	damage threat assessment
EFT-1	Exploration Flight Test 1
ELC	elasticity laminate checker
EOP	edge of port
ET	external tank
ETW	elevated temperature wet
EUS	Exploration Upper Stage
EWC	edge-wise compression
FCB	fraction control board
FE	finite element

LIST OF ACRONYMS, SYMBOLS, AND ABBREVIATIONS (Continued)

FEA	finite element analysis
FEM	finite element model
FEP	fluorinated ethylene propylene
FI	failure index
FS	factors of safety
FV	fiber volume
FWC	filament wound case
GH ₂	gaseous hydrogen
GRC	Glenn Research Center
GSFC	Goddard Space Flight Center
HEOMD	Human Exploration and Operations Mission Directorate
HST	Hubble Space Telescope
IDPP	impact damage protection plan
ISSAC	integrated structural assembly of advanced composites
ITAR	International Traffic in Arms Regulation
LaRC	Langley Research Center
LH ₂	liquid hydrogen
LOX	liquid oxygen
LSSM	lightweight spacecraft structures and materials
MPCV	multipurpose crew vehicle
MPR	Marshall Procedural Requirements
MRL	manufacturing readiness assessment
MSA	MPCV stage adapter
MSFC	Marshall Space Flight Center
NASA	National Aeronautics and Space Administration
NCAMP	National Center for Advanced Materials Performance

LIST OF ACRONYMS, SYMBOLS, AND ABBREVIATIONS (Continued)

NDE	nondestructive evaluation
NIAR	National Institute of Aviation Research
OHC	open-hole compression
OHT	open-hole tension
OML	outer mold line
OOA	out-of-autoclave
PDR	preliminary design review
PM	project manager
PMT	project management team
psf	pounds per square foot
RMS	root-mean-square
RTD	room temperature dry
RVE	representative volume element
SBKF	shell buckling knockdown factor
SBS	short beam shear
SLIC	super-lightweight interchangeable carrier
SLS	Space Launch System
SMA	safety and mission assurance
SRB	solid rocket booster
SSR	systems requirements review
STA	structural test article
STMD	Space Technology Mission Directorate
TPS	Thermal Protection System
TRL	technology readiness level
USA	universal stage adapter
VCCT	virtual crack closure technique

LIST OF ACRONYMS, SYMBOLS, AND ABBREVIATIONS (Continued)

VCP	VERICUT for Composites Programming
VCPe	VERICUT for Composite Paths for Engineering
VCS	VERICUT for Composites Simulation
VFM	virtual flight model
WBS	Work Breakdown Structure

NOMENCLATURE

D	diameter
E	modulus of elasticity
E'	storage modulus
E''	loss modulus
F_z	avail load force (z direction)
h	height
I	damage initiation
M_y	moment (y direction)
N	load displacement nonlinearity
N_y	loading direction
P	peak load
T_g	transition
t_c	core thickness
t_f	facesheet thickness
w	width
x	location on x -axis
y	location on y -axis
z	location on z -axis
δ	loss tangent
η	viscosity

TECHNICAL MEMORANDUM

COMPOSITES FOR EXPLORATION UPPER STAGE

1. PROJECT OVERVIEW

The Composite for Exploration Upper Stage (CEUS) project technical scope was developed to (1) reduce technical impediments for the use of composites in launch vehicles and other NASA missions; (2) bridge the gap between technology demonstration and the final infusion into NASA missions; (3) streamline the design and manufacturing processes for launch vehicle applications to reduce development costs; and (4) address the use of conservative knockdown factors and limiting damage tolerance techniques. This scope was organized into the following four primary areas: materials, structures, manufacturing, and testing. The initial activity content was focused on the liquid hydrogen (LH_2) tank forward and aft skirt of the Exploration Upper Stage (EUS). Level 1 requirements were generated for the initial CEUS technical scope (shown in table 1) and were updated during the project scope trade studies. The tasks for the initial scope included the following:

- (1) Accelerated building block approach:
 - Coupon program.
 - Joint development (out-of-autoclave (OOA) jointing activity with composite joints).
 - Tool design and fabrication.
- (2) Eight-segment forward LH_2 skirt and aft LH_2 skirt:
 - Fit in 20-ft autoclave.
 - Metallic joints (optional).
 - Analyze and test critical subcomponent specimens to develop and validate the composite design database.
- (3) Design in a model-based environment:
 - Failure modes and loads predicted within 5% of measured values.
- (4) Modeling and simulation included in manufacturing flow.
- (5) Assessment of structural secondary attachments.
- (6) Thermal testing:
- (7) Multipurpose tool for LH_2 forward skirt and LH_2 aft skirt (outer mold line (OML) structures).

Table 1. Level 1 requirements for CEUS-1 through CEUS-7.

Structure	Level 1 Requirements*
CEUS-1	The CEUS project shall fabricate at least one full-scale technology demonstration unit Space Launch System (SLS)/EUS hydrogen tank skirt assembly.
CEUS-2	The assembly shall include interfaces representative of those in the SRR SLS/EUS baseline design.
CEUS-3	The assembly shall demonstrate structural integrity when exposed to qualification-level loads and environments representative of the anticipated SLS/EUS-induced and natural environments.
CEUS-4	The assembly, including planned penetrations and interfaces, shall be at least 20% less massive than an analogous metallic skirt.
CEUS-5	The CEUS project shall document design, analysis, manufacturing, inspection, and test data relevant to qualifying large composite structures and infusing them into future human exploration vehicles.
CEUS-6	The CEUS project shall provide estimated DDT&E costs for producing flight-qualified composite skirts.
CEUS-7	The CEUS project shall use DDT&E methodologies consistent with SLS/EUS composite structure certification requirements.

*All CEUS level 1 requirements were approved.

- (8) Forward skirt and aft skirt testing in a relevant environment.
- (9) Forward skirt and aft skirt development for qualification.
- (10) Publically disseminate all results.

The project successfully completed the Systems Requirements Review (SRR) for the initial technical scope. Several scope trade studies were accomplished after SRR that assessed deleting the aft skirt and adding additional large panel testing, and assessed technical scope related to the universal stage adapter (USA) instead of the LH₂ skirts. These trades were either complete or nearing completion when the project was cancelled. Figure 1(a) depicts the scope options the project evaluated with the EUS LH₂ skirts, and (b) depicts the USA risk reduction.

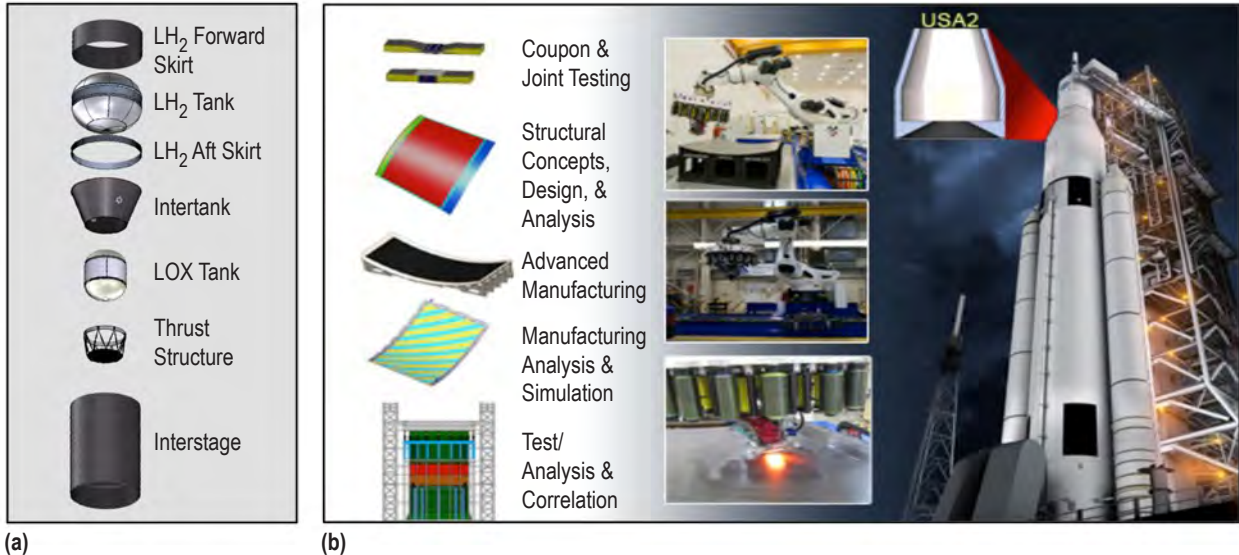


Figure 1. Project evaluation: (a) Scope options and (b) USA risk reduction evaluation.

1.1 Management Approach

NASA's Glenn Research Center (GRC), Langley Research Center (LaRC), and Marshall Space Flight Center (MSFC) formed a strong technical and management team to support the CEUS project. Collaborative partnership arrangements were made between the three NASA Centers to ensure the success of the project. Project team members were carefully selected based on previous experience and suitability to help the project reach its objectives and specific aims. GRC was responsible for leading the Materials Work Breakdown Structure (WBS) element, LaRC was responsible for leading the Joint Development and Structural Analysis WBS elements, and MSFC was responsible for design, manufacturing, testing, and project management. All Centers were responsible for the work in their lead roles, providing support roles in other WBS areas, as well as insight/oversight work with the in-house and contractor activities, developing requirements, and performing reviews. The organization chart in figure 2 indicates the LaRC, GRC, and MSFC roles in the project organization. The organization structure was designed to establish lines of responsibility and management accountability. Core management came from within MSFC to create a centralized project management team (PMT). The PMT consisted of the project manager (PM), the deputy project manager, and the chief engineer (CE). Project resource administrators (RAs) at each Center managed the business side of their Center's tasks. The PM's support staff was drawn from MSFC's directorates and provided the PM with effective project control, permitted delegation of authority and responsibility, ensured short lines of communication and reporting, and permitted corrective actions to be taken at the proper level of responsibility.

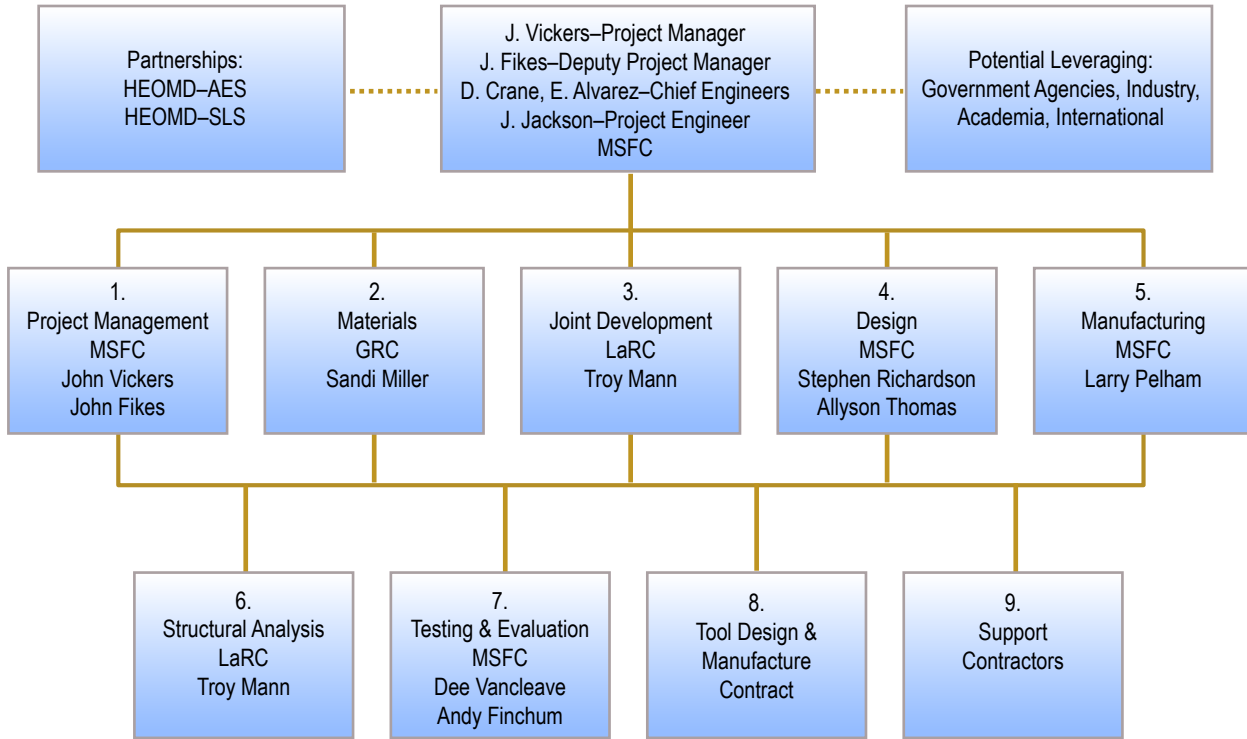


Figure 2. Project organization structure.

1.2 Risk Management

The CEUS project managed risk according to tailored requirements outlined in MPR 7120.1, Rev. G, “MSFC Engineering and Program/Project Management Requirements,” dated August 26, 2014.¹ The Risk Management process consisted of the following:

- Identification of risk contributors.
- Analyses to estimate probability and consequences.
- Planning of risk mitigation.
- Tracking to performance measures.
- Controlling risk through adjustments to plans and control measures.
- Communication of risk management activity.
- Documentation throughout the process.

Risk was evaluated on a 5×5 matrix of likelihood and consequence, and the PM, CE, and chief safety officer had the authority to determine risk items to be entered in the system and to adjust the likelihood and consequence levels. The project assigned a risk owner for each risk item. In addition to the 5×5 assessment, each risk owner prepared and presented the tasks, funding, and schedule required to mitigate the risk and the impacts of not mitigating (technical, cost, schedule, safety).

At the time of termination, the project had eleven open risks, of which none were high (red), six were moderate (yellow), and five were low (green). As a result of several trade studies that kept the project in a transient state for several months prior to termination, several of the risks were still being formulated. As a result, many mitigation plans and risk statements were still to be defined at the time of termination. The open moderate risks are shown in table 2.

Table 2. Open moderate risks at project termination.

Risk	Likelihood	Consequence	Risk Mitigation	Impact of Not Mitigating
CEUS-01	2x5	Autoclave failure	Watch	If the MSFC 20-ft autoclave should fail, the CEUS schedule may be delayed by up to 6 months into FY 2018.
CEUS-14	3x3	Technical design criteria	Mitigate	Given the current design criteria for composites, design decisions could lead the effort to overly conservative solutions that will cost time, budget, and performance with no significant reduction in risk and not taking full advantage of potential savings.
CEUS-22	2x5	SLS test failure	Watch	Given that major SLS structural tests and test related activities will be performed concurrently at MSFC, a test failure in an adjacent test stand could damage the CEUS test article.
CEUS-105	3x3	Scale up—large composite structures	Mitigate	Manufacturing processes for composite structures typically do not lend themselves to linear scaling. As a result, there is inherent risk with the scaling of structures. Unforeseen issues that could arise may impact both cost and schedule.
CEUS-108	3x2	OOA joint manufacturing	Mitigate	Demonstration of large-scale OOA joint manufacturing.
CEUS-111	2x4	Assembly fixture—end ring	Mitigate	End ring for assembly fixture is schedule critical.

1.3 Lessons Learned

1.3.1 Review of Historical Lessons Learned

A review of the NASA Lessons Learned database and of previous composites projects was conducted. The purpose of the review was to capture lessons learned from prior Agency efforts and to build a plan to address those lessons specifically for the CEUS project. The information reviewed included the following:

- Composite Crew Module – NESC-RP-06-019, series of seven NASA Technical Memoranda (NASA/TM—2011-217185 through NASA/TM—2011-217191) detailing primary structure, design, materials, and processes, analysis, manufacturing, test, and nondestructive evaluation (NDE).
- Final Report of the X-33 Liquid Hydrogen Tank Test Investigation team (no document number assigned).
- Ares 1 Interstage – MSFC/EV31 internal documentation.
- Composite Cryotank – MSFC/EV31 internal documentation.
- SRB Composite Nose Cap Project – MSFC strength analysis group internal documentation.
- Composite Interstage Structural Concepts for Heavy Lift Launch Vehicles – Lightweight Spacecraft Structures & Materials (LSSM) project internal documentation.
- Composite Chronicles: A Study of the Lessons Learned in the Development, Production, and Service of Composite Structures – NASA-CR-4620.
- Boeing Lessons Learned: Delta IV Centerbody and Interstage, Sea Launch Fairings, and Payload Attach Structures – Boeing internal documentation.
- NASA Preferred Reliability Practices – NASA-TM-4322A.
- NASA Lessons Learned Information System – Various lessons learned found using keyword composites.

The information was collected in a spreadsheet (app. A). Each lesson learned was entered in its own row with document number, document name, date, LLIS# (if applicable), statement of the lesson learned, applicability of the lesson to the CEUS project, and the plan to address the lesson in the CEUS project. A total of 94 lessons learned were considered for applicability to the CEUS project. The lessons learned were reviewed during the design and analysis meetings held for this project. The project was cancelled before a plan for every lesson could be formulated. Historic lessons learned are listed in table 3.

Table 3. Historic lessons learned March 2015.

Document Number	Document Name	Date	Lesson Learned	Applicable?	Plan
NASA/TM—2011-217185; NESC-RP-06-019	<i>Composite Crew Module: Primary Structure</i>	Nov. 2011	F-1: Many of the design, analysis, materials, and manufacturing lessons learned were not evident in the coupon, element, or subcomponent testing and only became evident when building the full-scale assembly.	Yes	The CEUS project is aware that there can be scaling issues in manufacturing and analysis. The project is going to build a full-scale test article for final verification of the design and manufacturing.
NASA/TM—2011-217188; NESC-RP-06-019	<i>Composite Crew Module: Analysis</i>	Nov. 2011	F-5: Manufacturability, symmetry, and other derived requirements resulted in a CCM structure that does not have zero MS everywhere. These derived requirements can lead to higher MS, thus higher mass than expected.	No	No flight structure is ever perfectly optimized. All engineering designs are a compromise to meet sometimes conflicting requirements.
NASA/TM—2011-217189; NESC-RP-06-019	<i>Composite Crew Module: Manufacturing</i>	Nov. 2011	F-11: The need for repair was caused by a variety of sources including inadvertent impact damage, failed secondary cures, and secondary mechanical fastener hole misalignment.	Yes	Take special care with tooling (tethers?) to avoid impact damage. Make sure procedures for curing are followed correctly. Take special care with the placement of fastener holes; designers, make sure to accommodate existing location constraints; manufacturing, make sure to follow drawings (STA design and manufacturing)
NASA/TM—2011-217190; NESC-RP-06-019	<i>Composite Crew Module: Test</i>	Nov. 2011	F-1: Real-time monitoring of test results against analytical predictions was central to the success of the full-scale test program. This enabled the team to push the applied load limits progressively while minimizing the risk of catastrophic failure.	Yes	Generate pretest predictions and have analysts at stress stations during test (STA analysis and test).

1.3.2 Review of Previous Composites Program Fracture Control Plans and Certification Strategies

A review of previous NASA composites projects for human-rated hardware was conducted. The purpose of the review was to compare the approaches the projects used to satisfy fracture control and damage tolerance requirements and compare those to the intent of the current Agency damage tolerance standards. The projects reviewed were as follows:

- Ares I Interstage.
- Ares I First Stage Frustum.
- Space Shuttle External Tank (ET) Fwd Gaseous Hydrogen (GH_2) Press Line Fairing.
- Space Shuttle ET Intertank Access Door.
- Space Shuttle ET Composite Nose Cone.
- Space Shuttle Filament Wound Case (FWC).

- Hubble Space Telescope (HST) Super Lightweight Interchangeable Carrier (SLIC).
- Orion Multi-Purpose Crew Vehicle (MPCV).

Of the projects in this list, Ares I and the Space Shuttle FWC were cancelled for programmatic reasons prior to first flight. The remaining Shuttle and Hubble structures were successfully flown, and, at the time of writing this Technical Memorandum, Orion is still in development. Additionally, the SLS Block 1 MPCV Stage Adapter (MSA) composite diaphragm (flown on Orion Exploration Flight Test 1 (EFT-1) and scheduled to fly on SLS Exploration Mission 1 (EM-1)) and the Space Shuttle payload bay doors were being studied for this effort, but the CEUS project was overcome by events before the summaries could be made available to the team for review.

Fracture control requirements are provided in NASA-STD-5019, “Fracture Control Requirements for Spaceflight Hardware.” NASA-STD-5019 points to MSFC-RQMT-3479, “Fracture Control Requirements for Composite and Bonded Vehicle and Payload Structures,” for fracture control of composite structures.² At the time of this study, the Agency damage tolerance requirements for fracture critical composite structures were specified in NASA-STD-5019, which invoked MSFC-RQMT-3479.³ Subsequent to this study, Revision A to NASA-STD-5019 was released, which contained all mandatory composite damage tolerance requirements directly in the standard in lieu of invoking MSFC-RQMT-3479. The expectation is that MSFC-RQMT-3479 will become inactive for new design, and fracture critical composite structures on future projects will have to satisfy the damage tolerance requirements of NASA-STD-5019, Rev A.

As stated in MSFC-RQMT-3479, the damage tolerant approach is the preferred approach for accepting fracture critical parts. In the event the required steps cannot be accomplished for a specific structure or joint, the developer may propose an alternate approach to the NASA Project Office through the fracture control plan. The Responsible Fracture Control Board (FCB) reviews the technical adequacy of the plan for the Project Office.

Fracture control of composite structures using the damage tolerant approach shall meet the steps listed below. Note that the damage tolerant approach does include a proof/acceptance test of the flight article. The following steps are the minimum required:

- (1) Damage threat assessment (DTA).
- (2) Impact damage protection plan (IDPP).
- (3) Damage tolerant coupon tests.
- (4) Damage tolerant development tests.
- (5) Analytical support.
- (6) Damage tolerant full-scale component tests.
- (7) Implement impact damage protection plan.
- (8) NDE parts.
- (9) Acceptance proof test to 1.05 minimum.
- (10) Post-proof NDE.
- (11) In-service inspection.

MSFC-RQMT-3479 was released on June 29, 2006. Thus, MSFC-RQMT-3479 did not exist at the time of composite hardware development for projects prior to 2006, but the principal concepts of composite damage tolerance existed, and each project was required to meet fracture control for composite/bonded structures as shown in tables 4–11 in sections 1.3.2.1 through 1.3.2.8. In this summary, these projects were assessed for whether their activities met the intent of MSFC-RQMT-3479. The summaries were put together by members of the CEUS team as part of researching background information; i.e., the summaries were not performed by any agency-chartered FCB.

In tables 4–11, each of the projects reviewed is mapped to the requirements in MSFC-RQMT-3479. Each of these summaries provides objective evidence to demonstrate successful certification of composite flight structure. It should be noted that for every project, the damage tolerance plan was vetted by an FCB and had Board approval.

1.3.2.1 Ares I Interstage. Design work for the Ares I Interstage began c. 2008. MSFC-RQMT-3479 was levied on the project via NASA-STD-5019. The fracture control plan was approved by the MSFC FCB on June 10, 2008, in memo EM20-08-FCB-014.

Table 4. Ares I Interstage mapping to MSFC-RQMT-3479.*

Assessment	Completed?
DTA	In work at time of cancellation
IDPP	Yes
Damage tolerant coupon tests	Yes
Damage tolerant development tests	Yes
Damage tolerance analysis	Yes
Damage tolerant full-scale component tests	Yes
Implement IDPP	In work at time of cancellation
NDE of flight parts	Yes
Acceptance proof test	Yes
Post-proof NDE	Yes
In-service inspection	NA (single flight part)

* Assessment of MSFC/R. Wingate.

1.3.2.2 Ares I First Stage Frustum. Design work for the Ares I First Stage Frustum began after the release of MSFC-RQMT-3479 in 2006 and thus had those requirements levied on the project via NASA-STD-5019. The MSFC FCB approved the fracture control plan on April 21, 2011, in memo EM20-11-FCB-006.

Table 5. Ares I First Stage Frustum mapping to MSFC-RQMT-3479.*

Assessment	Completed?
DTA	Yes
DPP.	Yes
Damage tolerant coupon tests	Yes
Damage tolerant development tests	Yes
Damage tolerance analysis	Yes
Damage tolerant full-scale component tests	Yes
Implement IDPP	In work at time of cancellation
NDE of flight parts	Yes
Acceptance proof test	Yes
Post-proof NDE	Yes
In-service inspection	NA (single flight part)

* Assessment of MSFC/D. Phillips based on information collected by MSFC/R. Wingate.

1.3.2.3 Space Shuttle External Tank Fwd Gaseous Hydrogen Press Line Fairing. Design work for the Space Shuttle ET Fwd GH₂ press line fairing began around 1985. MSFC-RQMT-3479 did not exist yet. The damage tolerance approach for this project would today be considered an alternate approach per MSFC-RQMT-3479.

Table 6. Space Shuttle ET Fwd GH₂ Press Line Fairing mapping to MSFC-RQMT-3479.*

Assessment	Completed?
DTA	Unknown
IDPP	Unknown
Damage tolerant coupon tests	No
Damage tolerant development tests	No
Damage tolerance analysis	No
Damage tolerant full-scale component tests	No
Implement IDPP	Unknown
NDE of flight parts	Yes
Acceptance proof test	Unknown
Post-proof NDE	Unknown
In-service inspection	NA (single flight part)

* Assessment of MSFC/D. Phillips based on information collected by MSFC/R. Wingate.

1.3.2.4 Space Shuttle External Tank Intertank Access Door. Design work for the Space Shuttle ET intertank access door began around 1985 with damage tolerance requirements per MMC-ET-SE13-C, “Space Shuttle External Tank Fracture Control Program Requirements and Implementation Document” and MSFC-HDBK-1453, Fracture Control Program Requirements. This was also before MSFC-RQMT-3479, “Fracture Control Requirements for Composite and Bonded Vehicle Payload Structures.” The damage tolerance approach for this project would today be considered an alternate approach per MSFC-RQMT-3479. The damage tolerance approach for the intertank access door was reviewed and approved by the MSFC FCB in October 1991.

Table 7. Space Shuttle ET Intertank Access Door mapping to MSFC-RQMT-3479.*

Assessment	Completed?
DTA	Intent** (potential flaw types defined)
IDPP	Intent (photos show protective cover)
Damage tolerant coupon tests	Yes
Damage tolerant development tests	No
Damage tolerance analysis	Intent
Damage tolerant full-scale component tests	No
Implement IDPP	Intent
NDE of flight parts	Yes
Acceptance proof test	No
Post-proof NDE	No
In-service inspection	NA (single flight part)

* Assessment of MSFC/R. Wingate.

** Intent means engineering activities were conducted that are considered to partially address the intent of the MSFC-RQMT-3479 requirement, though methods used may not be what would be used in a current effort. MSFC-RQMT-3479 did not exist at the time of ET composite hardware development, but the principal concepts of composite damage tolerance existed well before MSFC-RQMT-3479.

1.3.2.5 Space Shuttle External Tank Composite Nose Cone. Design work for the Space Shuttle ET composite nose cone began around 1985 with damage tolerance requirements per MMC-ET-SE13-C, “Space Shuttle External Tank Fracture Control Program Requirements and Implementation Document” and MSFC-HDBK-1453, “Fracture Control Program Requirements.” This project was also pre-MSFC-RQMT-3479. The damage tolerance approach for this project would today be considered an alternate approach per MSFC-RQMT-3479. The damage tolerance approach for the composite nose cone was reviewed and approved in the mid-1990s.

Table 8. Space Shuttle ET composite nose cone mapping to MSFC-RQMT-3479.*

Assessment	Completed?
DTA	Intent** (potential flaw types defined)
IDPP	Unknown
Damage tolerant coupon tests	Yes
Damage tolerant development tests	No
Damage tolerance analysis	Intent
Damage tolerant full-scale component tests	Yes
Implement IDPP	Unknown
NDE of flight parts	Yes
Acceptance proof test	No
Post-proof NDE	No
In-service inspection	NA (single flight part)

* Assessment of MSFC/R. Wingate.

** Intent means engineering activities were conducted that are considered to partially address the intent of the MSFC-RQMT-3479 requirement, though methods used may not be what would be used in a current effort. MSFC-RQMT-3479 did not exist at the time of ET composite hardware development, but the principal concepts of composite damage tolerance existed well before MSFC-RQMT-3479.

1.4.2.6 Space Shuttle Filament Wound Case. Design work for the Space Shuttle FWC began in the early 1980s (the first flight was to have been in 1986). MSFC-RQMT-3479 was not in existence. Fracture control requirements were required to be specified in a supplier-prepared fracture control plan, and damage tolerance was to be determined by methods approved by Morton Thiokol and MSFC. The damage tolerance approach for this project would today be considered an alternate approach per MSFC-RQMT-3479.

Table 9. Space Shuttle FWC mapping to MSFC-RQMT-3479.*

Assessment	Completed?
DTA	Intent** (potential flaw types defined)
IDPP	Yes***
Damage tolerant coupon tests	Yes
Damage tolerant development tests	Yes
Damage tolerance analysis	Yes
Damage tolerant full-scale component tests	Yes
Implement IDPP	Yes
NDE of flight parts	Yes
Acceptance proof test	Yes
Post-proof NDE	Yes
In-service inspection	N/A (single flight part)

* Assessment of MSFC-Auburn/F. Ledbetter

** Intent means that engineering activities were conducted that are considered to partially address the intent of the MSFC-RQMT-3479 requirement, though methods used may not be what would be used in a current effort. MSFC-RQMT-3479 did not exist at the time of Space Shuttle FWC hardware development, but the principal concepts of composite damage tolerance existed well before MSFC-RQMT-3479.

*** Although not documented in this presentation, it is known that the FWC Program developed a protective cover for each case segment for all transportation operations.

1.3.2.7 Hubble Space Telescope Super Lightweight Interchangeable Carrier. The HST SLIC flew in 2009. MSFC-RQMT-3479 was not in existence when the design began; it was required to conform to NASA-STD-5003, “Fracture Control Requirements for Payloads Using the Space Shuttle.” The damage tolerance approach for this project would today be considered an alternate approach per MSFC-RQMT-3479. The damage tolerance approach for the SLIC was approved by an FCB.

Table 10. HST SLIC mapping to MSFC-RQMT-3479.*

Assessment	Completed?
DTA	Intent** (potential flaw types defined)
IDPP	Yes
Damage tolerant coupon tests	No
Damage tolerant development tests	No
Damage tolerance analysis	No
Damage tolerant full-scale component tests	Intent***
Implement IDPP	Yes
NDE of flight parts	Yes
Acceptance proof test	Yes†
Post-proof NDE	Yes
In-service inspection	NA (single flight part)

* Assessment of GSFC/K. Segal.

** Intent means that engineering activities were conducted that are considered to partially address the intent of the MSFC-RQMT-3479 requirement, though methods used may not be what would be used in a current effort. MSFC-RQMT-3479 did not exist at the time of HST SLIC, but the principal concepts of composite damage tolerance existed.

*** Full-scale-sized, flight-like component tests performed for allowables; manufacturing defects would be present.

† Designed for high margins of safety and acceptance proof test at $1.2 \times$ design limit load on the prototypical structure performed to address damage risks.

1.3.2.8 Orion Multi-Purpose Crew Vehicle. Design work for the Orion MPCV began c. 2006. MSFC-RQMT-3479 was levied on the project.

Table 11. Orion MPCV mapping to MSFC-RQMT-3479.*

Assessment	Completed?
DTA	Yes
IDPP	Yes
Damage tolerant coupon tests	Yes
Damage tolerant development tests	Yes
Damage tolerance analysis	Intent
Damage tolerant full-scale component tests	Fracture critical proof; structural element only
Implement IDPP	Yes
NDE of flight parts	Yes
Acceptance proof test	Yes
Post-proof NDE	Yes
In-service inspection	N/A (single flight part)

* Assessment of GRC-LMC/J. Thesken.

2. MATERIALS

The primary goals of the CEUS project materials WBS included (1) materials selection/procurement and (2) coordination of a laminate equivalency test activity. Manufacturability, co-cure compatibility and, with the prepreg, availability of existing data were factored into the material selection. Availability of an existing materials database enabled equivalency testing as a means to reduce the scope of coupon testing. The prepreg selected for the project was IM7/8552-1, a variant of the IM7/8552 material used to generate test data reported within a database established by the National Center for Advanced Materials Performance (NCAMP). Laminate panels for the CEUS project were fabricated at three NASA Centers to determine equivalency of the material to the database and additionally, equivalence of fiber placement fabrication available at MSFC and LaRC. Coupons from the laminate panels were machined and tested at the National Institute of Aviation Research (NIAR). Statistical analysis methods were used to determine equivalency between the IM7/8552-1 coupons and the NCAMP database for IM7/8552.⁴ Equivalence of the remotely manufactured composite panels was evaluated by Analysis of Variance (ANOVA).

Along with leveraging the NCAMP database to establish design allowables, a CEUS objective was to evaluate Digimat from e-Xstream engineering/MSC-Software®, a nonlinear multiscale material modeling tool, as a method to provide fiber-reinforced polymer matrix composites for both establishing initial design allowables and enabling an ‘as-built’ digital material for in-service performance predictions.

2.1 Selection and Preexisting Data

Hexcel’s IM7/8552-1 prepreg tape was selected as the STA facesheet material based on its amenability to fiber placement and the available NCAMP materials database. Hexcel’s 8552-1 epoxy resin is a variant of the baseline 8552 resin and was designed for fiber placement. Compared to 8552, the 8552-1 variant demonstrates a lower tack, facilitating movement through the fiber placement head. As data for the 8552 form of the material is available through the NCAMP database,⁴ the project adopted an accelerated building block approach in the form of an equivalency test matrix to reduce risk related to materials and schedule. The Composite Material Handbook -17 allows equivalency to be demonstrated for design allowables in the case where the differences between the original and new material and/or process are minimals.⁵

Cytec’s FM300-2M, with 0.06-psf areal weight, was selected as the film adhesive for sandwich panel construction. Cytec’s FM309-1 was initially selected, but the quoted lead time was prohibitive. The FM300-2M film adhesive is a 121 °C cure variant of Cytec’s FM300M adhesive. Previous work had focused on FM300M; however, the 177 °C cure led to co-mingling of the adhesive and the epoxy resin from the facesheet. The 121 °C cure variant was selected to initiate adhesive cure prior to that of the facesheet, and reduce mixing of adhesive and resin during cure. For this project, there was no investigation of the mat-versus-knit carrier, but such a study could have been beneficial, in particular, where foam core may be considered.

The 20-day out-time specified by the vendor was a concern with the FM300-2 film adhesive. An out-time study was carried out to address these concerns; the results are outlined in section 2.4.

Aluminum (Al) honeycomb core was procured from Alcore in flat sheets for process development. The core was phosphoric acid, anodized 5052 aluminum honeycomb, perforated, 1 in thick and $\frac{1}{8}$ in cell size.

2.2 Prepreg Procurement Specification

The IM7/8552-1 prepreg material was ordered from Hexcel. The 12-in parent tape was fabricated at Hexcel Corp, Salt Lake City, Utah, and slit at Web Industries, Atlanta, Georgia. The slit tape width specifications included $\frac{1}{4}$ -in-wide tape provided to LaRC and a $\frac{1}{2}$ -in-wide tape provided to MSFC.

There was considerable discussion within the project regarding the development of an internal NASA specification for the prepreg material. Ultimately, the schedule did not allow for such development, particularly as a portion of the material was procured early within the project for process development and equivalency test panels. Deviating from the specification of the first procurement was not an option.

2.3 Storage and Handling

Guidelines were established to address risk associated with material storage and handling. Specifically, the document described the requirements and methods for storage and handling of temperature-sensitive materials, including Hexcel's Hexply 8552-1, carbon fiber-reinforced epoxy prepreg. The scope of the storage and handling document included requirements for inspection on material delivery, usage, and requalification of a material that exceeded the manufacturer specified out-life or shelf life. Throughout the CEUS project, prepreg and film adhesive were stored in a freezer, at or below 0 °F, and out-time was recorded as the material was used. Acceptance tests included the Differential Scanning Calorimetry (DSC) test for extent of cure and the High-Pressure Liquid Chromatography test for relative constituent concentrations, as well as physical and mechanical test data provided by Hexcel on delivery. This activity was coordinated with Safety and Mission Assurance (SMA). A full description of the SMA activities within the CEUS project is provided in section 4.

2.4 Film Adhesive Out-Time Study

The CEUS manufacturing schedule estimated 20 days to manufacture each $\frac{1}{8}$ -in skirt segment; the film adhesive would sit on the tool through most of that manufacturing process. During this out-time period, the physical and/or chemical properties of the material may change as a result of room temperature cure advancement. A study on the room temperature stability of the film adhesive was initiated to mitigate risk related to film adhesive out-time and to ensure that material manufacturability, strength, durability, and other physical properties are not adversely affected by out-time. The film adhesive was aged at room temperature for 30 days, and the thermal

response of both the baseline and aged materials was evaluated by DSC and rheology measurements. Flat-wise tensile strength of sandwich panels fabricated from baseline and aged adhesive was also evaluated. Photos of failed coupons are shown in figure 3. Both core and adhesive failure was observed within the set of coupons tested with 20-day-aged adhesive; however, there was no overall drop in flatwise tensile strength. In conclusion, the study found no effect on the degree of cure nor reaction temperature following a 30-day out-time. The rheological cure behavior showed a constant gelation temperature through 30 days of out-time, whereas the vitrification temperature decreased with out-time. The time to gelation and vitrification also decreased with increasing out-time. Flatwise tensile strength showed no significant change with film adhesive out-time; however, failure was primarily observed within the 4.5-pcf core.

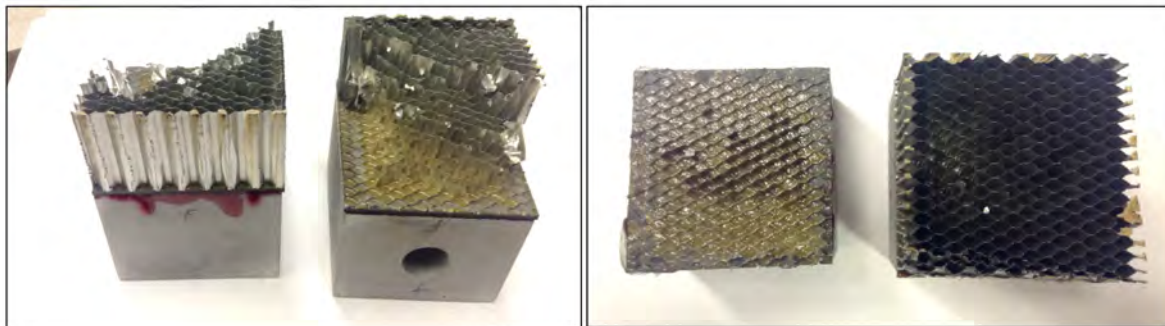


Figure 3. Core and adhesive failure within the coupons fabricated from 20-day-aged film adhesive.

2.5 Equivalency Tests

The purpose of the equivalency test matrix was to reduce the scope of coupon testing within the CEUS project and enable application of the NCAMP-generated materials data to the STA design. Panels for equivalency tests were fabricated at three NASA Centers with the goal of demonstrating material equivalency and equivalency of the manufacturing method, i.e., fiber placement to hand layup. Panels from each Center were shipped to the NIAR where coupons were machined, conditioned, and tested.

2.5.1 Panel Processing Specification

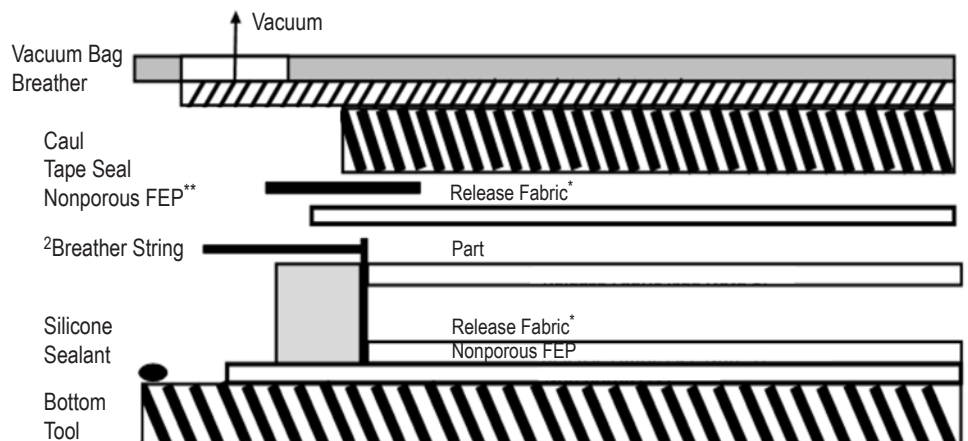
A processing specification was established to ensure consistency of fabrication and processing methods between remote Centers. The document, available on SharePoint, was based off of an NCAMP provided processing document, thereby ensuring consistency with panels fabricated for database development.⁶

2.5.2 Equivalency Panel Fabrication

Figure 4 details the bagging arrangement used to manufacture equivalency test panels. The cure cycle followed NCAMP processing conditions. This cure profile, identified as ‘baseline/medium cure cycle (M),’ varied from the vendor-recommended cycle.

Baseline/Medium Cure Cycle (M): Check vacuum bag integrity prior to starting the cure cycle; leak rate shall not exceed 5 in Hg in 5 minutes. All temperatures are part temperatures. Steps (1)–(6) are based on leading thermocouple, except step 5 is based on lagging thermocouple.

- (1) Pull vacuum (min 22 in Hg).
- (2) Heat at 2° F/min to 355 ± 10 $^{\circ}$ F, and ramp autoclave pressure to 100 psig.
- (3) Before temperature reaches 140 $^{\circ}$ F and when autoclave pressure is 20 ± 10 psig, vent vacuum bag to atmosphere.
- (4) From 325 $^{\circ}$ F to 355 ± 10 $^{\circ}$ F, a minimum heat up rate of 0.3 $^{\circ}$ F/min is acceptable.
- (5) Hold 355 ± 10 $^{\circ}$ F for $120 +60^{\circ}/-0$ min.
- (6) Cooldown rates from cure temperature to 150 $^{\circ}$ F shall be no more than 10 $^{\circ}$ F/min.
- (7) Release autoclave pressure when lagging thermocouple is below 150 $^{\circ}$ F or minimum of 1 hr into cooldown, whichever occurs sooner.
- (8) Remove from autoclave when autoclave temperature is less than 120 $^{\circ}$ F.



* Release fabric is to be used on 0° , unidirectional tension (longitudinal tension, LT) panels only.

** The breather string must be in the edge of the part, not laid on the top of the panel, and must extend out past the seal to touch the breather pad material as shown.

Figure 4. Recommended bagging sequence.

LaRC and MSFC each fabricated three equivalency test panels by fiber placement, where panel dimensions were determined by the dimensions and quantity of coupons required for mechanical tests. Due to the size of the GRC autoclave, smaller panels were fabricated and a total of 16 panels were made to meet the coupon requirements. The key difference between these three sets of panels was the use of $\frac{1}{4}$ -in-wide slit tape at LaRC, $\frac{1}{2}$ -in-wide slit tape for fiber placement at MSFC, and 12-in-wide unidirectional prepreg for hand layup at GRC.

Panel Fabrication, LaRC: The ISAAC system⁷ (fig. 5) at LaRC was used to fabricate three panels (fig. 6) from $\frac{1}{4}$ -in-wide IM7G/8552-1 graphite/epoxy prepreg slit tape.⁸ The panels included a unidirectional 6-ply panel (14 in \times 26 in), a quasi-isotropic 16-ply panel (24 \times 24 in 2), and a quasi-isotropic 24-ply panel (24 in \times 24 in).



Figure 5. LaRC ISAAC system.



Figure 6. Equivalency panel fabrication at LaRC.

The panel layups were first programmed using the CGTech VERICUT® for Composites Programming (VCP) software, tested virtually prior to running on the ISAAC hardware using the CGTech VERICUT for Composites Simulation (VCS) software (fig. 7), and tested virtually (fig. 8) prior to running on the ISAAC hardware using the CGTech VCS. After layup on ISAAC, the panels were then cured at LaRC using the cure cycle specified by the CEUS processing document.

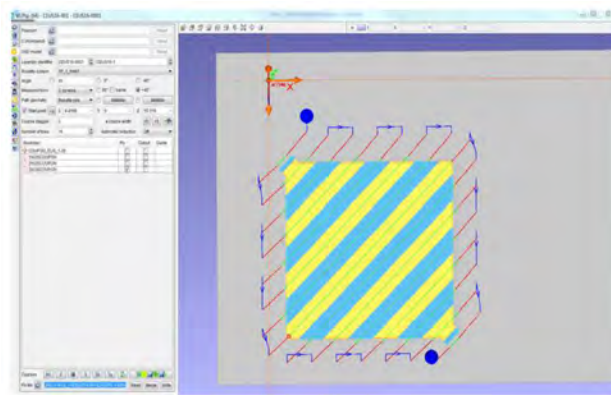


Figure 7. Panel layups tested on CGtech VCP.



Figure 8. CGTech VERICUT tested virtually.

Panel Fabrication, MSFC: Details of MSFC panel fabrication will be provided in the manufacturing section.

Panel Fabrication, GRC: Panels were hand laid from 12-in-wide parent tape and followed the CEUS processing document. Panels were a maximum of 12×12 in, requiring 16 panels to be fabricated for equivalency testing.

2.5.2.1 Panel Quality. Panel quality was characterized at NIAR by ultrasonic C-scan to ensure acceptable consolidation prior to test. Representative images from panels fabricated at GRC, LaRC, and MSFC are shown, respectively, in figure 9. These images represent the [45/0/-45/90]_{2s} ply configuration.

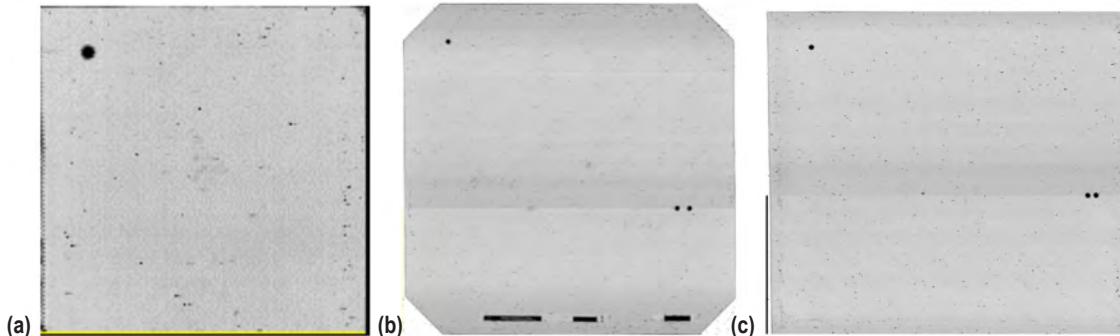


Figure 9. C-scan images of the 16-ply panels fabricated for (a) UNT, (b) UNC, and (c) OHT tests.

Coupons from each panel were sectioned for optical microscopy and acid digestion. Representative photomicrographs in figure 10 support NDE indicating low void content throughout the panels. Acid digestion showed less than 1% void content in panels evaluated.

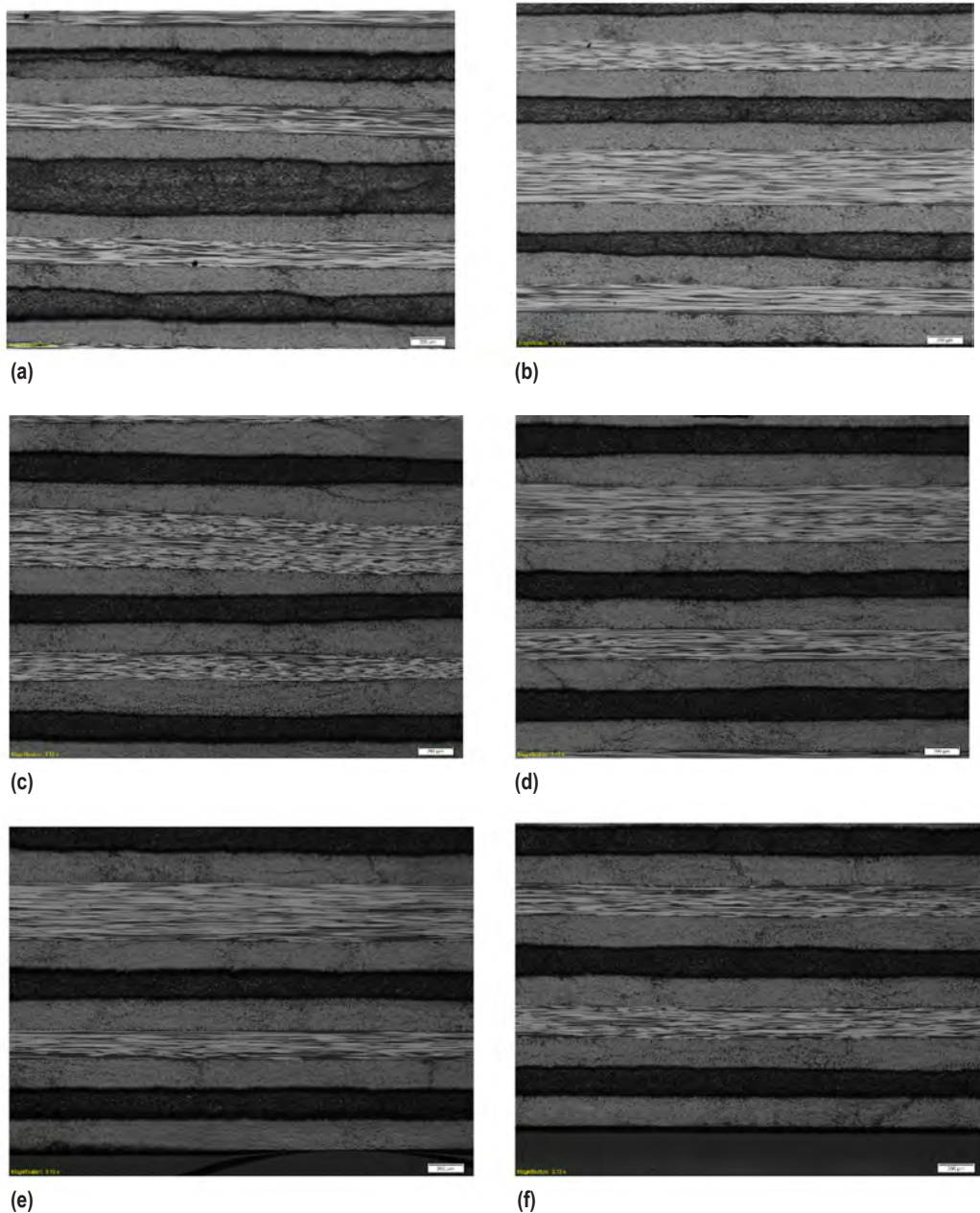


Figure 10. Photomicrograph of GRC panels: (a) 24 ply and (b) 36 ply, LaRC panels: (c) 24 ply and (d) 36 ply, and MSFC panels: (e) 24 ply and (f) 36 ply.

2.5.3 Test Matrix and Data

The equivalency test matrix outlined in table 12 reflects a portion of the data available within the NCAMP database. The identified coupon tests were chosen to provide confidence in the material and manufacturing method. Ply configurations matched those used to generate the NCAMP database. Coupons were machined by wet diamond saw to be oversized, then ground to meet American Society for Testing and Materials (ASTM) specifications. Details on coupon size are also outlined in table 12. Test conditions matched those used in the NCAMP database, where the cold temperature dry condition was defined as –65 °F, room temperature dry (RTD) condition was 70 °F, and the elevated temperature wet (ETW) condition was 250 °F.

Table 12. Test matrix.

Test Description	Test Standard	Test Type	Condition	Specimens		Panel Thickness		Specimen Size (in)	
				Test per Center	Spare per Center	No. of Plies	Nom. Thick (in)	0 Dir.	90 Dir.
Solid Panels									
Lamina-tension, 0-deg direction	ASTM D3039	T	CTD	6	1	6	0.04	10	1
			RTD	6	1				
			ETW	6	1				
Laminate tension (Q/I)	ASTM D3039	UNT	CTD	6	1	16	0.12	10	1
			RTD	6	1				
			ETW	6	1				
Laminate compression (Q/I)	ASTM D6641	UNC	CTD	6	1	16	0.12	5.5	0.5
			RTD	6	1				
			ETW	6	1				
Short beam shear strength	ASTM D2344	S	CTD	6	1	24	0.17	1.5	0.5
			RTD	6	1				
			ETW	6	1				
Open-hole compression	ASTM D6484	OHC	CTD	6	1	24	0.17	12	1.5
			RTD	6	1				
			ETW	6	1				
Open-hole tension	ASTM D5766	OHT	CTD	6	1	16	0.12	12	1.5
			RTD	6	1				
			ETW	6	1				
Compression after impact	ASTM D7137	CAI	CTD	6	1	24	0.14	6	4
			RTD	6	1				
			ETW	6	1				

Mechanical test data were generated for coupons fabricated at each Center and preliminary statistical analysis determined a ‘per-Center’ equivalency to the NCAMP database. The coupons prepared at separate locations could not be grouped for equivalency analysis because doing so would imply equivalency of those panels. Panels made at separate locations could not be assumed to be equivalent; a component of this effort was to demonstrate equivalency of the processing methods. While each center routinely passed the equivalency metric, that pass came with the caveat of ‘insufficient data.’ Per CMH-17 guidelines, eight coupons are required to determine equivalency, and each Center individually offered only four to six coupons per test.

ANOVA was performed on the test data to determine statistical equivalence of coupons from separate Centers, therefore allowing those coupons to be grouped in the analysis for equivalency. ANOVA is a well-known statistical method used to determine whether independently fabricated panels can be considered equivalent, although this level of equivalency is, in general, very difficult to establish. Equivalency between even two of the Centers would provide a sufficient coupon count to remove the ‘insufficient data’ descriptor. ANOVA allowed data pooling in most cases. Where allowed, these data are presented in tables 13–18 as ‘Combined Data.’

The mechanical test data generated by NIAR is tabulated in table 13, with the Pass/Fail column indicative of the equivalency metric. For statistical analysis for equivalency testing of composite materials, alpha is set at 0.05, which corresponds to a confidence level of 95%. This means that if the null is rejected and the two materials are not equivalent with respect to a particular test, the probability that this is a correct decision is no less than 95%.

The NIAR report utilized a modified coefficient of variation (CV); in accordance with section 8.4.4 of CMH-17 Rev. G. It is a method of adjusting the original basis values downward in anticipation of the expected additional variation. Composite materials are expected to have a CV of at least 6%. When the CV is less than 8%, a modification is made that adjusts the CV upwards. Several datasets in the CEUS equivalency matrix passed the equivalency standard under the Modified CV condition. Complete details on this method are provided in the NIAR report.

The mean value of each dataset is tabulated in tables 13–18, with the coefficient of variation noted parenthetically. The following items are important to note:

- (1) Different materials were used. Hexcel expects a reduction in compressive strength of the 8552-1 variant compared to the baseline 8552 matrix resin. Internal Hexcel testing has confirmed this to be the case; however, modification of the test method reduced the gap in measured compressive strength between the two materials.
- (2) The statistical analysis was performed with cured ply thickness (CPT) normalized to 0.0072 in. The average CPT of NASA-generated panels was 0.0070 in.
- (3) All ‘passes’ are with the ‘Insufficient Data’ caveat, and a ‘pass’ with Modified CV was considered a ‘pass’.

Table 13. Lamina tensile strength and modulus data.

Panel [0]6	CTD			RTD			ETW		
	Raw Data (CV)	Normalized Data	Pass/Fail	Raw Data (CV)	Normalized Data	Pass/Fail	Raw Data (CV)	Normalized Data	Pass/Fail
NCAMP Database									
Strength (ksi)	353.7	357.4 (6)	–	371.1	362.7 (6.2)	–	328.0	33.5 (11.7)	–
Modulus (Msi)	22.3	22.6 (1.7)	–	23.5	23.0	–	23.8	24.0	–
COMBINED DATA									
Strength (ksi)	–	363.3 (3.0)	Pass	–	389.1 (3.1)	Pass	–	360.0 (3.5)	Pass
Modulus (Msi)	–	22.3 (1.6)	Pass	–	22.4 (1.6)	Pass	–	23.1 (1.5)	Fail
HXL-H12-GRC									
Strength (ksi)	404.5 (3.7)	363.7 (3.5)	Pass	427.1 (1.4)	388.3 (1.7)	Pass	394.3 (3.5)	356.4 (3.2)	Pass
Modulus (Msi)	24.7 (0.7)	22.2 (0.6)	Pass	24.8 (0.8)	22.5 (2.2)	Pass	25.7 (1.3)	23.2 (1.7)	Pass
HXL-H12-LaRC									
Strength (ksi)	387.0 (3.4)	368.2 (3.2)	Pass	412.1 (3.7)	381.7(14.2)	Pass	380.8 (3.8)	358.1 (3.7)	Pass
Modulus (Msi)	23.3 (1.0)	22.1 (0.9)	Pass	24.1 (2.4)	22.4 (2.4)	Pass	24.6 (1.8)	23.2 (1.6)	Pass
HXL-H12-MSFC									
Strength (ksi)	371.5 (1.8)	358.0 (1.9)	Pass	416.8 (3.7)	397.1 (2.7)	Pass	380.8 (3.5)	366.5 (3.5)	Pass
Modulus (Msi)	23.0 (1.1)	22.1 (1.0)	Pass	23.7 (1.6)	22.6 (0.3)	Pass	23.7 (1.0)	22.8 (0.9)	Pass

Table 14. Unnotched tensile strength and modulus data.

Panel [45/0/-45/90]2s	CTD			RTD			ETW		
	Raw Data (CV)	Normalized Data	Pass/Fail	Raw Data (CV)	Normalized Data	Pass/Fail	Raw Data (CV)	Normalized Data	Pass/Fail
NCAMP Database									
Strength (ksi)	–	97.2 (6.1)	–	–	103.4 (7.1)	–	–	110.5 (5.8)	–
Modulus (Msi)	–	8.1	–	–	8.2	–	–	7.6	–
COMBINED DATA									
Strength (ksi)	–	108.8 (2.3)	Pass	–	106.9 (3.9)	Pass	–	Could not pool data	NA
Modulus (Msi)	–	Could not pool data	NA	–	8.1 (3.6)	Fail	–	8.0 (1.5)	Pass
HXL-H12-GRC									
Strength (ksi)	116.8 (3.7)	109.9 (3.0)	Pass	113.7 (1.7)	105.3 (6.7)	Pass	118.4 (2.9)	108.3 (3.0)	Pass
Modulus (Msi)	8.7 (2.2)	8.2 (1.4)	Pass	8.6 (3.7)	7.9 (5.7)	Pass	8.7 (1.8)	8.0 (1.0)	Pass
HXL-H12-LaRC									
Strength (ksi)	110.1 (1.8)	107.1 (1.4)	Pass	111.0 (1.6)	108.0 (1.4)	Pass	119.3 (1.9)	116.1 (2.4)	Pass
Modulus (Msi)	8.7 (1.6)	8.4 (1.3)	Pass	8.4 (1.8)	8.2 (2.0)	Pass	8.2 (1.4)	8.0 (1.8)	Pass
HXL-H12-MSFC									
Strength (ksi)	112.8 (1.6)	109.5 (1.6)	Pass	110.5 (1.4)	107.4 (1.5)	Pass	114. (2.6)	110.9 (2.5)	Pass
Modulus (Msi)	8.6 (0.5)	8.3 (0.5)	Pass	8.3 (1.4)	8.1 (1.2)	Pass	8.1 (1.8)	7.9 (1.6)	Pass

Table 15. Unnotched compression strength and modulus data.

Panel [45/0/-45/90]2s	CTD			RTD			ETW		
	Raw Data (CV)	Normalized Data	Pass/Fail	Raw Data (CV)	Normalized Data	Pass/ Fail	Raw Data (CV)	Normalized Data	Pass/Fail
NCAMP Database									
Strength (ksi)	–	–	–	–	87.1 (9.3)	–	–	57.7 (11.0)	–
Modulus (Msi)	–	–	–	–	7.6 (4.8)	–	–	7.1 (1.8)	–
COMBINED DATA									
Strength (ksi)	–	–	–	–	92.4 (5.1)	Pass	–	57.7 (8.6)	Pass
Modulus (Msi)	–	–	–	–	7.7 (1.8)	Pass	–	Could not pool data	NA
HXL-H12-GRC									
Strength (ksi)	112.8 (4.5)	–	–	95.1 (4.3)	94.5 (7.8)	Pass	59.6 (12.6)	60.5 (12.7)	Pass
Modulus (Msi)	7.9 (1.9)	–	–	8.0 (0.8)	8.0 (4.5)	Pass	7.7 (1.3)	7.8 (1.6)	Fail (2.9%)
HXL-H12-LaRC									
Strength (ksi)	119.8 (3.7)	–	–	94.1 (2.2)	92.2 (2.3)	Pass	57.9 (7.5)	56.4 (7.5)	Pass
Modulus (Msi)	7.9 (1.2)	–	–	7.8 (1.3)	7.6 (1.3)	Pass	7.6 (0.9)	7.4 (0.8)	Pass
HXL-H12-MSFC									
Strength (ksi)	114.3 (5.3)	–	–	97.7 (3.3)	95.0 (3.3)	Pass	62.1 (2.7)	60.3 (2.8)	Pass
Modulus (Msi)	8.1 (0.7)	–	–	7.9 (0.4)	7.7 (0.5)	Pass	7.7 (1.2)	7.5 (1.2)	Pass

Note: The fail in the compression modulus is due to a measured value that is greater than the modulus reported in the database.

Table 16. Laminate short beam shear data.

Panel [45/0/-45/90]3s	CTD			RTD			ETW		
	Raw Data (CV)	Normalized Data	Pass/Fail	Raw Data (CV)	Normalized Data	Pass/Fail	Raw Data (CV)	Normalized Data	Pass/Fail
NCAMP Database									
Strength (ksi)	–	–	–	NA	12.13 (6.9)	–	–	6.99 (3.7)	–
COMBINED DATA									
Strength (ksi)	–	–	–	–	12.3 (3.7)	Pass	–	6.8 (3.6)	Fail
HXL-H12-GRC									
Strength (ksi)	12.89 (2.9)	–	–	12.45 (3.2)	12.4 (3.2)	Pass	6.8 (4.0)	6.8 (4.4)	Pass
HXL-H12-LaRC									
Strength (ksi)	11.31 (7.8)	–	–	12.03 (3.9)	12.0 (3.9)	Pass	7.0 (2.3)	7.0 (2.3)	Pass
HXL-H12-MSFC									
Strength (ksi)	13.55 (2.2)	–	–	12.4 (3.8)	12.4 (3.8)	Pass	6.7 (3.1)	6.7 (3.2)	Fail (0.1%)

Table 17. Open-hole tension data.

Panel [45/0/-45/90]2s	CTD			RTD			ETW		
	Raw Data (CV)	Normalized Data	Pass/Fail	Raw Data (CV)	Normalized Data	Pass/Fail	Raw Data (CV)	Normalized Data	Pass/Fail
NCAMP Database									
Strength (ksi)		57.8 (4.2)	-		59.0 (4.0)	-		67.0 (4.3)	-
COMBINED DATA									
Strength (ksi)		63.6 (2.6)	Pass		Could not pool data	NA		69.2 (4.4)	Pass
HXL-H12-GRC									
Strength (ksi)		64.6 (2.3)	Pass		66.0 (2.8)	Pass		69.2 (6.9)	Pass
HXL-H12-LaRC									
Strength (ksi)		63.6 (2.8)	Pass		62.4 (1.8)	Pass		69.0 (2.4)	Pass
HXL-H12-MSFC									
Strength (ksi)		62.6 (2.2)	Pass		64.1 (2.6)	Pass		69.4 (3.4)	Pass

Table 18. Open-hole compression data.

Panel [45/0/-45/90]3s	CTD			RTD			ETW		
	Raw Data (CV)	Normalized Data	Pass/Fail	Raw Data (CV)	Normalized Data	Pass/ Fail	Raw Data (CV)	Normalized Data	Pass/Fail
NCAMP Database	-	-	-	-	-	-	-	-	-
Strength (ksi)	-	-	-	-	49.1 (3.7)	NA	-	35.5 (4.1)	-
COMBINED DATA									
Strength (ksi)	-	-	-	-	46.9 (2.8)	Fail	-	32.5 (2.9)	Fail
HXL-H12-GRC									
Strength (ksi)	-	-	-	-	45.8 (2.1)	Fail (1.1%)	-	31.8 (1.4)	Fail (5.1%)
HXL-H12-LaRC									
Strength (ksi)	-	-	-	-	47.1 (2.9)	Pass	-	32.2 (2.4)	Fail (4.8%)
HXL-H12-MSFC									
Strength (ksi)	-	-	-		47.5 (3.7)	Pass	-	33.2 (2.7)	Fail (1.9%)

NIAR characterized a failure as mild if the percent fail is $\leq 4\%$ for modulus and $\leq 5\%$ for strength. The majority of failures observed in this study would be considered mild. The Glenn open-hole compression (OHC)/ETW coupons had a percentage failure of 5.1%, which is characterized as a mild to moderate failure. Although generally mild, the failures in the equivalency test matrix are addressed below.

The tests that failed were the (1) unnotched compression modulus at elevated temperature, (2) short beam shear (SBS) at elevated temperature, and (3) open-hole compression. The failure in unnotched compression was due to a modulus value that exceeded the database value. A higher value is not an issue.

The SBS and OHC failures are likely related to the variation of the matrix resin, as predicted by the vendor.

The NIAR statistical report, which includes the ANOVA analysis, is presented as appendix B. The report includes data for GRC-generated coupons labeled as (1) slow ramp and (2) low vacuum. The low vacuum coupons are mislabeled and should read ‘low pressure.’ These coupons were tested to represent realistic manufacturing conditions of the STA. The mass of the STA $\frac{1}{8}$ arc segment would likely slow the part ramp temperature to less than the $2\text{ }^{\circ}\text{F}/\text{min}$ used to generate equivalency data. The ‘slow-ramp’ coupons were generated using a $0.5\text{ }^{\circ}\text{F}/\text{min}$ ramp rate. In addition, the pressure on the sandwich panel facesheet will be in the range of 45 psi, as opposed to the 100 psi used to manufacture the equivalency panels, and this condition is represented by the ‘low vacuum (pressure)’ coupons. As these coupons were outside the scope of the equivalency matrix, they were not included in the above tables.

2.6 Safety and Mission Assurance

The CEUS and later Composites for the Universal Stage Adapter 2 (CUSA2), and later the SMA effort, was an initiative including multiple NASA Centers. MSFC led a collaborative bimonthly discussion between LaRC, GRC, and Goddard Space Flight Center (GSFC). The collaboration provided a synergistic opportunity for the Centers to compare and choose the best path between respective Center quality plans and best practices.

Project deliverables, e.g., SMA and test plans, were generated in support of the CEUS-CUSA2 project plan to advance the technology readiness level (TRL) (see app. C) of composites for launch vehicles from TRL 5 to TRL 6, initially planned to complete in time for the EUS preliminary design review (PDR) and potential infusion onto the SLS. Additionally, a qualification path leading to potential human-rating certification requirements for composites was proposed as a key deliverable, but the project was cancelled before its completion. In fulfillment of the CEUS-CUSA2 SMA requirements before its cancellation, input was provided in the “Processes for Storage and Handling of Prepreg Including Guidelines for Receiving Inspection and Re-Qualification of Carbon Fiber/Epoxy Prepreg Materials” led by the GRC CEUS-CUSA2 material lead. GRC SMA developed a ‘quality engineering and assurance checklist’ for the coupon testing scheduled to be performed. Either the SMA lead or a delegate, reviewed the CEUS-CUSA2 requirements. Receiving inspections were performed at delivery.

The MSFC Science and Mission Systems Assurance Branch (QD22) prepared both the SMA and Mishap plans to define the Industrial Safety and Quality Plan for the CEUS-CUSA2 project. The successful implementation of the SMA plan required a coordinated effort from all members of the CEUS-CUSA2 team involved in the proposed procurement, testing, handling, and storage of the CEUS-CUSA2 coupons, test panels, and static test articles. CEUS-CUSA2 test articles were developmental/nonflight; however, at one point, various configurations were proposed ranging from a USA2 prototype static test article to single test panels. The associated costs of these proposed configurations ranged from approximately \$20 million to \$50 million. SMA was prepared to meet the needs of the CEUS-CUSA2 project whichever path was chosen. The final configuration resided along the less expensive test article path.

The SMA lead coordinated the development of the SMA plan across the project and other Centers with the CEUS PM and CE. The SMA lead or quality assurance delegate(s) representing QD22 at each Center were responsible for specific duties and sharing applicable quality records on the CEUS-CUSA2 share site until the date of its cancellation. The duties were as follows:

- Witness testing activities.
- Verify that testing procedures were being followed.
- Verify test equipment and instrumentation calibration was up-to-date.
- Assure that necessary data were recorded and reported.
- Approve fabrication requests and manufacturing documents.
- Review calibration records and test procedure for testing performed through contract at the NIAR.

2.7 Computational/Model Based Materials

Composite laminate property allowable determination is a core effort for any composite structure development. Test programs are executed in a number of ways, including full test programs based on Composite Material Handbook-17 (CMH-17), with high costs and long execution time. Some programs opt to reuse past databases with no testing, such as when the prime contractor uses in-house, established databases. This is good when a plethora of data have been collected, and the same material and processes are used. Other programs might leverage published data with targeted testing to validate program specific design variants; the CEUS equivalency program is an example. All approaches have a common goal—establishing design allowables that can be used with confidence to predict the service life of composite structures. All of these methods rely on experimental approaches. New computing power and simulation capabilities are enabling finite element (FE) modeling down at the constituent levels, a new world into determining composites material allowability. This enables constituent material modeling to evaluate microscale material effects on the macroscale material response. This digital approach provides the opportunity to capture constituent material variability, process variables, and test variables—traditionally captured through testing multiple batches and many replicates—without all the testing.

2.7.1 Digimat (for CEUS)—Introduction

Digimat is a nonlinear, multiscale, material and structural modeling platform that allows for describing micro- and macro-level composite behavior and for bridging the gap between manufacturing and performance. A 1-year lease of the tool allows for evaluating the software capabilities that are in line with CEUS scopes during 2016. Digimat offers several tools and solution modules for several applications (fig. 11). The following is a brief description of each module:

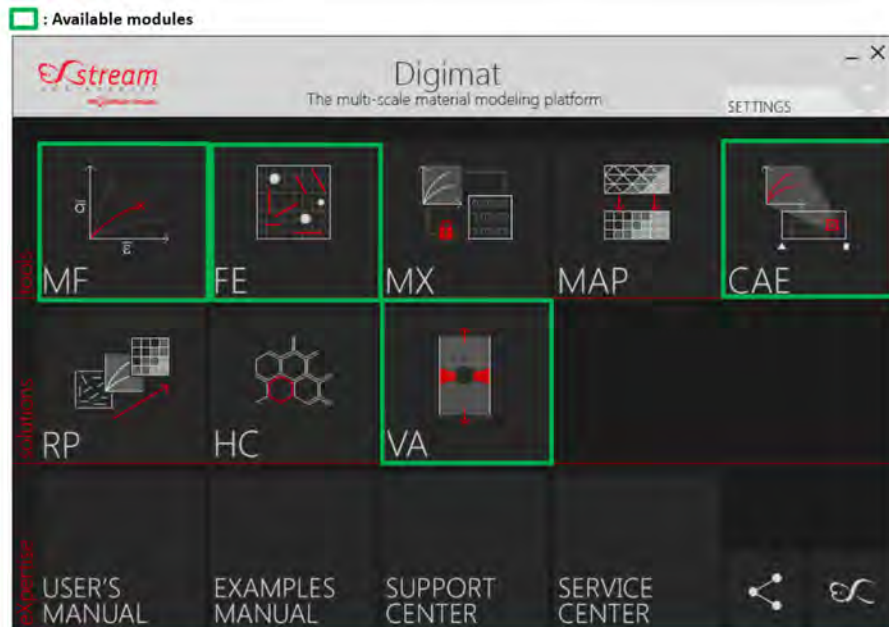


Figure 11. Digimat platform and available modulus at GSFC.

- Digimat-MF: Computes the macroscopic performance of composite materials from their per-phase properties and microstructure definition.
- Digimat-FE: Microscopic level FE approach to obtain an in-depth view into the composite material by the direct investigation of representative volume elements (RVEs).
- Digimat-VA: Computes, instead of tests, the behavior of composite coupons to screen, select and compute allowables of composite materials.
- Digimat-CAE: Interface to finite element analysis (FEA) packages for structural analysis level.

As mentioned, at the CEUS, an objective was defined to demonstrate and validate the software capabilities. Some of the potential benefits of adapting this tool, after verification, are as follows:

- The capability of computing (instead of extensive testing) statistical basis material allowables:
 - Compare to CUSA material (equivalency) test data (established for analysis).
 - How does a Digimat computed B-Basis allowables (using 8552-1 limited test data) compared with the published 8552 B-Basis allowables?

- Being able to understand material properties' sensitivity to manufacturing processes, such as void content and fiber volume fraction:
 - How well the imperfection-affected properties computed by Digimat compare to the test data. (See demo 1.)
- Executing accelerated (instead of traditional) building block with virtual tests and reduce test matrices:
 - Using unnotched test data to statistically compute open-hole allowables.
- The possibility of efficient materials development across programs (cost and schedule), e.g., design the architecture of 3D woven composites for joint applications. (See demo 2.)

Demo Example 1: Using Digimat-FE, it is possible to create/design an RVE of the composite material of interest and compute the composite properties based on its constituent's properties. Figure 12 illustrates a simple process of creating an RVE, for a unitape material, and extracting the material in-plane and out-of-plane stiffness responses (E_{11} , E_{22} , and E_{33}) under an applied load.

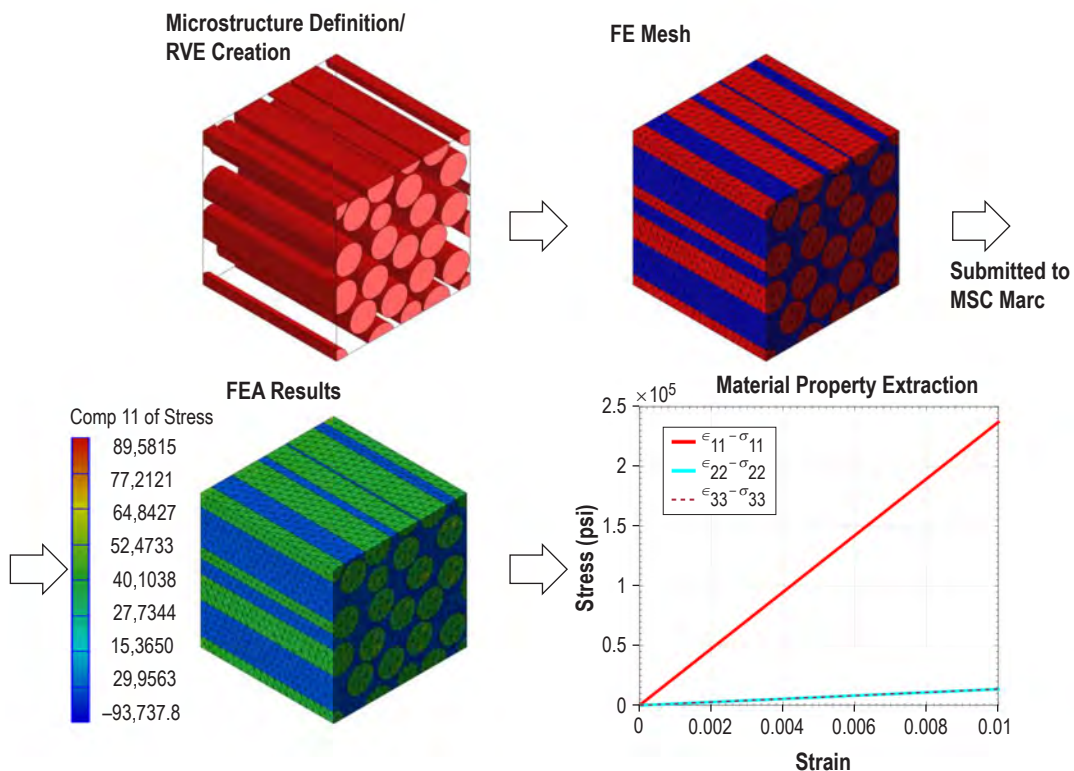


Figure 12. Design and material property computation of a unitape material.

Demo Example 2: Similar to example 1, a more complicated architecture can also be designed, and properties in different directions can be computed. Figures 13 and 14 show the design of a 3D woven RVE and FEA results for material property extractions, respectively. This is of interest to composite joint technology development activity where a preform joint material can be designed (i.e., going through a trade study) to meet predefined requirements, prior to procuring

materials and performing any testing. In this particular application, the design-adjustable parameters include: individual phase material properties, different materials for different phases, and fabric characteristics (e.g., number of warp/weft yarns, number of layers, weave steps, warp/weft/linker yarn, warp/weft yarn count, etc.).

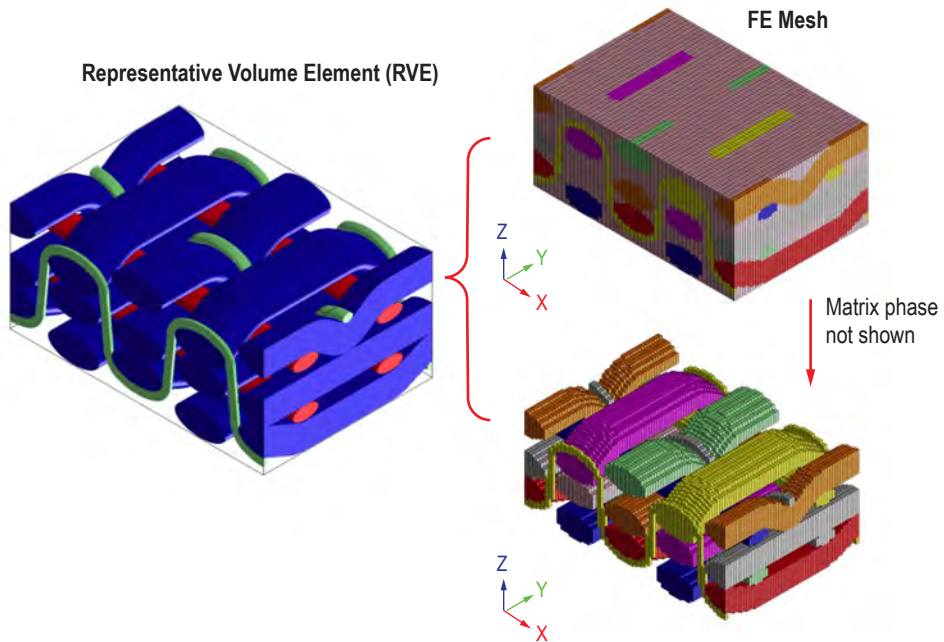


Figure 13. A 3D woven RVE creation and corresponding FE mesh.

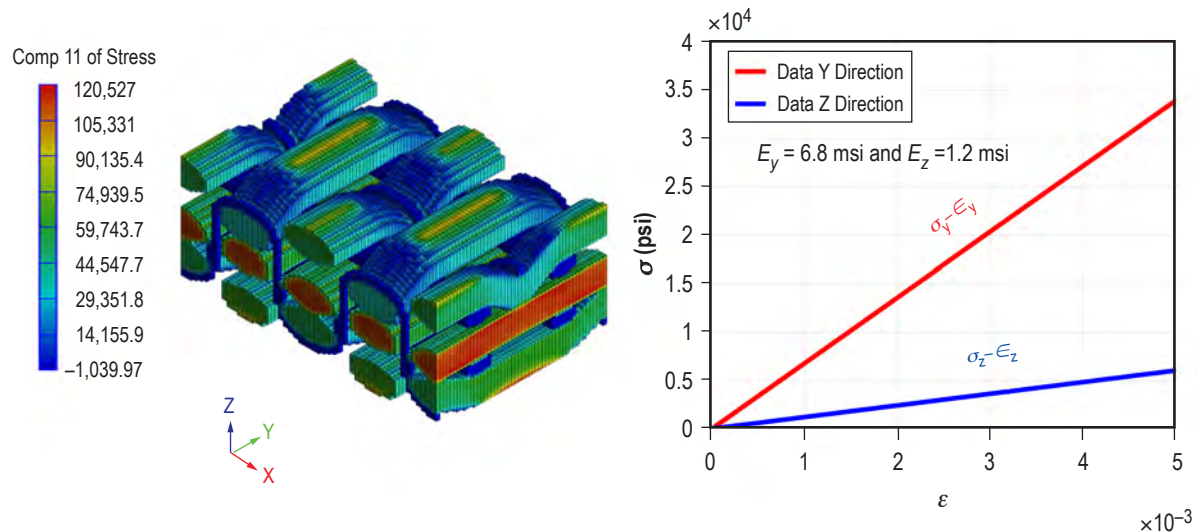


Figure 14. FEA results and property extraction for a 3D woven RVE.

2.8 Digimat Test Simulation

Digimat-VA makes it possible to reduce material property characterization test programs by taking advantage of virtual testing and virtual allowable computation. Instead of executing an extensive test program, a selected number of experiments can be performed, and results can be used to compute for the rest. Virtual test matrices can be created, and execution (through FE analysis) of the test matrix provide the selected material virtual allowables. The following general steps are needed to create and execute a virtual test program:

- Test matrix definition includes defining material, layups, type of test, and environmental conditions (fig. 15).

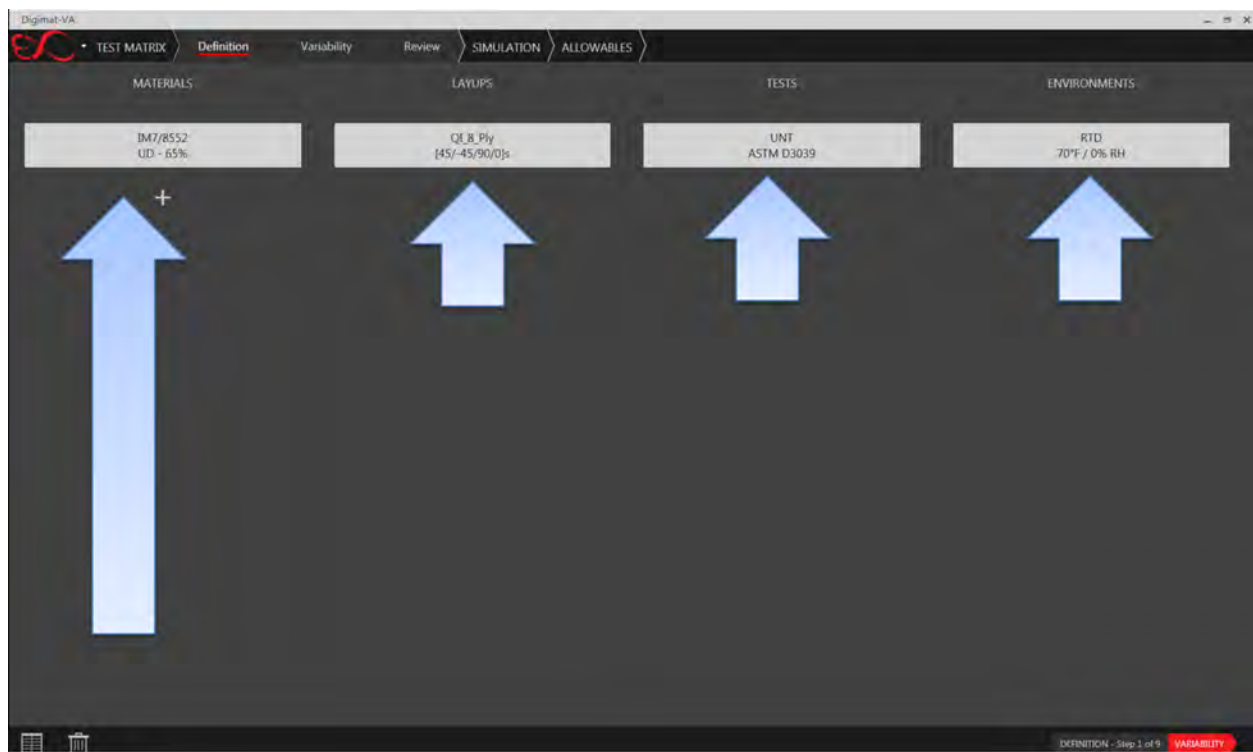


Figure 15. Test matrix definition.

- Test variability definition: includes a set of adjustable parameters that accounts for probable variabilities such as constituent variability, process variability, and testing variability (fig. 16).

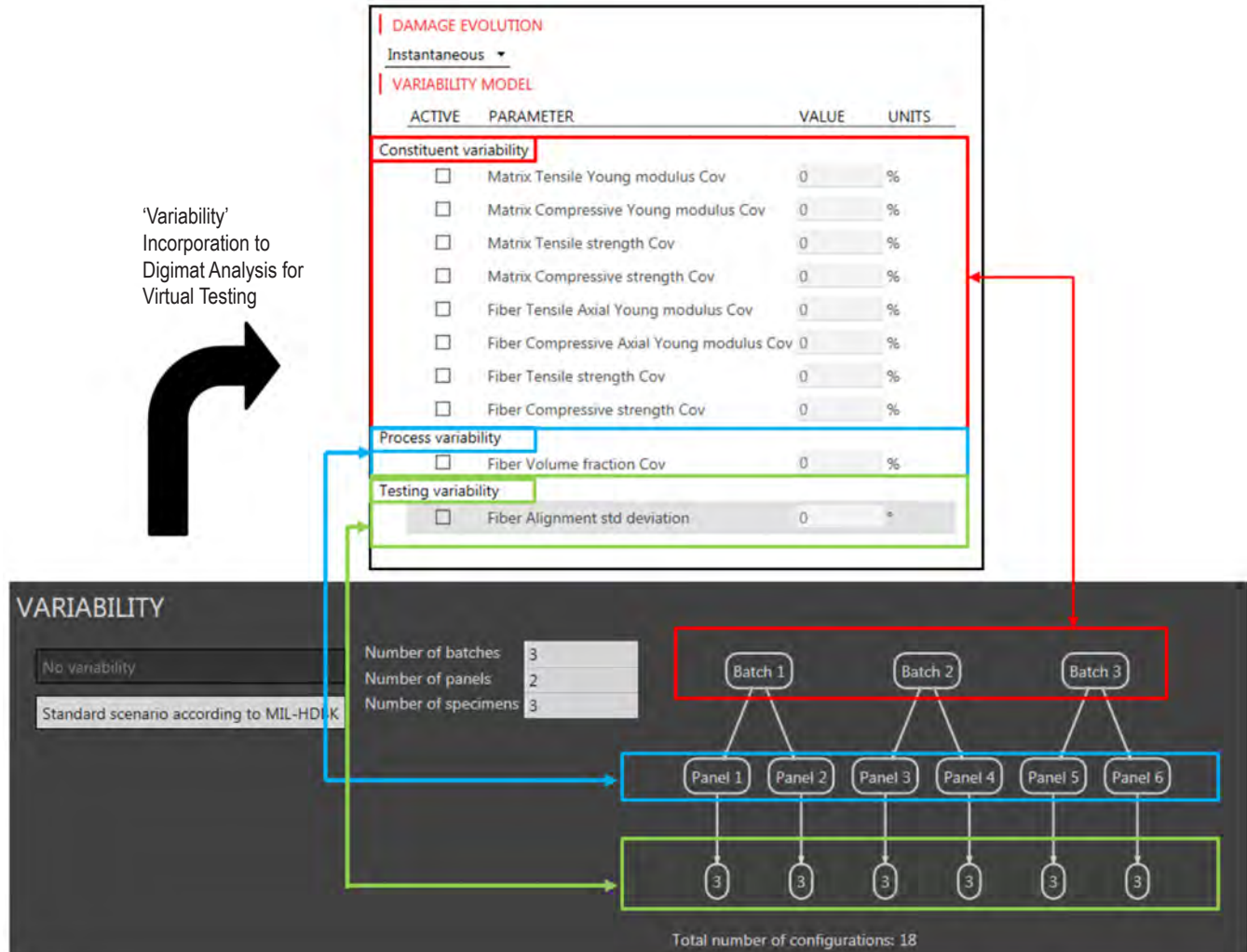


Figure 16. Test variability definition.

- Simulation and allowable computation: Based on the selected variabilities and type of ASTM test, each coupon is analyzed, and a family of allowables will be generated to calculate A- and B-basis allowable, etc. Figure 17 shows the selected variabilities and results for 18 virtual unnotched tension tests, and calculated allowable for IM7-8552 QI [45/-45/90/0]_S laminate.

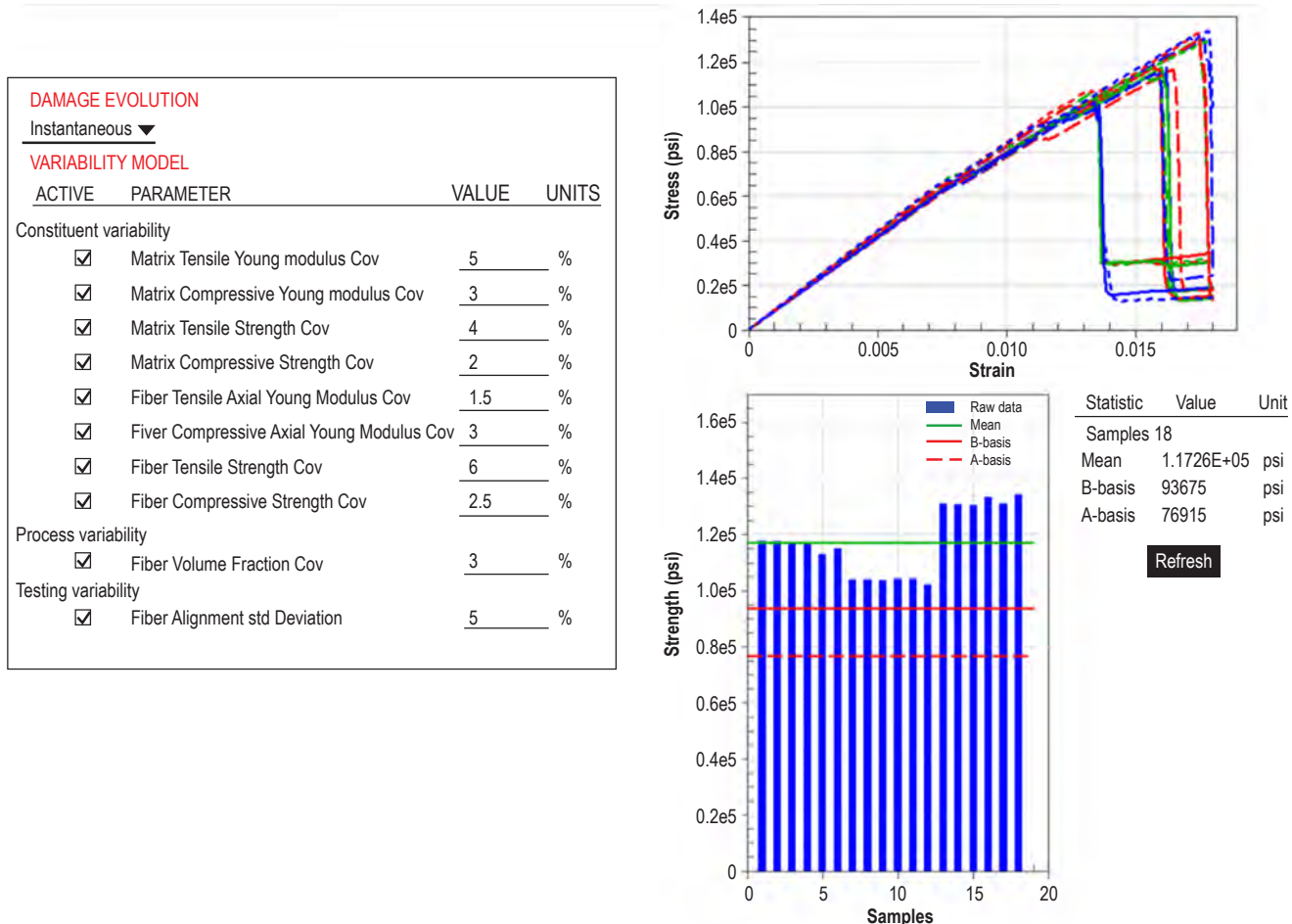


Figure 17. Simulation and allowable computation.

2.8.1 Computational Materials and CEUS Lifecycle

Materials can change over a lifetime of service. The allowables derived from testing during the program inception, as well as derived from ASTM flat panel specimens in the small scale, do not necessarily represent the final part. How the part was made and what the environmental exposures were during storage, testing, and loading can all influence properties. The CEUS computational material plan was to validate the software and collect relevant data during the development lifecycle for an ‘as-built’ structure for evaluation. The as-built data were to include constituent material properties variations in modulus and strength, fiber volumes, and void content of individually built parts. This was to include tool-side and bag-side facesheets for each panel.

After manufacturing, environmental exposure would be captured for material updates. These data points were to provide the basis to adjust composite facesheet material properties in Digimat. The updated facesheet material properties applied to a given panel would be input to the structure model for as-built pretest analyses performance predictions. The as-built structure performance model would be used in conjunction with the initial analytical models with pristine material property to evaluate the structure test performance for comparison.

2.8.2 Verification Approach

In order to evaluate the fidelity of the adapted Digimat software, a verification plan, including a test program, was proposed and adopted. Figure 18 shows a complete verification plan with the following three linked phases: (1) Fiber and matrix testing with ‘lamina’-level property predictions and verifications, (2) lamina-level testing with laminate-level property predictions and verifications, and (3) laminate level testing and verifications. Test data generated within this project are presented in appendices A.1, A.2, and A.3.

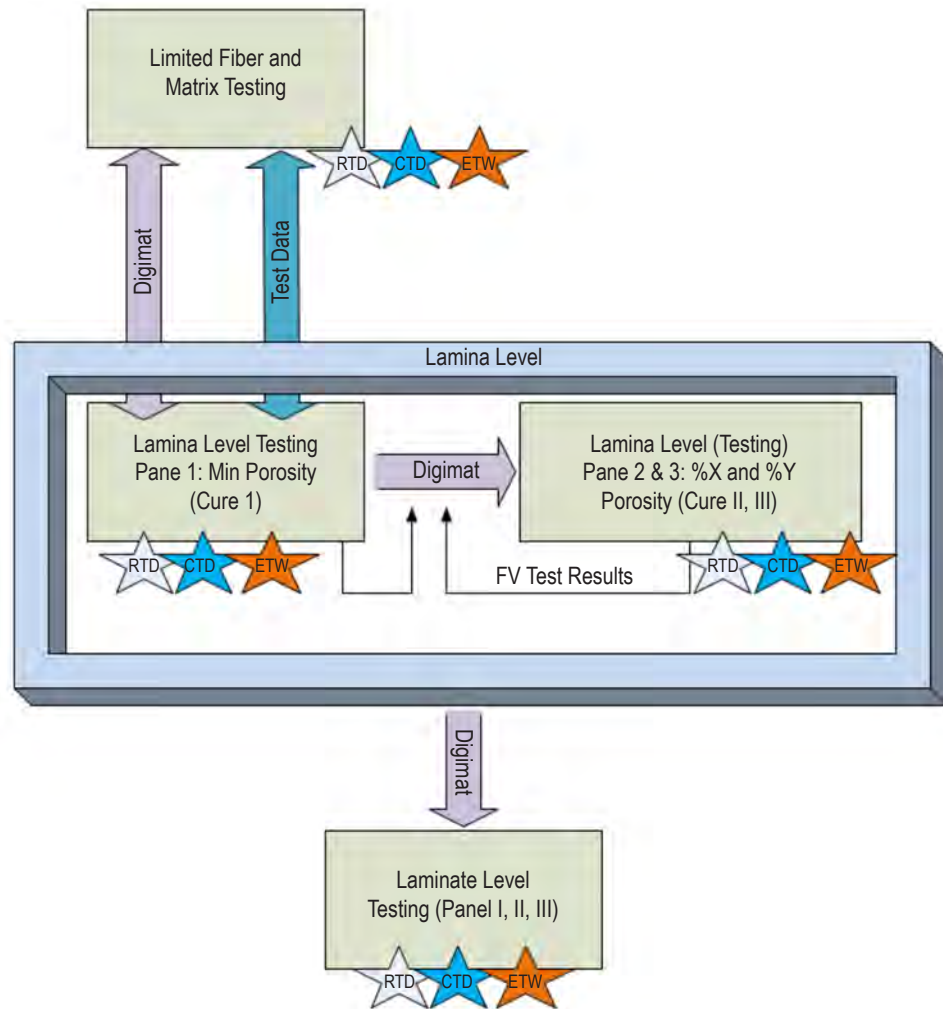


Figure 18. Digimat software verification approach.

The plan includes the verification in three different standard environmental conditions—RTD, CTD, and ETW. Characterizing constituents (i.e., fiber and matrix), separately allows for creation (Digimat modeling) of unitape lamina while parameters such as fiber volume (FV), void content, etc., can be accounted for and considered in subsequent analysis. Figure 19(a) shows an RVE with 60% fiber volume fraction, while figure 19(b) illustrates the same RVE with addition of 7% distributed porosity. The idea is to explore whether, for instance, using an input test data of a lamina/laminate with minimum level of porosity (fig. 19(a)) to Digimat along with characterized porosity level of another lamina/laminate (fig. 19(b), for instance) can be accurately predicted/computed.

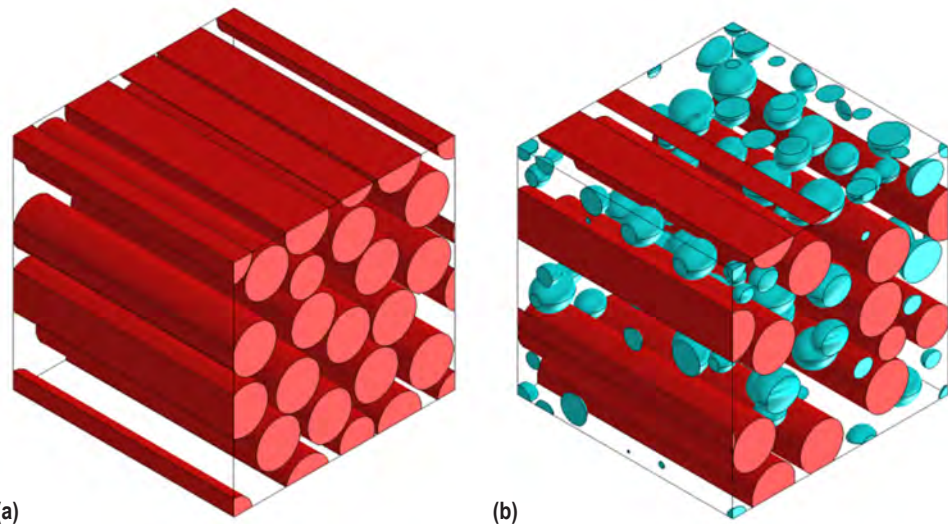


Figure 19. RVE: (a) With 60% FV and (b) with 60% FV and 7% void content.

Upon computation of properties of these RVEs, the results can be compared with lamina level test data for verification purposes. Prior to conducting the tests, coupons (or the parent panel) will undergo NDE to characterize the level of porosity and other imperfections.

The verification approach, as shown in figure 18, also scales up the validation approach to lamina and laminate levels where the test data of lower size scale will be used as an input for computing/predicting properties of the next higher size scale constituent. The higher size scale test data will then determine the fidelity of computation/prediction. The proposed complete verification plan entertains the above process using lamina and laminate IM7-8552-1 panels of three different porosity (cure) levels.

3. DESIGN

3.1 Composites for Exploration Upper Stage Skirt Design

The initial task for this project was to design, analyze, fabricate, and test two large-scale articles representative of the skirt structures for the EUS, the second stage of the SLS. These skirt structures are now referred to as adapters for clarity in differentiating the structures between the SLS Core Stage and the EUS. Initial concepts for the stage, as shown in figure 20, had a forward skirt approximately 10 ft tall, while the aft skirt was approximately 30 in tall.

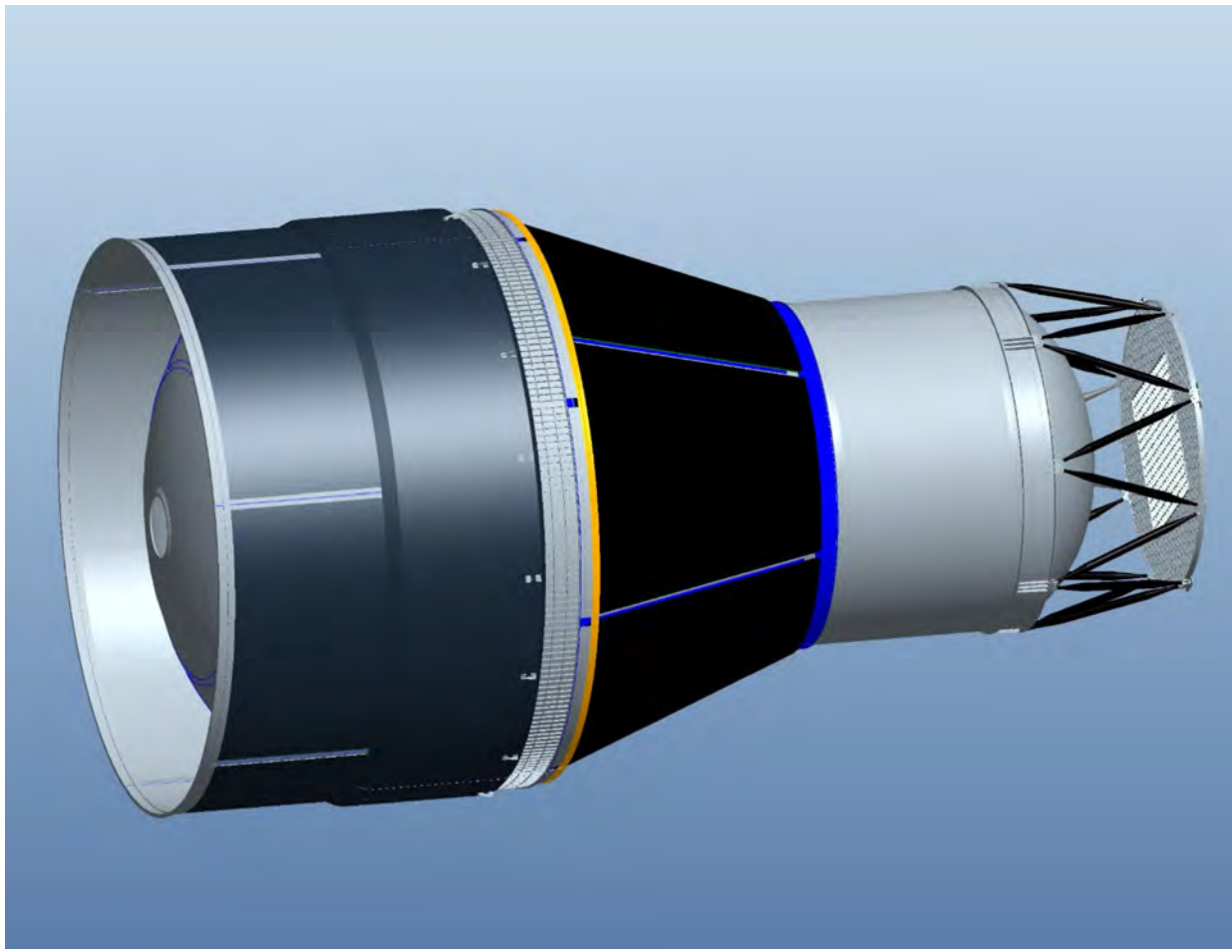


Figure 20. Early concept of a cryogenic Upper Stage for the SLS.

The launch vehicle skirt application poses an interesting challenge for composite structure. Composite structures used on launch vehicles typically utilize metallic end rings to join to the adjacent component. This may be due to considerations of assembly/disassembly, tolerance/alignment, or stiffness. Because of shrinkage at the cryogenic tank interface, the joint was examined as to efficient methods to accommodate the mismatch. The design baseline was to use a mechanically-fastened aluminum flange that extended until the ambient purge temperatures were reached. Another innovative method was to look at the possibility of tow steering to tailor the effective coefficient of thermal expansion for the structure to more closely align with the hoop contraction witnessed by the LH₂ tank.

The aft skirt, in addition to having the same thermal considerations, also had the challenge of interfacing with the structure used to provide the structural interface between the suspended LOX tank and the vehicle OML. This structure delivered out-of-plane loading at locations in the acreage area of the skirt. This would have required significant local reinforcement. Attaching the intertank, or mid-body, type of structure to the aft flange may have been an option to alleviate the imparting of loads in the skirt acreage.

Prior to the SRR for the CEUS, a systems design review was conducted for the EUS. This brought about a major change to the hardware being targeted for composite implementation. The forward and aft skirts were brought to a uniform height of 70 in. While this improved the application for the aft skirt, the loss of 50 in of height for the forward skirt meant that the metallic interface to the tank was a greater percentage of the overall mass of the structure. Due to the integrated SLS vehicle baselining this change, these criteria were adopted for the CEUS activity. This simplified the analysis activity that was being conducted in support of the wall construction trade outlined in section 3.2. Essentially, the higher loads for the aft skirt could then be used as the driving design loads for the trade.

3.2 Wall Construction Trade Study

The wall construction trade study was conducted to assess whether the architecture would be optimal for the EUS skirts. A key criteria, assuming that any structure would be required to satisfy the requirements for structural qualification and material compatibility, is to minimize mass. Other factors must also be considered including cost and schedule to develop. The CEUS project thus undertook a trade with a planned completion date shortly after the SRR was to be conducted. Figure 21 is a slide from the summary charts for the trade indicating the criteria used to assess the options. The analysis for the wall construction trade is detailed in section 4, Joints and Analysis.

Composites for Exploration Upper Stage

CEUS-TRADE-001



- **Objective of trade**

- Establish the appropriate wall construction type for a composite skirt structural test article designed to launch vehicle requirements (standards and environments). Potential candidates include sandwich (aluminum honeycomb, corrugated composite core and foam core) and skin stringer (blade or hat stiffened) options.

- **Criteria**

- Mass Savings
- Heat Leak
- Cost
- Schedule
- Manufacturability
- Inspection
- Damage Tolerance
- Integration of Late Hardware Changes

Figure 21. Composites for Upper Exploration Stage CEUS-TRADE-001.

Considered in the trade were sandwich-type wall constructions, including both honeycomb and foam-reinforced sandwich, as well as stringer-stiffened configurations. The composite material selected was a commercially available, toughened carbon/epoxy. The properties for the composite were extracted from existing databases and assumed an autoclave curing process. Schedule and cost were judged relative to the CEUS project constraints and possibly more limited than an architecture trade for a structure with a one-to-one payload ratio. Cost and schedule thus eliminated all skin-stringer variants for the STA for the CEUS project, due to the process development required for the manual fabrication process.

A concern regarding agency polymer matrix composite development efforts is that each task may not fully utilize the knowledge gained on prior NASA-funded composite projects. This may be more of an artifact of attempting to satisfy aggressive mass- and cost-savings goals for a particular structure, as opposed to heavy-weighting of commonality (e.g., wall construction, material, fabrication techniques, etc.) for a launch vehicle due to cost and schedule concerns. It is often contrasted to metallic hardware design, where it is assumed an alloy and construction (isogrid, orthogrid or hat-stiffened structure) are selected early in the program stages, leading to structural sizing and integrated design activities within months of design authorization. This may be true for applications where mass optimization is not required, but recent experience shows that for metallic structures, alloys and construction are still traded up to milestone reviews, primarily the PDR.

Because one of the challenges for composite structures was an efficient design process, one of the goals of this project was to utilize the previous studies to streamline the decision on what construction to utilize for the wall of the structure.

As stated, the trade space for the STA was reduced to selection of core material for a sandwich configuration. A Figure of Merit trade study was discussed, but the decision was made to use an alternate trade form utilized on the early SLS trades which was an advantages/disadvantages trade. In this trade form, the metrics that can be calculated or estimated are reported and then items such as manufacturability, inspectability, or integration of late hardware changes were discussed without assigning a comparative numeric value.

Honeycomb core and foam core structures are both utilized in the aerospace industry, thus indicating that both construction configurations have been manufactured and inspected. For manufacturability, while the two cores are utilized by industry, foam core was preferred over aluminum honeycomb. The rationale is listed in table 19.

Table 19. OHT data.

Foam Core	Core used on Delta IV for most all 5-m dry structure. Extensively used by transportation, energy, medical, and architectural industry for lightweight stiffness driver structures. Fabrication requires relatively simple tooling. May require additional step to dry foam before lamination process and seal exposed core immediately. This construction method is the baseline for the established CEUS budget and schedule.
Al Honeycomb	Extensively used by industry for launch vehicle dry structure fabrication. Lower density core is more prone to damage from handling. Dimpling and ply waviness will occur in piles adjacent to core unless skins are precured. Specific core splice methods are part specific, vendor proprietary, and will require process development to establish a reliable/repeatable core splice application method. Selecting this construction method will exceed the CEUS established schedule.

As listed, any potential advantages of heat leak for one configuration over another was deemed an important criterion for wall-construction selection. The mass savings realized by utilizing composites could thus be enhanced by a reduction in boil-off of hydrogen for on-orbit applications. The Thermal Analysis & Control Branch at MSFC utilized Thermal Desktop to perform a heat leak comparison. The analysis indicated that heat leak during on-pad and ascent may exceed the metallic baseline if a surface treatment was not utilized. On-orbit calculations did indicate potential benefit for composite structures, but at the fidelity of the trade, it was recommended that the foam and aluminum core numbers were within a range that was close enough as to state that heat leak should not be used as a discriminator for core selection.

Damage susceptibility and repairability were criteria assessed in previous trade studies, including the Composite Payload Fairing Structural Architecture Assessment and Selection documented by Krivanek and Yount.⁹ That trade study rated damage tolerance equivalent for honeycomb and foam sandwich structures but did indicate that foam sandwich structures were less susceptible to fabrication defects. The Lightweight Spacecraft Structures & Materials (LSSM) project report entitled, “Ares V Interstage Structural Concepts Down Select Process and Results,” also indicated that, from a damage tolerance perspective, foam and honeycomb sandwich were equivalent. This report also rated the two cores as being equivalent from a repairability standpoint.

Inspection capability was also acknowledged as a key component for composite structures. MSFC Non-Destructive Evaluation personnel provided the assessments in table 20 with consultation from other Agency personnel. From this aspect, aluminum honeycomb possessed an advantage over foam core.

Table 20. OHC data.

Al Honeycomb	Much more field experience than other candidate designs and proven methods exist that can be used right off the shelf. The aluminum provides a good contrast (attenuation) to voids (air).
Foam Core	The form core does not provide a good contrast (attenuation) to voids (air).

Discussion was held about the extensibility of the selection—whether or not the construction would be able to be utilized for structures on other parts of the vehicle, or for on-orbit application. This led to discussion of NASA-STD-6016, specifically section 4.2.6.2 which governs Sandwich Assemblies.¹⁰ Section 4.2.6.2.c. of NASA-STD-6016 states that perforated and moisture-absorbing cores shall not be used in sandwich assemblies. This indicated that a Material Usage Agreement would have to be obtained for whichever construction was selected. A previous Advanced Composites Technologies task had performed a moisture-absorption test. The composites for that particular study did not have any surface treatment on the skins. That study indicated that honeycomb sandwich would lead to less moisture update than the foam core tested.

Another area of extensibility considerations or its own unique criteria was response to vibro-acoustic loading. The previously referenced Composite Payload Fairing trade rated the foam core as possessing better performance as compared to honeycomb. However, the ratings were very close for the two core types.

Another consideration for the wall construction trade was the ability to incorporate penetration and secondary attachments. The Interstage Trade Phase 1 Down Select FOM results had rated honeycomb as preferable to foam core for this consideration. However, discussions for the CEUS project resulted in concurrence for the condition that the methods for local reinforcement were well understood for sandwich construction, regardless of core type.

The following schedule and cost impact differences were also considered for the trade:

- Each unique core segment will require a design model:
 - Element properties will be adjusted for different densities of cores.
- If the buildups are to the inside, this could require machining of the core, which increases in difficulty with decreasing density of core.
- Segment-to-segment honeycomb cell communication may require stints or slots of cores that require additional panels and coupons to demonstrate viability of method and any impact to properties.
- Methods of joining foam could require development.
- Ensuring proper conditioning of foam to obtain a successful core to facesheet bond could require development.

- Core splice of honeycomb could cause facesheet issues and requirement development panels
- Core dimpling of facesheets may require limited development to determine optimal cure pressure.

The Interstage trade had indicated the total cost for a foam core structure would be less than a honeycomb structure. However, for this project, both sandwich construction methods were determined to meet the cost and schedule constraints to produce a skirt STA.

One of the driving requirements from the CEUS Systems Requirements document states the assembly, including planned penetrations and interfaces, shall be at least 20% less massive than an analogous metallic skirt.

In the absence of meaningful differentiation between the sandwich configurations, this requirement was the driving factor in the recommendation to select the core type. The only mass data obtained during the wall construction trade, as outlined in the analysis section (sec. 4), was for a condition limited to one penetration. One of the concerns cited for composite structure implementation is that during preliminary sizing, activities composites offer significant weight advantages; but once penetrations and attachments are included, the mass savings are not as substantial as originally anticipated. Due to the limited time to conduct the wall trade and design as well as build and test a STA from the selected configuration, there exists some possibility that the mass growth of one configuration over the other could have brought the numbers within a range where factors, including cost and schedule, may have been influential in selection of the appropriate core type. However, this could not be assessed for this project; thus, honeycomb sandwich was selected as the wall configuration for the remainder of the STA activities on the project. Local reinforcement would be traded as the design matured as to utilize high-density aluminum core or potted aluminum core, or high-density foam core or inserts.

Additionally, it should be noted the Ares V Interstage report that had stiffened composite structure offers the potential to minimize mass for certain launch vehicle applications. During the timeframe of the Wall Construction trade and post SRR, it was assumed that a design could revisit other configurations for the skirts that may lead to optimal mass savings, but that exceeded CEUS program constraints.

3.3 Design Requirements for Structural Test Article

The method adopted for structures design tasks by the Structural & Mechanical Design Branch at MSFC is to have a document referred to as a design data sheet (DDS) that lists criteria that must be met for the structure. Other design activities have similar products, where the criteria for determining the design are listed in a design and analysis notebook. The formal documentation for the criteria will be the Engineering or Element Requirements documents and/or NASA standards invoked in the signed stress report that accompanies the release of the drawings or delivered at the product critical design review. Due to the desire of this activity to use the loads applicable to the actual EUS, the DDS is marked as an International Traffic in Arms Regulation (ITAR) document. Figure 22 is the cover sheet included with the document.

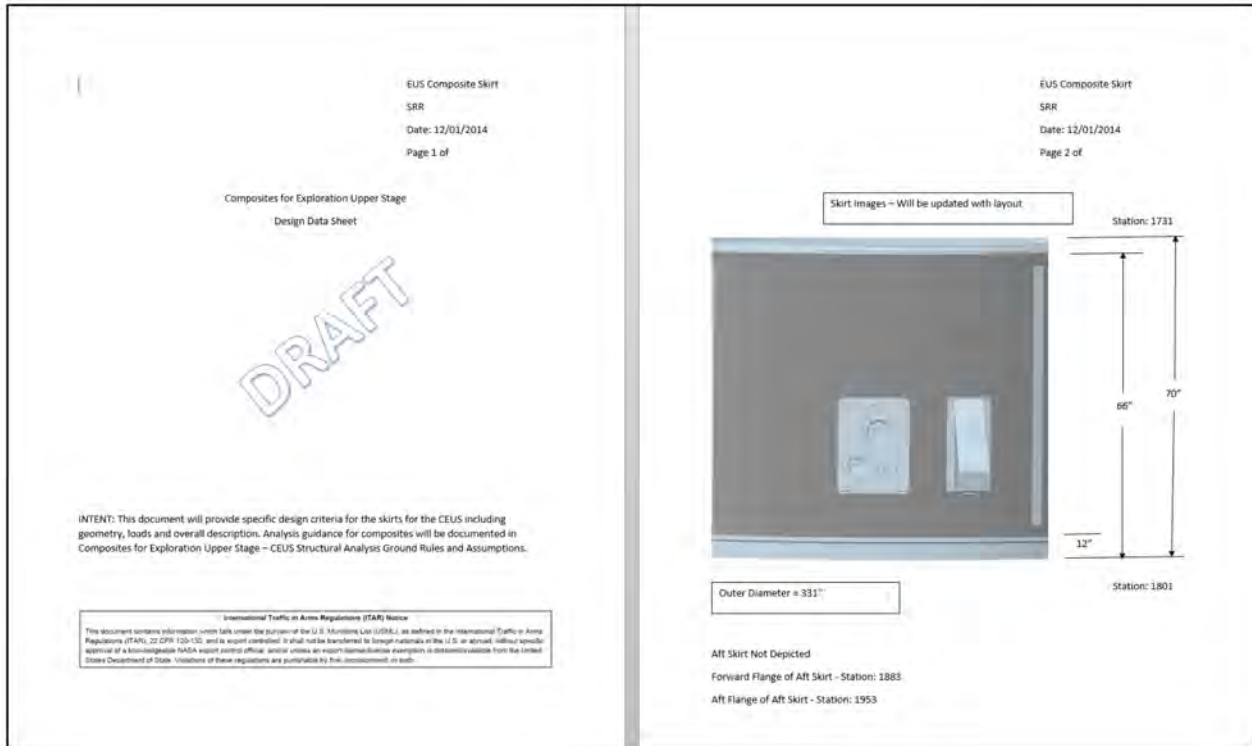


Figure 22. DDS for the forward skirt STA.

The method of configuration management for this project was to utilize a Microsoft SharePoint site hosted by MSFC with limited access folders to provide configuration control. This document, however, is a preliminary document and was thus kept in the design folder. Configuration management for the DDS was to be by listing the date at the end of file name to provide a means of version control. The DDS for the target application at the completion of the program are included in appendix D—Design. All of the loads and information that would render the document to be marked with ITAR have been removed.

3.4 Development of the Skirt Structural Test Article Layout

The flange-to-flange height for the skirt STA was assumed to be 70 in. The OML of the article was derived based on multiple criteria. First, the vertical leg of the metallic end rings was designed so that the centerline closely aligned with existing test simulator dimensions. From this constraint, the OML of the composite section was developed based on a thickness of core that would satisfy a load set that could be considered representative of vehicle loads for the targeted components. The OML was determined based on the honeycomb sandwich design as selected in the wall construction trade. Honeycomb core properties considered conducive to manufacturing were utilized in determining the thickness of the core.

Based on the CEUS-PROG-02—the assembly shall include interfaces representative of those in the SRR SLS/EUS baseline design, the following list of penetration and attachments were developed for the skirt STA layout:

- Forward skirt panel penetrations:
 - Umbilical plate (electrical, LH₂ vent/relief, purge).
 - LH₂ vents (two propulsive, two relief) (opening w/ gasket/seal).
 - Systems tunnel/panel.
 - Vents (if not provided by payload above), (opening w/ gasket/seal).
 - Cameras/fairings (mounting/cable penetration).
- Forward skirt panel secondary mounting/loads:
 - Flight computers (shelf-mounts).
 - Antenna (mounting).
 - Purge vent ducts.
 - Press line mounts.
 - Harness mounts.
 - Sensors (mounting/opening).
 - Ground support equipment hardware mounts.
- External interfaces:
 - Forward ring flange.
 - Aft ring flange.

It was decided that only the major penetrations would be represented in the STA. Secondary hardware was to be left to a decision of whether it was to be conducted on a panel level type test or assessed analytically. The STA layout (figs. 23 and 24), was thus generated as a baseline for detailed design to be initiated and to facilitate discussions with assembly fixture design and test hardware planning. The layout was distributed to the team through SharePoint.

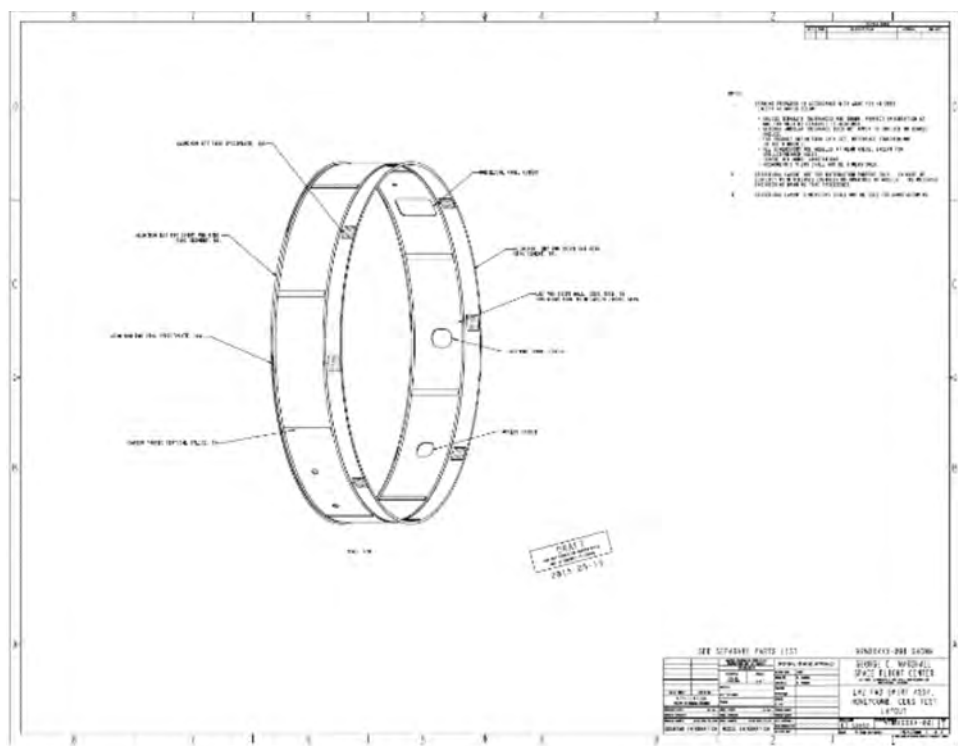


Figure 23. Forward skirt STA layout.

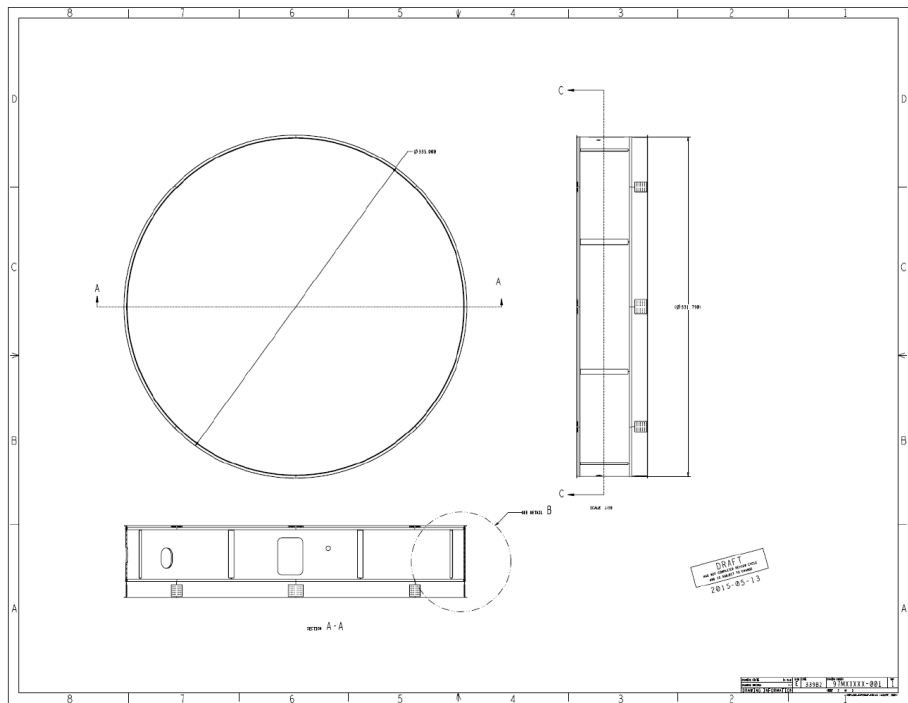


Figure 24. Forward skirt STA layout second angle.

3.5 Evaluation of Model Based Design Tools

One of the objectives for the CEUS was to examine efficiencies related to model based design. Model based design has many variations and can range from no production of 2D products, e.g., drawings, to an approach where models are controlled but drawings are still utilized for integration, communication to multiple disciplines, and as a basis for quality control or inspection. If the models are controlled, then they can be distributed to Analysis or Manufacturing, but a system must be in place to maintain configuration control if the models are modified from the original computer-aided design (CAD) format. A proposal for the definition of ‘model based’ for this project was presented to the MSFC Design Skill Leads as well as submitted to the CEUS project management. This definition, as included in the SRR package, was ‘the design model will be analyzed for producibility utilizing manufacturing simulations prior to design approval. The approved design model should also provide sufficient definition of ply geometry to ensure corresponding structural analyses can be iterated efficiently with a maturing design.’

3.5.1 Evaluation of Alternate Tools

The CAD software primarily utilized at NASA for hardware design is Creo from PTC. The companion product data management system Windchill has an instance for NASA specified as ICE Windchill. The configuration and data management processes for flight hardware development are based on this suite of tools and reflected in the corresponding quality instructions of the Agency. The standalone Creo tool, however, did not provide for manufacturing simulations of a composite article, nor did it provide an automated manner to address ply drops. For manufacturing simulations, the decision was made to use CGTech VERICUT for Composite Paths for engineering (VCPe), a companion software to the CGTech VERICUT VCP used to drive the automated fiber placement (AFP) robot possessed by both MSFC and LaRC. Fibersim, a CAD supplemental package supplied by Siemens, was utilized for ply drop definition and to facilitate manufacturing drawing generation.

In addition to the baseline suite of tools that required the VERICUT and Fibersim augmentations listed above, a fully integrated solution provided by Dassault Systèmes was evaluated. The functionality between the two toolsets was compared, and for this activity, the augmented PTC Creo capability was selected. This decision was based on the fact that flight hardware design processes at MSFC are currently being tailored to the PTC toolset and the familiarity of the NASA user community.

3.5.2 Approach to be Utilized to Enable Models to Serve as Basis From Design to Manufacturing

The following approach was established in order to meet the definition for model based approach for this project as defined in the SRR package. Models are generated using Creo CAD software (fig. 25). The Fibersim supplemental package is used within Creo to generate ply information, including definition of ply drop locations (fig. 26).



Figure 25. Creo model of tool surface.

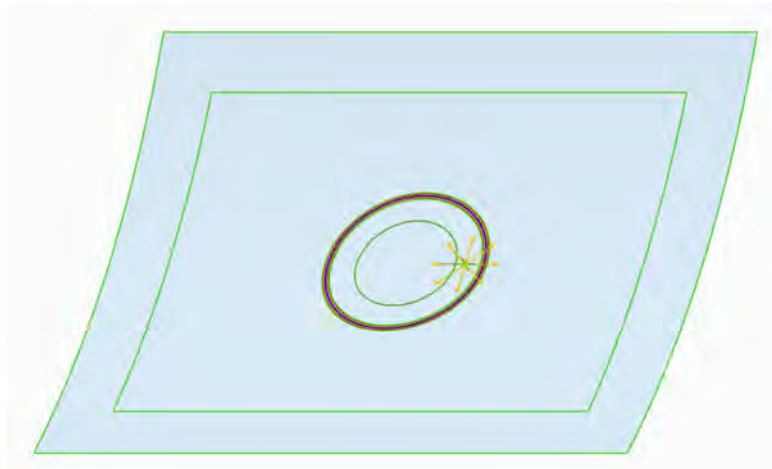


Figure 26. Fibersim is used to generate plies.

Fibersim generates cross sections of plies that can be used by the designer to visualize ply drops (fig. 27). Generated cross sections are also used in manufacturing drawings. The cross section is a drawing detail that is required to properly communicate the ply configuration by defining the boundaries for every ply dropoff or buildup area. Depending on the complexity of the design, cross-section views could take an extensive amount of time to generate manually using Creo without the Fibersim supplemental package. With Fibersim, the views can be generated in a matter of minutes. Furthermore, Fibersim is designed to allow ply definition and ply cross sections to be easily updated as the design evolves (fig. 28).

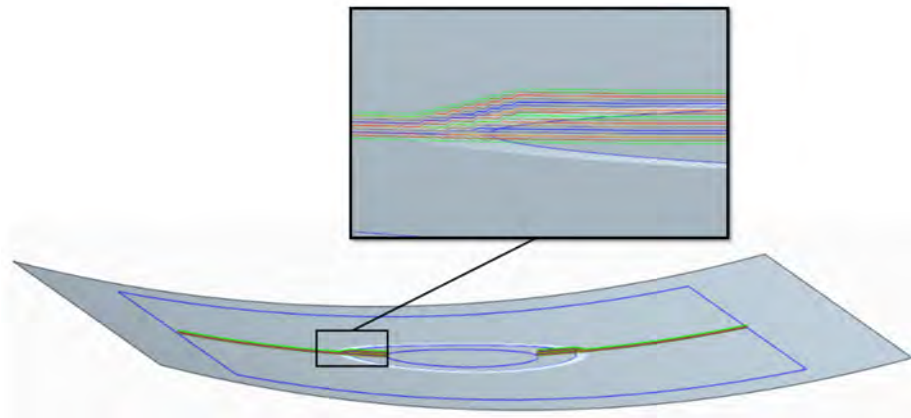


Figure 27. Fibersim generated 3D cross section of laminate showing interleaved plies.

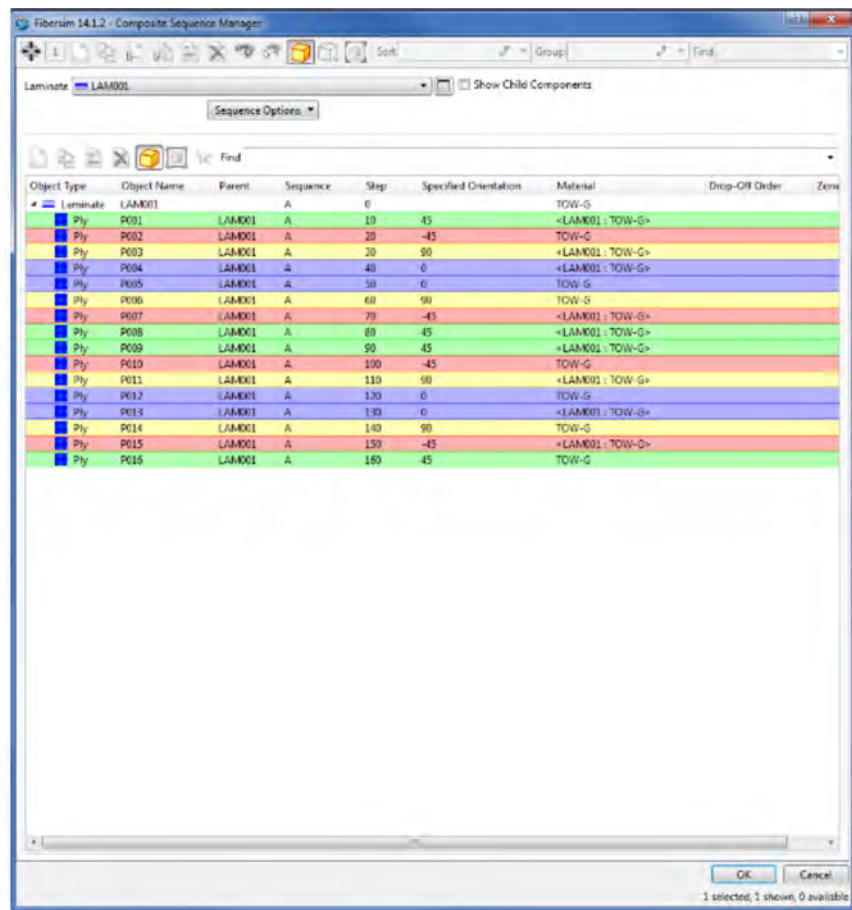


Figure 28. Fibersim has a ply sequence editor that allows the designer to easily edit the ply sequence.

When the design is finalized, the Creo model and the Fibersim ply data are used to generate manufacturing simulations to assess the manufacturability of the part. The Creo model and the Fibersim ply data are imported into VERICUT VCPe (fig. 29). Within VCS, the model and ply data are used to generate manufacturing simulations (fig. 30). That same information can be used in CGTech VERICUT VCP to generate course data for the AFP machine (fig. 31).

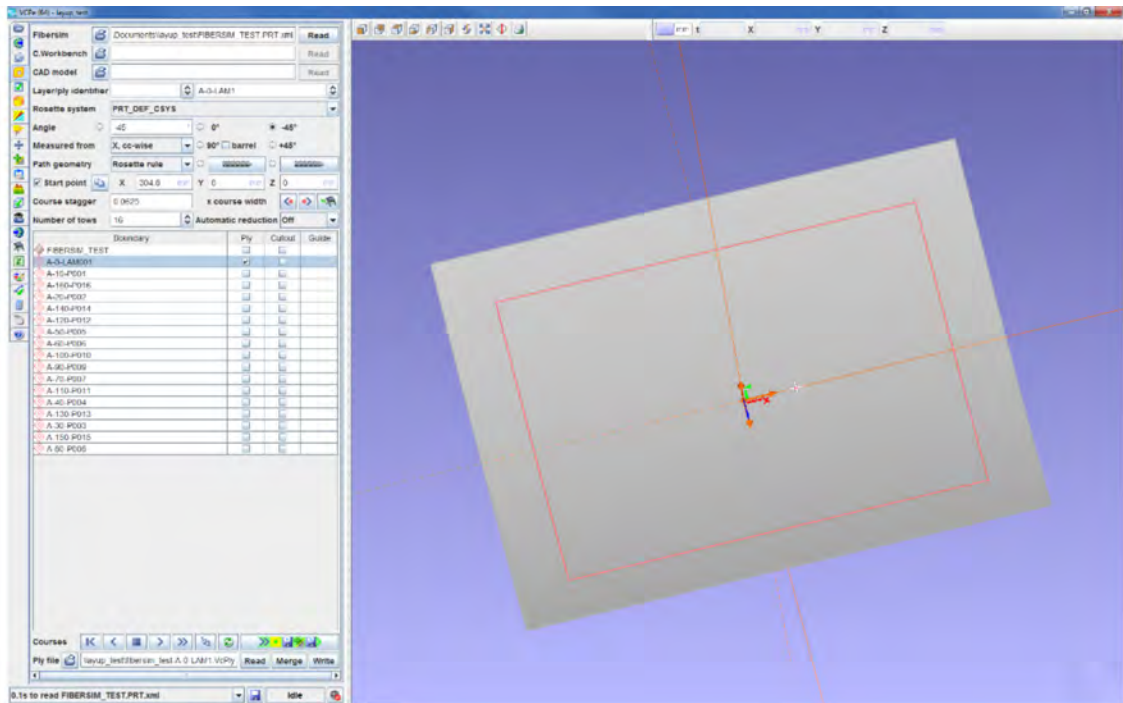


Figure 29. CGTech VERICUT VCPe with imported Creo model and Fibersim ply data.

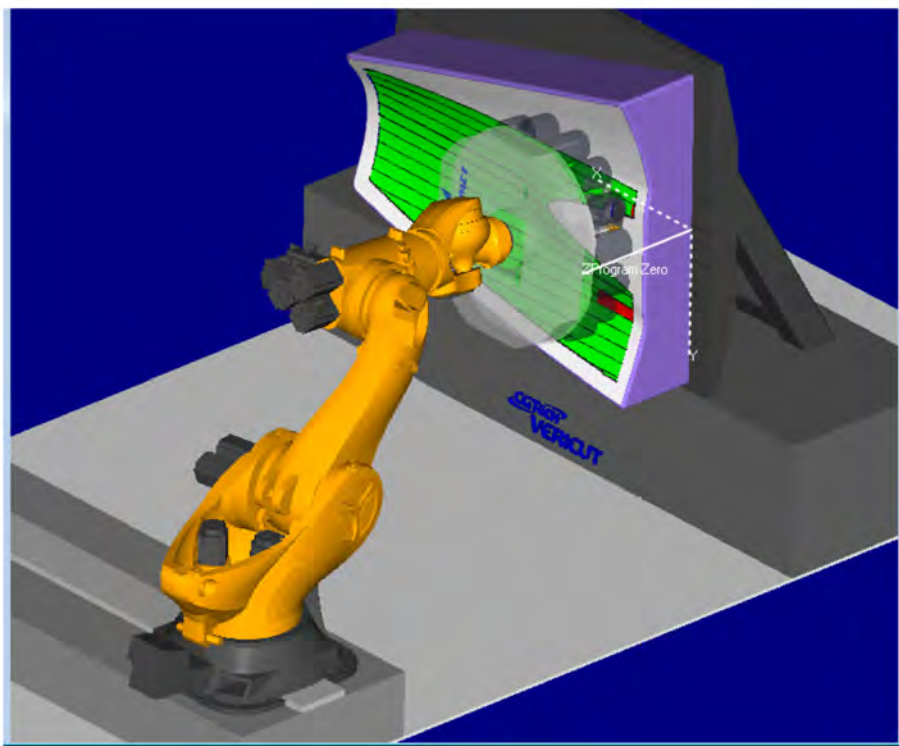


Figure 30. CGTech VCS manufacturing simulation.

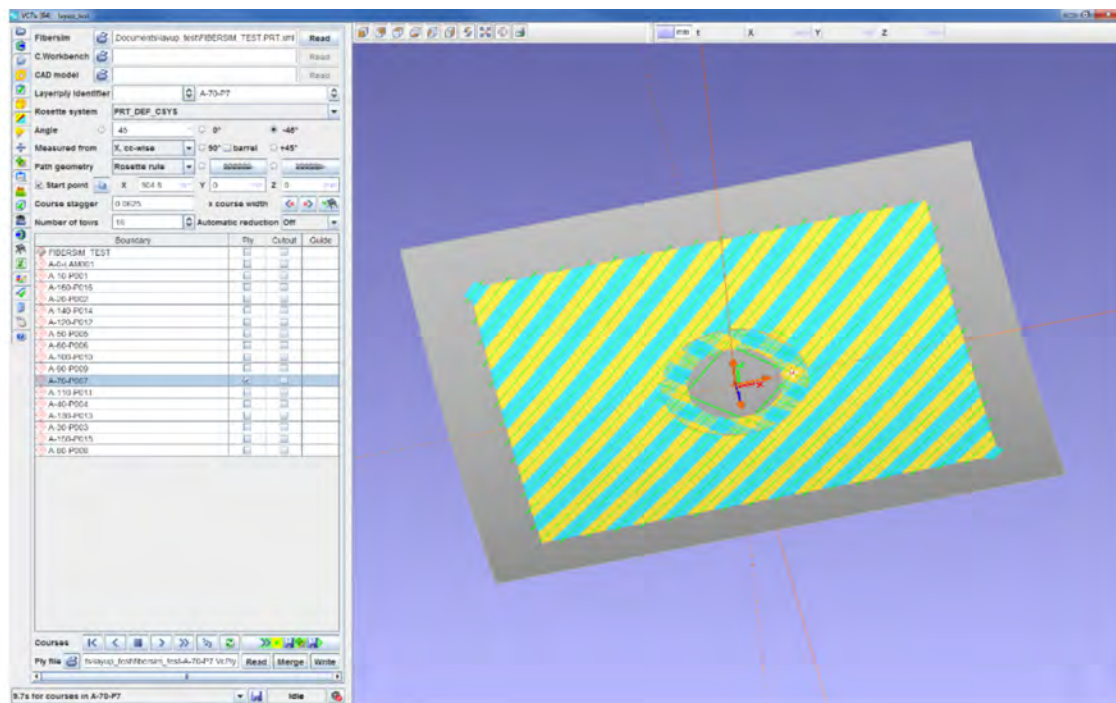


Figure 31. CGTech VERICUT VCPe-generated course data for AFP (reinforcement ply).

3.6 Composite Universal Stage Adapter

Upon completion of the CEUS skirt layout and prior to the detailed design progressing to the PDR, the project received direction to ensure that the products had extensibility for SLS hardware development. Due to budget and time limitations, panel test options for SLS hardware risk reduction were considered. However, it was decided to focus on the USA2, a structural component of the SLS forward of the EUS. The baseline USA2 design was sandwich composite with aluminum honeycomb core, and was divided into four cone-cylinder petals that were connected with metallic, vertical separation joints.

A trade study was conducted to determine the most applicable test within the budgetary constraints of the project. The scope of the trade extended from a STA that replicated the structure of a flight USA2 (with a slightly shortened barrel that would be constructed using the tool procured for the CEUS skirt) to testing a peta—a one-fourth section of the cone and cylinder. Also considered within the trade was a test of either just the conic or just the cylinder sections of the USA2. The configurations considered in the trade are shown in figure 32.

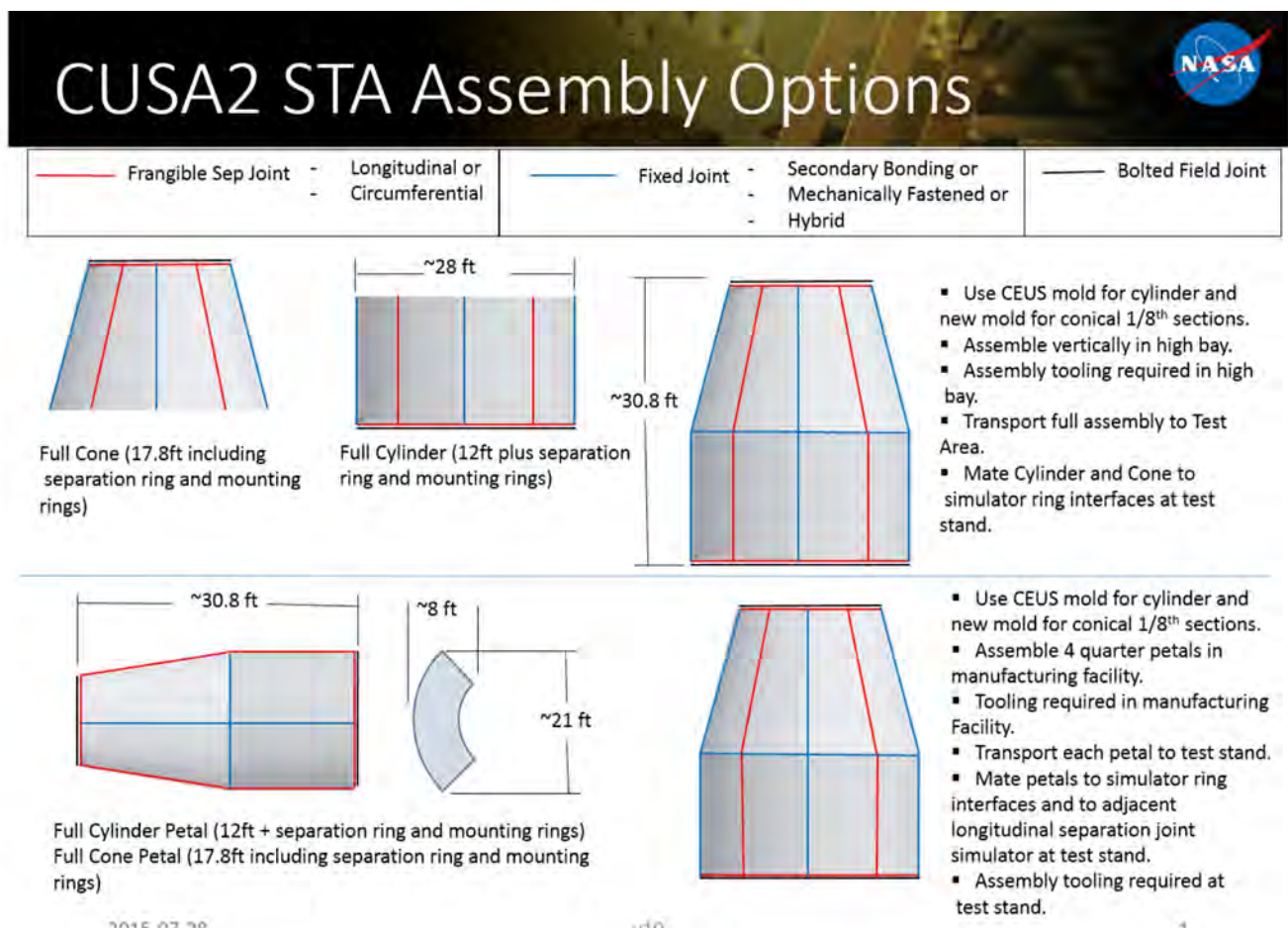


Figure 32. CUSA2 STA traded assembly options.

3.7 Structural Test Article

The trade for the USA2 had a comprehensive scope that led to the selection of a cylindrical test article utilizing the cylindrical tool already procured during the CEUS skirt section of the project. The CEUS had higher loads than the USA2, so the CEUS tool was designed for a thicker core than the USA2 required. This resulted in offsets of the neutral axis between the existing test simulators and the test article. The end rings had to be designed to account for this offset. The STA would be between 12 and 13 ft tall with an outer diameter, D , of 331.2 in, and it would include one 36-in penetration positioned at least $1D$ from the top of the panel. The STA would be constructed of eight sandwich composite panels to be joined with OOA, out-of-oven vertical joints. Excluding the metallic vertical separation joints from the STA reduced complexity. At the time of this decision, a trade was being conducted as to whether vertical separation joints were required for the flight USA2. The panels would have intermediate modulus/toughened epoxy facesheets bonded to an aluminum honeycomb core using epoxy. The metallic end rings would be a separable clevis design with eight segments joined together with splice plates. The STA would be manufactured using the AFP machine to lay up the facesheets of the eight panels. The panels would be placed in the autoclave to cure the facesheets. An assembly fixture would be used to support the formation of the OOA, out-of-oven vertical joints connecting the panels.

Dynetics was contracted to design the assembly fixture for the CUSA2 STA. Interface information was provided to Dynetics for the STA interface with the test simulators. Dynetics began to use this information to design an assembly fixture interface that would use the same bolt hole pattern as the test simulators. Figures 33 and 34 depict the drawing created to communicate this interface. (All ITAR information has been removed.)

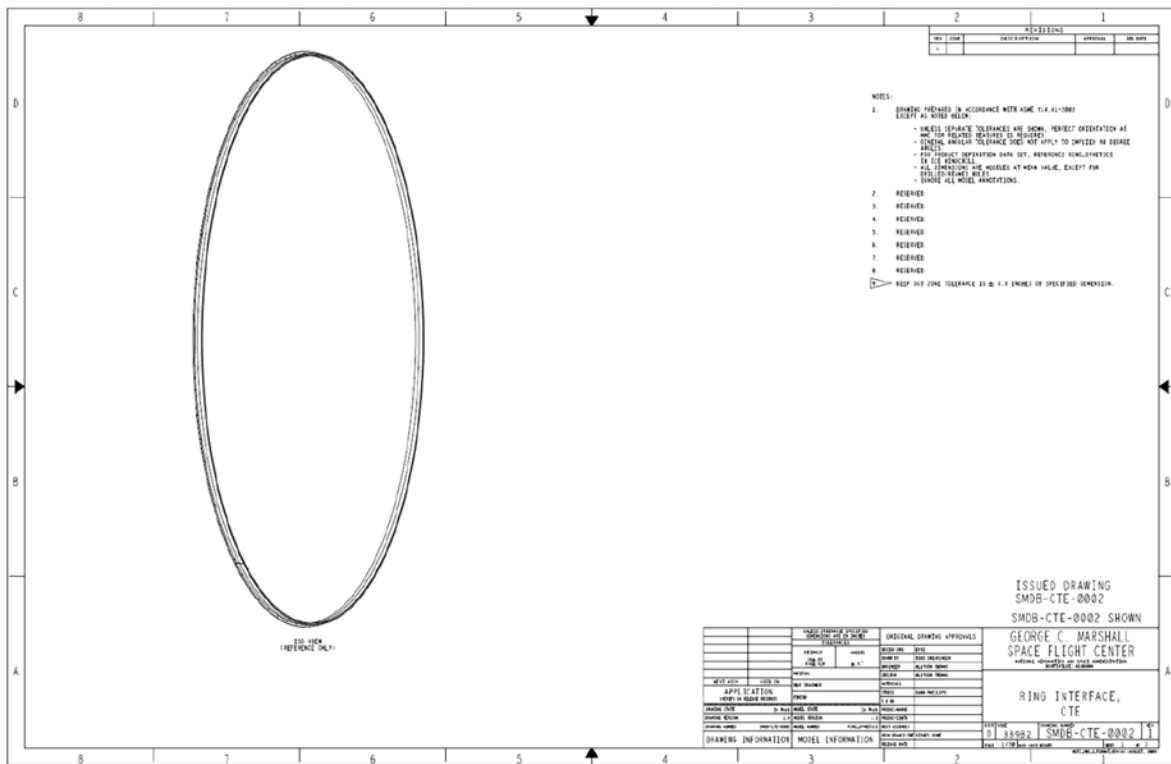


Figure 33. Interface definition for the STA assembly fixture (sheet 1).

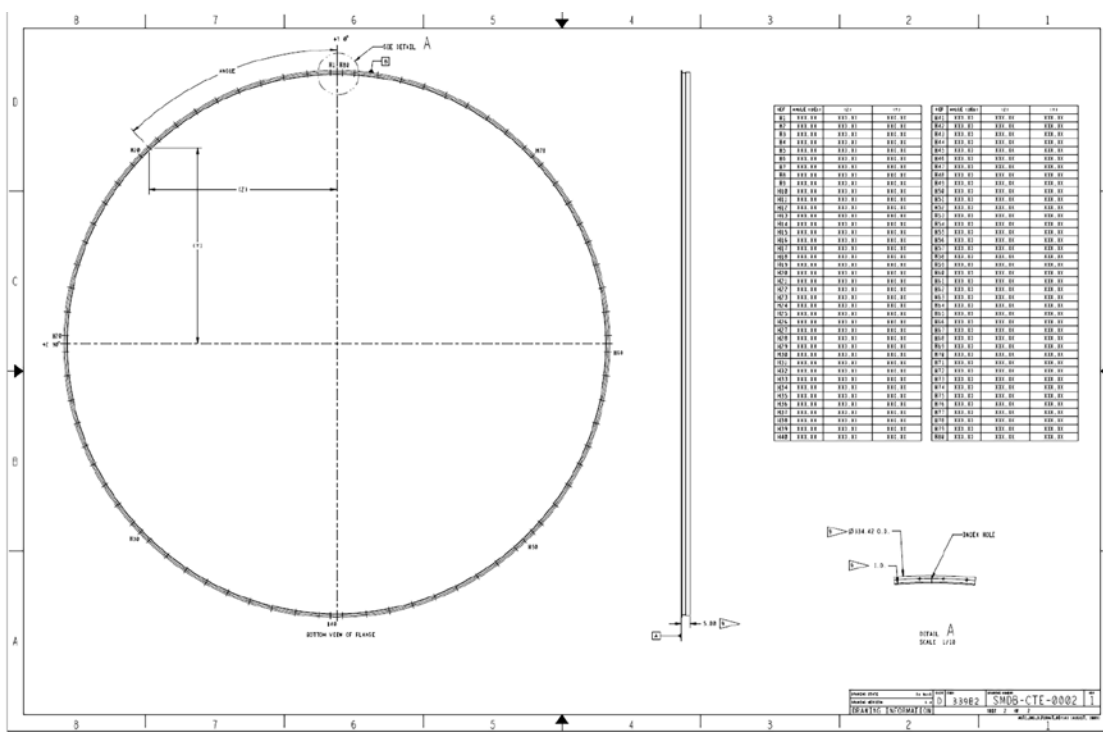


Figure 34. Interface definition for the STA assembly fixture (sheet 2).

To meet the requirement of testing the STA to a representative flight load case, the loads were reviewed for the DAC-0 Block 1B Cargo and Crew Configurations. An ascent load case was chosen for the STA to facilitate using the existing ET test simulators without structural modification. No burst or crush pressure loads would be tested because the complexity of pressurizing the test setup was a cost and schedule risk to the project. The test would be conducted at an ambient temperature. A DDS was generated for the STA that summarizes the material, construction, and load information. The geometry of the STA was defined in a layout drawing (shown in figs. 35–37). (All ITAR information has been removed.)

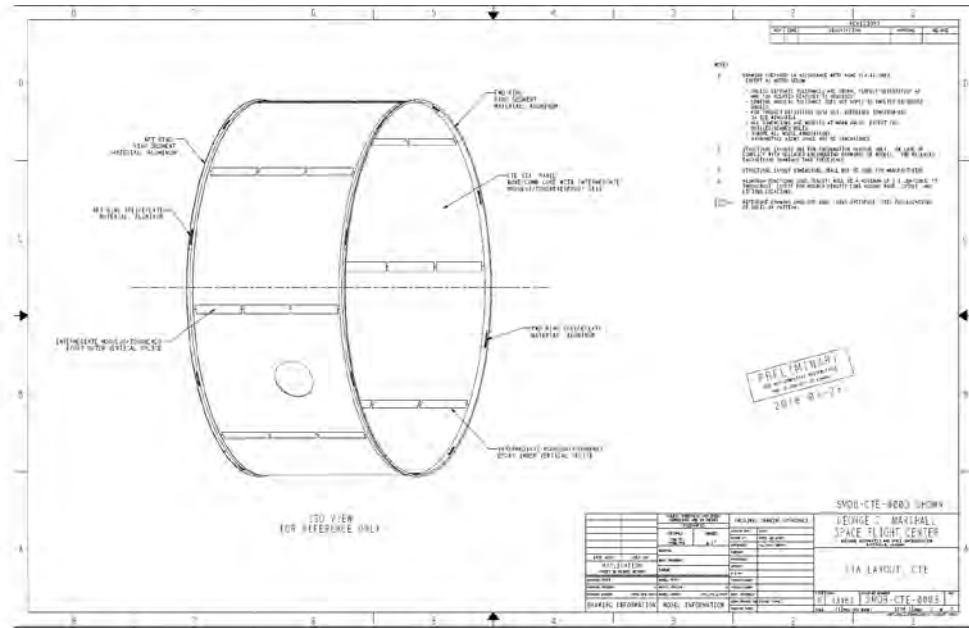


Figure 35. Layout drawing for the STA (sheet 1).

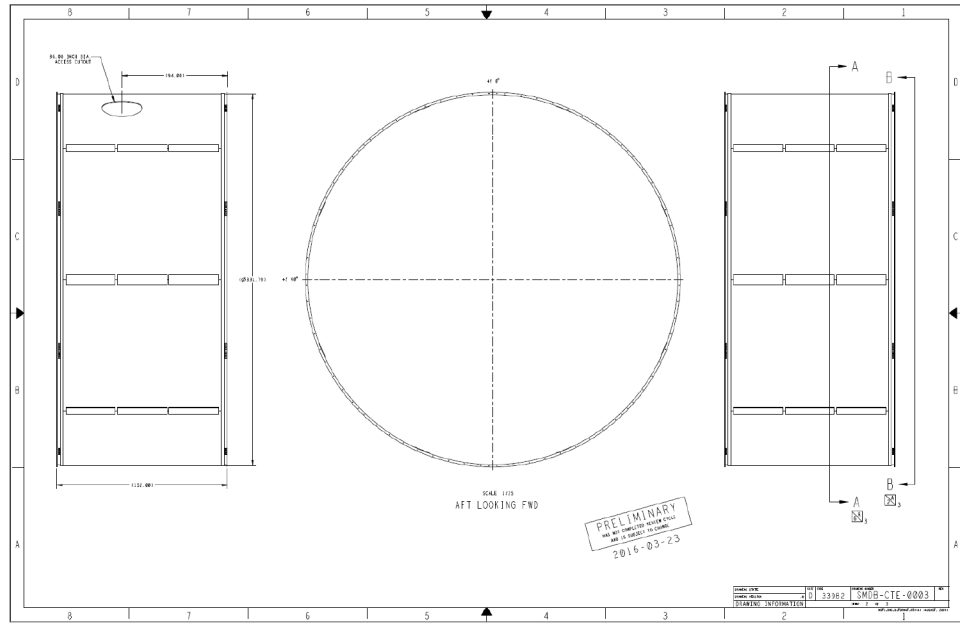


Figure 36. Layout drawing for the STA (sheet 2).

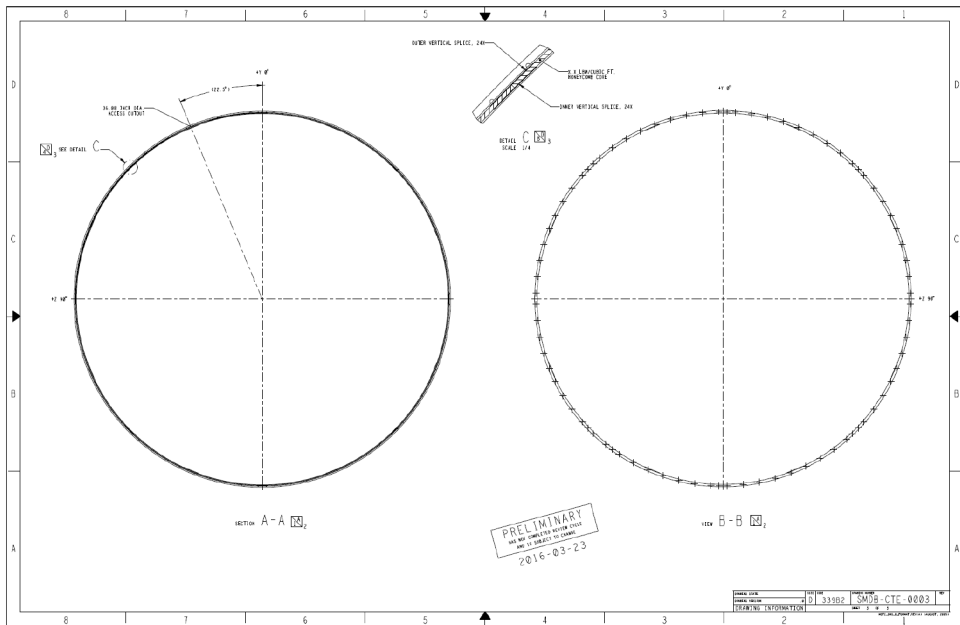


Figure 37. Layout drawing for the STA (sheet 3).

3.8 Pathfinder Design Effort

In addition to the STA, a Pathfinder design effort was proposed that would essentially conduct a PDR for CUSA2, with the assessment of the product limited to an analytical assessment. The Pathfinder would be designed to encompass all of the load cases for the DAC-0 Block 1B Cargo and Crew Configurations. Figure 38 is an illustration of the conceptual model design. The Pathfinder load cases would also incorporate the crush and burst pressure loads. All load cases including stiffness requirements are documented in the Pathfinder DDS.



Figure 38. Pathfinder conceptual model.

Trades planned for the Pathfinder study included a trade of the OML shape of the structure. In this trade, a two-part cone and cylinder construction would be compared with alternate geometries that incorporated a smooth, curved transition between the cone and the cylinder portions of the USA2 (fig. 39). Factors such as manufacturability, mass impact, and aerodynamic properties would be considered in the trade. Other trades that were planned within the Pathfinder effort were a core material and density study, knockdown factor evaluation based on imperfection sensitivity, a vertical separation joint trade, and a discontinuity factor sensitivity study.

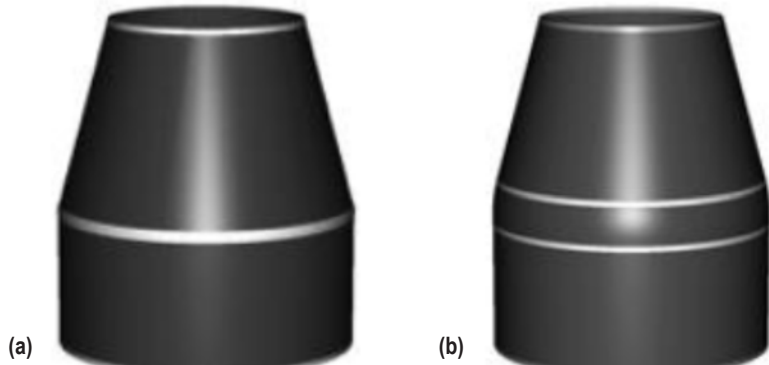


Figure 39. OML trade study considerations: (a) Two-part cone and cylinder and (b) alternate geometries.

For the Pathfinder effort, transient temperature profiles would be developed for hot/cold prelaunch (DSNE) terrestrial environments (e.g., rollout, on-pad, tanking) as well as ascent aerothermodynamic environments. It was determined that the initial case would assume no Thermal Protection System (TPS). Aero thermal heating data were not available for USA2 in the Block 1B DAC-0 database, so the Thermal Branch (EV34) planned to coordinate with the Aerosciences Branch (EV33) to determine reasonable aeroheating assumptions for the preliminary assessment.

4. JOINTS AND ANALYSIS OVERVIEW

4.1 Composite for Exploration Upper Stage Skirt Activities

The CEUS project began with a focus on the skirts that provide connections between the service module and the LH₂ tank for the EUS at one end, and between the LH₂ tank and the Interstage at the other end. In addition to the normal launch and ascent loads, the skirts experience significant thermal gradients because of their proximity to the cryogenic propellants.

4.1.1 Wall Trade Analysis

The first trade study carried out for the CEUS program was designed to determine an appropriate wall construction for a composite skirt STA designed to launch vehicle requirements. Included in the trade were the following construction types:

- Aluminum honeycomb core sandwich.
- Foam core sandwich.
- Corrugated panel.
- Blade stiffened skin.
- Hat stiffened skin.

These composite construction concepts were sized for the SLS loads and environments and compared against metallic orthogrid and isogrid concepts. Ground rules and assumptions, as well as trade study results, are included in the wall construction trade study.

4.1.1.1 Models. A finite element model (FEM) of the hydrogen tank aft skirt was developed utilizing eight panels joined with longitudinal joints (because of the physical limitations of the autoclave that was to be used). This skirt model was then attached to the load introduction structure at the fore and aft of the skirt to simulate the structure at these locations and provide appropriate stiffness (fig. 40). The attachments at these locations were made with representative metallic clevis joints. Additionally, a 12-in segment of metallic structure (a simple ring) was included to provide separation between the composite part and the extreme temperatures seen at the tank interface (fig. 41). Finally, a penetration to the primary structure (for human access) was also modeled to understand the impact of this design detail on the results.

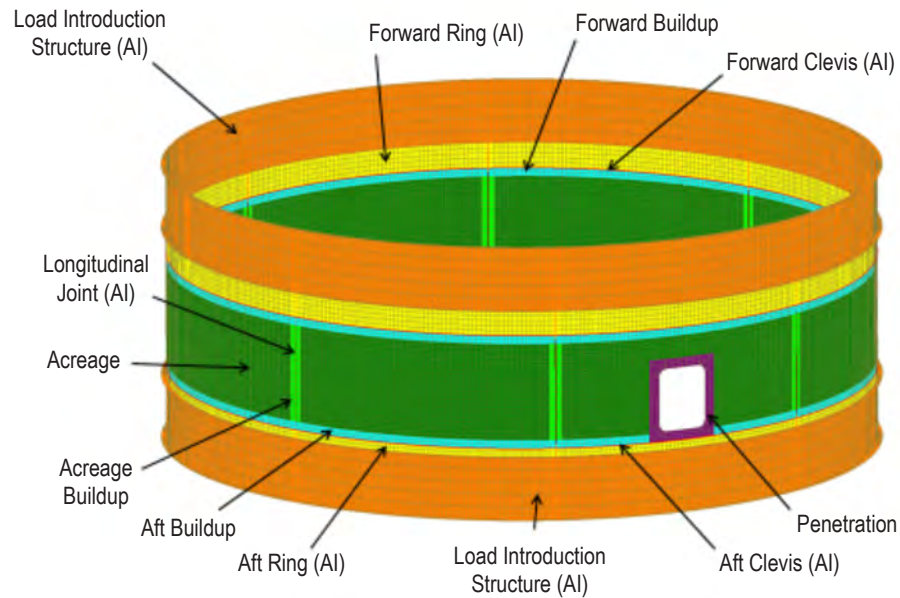


Figure 40. Aft skirt sizing model.

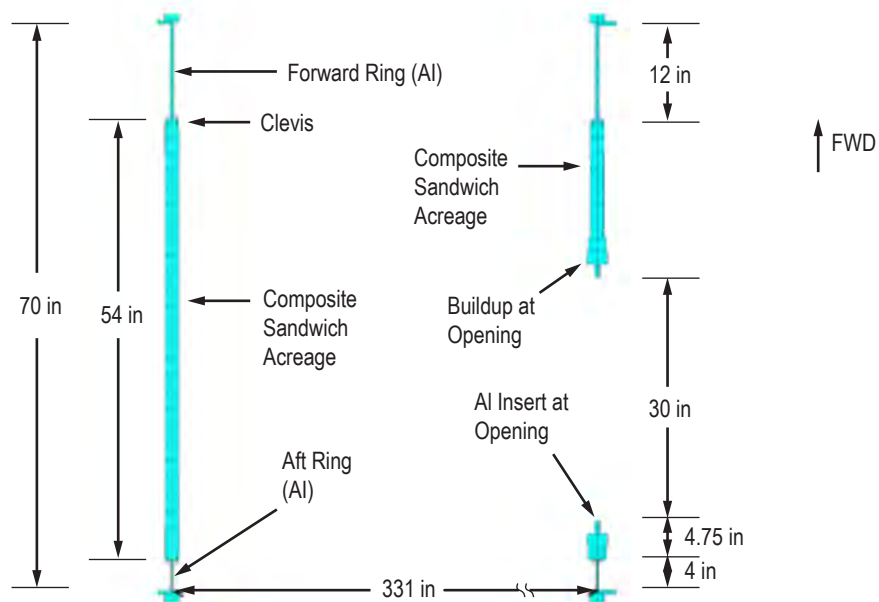


Figure 41. Joint interface details.

4.1.1.2 Sizing Results. The skirt sizing was performed with HyperSizer and NASTRAN as the analysis tools. The sizing results are shown in table 21. Several important results came out of the sizing results. The mass of the interface rings and joints were much more than the acreage masses of any of the concepts. Additionally, all of the sandwich constructions ended up at an assumed minimum gauge thickness (8 plies) as the principal failure mode was buckling. This allowed for some assumption of damage tolerance, as the design was nearly identical for pristine material properties or open-hole compression equivalent material properties. It was initially assumed that the stiffened designs might prove to be more efficient than the sandwich constructions. However, the large thermal gradients at the tank interface caused a bi-axial stress state that was more effectively reacted by the sandwich constructions. There were several design concepts that met the required 20% mass benefit compared with the metallic baseline.

Table 21. Wall construction trade study mass results.

Aft Skirt	Acreage Mass (lb)	Buildup Mass (lb)	Adhesive Mass (lb)	Total Mass (lb)	Buckling Eigenvalue	Mass Savings (Metallic Baseline) (%)
Damage Tolerant Material Properties						
Honeycomb core (3.1 pcf core)	398	123	62	1,580	2.50	42
Honeycomb core (4.5 pcf core)	474	150	62	1,683	2.84	38
Honeycomb core w/penetration (4.5)	462	191	62	1,712	3.01	39
Foam core	637	195	62	1,891	2.85	31
Foam core w/penetration	632	280	62	1,971	3.00	30
Corrugated core	634	165	31	1,828	3.07	33
Blade stiffened	1,451	253	16	2,717	2.24	1
Hat stiffened (2-in hats)	970	205	16	2,187	2.16	20
Hat stiffened (4-in hats)	842	195	16	2,050	2.21	25
Pristine Material Properties						
Honeycomb core (4.5 pcf core)	556	147	62	1,700	–	38
Corrugated core	634	137	31	1,800	3.08	34
Blade stiffened	1,451	253	16	2,717	2.24	1
Hat stiffened	780	148	16	1,941	2.48	29
Metallic orthogrid	1,345	710	–	3,052	2.22	-12
Metallic isogrid	1,442	296	–	2,735	3.30	–
Metallic isogrid-w/penetration	1,472	332	–	2,802	2.47	–

Note: Metal frame weight = 997 lb.

4.1.1.3 Figures of Merit Evaluations. Other figures of merit used to determine the preferred acreage construction are documented in section 4.2.1.1.

4.1.2 Joint Trade Study

Following the wall construction trade study, a second trade study was undertaken to determine the appropriate joints for the STA. The STA required eight longitudinal joints because of the facility limitations. Circumferential joints were also evaluated at the forward and aft interfaces. The joint concepts evaluated included the following:

- Longitudinal joints:
 - Double-lap, composite bonded joint.
 - Double-lap, composite bolted joint.
 - Double-lap, metallic bolted joint.
 - No longitudinal joint (remove these altogether—allow separation of panels).
- Circumferential joints:
 - Metallic clevis-bolted joint.
 - Metallic clevis-bonded joint.
 - 3D woven F-preform joint (bonded).
 - 3D woven Pi-preform joint (bonded).
 - Builtup F-preform joint (bonded).

Masses for each of the joint concepts were evaluated with spreadsheet calculations as well as open-source code (A4EI) for the adhesive connections. Additionally, the concepts were evaluated in other key areas, in much the same way the wall construction was evaluated. These key areas were:

- Structural integrity.
- Inspectability.
- Minimum recurring cost.
- Minimum nonrecurring cost.
- Minimal development cost.
- Design/analysis uncertainty.
- Producability/complexity.

The joint trade study was not completed prior to the program request to consider alternate hardware.

4.1.3 Kissing Bond Evaluation

A kissing bond describes a region where substrates intended to be bonded in contact are held together by a very weak bond, but cannot sustain tensile or shear stresses required by the design. A kissing bond is the limiting case of a weak bond (i.e., a very weak bond that will likely fail under service loads). The likelihood of a kissing bond occurrence can be minimized using manufacturing process controls since kissing bonds result from manufacturing process errors. For composite sandwich structure, a kissing bond at the facesheet-core interface is a relevant failure mode that must be considered in structural certification. In this work, the effect of local disbonds

on the strength of sandwich structure is considered. This work complements a similar investigation into the effect of facesheet-core disbonds on buckling of sandwich panels.¹¹

Structural substantiation of disbonds can be accomplished using a damage tolerance approach. For a damage tolerance approach, a critical flaw size and detectable threshold must be established. A margin of safety is established by ensuring that the critical flaw size is at least two times larger than the detectable size.

In this section, a preliminary damage tolerance evaluation of facesheet-core disbonds in composite sandwich structures is described. Several analyses were conducted using Abaqus Standard version 6.14. Material property data available in the literature were used. The geometrical configuration, facesheet layup, and materials were assumed based on guidelines from the CEUS trade study activity, which were conducted in parallel. Though the particular model configuration does not match the outcome of the CEUS panel sizing, the configuration used here is representative and the model is parametric so accommodating different configurations in future analyses is simple.

No experimental validation was performed. Further work, including detailed experimental validation, is required to establish confidence in the analysis results described in the following subsections.

Section 4.1.3.1 describes investigation into the critical size of facesheet-core disbonds subjected to relevant loading conditions, and section 4.1.3.2 discusses two concepts for disbond detection.

4.1.3.1 Critical Size. For the purpose of structural substantiation, kissing bonds can be treated as disbonds since they effectively have no strength. Structural test and analysis of facesheet-core disbonds has been conducted in prior investigations. For example, Rinker¹² and Glaessgen¹³ have used the virtual crack closure technique (VCCT) to analyze facesheet-core disbonds in the presence of internal pressure. In order to use a fracture mechanics approach such as the VCCT, the fracture toughness of the facesheet-core interface must be characterized. Ratcliffe presents a recommended procedure for characterization of facesheet-core fracture toughness and have tabulated the fracture toughness of the facesheet-core interface for several facesheet and core materials from data available in the literature.¹⁴ In this project, a 3D parametric model was developed by building on the previous work referenced above. The purpose of the model is to evaluate the effect of a facesheet-core disbond on the strength of sandwich structure subjected to edgewise compression load. The details of this analysis are described in this section.

4.1.3.1.1 Model Configuration. The model configuration was chosen to resemble the standard test for edgewise compressive strength of composite sandwich construction (e.g., ASTM C364), as shown in figure 42.

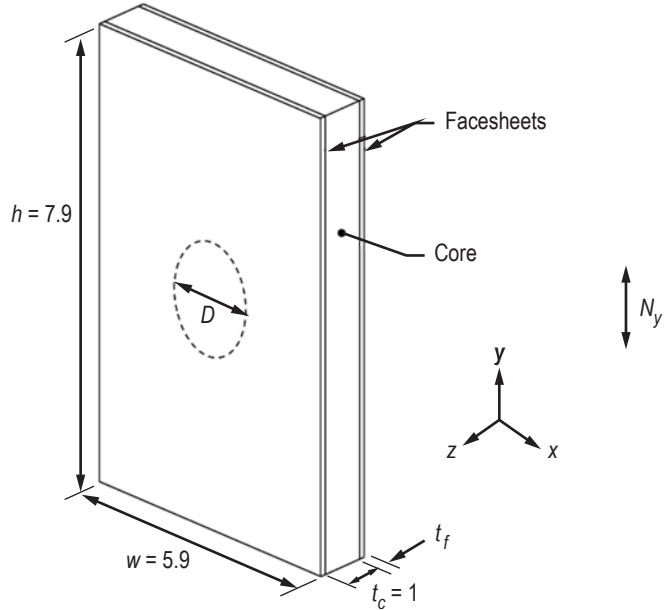


Figure 42. Configuration used for analysis of the critical size of kissing bonds at the facesheet-core interface.

The key difference between the configuration shown in figure 42 and the standard test is that a circular disbond is considered with diameter, D . The disbond is placed at one facesheet-core interface. The configuration has a width, w , of 5.9 in and a height, h , of 7.9 in. The overall dimensions were chosen so that the behavior of the disbond is not influenced by edge effects. The core and facesheets have thickness, $t_c=1$ in and, $t_f=0.057$ in, respectively. A python script was used to automatically generate models with various disbond sizes, which will greatly assist future studies.

Since the primary load for the CEUS structures is axial compression, it is assumed that a compressive load acts on the model in the y -direction as shown in figure 42. Under this edgewise compressive load, the driving force for initiation and propagation of the disbond is local buckling of the debonded region. Therefore, a postbuckling analysis procedure was used with two steps. In the first step, a linear eigenvalue buckling analysis is conducted. The first buckling mode (local buckling of the disbond region) is used to seed an imperfection in the mesh for the subsequent analysis with an amplitude of $0.03 t_f$ for the second step. In the second step, a geometrically nonlinear postbuckling analysis procedure is used where the edgewise compressive load is applied as a prescribed end shortening and cohesive elements or the VCCT are used to capture growth of the disbond and thus predict the strength of the specimen. This analysis procedure extends the work of Reeder et al. to the case of sandwich constructions.¹⁵

4.1.3.1.2 Mesh and Boundary Conditions. A typical mesh is shown in figure 43. The core and facesheets were represented with one layer of continuum shell elements (SC8R) each. A refined mesh was used in the region near the disbond front and a coarser mesh was used in the far-field region. The typical far-field mesh size was 0.25 in. For models that used cohesive elements, the mesh size in the refined mesh region was 0.01 in to satisfy guidelines for cohesive element size.¹⁶ The cohesive elements (COH3D8) were placed in the region highlighted in green in figure 44. The cohesive elements were replaced with tie constraints during the first analysis step (eigenvalue buckling analysis). For models that used VCCT, a typical refined mesh size of 0.08 in was used, as established by a mesh convergence study. For both models with cohesive elements and models that used the VCCT, a contact condition was used in the second step to prevent the facesheet from penetrating the core within the disbond region. Also, in both models, damage growth was only allowed within the refined mesh region. Once damage propagation reached the transition region, the model results were truncated, since damage is artificially arrested at this point the results are no longer physically meaningful.

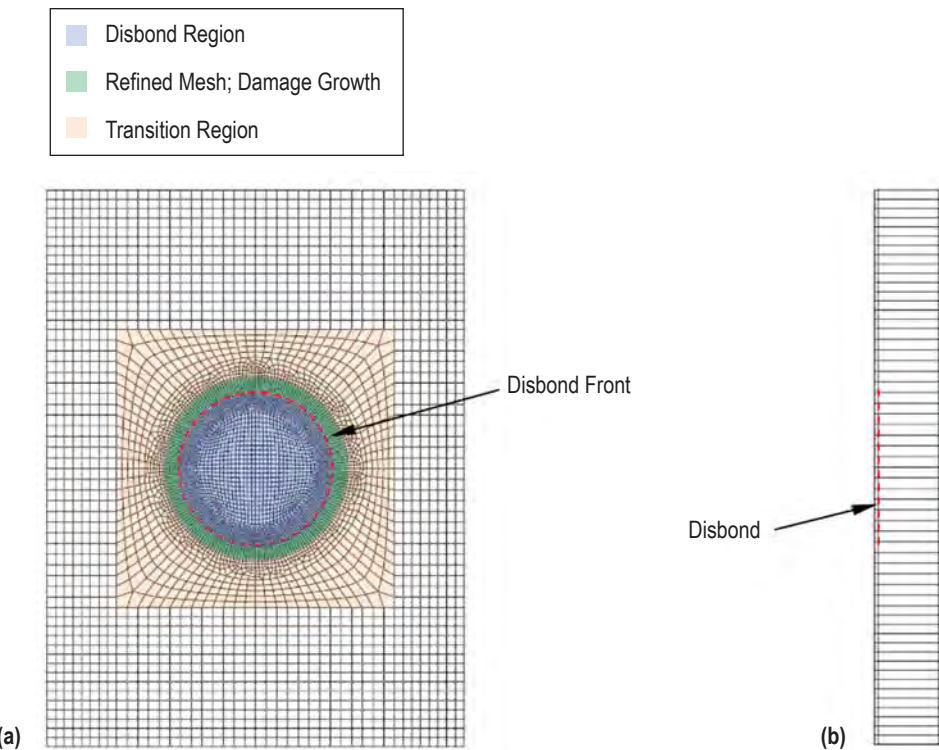


Figure 43. Typical mesh used for the critical disbond size analysis: (a) Front and (b) side.

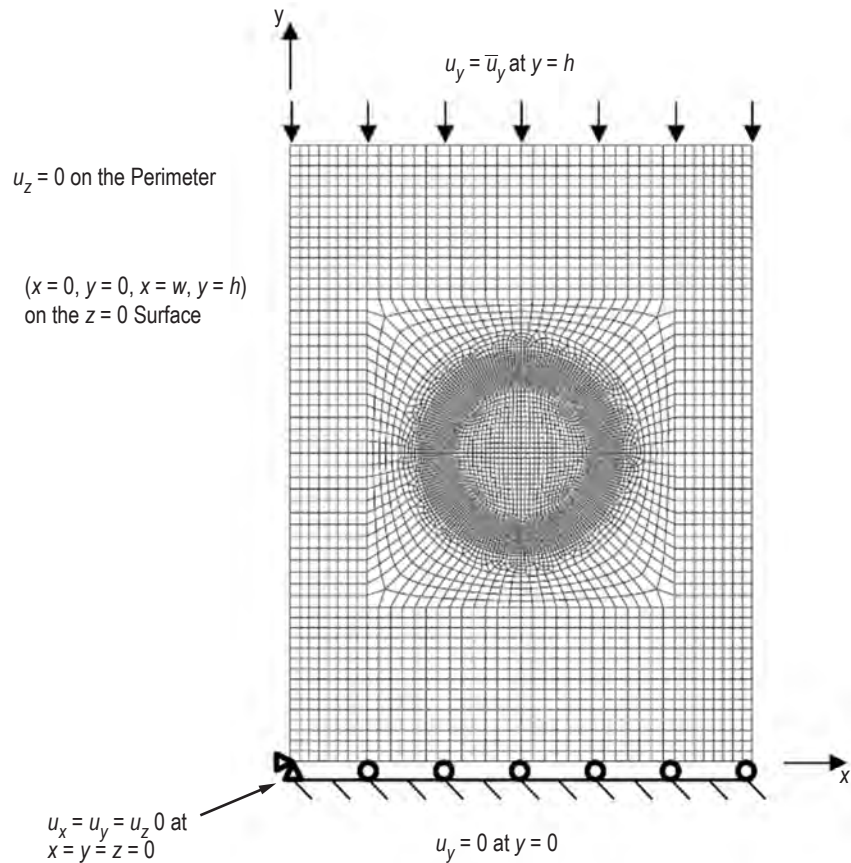


Figure 44. Boundary conditions for the critical disbond size analysis.

4.1.3.1.3 Material Properties. Material properties for the facesheets, core, and facesheet–core interface were assumed based on published data summarized in NASA Internal Memorandum, Property Values for Preliminary Design of the Ares I Composite Interstage, J. Reeder, 2007). The facesheets are assumed to be IM7/8552 with a 0.0057-in ply thickness and a [45/-45/0₂/90₂/0₂/-45/45] layup. The core material was assumed to be Rohacell® 110 HERO foam. Core elastic properties for Rohacell HERO foam is $E = 27$ ksi and $\nu = 0.3$. Mode-independent damage propagation was assumed for the facesheet–core interface using a Mode I value for fracture toughness, which is a conservative assumption since Mode II and mixed-mode fracture toughnesses are typically higher than the Mode I fracture toughness. The fracture toughness was assumed as 5.71 lbf/in.¹⁴ For the cohesive elements, the strength was assumed as 1,827 psi,¹⁶ and the penalty stiffness was calculated following the recommendation by Turon et al.¹⁷

4.1.3.1.4 Results. A typical contour plot of u_z from the eigenvalue buckling analysis for the first eigenmode is shown in figure 45 where the disbond size is 1.6 in. This deformation is used to seed an imperfection in the subsequent postbuckling analysis.

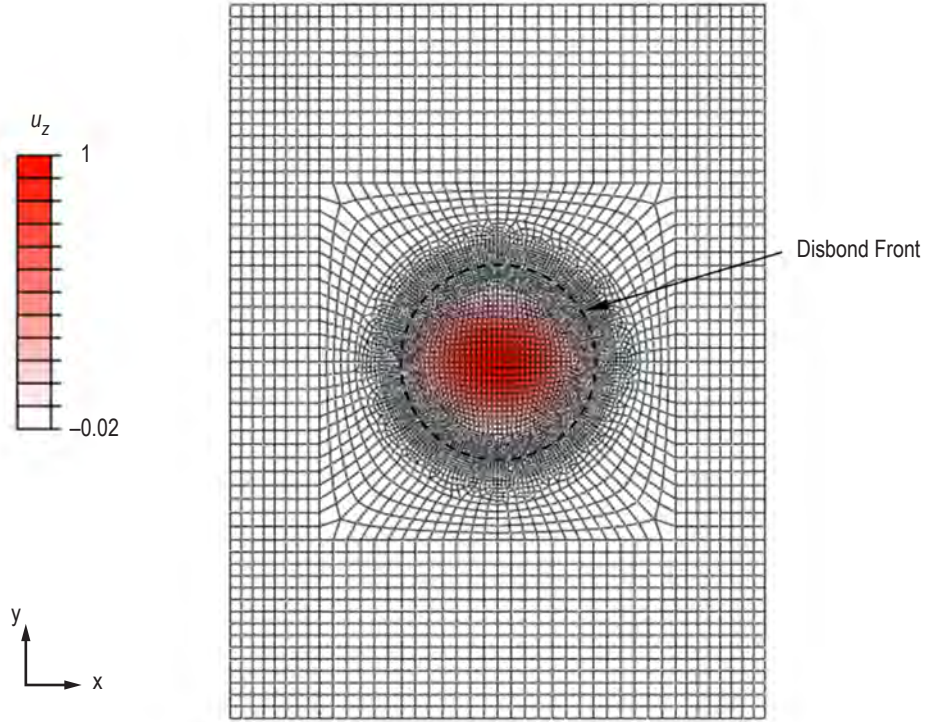


Figure 45. Typical first mode of eigenvalue buckling analysis.

Typical load-displacement responses, damage propagation, and deformation are shown in figure 46 for a model with cohesive elements and in figure 47 for a model with VCCT. In both cases the initial disbond size is 1.6 in. In figure 46, three key points in the load-displacement response are designated as follows: damage initiation, I ; onset of load-displacement nonlinearity, N ; and peak load, P . The damage state and out-of-plane displacement are shown as contour plots for each key point in the load-displacement history. It is observed that damage has initiated and propagated to a critical length when the peak load is reached. Similarly, in figure 47, the peak load point is highlighted, and corresponding contour plots of the damage state and out-of-plane displacement are shown. The VCCT prediction does not indicate damage initiation prior to the peak load.

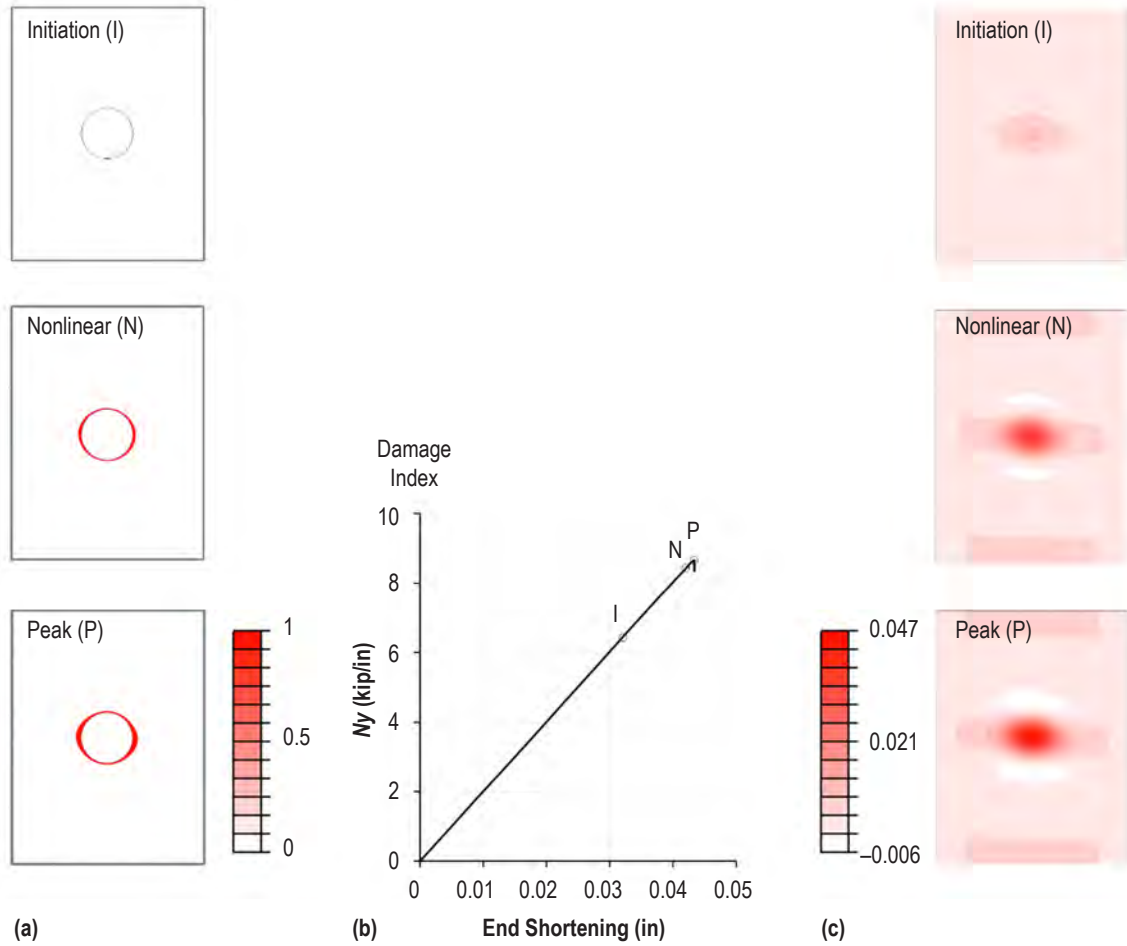


Figure 46. Damage, load-displacement response, and out-of-plane deformation predicted using cohesive elements: (a) Damage propagation, (b) load displaced response, and (c) u_z (in).

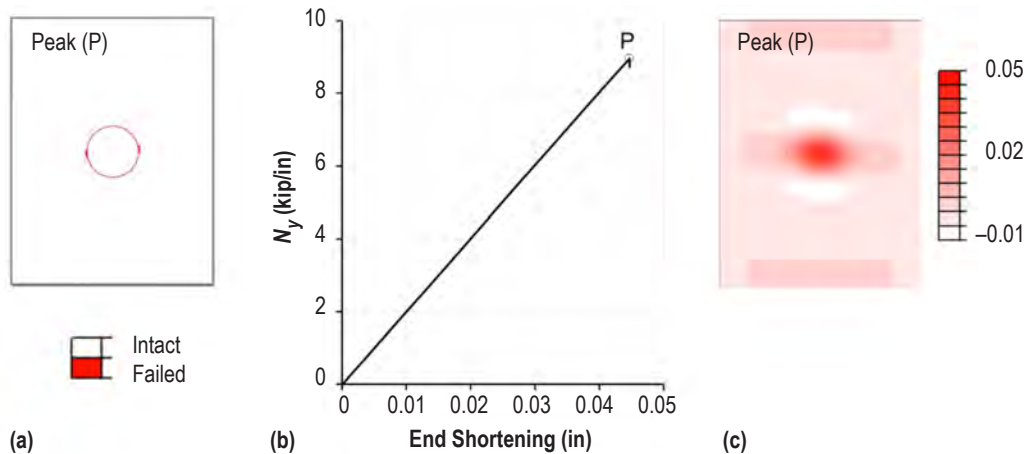


Figure 47. Damage, load-displacement response, and out-of-plane deformation predicted using VCCT: (a) Damage propagation, (b) load displacement response, and (c) u_z (in).

In contrast to the prediction using cohesive elements, the model with VCCT does not capture damage initiation and initial accumulation, but it does capture damage propagation at peak load. The differences between the predictions from the two fracture mechanics approaches are expected due to the fact that the VCCT approach is based on a linear elastic fracture mechanics formulation while the cohesive elements consider both strength and fracture through a nonlinear fracture mechanics formulation. While the model using the VCCT provides less insight into the damage process compared with the model using cohesive elements, the model using the VCCT requires only 20% of the computational time of the model with cohesive elements. The difference in computational expense between the two models is due to (1) the difference in mesh size and (2) the cohesive element model suffering from more extensive load-increment convergence difficulties than the VCCT model.

Both models require the analyst to specify solution parameters that can have a significant impact on the results. For the VCCT model, a contact stabilization parameter of 1×10^{-6} was used as recommended by Krueger.¹⁸ Trial and error showed that larger values of this parameter and automatic selection of this parameter by Abaqus yielded varying results that were in poor agreement with the predictions from the model with cohesive elements. For the model with cohesive elements, viscous regularization was used to limit the convergence difficulties. A viscous regularization coefficient of 1×10^{-6} was found to provide a good balance between improving convergence behavior and having a minimal effect on the load-displacement response. Increasing the viscous regularization coefficient resulted in a load-displacement behavior with a rounded peak load instead of a sharp load drop. Models with smaller values of the viscous regularization coefficient converged significantly more slowly and had little effect on the load-displacement response. Though both solution parameters (contact stabilization parameter and viscous regularization coefficient) are the same, this is likely a coincidence for the particular structure considered here. It is assumed that the solution parameters established here are valid for the range of model configurations considered and that vastly different structures will require different solution parameters.

The disbond size was varied to obtain the load-carrying capability as a function of disbond size for this sandwich structure. The results are shown in figure 48 as predicted by the linear eigenvalue buckling analysis, the postbuckling analysis using cohesive element, and postbuckling analysis using VCCT. The results show that the models using cohesive elements and VCCT are in good agreement for the range of disbond sizes considered. The eigenvalue buckling analysis under-predicts the load-carrying capability when the disbond is large. However, the eigenvalue buckling analysis is useful as a quick and conservative preliminary design tool for assessing the severity of this failure mode.

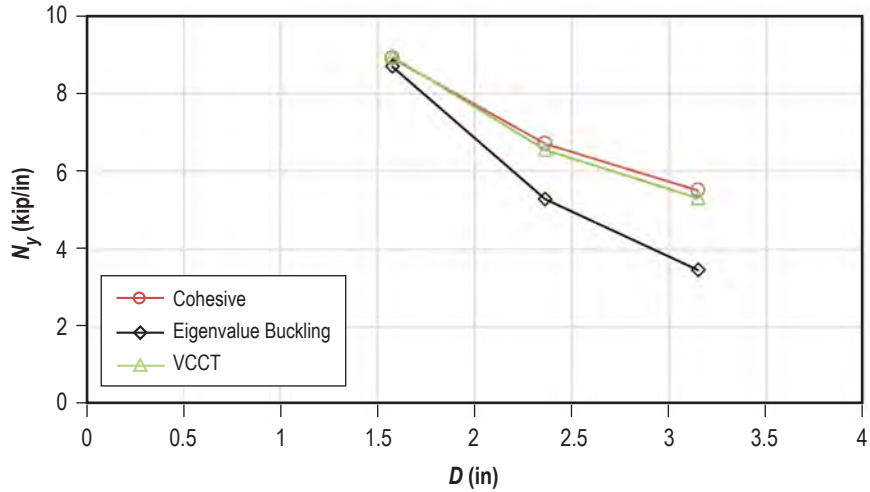


Figure 48. Critical disbond size.

4.1.3.1.5 Conclusions and Recommendations for Future Work. A parametric FEM was developed to assess the critical size of facesheet-core disbonds in sandwich structures subjected to edgewise compressive load. Two fracture mechanics-based approaches were considered to model propagation of the disbond: the VCCT and cohesive elements. Material properties available in the literature were used for the analyses. Model results show good correlation between the two modeling approaches. As a result, the use of the VCCT is recommended for future evaluations due to its lower computational cost. The results suggest that, for the CEUS design load levels, facesheet-core disbonds must be very large (≥ 4 inches) before this defect poses a threat to the structural configuration considered.

Detailed experimental characterization of material property inputs and validation of model predictions has not been conducted and is a required next step. In addition, the parametric model developed here could be used to develop critical disbond size data for a wide variety of sandwich configurations. Such data would be valuable tools for assessing the severity of the facesheet-core disbond failure mode in preliminary design. Further investigation for particular structural configurations including the effect of curvature, combined loads, environment, disbond shape, and disbond proximity to structural features such as joints are needed to assess the severity of this damage mode fully.

4.1.3.2 Detection. Detection of kissing disbonds is challenging since conventional NDE methods (ultrasound and thermography) identify defects through the presence of voids and, by definition, kissing bonds do not have a void. Therefore, conventional NDE techniques are not capable of detecting kissing bonds and weak bonds. However, if the assumption is that the kissing bonds are localized and have no strength, they can be detected using a nonconventional approach, where the sandwich structure is inspected while subjected to a pressurization load so that the structural deformation reveals the presence of a kissing bond by its lower local bending stiffness. This approach may be suitable for identifying very weak bonds since the loading could lead to failure in the weak region. However, in this study, the approach is considered for disbonds

only. Two applications of this approach are reviewed in this section: (1) A commercially available product for local inspection called the elasticity laminate checker (ELC) and (2) a newly proposed wide-area inspection method.

4.1.3.2.1 Elasticity Laminate Checker. The ELC was developed by Airbus¹⁹ as a local inspection method to identify facesheet-core disbonds in sandwich structures. Figure 49 depicts a schematic of the device. The ELC operates by applying a vacuum to a local region on one side of a sandwich panel and measuring the relative displacement of the skin. The skin will deform significantly more in areas where disbonds are present since the bending stiffness of one facesheet is much less than the bending stiffness of the sandwich. The ELC will only detect facesheet-core disbonds on one side at a time. To have confidence that the structure has no facesheet-core disbonds, inspections must be conducted on all regions (including both sides) of the sandwich panel. The ELC is a commercially available product that has been validated and used in field applications by Airbus.

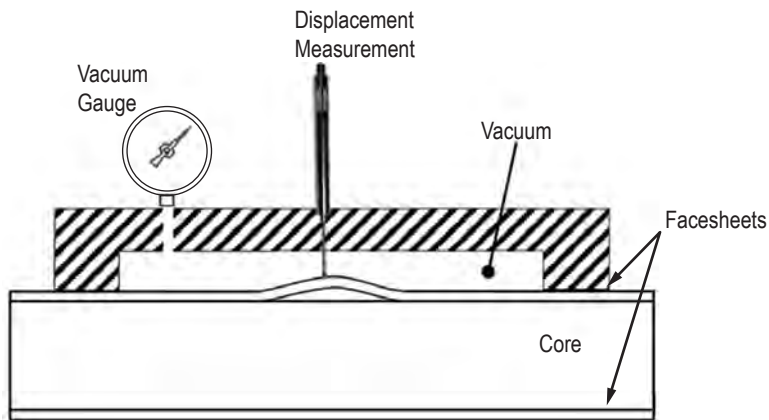


Figure 49. Schematic of the ELC.

4.1.3.2.2 Vacuum-Assisted Wide Area Inspection for Facesheet-Core Disbonds. While the ELC is a useful tool for local inspections, it is time-consuming to scan large areas. Using a similar approach, a vacuum-assisted, wide-area inspection concept is proposed. The concept is illustrated in figure 50. The panel to be inspected (shown with black solid lines) is installed on a vacuum fixture (shown with blue dashed lines). The air within the enclosed region is evacuated. Following the concept of the ELC, localized deformation in the out-of-plane direction will occur in regions where facesheet-core disbonds are present. The vacuum loading condition should be designed such that weak bonds fail and, thus, are readily detectable while nominal bonds are undamaged. With the vacuum applied, detection of disbonds can be accomplished through any technique that allows for full-field measurement of out-of-plane deformation including using a coordinate measuring machine (CMM), shearography, or digital image correlation. In contrast to the ELC, the vacuum-assisted, wide-area inspection concept allows for rapid inspection of large panels.

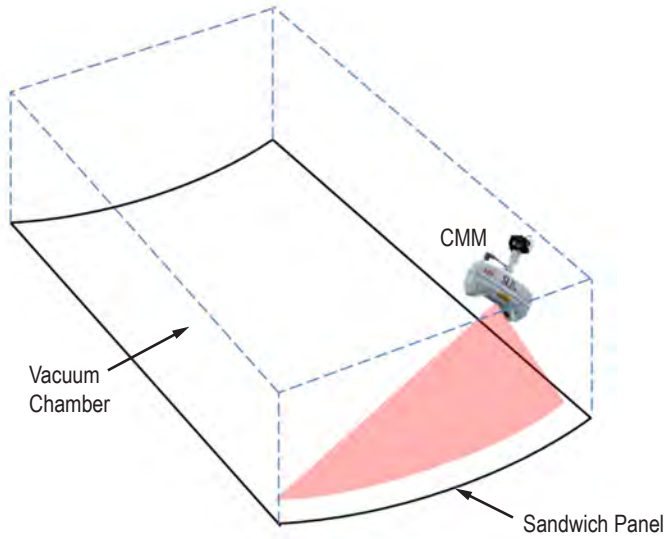


Figure 50. Wide-area, vacuum-assisted disbond inspection method.

4.1.3.2.3 Detectable Size. The model for eigenvalue buckling analysis described in section 4.1.3.1 was used to evaluate the detectable size for the particular combination of geometrical configuration, layup, and material properties that were assumed. The deflection, δ , as a function of disbond size for vacuum pressure of 14.5 psi, is shown in figure 51. These results suggest that the threshold of detectability of facesheet-core disbonds is on the order of 2 in and 0.75 in for CMM and shearography based systems, respectively.

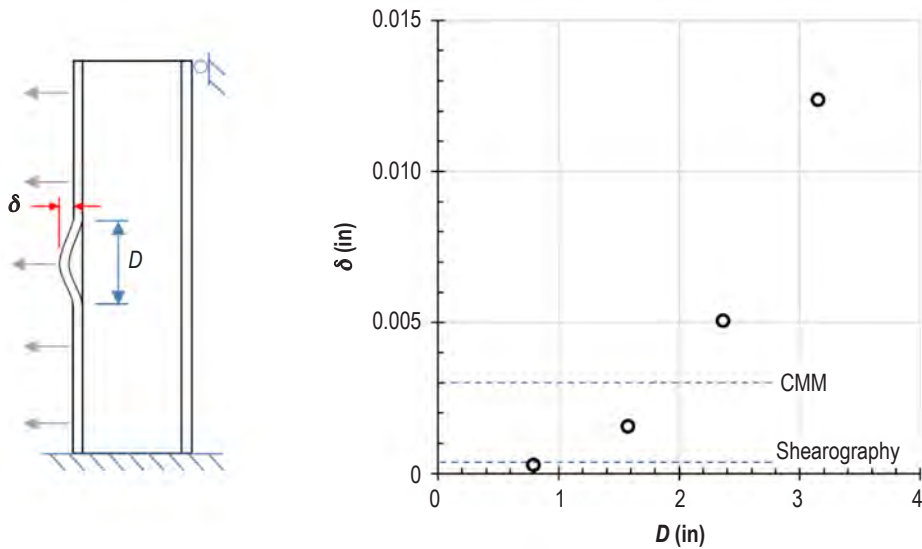


Figure 51. Detectable size for vacuum-assisted disbond inspection.

Considering the analysis described in section 4.1.3.1, which indicates that the critical disbond size is on the order of 4 in, the ratio of critical size to detectable size is 5.3 for a system using shearography, which compares favorably with the typical minimum acceptable value of 2. Therefore, these analysis results suggest that a damage tolerance approach to mitigating the risk of failure due to disbonds at the facesheet-core interface is feasible.

4.1.3.2.4 Conclusions and Recommendations for Future Work. The feasibility of detecting disbonds via local and wide-area, vacuum-assisted inspection methods was assessed. Considering a representative sandwich structure configuration, an FEA suggests that disbonds as small as 0.75 in are detectable for flat panels. Further work is required to explore the feasibility and limitations of the proposed approach for kissing bonds with varying strengths through experimental tests and additional analyses. Future tests and analyses should consider the effect of curvature carefully.

4.2 Composites for Exploration Upper Stage Universal Stage Adapter Activities

Following direction from the Space Technology Mission Directorate (STMD) and the SLS program, the focus of the CEUS program shifted from the skirts on the EUS to the USA. The USA provides an interface between the EUS and the MPCV. Additionally, it serves as a fairing for a secondary payload (fig. 52).



Figure 52. USA options.

4.2.1 Pathfinder Analysis

As the CEUS program began to consider the alternate geometry of the USA, initial sizing was completed to determine a point of departure for the flight-like construction of the USA. This became known as the Pathfinder design.

4.2.1.1 Initial Concepts. The CUSA Pathfinder Initial Concept design consisted of a conical portion and a cylindrical portion with a metal ‘hip joint’ clevis-type fitting to connect the cone to the cylinder. The entire assembly was divided into four petals that used a composite honeycomb core sandwich construction. The four petals were connected to each other using separation joints with clevis-type fittings to connect to the composite sandwich panels. The assembly was attached to the forward and aft structure using circumferential separation joints with clevis-type fittings.

The FEM was constructed using Patran (fig. 53). The model consisted of shell elements to represent the composite sandwich panels, metal separation joints, and other adjacent structures. Beam elements were used to represent the clevis fittings. The aft end of the model was restrained in the vertical and radial directions. The flight loads were applied as component loads to the forward end of the model and to the top of the cylinder using RBE3 connectors, as these do not add artificial stiffness. The flight loads used are the USA2 Loads – Crew Configuration dated December 18, 2014.

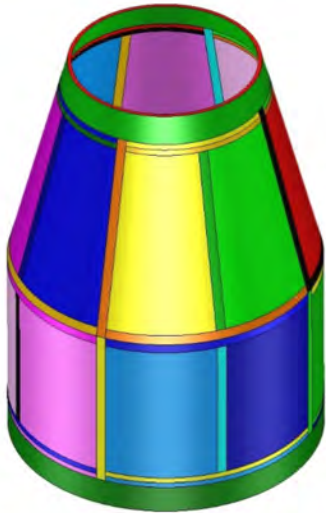


Figure 53. Analysis model for USA initial design concept.

Linear static analyses were performed on the FEM using NASTRAN. The structure was optimized for weight using a combination of HyperSizer and NASTRAN. Linear buckling analyses were then performed on the optimized structures.

This model was used to provide an initial core thickness and layup of the cone and cylinder acreage panels. Once the Alternate Geometry CUSA model was constructed, the initial model was no longer used.

The initial USA design (conic section on top of the cylindrical section) came about because of a requirement to use the conic system separately (called USA1 at the time). However, this requirement was removed, and the system was evaluated in the baseline configuration (shown in fig. 54).

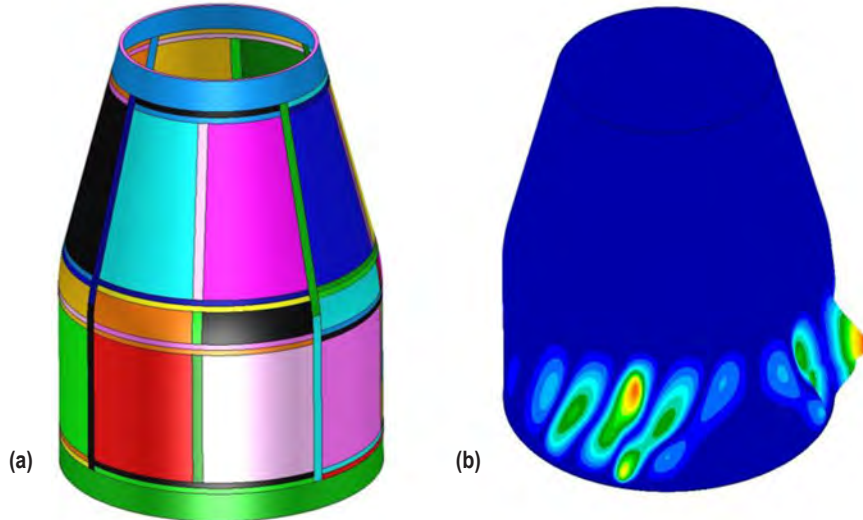


Figure 54. USA: (a) Baseline geometry and (b) representative buckling results.

4.2.1.2 Alternate Geometry. The CUSA Pathfinder Alternate Geometry design consisted of a conical portion, a cylindrical portion, and a blend portion that allowed for a smooth transition from the cone to the cylinder. The entire assembly was divided into four petals that used a composite honeycomb core sandwich construction. The four petals were connected to each other using separation joints with clevis-type fittings to connect to the composite sandwich panels. The assembly was attached to the forward and aft structure using circumferential separation joints with clevis-type fittings.

The FEM was constructed using Patran, shown in figure 54. The model consisted of shell elements to represent the composite sandwich panels, metal separation joints, and other adjacent structures. Beam elements were used to represent the clevis fittings. The aft end of the model was restrained in the vertical and radial directions. The flight loads were applied as component loads to the forward end of the model and to the top of the cylinder using RBE3 connectors as these do not add artificial stiffness. The flight loads used were the USA2 Loads – Crew Configuration dated 12/18/2014.

Linear static analyses were performed on the finite element model using NASTRAN. The structure was optimized for weight using a combination of HyperSizer and NASTRAN.. Linear buckling analyses were then performed on the optimized structures. Table 22 shows the resulting weights and buckling load factors (eigenvalues) of CUSA structures with varying facesheet layups, core thicknesses, and shell buckling knockdown factors (SBKFs).

Table 22. Buckling trade study results.

FS Plies	Cone- Blend SBKF	Core Thickness (in)				Weight (lb)			Cylinder		Cone		Blend	
		Lower Limit*	Cyl.	Cone	Blend	Frame	Panels	Diff	Mode	Eigne	Mode	Eigen	Mode	Eigen
7	0.33	0.500	0.500	0.625	0.500	1113	2827	–	1	2.477	102	5.278	173	6.149
7	0.65	0.500	0.500	0.500	0.500	1113	2778	-49	1	2.477	60	4.635	>400	>8.3
6	0.33	0.250	0.500	0.625	0.500	1113	2530	-297	1	2.161	121	4.643	>400	>7.4
6	0.65	0.250	0.500	0.375	0.250	1113	2406	-421	1	2.155	34	3.082	5	2.378

* Self-imposed lower limit of the core thickness range (core thickness may not be optimum).

4.2.2 Structural Test Article

The CEUS project investigated the potential of building and testing a test article that would represent all or a portion of the USA. After several iterations, it became clear the program would be unable to fund anything larger than a cylindrical section of the full USA article. As a result, some modifications to the sizing needed to be made to ensure that the test article would be representative, given facility limitations in manufacturing and in testing. The subsequent design was called the STA.

4.2.2.1 Initial Sizing. The STA composite laminate layups were based on the sizing for the Pathfinder cylindrical portion. The core thickness was based on the wall thickness evaluation and the load-carrying ability of the existing LOX and LH₂ simulators (interface test hardware from previous programs).

4.2.2.2 Wall Thickness Evaluation. The STA consists of a 12-ft-tall version of the cylindrical portion of the CUSA. The assembly consisted of eight composite honeycomb core sandwich panels joined longitudinally using composite laminate doublers on both the interior and the exterior. Coarse versions of the LOX and LH₂ tank simulators were used to emulate realistic boundary conditions for the STA (fig.55). The STA connects to the forward LOX tank simulator and aft LH₂ tank simulator using metal clevis-type fittings.

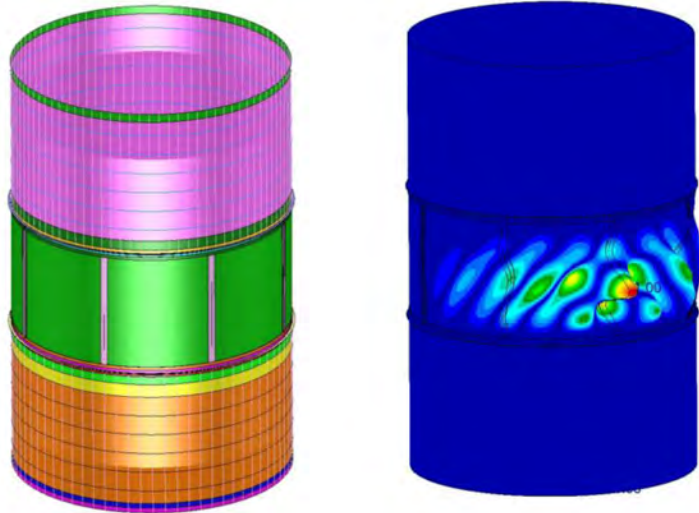


Figure 55. STA model with typical buckling eigenmode response.

The FEM was constructed using Patran. The model consisted of shell elements to represent the composite sandwich panels, composite laminate doublers, metal clevis fittings, and metal simulator structure. Beam elements were used to represent the simulator ring frames and vertical hat stiffeners. The doublers and clevis fitting were connected to the composite sandwich panels using glued contact. The aft end of the model was restrained in all directions. The flight loads were applied as component loads to the forward end of the model using an RBE3 connector, as it does not add artificial stiffness. The flight loads used are the Ascent Bin 8 – Max Q (Cylinder Aft) minus the shear load.

Linear buckling analyses were performed on the STA FEM with various core thicknesses, as the capability of the test stand hardware was being evaluated in parallel. Figure 56 shows the core depth versus the buckling load; this figure was used to estimate the core thickness required to ensure failure of the test article prior to the test facility hardware.

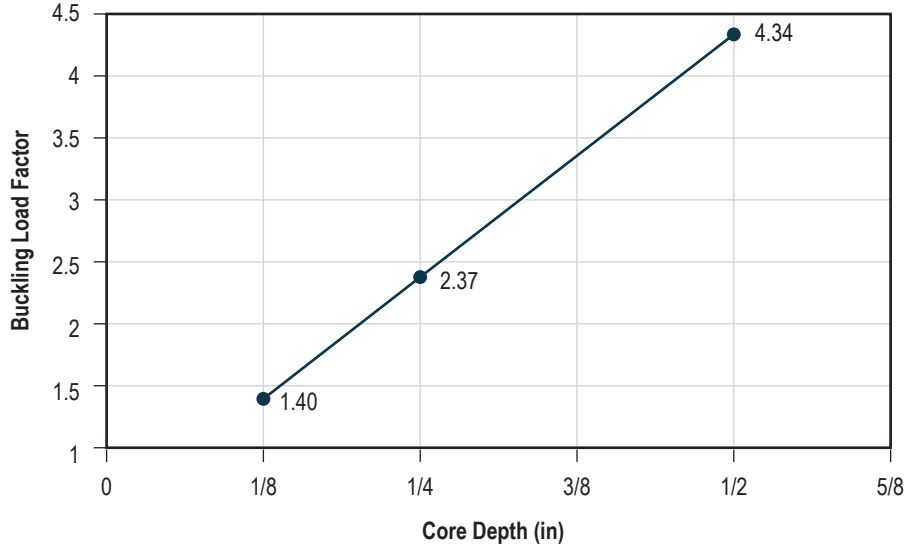


Figure 56. STA core depth study results.

4.2.2.3 Simulator Evaluations. The STA along with the test facility hardware (called simulators) and load ring models were analyzed to evaluate the buckling load of the STA and, most importantly, the strain distribution in the simulators. Based on an initial assessment of simulators by Dawn Phillips (fig. 57), the allowable line loads in the LO₂ and LH₂ simulators were limited to 3,300 lbf/in and 3,700 lbf/in, respectively. These line loads would result in an approximate factor of safety on yield of 1.1. Later assessment of the simulators based on modified failure criteria generated allowable line loads of 6,200 lbf/in and 4,900 lbf/in for LO₂ and LH₂ simulators, respectively. In order to estimate the load distribution in the simulators during actual testing of the STA in the full stack configuration, a transient dynamic analysis of a full stack model (consisting of load rings, simulators, and STA) was performed to evaluate buckling and postbuckling behavior of STA and also to obtain strain and displacement distribution at the interfaces of simulators and STA. The high-fidelity FEMs of the simulators and the loading rings were developed using shell elements in which frames and stringers were explicitly modeled. The full stack model (fig. 58) included loading jacks used in the simulation of load application points.

Simulator Capability Memorandum

From: Phillips, Dawn R. (MSFC-EV31)
Sent: Thursday, January 14, 2016 5:32 PM
To: Mann, Troy Owen (LARC-D206)
Cc: Richardson, Stephen W. (MSFC-EV32); Wingate, Robert J. (MSFC-EV31); Thomas, Allyson D. (MSFC-EV32)
Subject: Preliminary Simulator Capability

Troy,

Based on the simulator assessments we performed, we are estimating the following preliminary capabilities:

Lower (LH2) Simulator: 3700 lb/in
Upper (LO2) Simulator: 3300 lb/in

Each of these line loads results in an approximate factor of safety on yield of 1.1 for the simulators.

The simulator assessments did include some simplifying assumptions on how the line load is applied to the simulator. Because the buckling loads for the STA are coming in close to these capability values, it is now time to look more closely at the fidelity in the simulator assessment. We are working on that.

Thanks,
Dawn

From: Phillips, Dawn R. (MSFC-EV31)
Sent: Thursday, January 28, 2016 11:43 AM
To: Mann, Troy Owen (LARC-D206)
Cc: Richardson, Stephen W. (MSFC-EV32); Wingate, Robert J. (MSFC-EV31); Thomas, Allyson D. (MSFC-EV32)
Subject: RE: Preliminary Simulator Capability

Troy,

We modified our analyses for the simulators. We included effects from the clevis/ring for a $\frac{1}{2}$ -inch core to get the load path and neutral axis alignment more realistic. Based on these new analyses, we are estimating the following capabilities:

Lower (LH2) Simulator: 4900 lb/in
Upper (LO2) Simulator: 6200 lb/in

Each of these line loads results in an approximate factor of safety on yield of 1.1 for the simulators, where the critical condition is bending of the flange at the interface to the test article.

Thanks,
Dawn

Figure 57. Simulator capability memorandum.

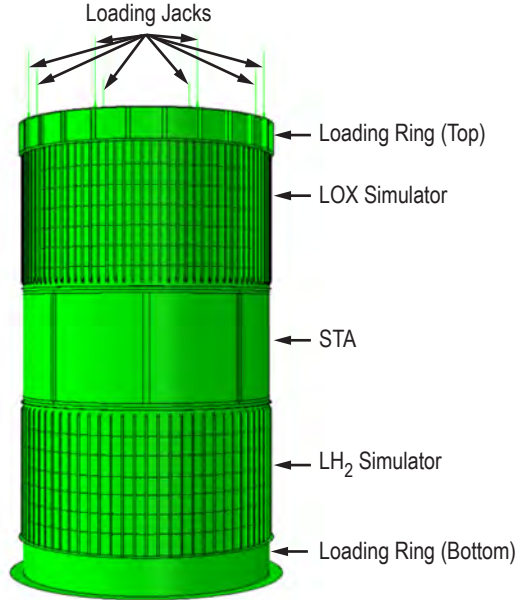


Figure 58. Full stack model—assembly of STA, simulators, loading rings, and load jacks.

A sandwich core thickness of 0.5 in was used (and fixed) in the STA model to evaluate the simulators. Nodes in the flange region of the bottom load ring were fixed in all degrees of freedom and a uniform axial displacement was applied to the top nodes of the loading jacks. The load versus displacement curve and radial displacement of the STA are presented in figure 59.

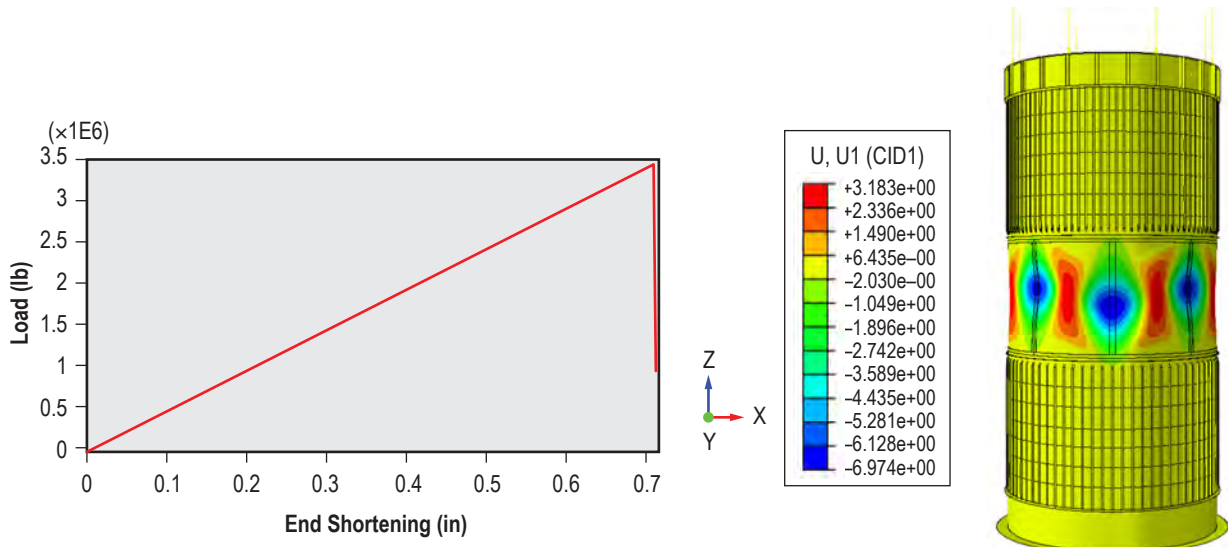


Figure 59. Load versus displacement curve and radial deformation contours in stack.

The radial deformation contours in the LH₂ simulator (to assess bending behavior of the simulator flange) are shown in figure 60. This initial assessment showed a test line load that was very close to the allowable limits for the simulators so a slightly different deformation configuration of load jacks (fig. 61) was considered to decrease the line load in the simulators. This deformation configuration resulted in generating axial and bending moment loads in the ratio as defined in Bin8. The load versus axial displacement of the STA and its radial deformation for displacement configuration defined above is shown in figure 62. This load configuration resulted in one side of the STA deforming more than the other. The radial deformation contours, before and after complete buckling, are shown in figure 63.

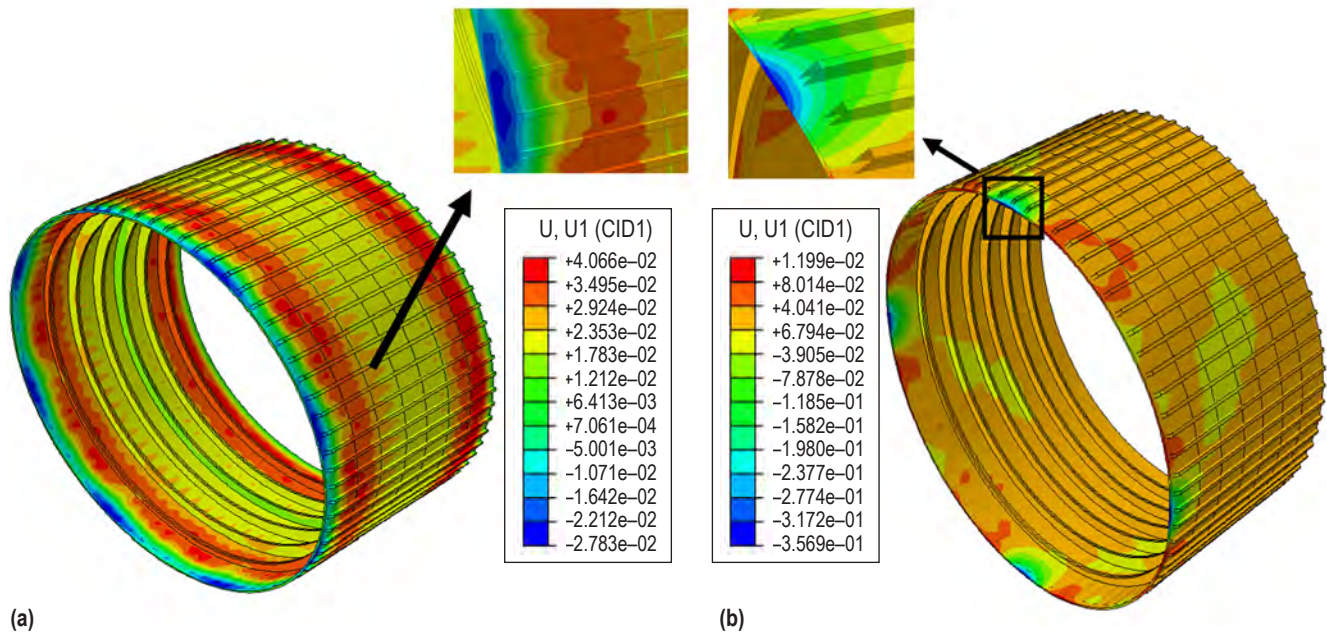


Figure 60 Radial deformations in LH₂ simulator: (a) Just before buckling, and (b) at the end of the analysis.

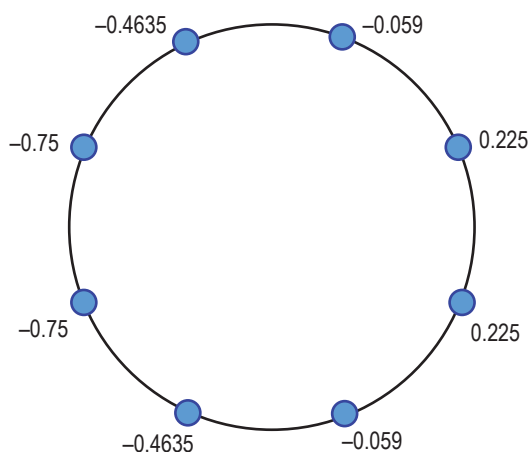


Figure 61. Axial displacement of load jacks (in inches).

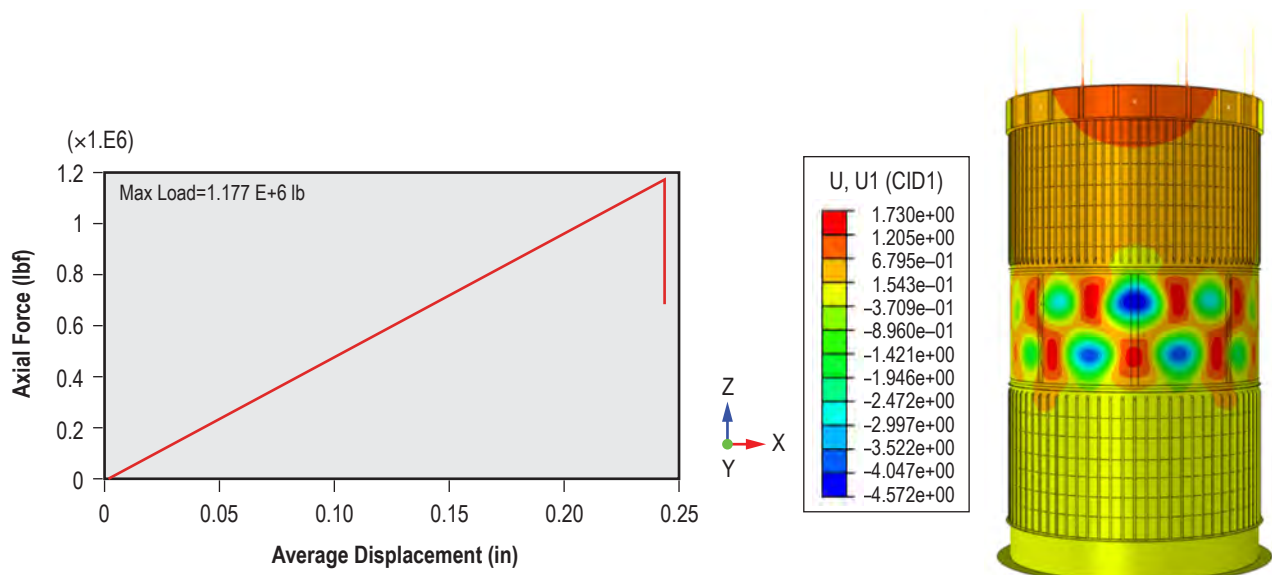


Figure 62. Load versus displacement curve and radial deformation contours in stack.

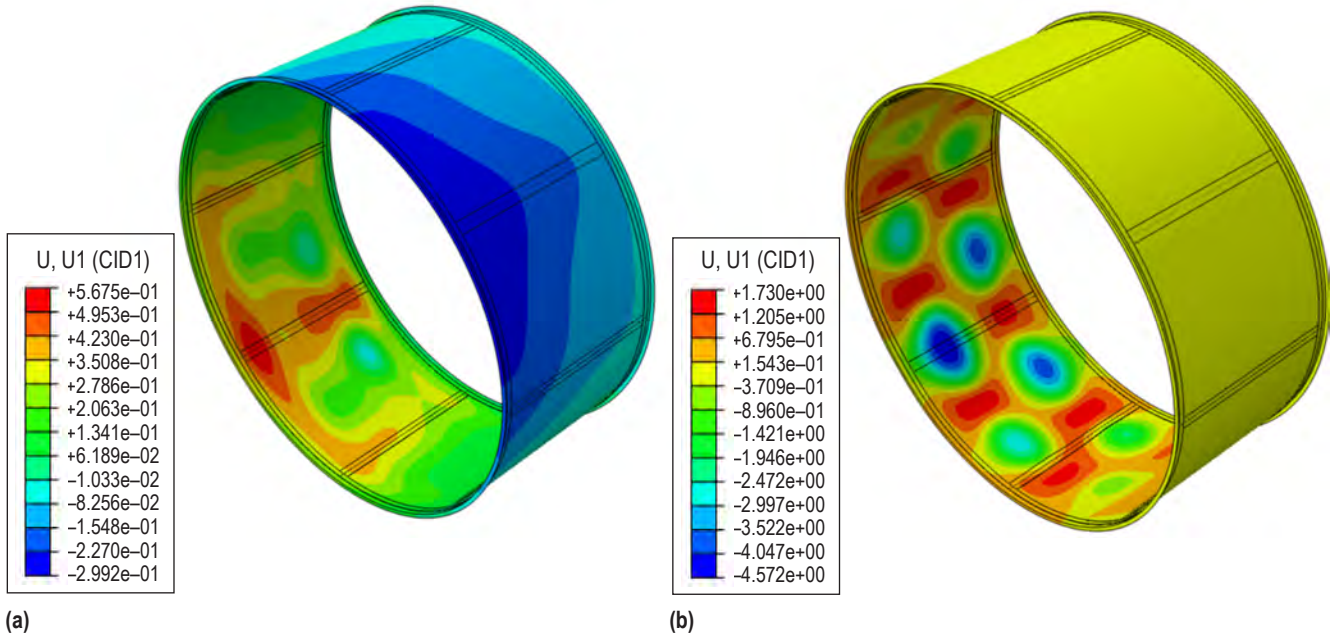


Figure 63. Radial deformation contours in the STA: (a) Just before buckling and (b) just after buckling.

In figure 64, the maximum in-plane, principal-strain distribution in the LH₂ simulator just before and after buckling is presented. Since strain values are not verified for convergence, they should be used for qualitative purposes only.

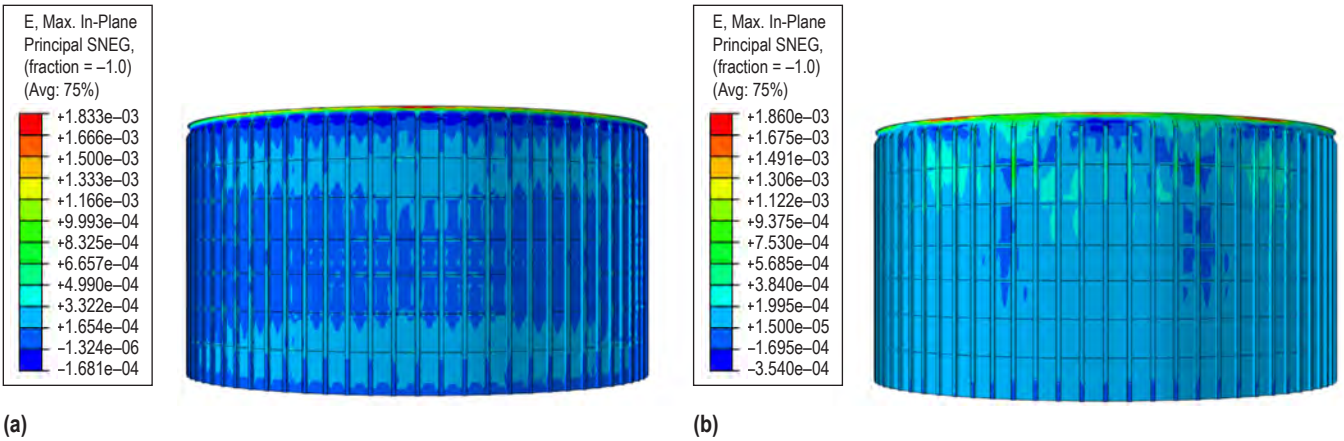


Figure 64. Strain contours in LH₂ simulator: (a) Just before buckling and (b) just after buckling.

There was still some residual concern that the test facility would be unable to test the STA to failure without damaging the simulators. A nonconventional approach to buckle the STA was explored to assess the performance of the full stack model without damaging the simulators. In this configuration, all of the load jacks were uniformly deformed by 0.75 in, and a transverse load of 1 kip was applied normal to the surface and in middle of the longitudinal joint as shown in figure 65. The transverse load resulted in an inward radial deflection of 0.19 in at the load application point. The intent was to ‘trip’ buckling failure prior to the nominal buckling load.

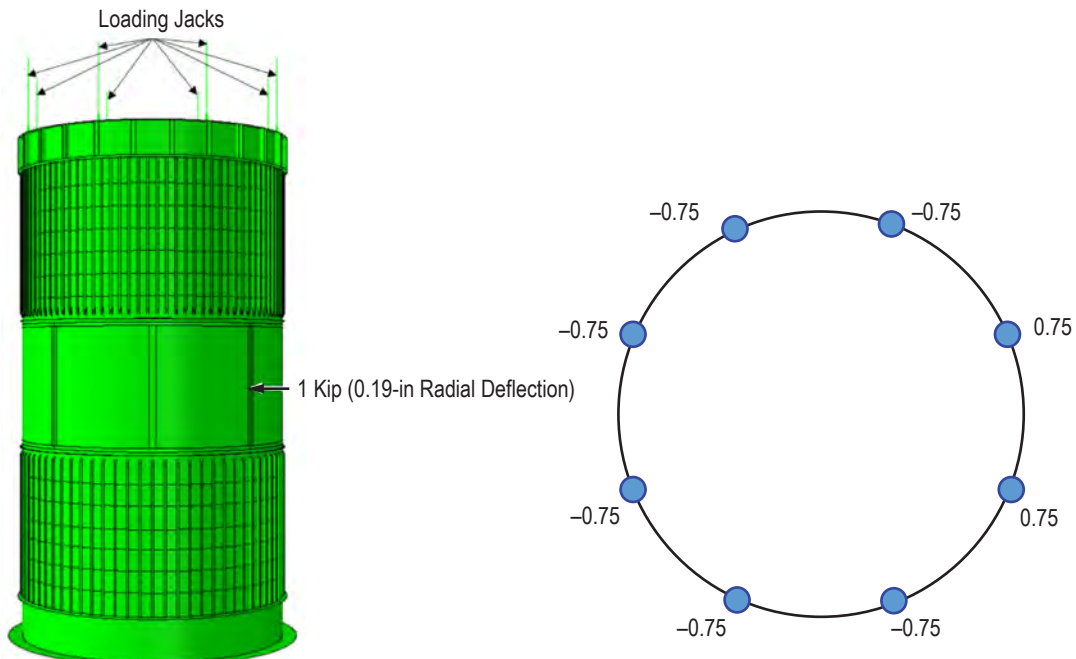


Figure 65. Displacement and load configurations (in inches).

This load configuration, like the previous one, resulted in one side of the STA experiencing more compression than the other side and resulted in nonuniform buckling of the STA as shown in figure 66. In figure 67, radial displacement of the STA before and after buckling is presented.

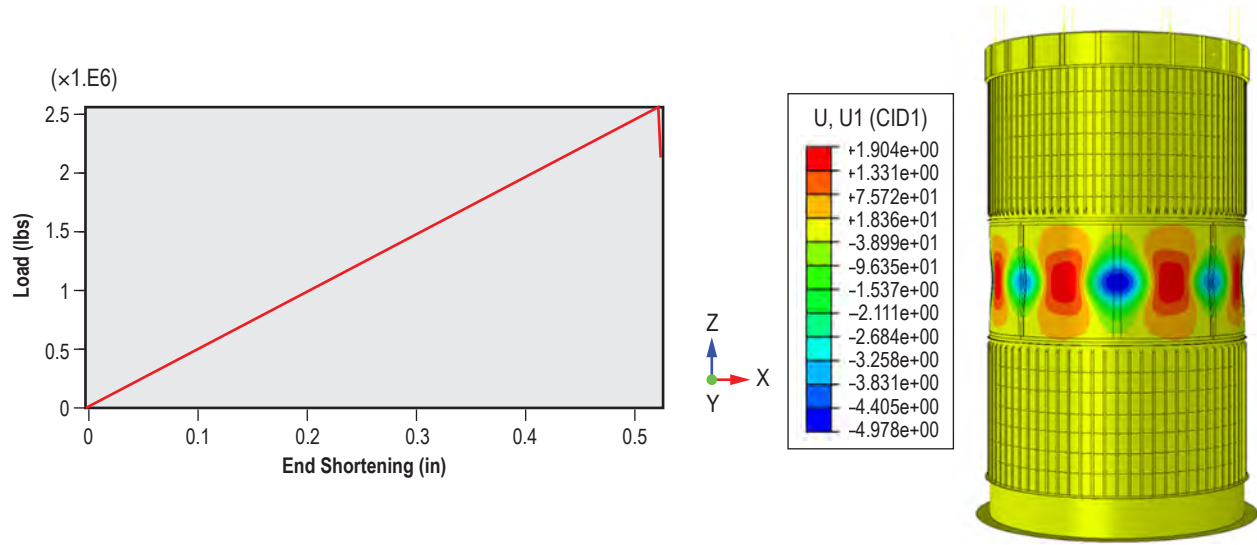


Figure 66. Load versus displacement curve and radial deformation contours in stack.

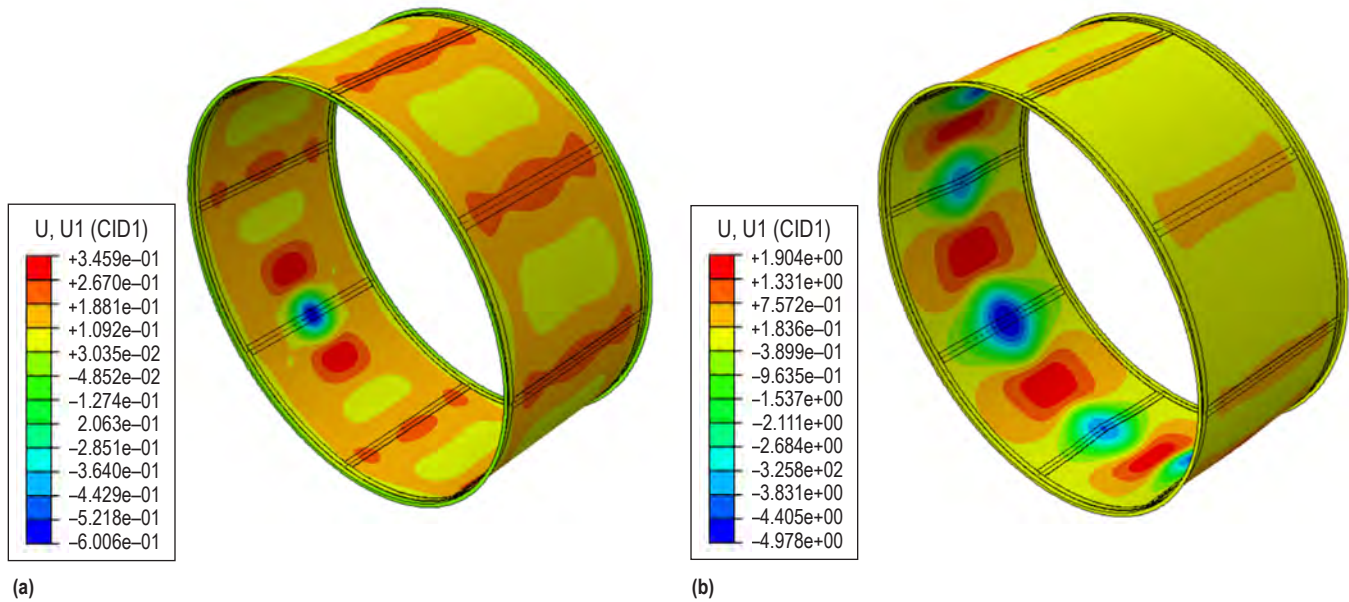


Figure 67. Radial deformation contours in the STA: (a) Just before buckling and (b) just after buckling.

Table 23 shows the buckling load, line load, and the in-plane principal strain in the LH₂ simulator for all three load configurations analyzed in this study. The in-plane principal strain should be used in assessing changes to the strain distribution in the simulator when the load configuration varied among the three load cases.

Table 23. Summary of buckling load line load and principal strain.

Type of Loading	Buckling Load (lb)	Max Principal Strain At Buckling (μ)	Line Load (lb/in)
Uniform axial displacement	3.46 E+6	1,549	3,327.35
Bending moment	1.18 E+6	1,833	1,134.76
Uniform axial displacement with 1 kip transverse load	2.55 E+6	1,232	2,454.24

4.2.2.4 Buckling Load Sensitivity to Geometric Imperfections Study. The STA along with the simulators and load ring models were analyzed to evaluate the sensitivity of the buckling load of the STA to manufacturing geometric imperfections. Axial displacements were applied to the load jacks as to simulate the Ascent Bin 8 (Max Q) loads (fig. 68). Transient dynamic nonlinear analyses were performed on a STA perfect geometry model and a STA model with imperfections that were scaled and superimposed on the nodal coordinates of the STA. The imperfections were taken from a composite 8-ft barrel mandrel from Griffin Aerospace. The magnitude of the imperfections was 1X the measured imperfections from the Griffin Aerospace 8-ft mandrel as shown in figure 68. In reality, the actual imperfections of a STA if manufactured could vary from the assumed imperfections in this study.

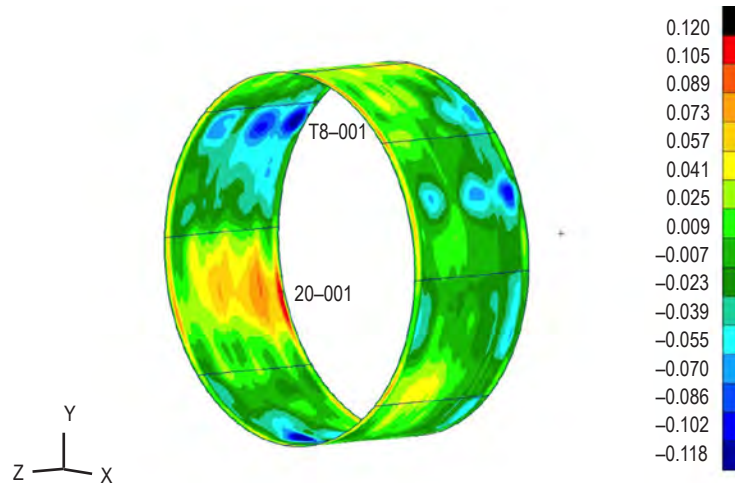


Figure 68. Nodal imperfections applied to the STA.

The load-deflection curve from the transient dynamic nonlinear analyses for the perfect STA and STA with imperfections is shown in figure 69. The perfect STA model a load ratio of 3.91 for F_z and 3.93 for M_y at buckling. The STA with imperfections has a load ratio of 3.62 for F_z and 3.64 for M_y at buckling which is a reduction in the buckling load by 7.4%. Figures 70 and 71 show the radial deformation for the perfect STA and STA with imperfections, respectively at the buckling load and the last load increment in the transient dynamic analysis.

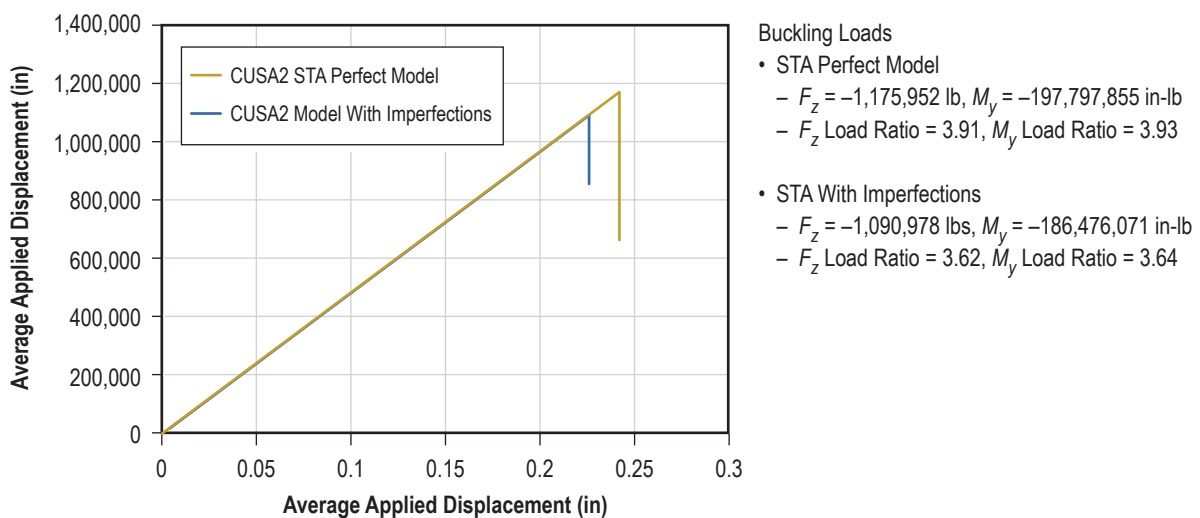


Figure 69. Load deflection curve of transient dynamic nonlinear analysis.

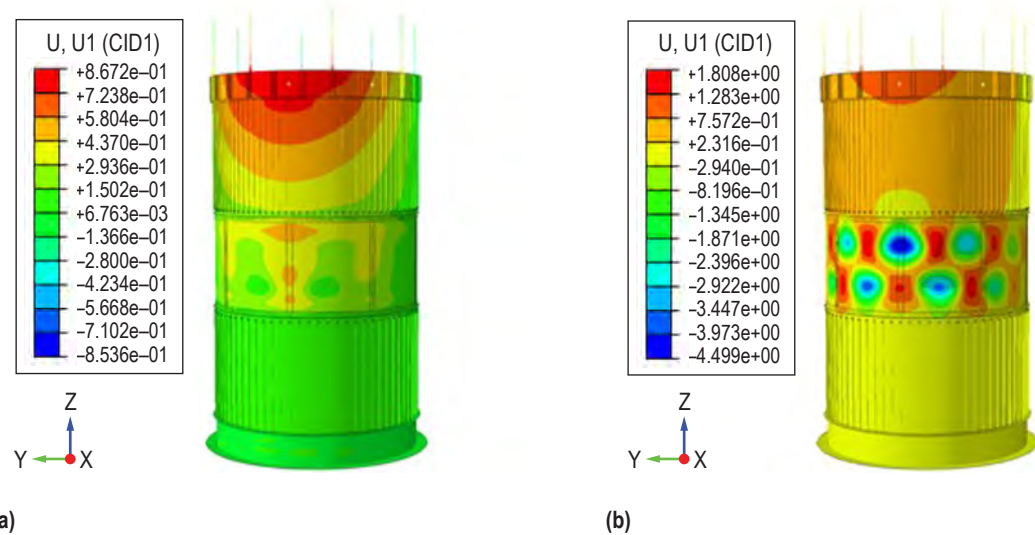


Figure 70. Radial deformation of perfect STA model: (a) At buckling load and (b) at last load increment in the transient dynamic analysis.

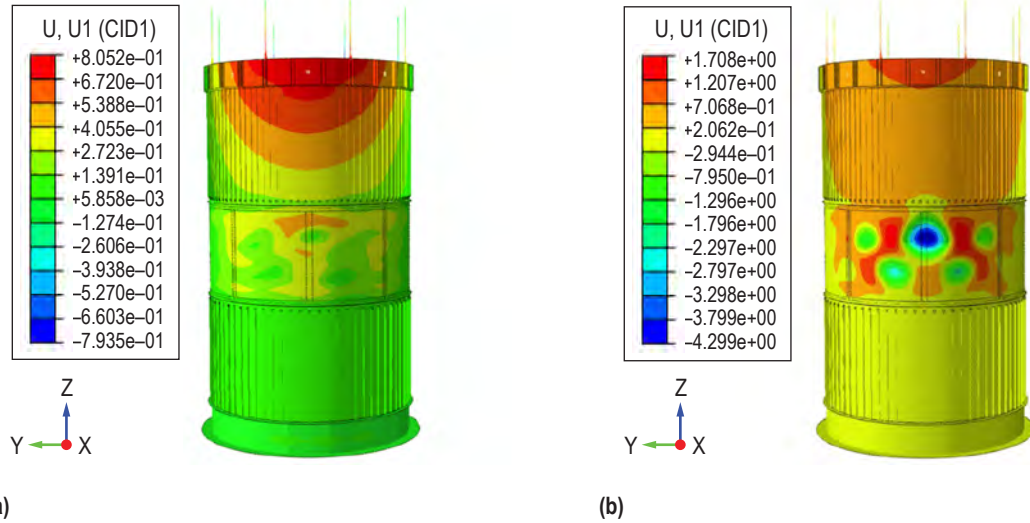


Figure 71. Radial deformation of STA model with imperfections: (a) At buckling load and (b) at last load increment in the transient dynamic analysis.

A comparison of the buckling load ratio and its corresponding compressive line load are listed in table 24, as well as an eigenvalue buckling analysis and the nonlinear transient dynamics analysis for the perfect STA model and STA model with imperfections.

Table 24. Summary of buckling load sensitivity to geometric imperfections study.

Model	Buckling Load Ration	Compressive Line Load (lb/in)
0.5-in sandwich core eigenvalue buckling analysis	4.03	3,522
0.5-in sandwich core transient dynamic analysis—perfect	3.91/3.93	3,426
0.5-in sandwich core transient dynamic analysis—imperfection	3.62	3,178

4.2.3 Trade Studies

4.2.3.1 Core Density (4.5 pcf versus 3.1 pcf). Initially, a honeycomb core with a density of 4.5 lb pcf was selected for the STA in order to simplify manufacturing. The thin foil used in some lighter core constructions can prove difficult to handle. However, there are opportunities to achieve mass reductions for the virtual flight model (VFM) using lower density core than the core planned for the STA. The Core Density trade study was an attempt to understand the impact of this type decision on the performance of the VFM.

Manufacturing large panel segments calls for handling 96-in×48-in aluminum honeycomb core segments. This can lead to core damage. The large spacecraft structures and materials manufacturing effort used 3.1-pcf-density core with 0.125-in cell size and 0.0007-in foil thickness. The big core segments with the thin foil damaged easily, and required lots of inspection and core

edge straightening. To mitigate damage, a 4.5-pcf core with $\frac{1}{8}$ -in cell size, 0.001 in foil thickness was selected for the STA. To show the potential for mass improvements a 3.1-pcf core with $\frac{3}{16}$ in cell size, 0.001-in foil thickness was selected for a trade study. This larger cell size could lead to print through and facesheet dimpling with the co-bonded manufacturing approach. This dimpling between larger cells has the potential to reduce ultimate buckling load (due to local imperfections) or to reduce facesheet strength. Table 25 shows the test matrix adopted to evaluate the buckling and strength concerns by using the larger cell size.

Table 25. Lightweight core validation test plan.

Test	Coupon	Environment	No. of Coupons
Edgewise Compression (ASTM C364)	3.1 pcf per drawing 1281253-001	RTD	5
Edgewise Compression (ASTM C364)	4.5 pcf per drawing 1281253-003	RTD	5
Buckling	3.1 pcf per drawing 1281251	RTD	5
Buckling	4.5 pcf per drawing 1281253	RTD	5

4.2.3.1.1 Panel Manufacturing. Two sets of panels (4.5- and 3.1-pcf core) were fabricated using the MSFC and LaRC AFP machines. The panels were of sandwich construction with 4.5- and 3.1-pcf, 1-in-thick perforated aluminum core (5052 and 5056) with ($\frac{3}{16}$ and $\frac{1}{8}$ in) hexagonal cell sizes and 8-ply quasi-isotropic graphite/epoxy facesheets (IM7/8552-1) with (45°/0°/-45°/90°)_s stacking sequence. The intent was to show equivalence between the two different tow widths on the AFP systems. At the end of the CEUS program, the MSFC panels were prepared in different samples to complete the testing, but budget and schedule constraints made it impossible to do the same for the panels fabricated at LaRC.

4.2.3.1.2 Panel Nondestructive Evaluation. The panels built at MSFC were verified by ultrasonic inspection. Inspection results showed a few indications of bad areas between facesheet and core; these areas were cut around and not part of the panel sections delivered for testing. The complete inspection report is given in appendix E—Manufacturing.

4.2.3.1.3 Pretest Predictions.

4.2.3.2 Test Articles and FEMs. The as-machined coupons from the parent panels were 40.2×6 in and 8.2×6 in for buckling and EWC specimens, respectively. The core material was removed from the ends (1.2-in deep) and EA 9394 was used to fill the 1.2×6×1-in empty space. The intent was to reduce the risk of crushing the core at the ends. After a full room temperature cure, the specimen ends were potted with EA 9394 epoxy grout, using 1-in-thick aluminum plates cut from 0.25-in-thick-wall extruded tubes. Prior to this, the specimen-end was centered in the slot and squared. The slots at the panel's corners at the edge remained unfilled to form an open cavity in order to act as stress relief features. Finally, the specimen ends were machined flat and parallel.

Femap and NX NASTRAN were used for pre- and post-processing and to assess buckling (SOL 105) and strength (SOL 101) performance. Two-dimensional plate (PCOMP) elements were used to model the facesheets, while solid elements were implemented for modeling the core (four elements through the thickness) and potted ends. The in-plane mesh size was in the order of 0.2×2 in. Rigid elements were used at the top and bottom to apply boundary conditions and a compressive axial load. The models and end condition details are shown in figure 70.

Core properties came from the Hexcel data sheet, while facesheet properties are from table 21 (Pristine allowables) (J. Reeder, NASA Internal Memo, Property Values for Preliminary Design of the Ares I Composite Interstage, 2007).

The coupons (and FEMs) were identical for both the buckling and edge-wise compression test articles, except for the EWC coupons that were 32 in shorter. Figure 72 shows both buckling and EWC FEMs with end-fitting details.

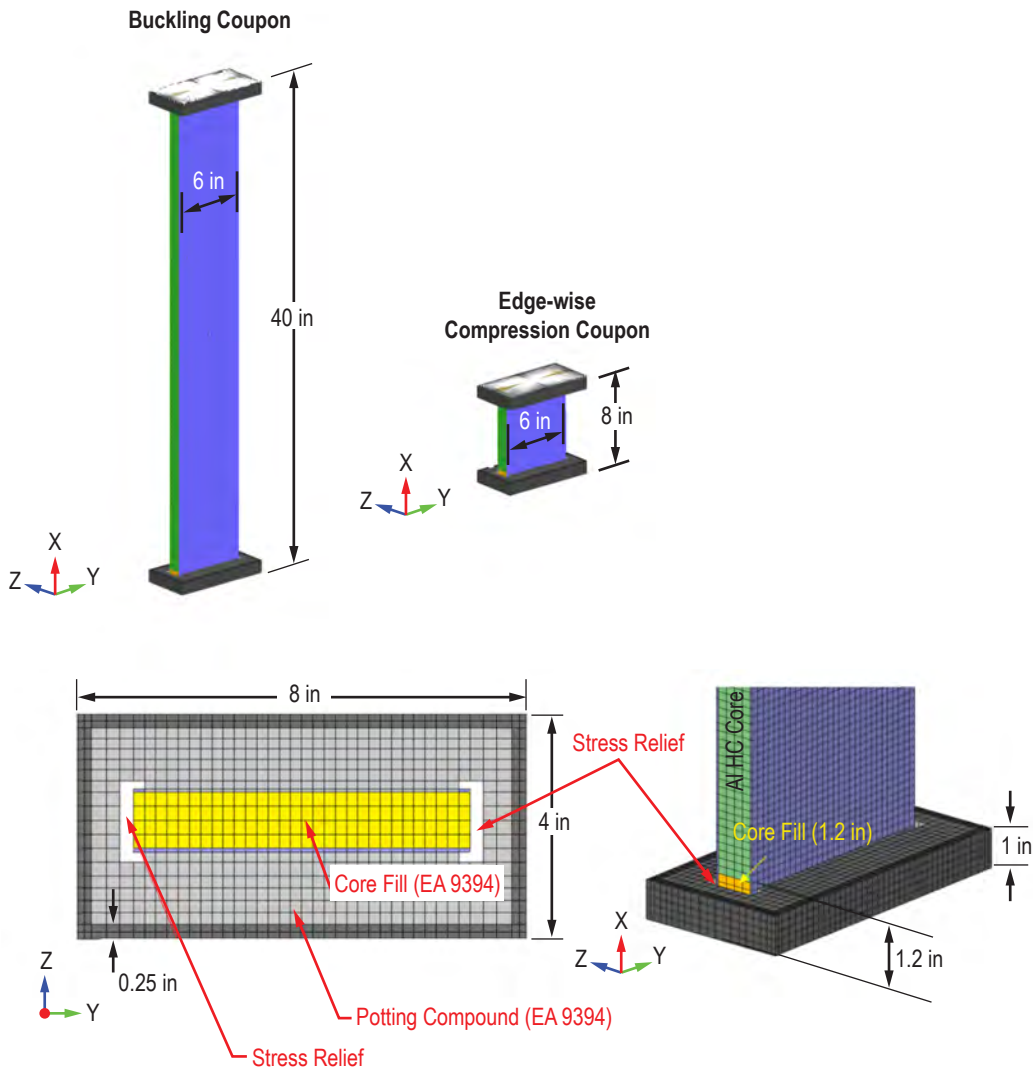


Figure 72. Buckling and EWC and FEMs with end-fitting details.

4.2.3.3 Finite Element Analysis (FEA) Results. Table 26 summarizes the predicted failure loads and end-shortening loads for both EWC and buckling specimens.

Table 26. Predicted loads and end-shortening: Core trade study.

Test	Core Density (pcf)	Predicted load at Failure (kip)	Predicted End-Shortening (in)
EWC	3.1	58.1	0.07
	4.5	58.1	0.07
Buckling	3.1	36.7	0.25
	4.5	38.4	0.26

Figure 73(a) and 73(b) also illustrate the buckling performance (SOL 105 results) for the 4.5 and 3.1 pcf core, respectively.

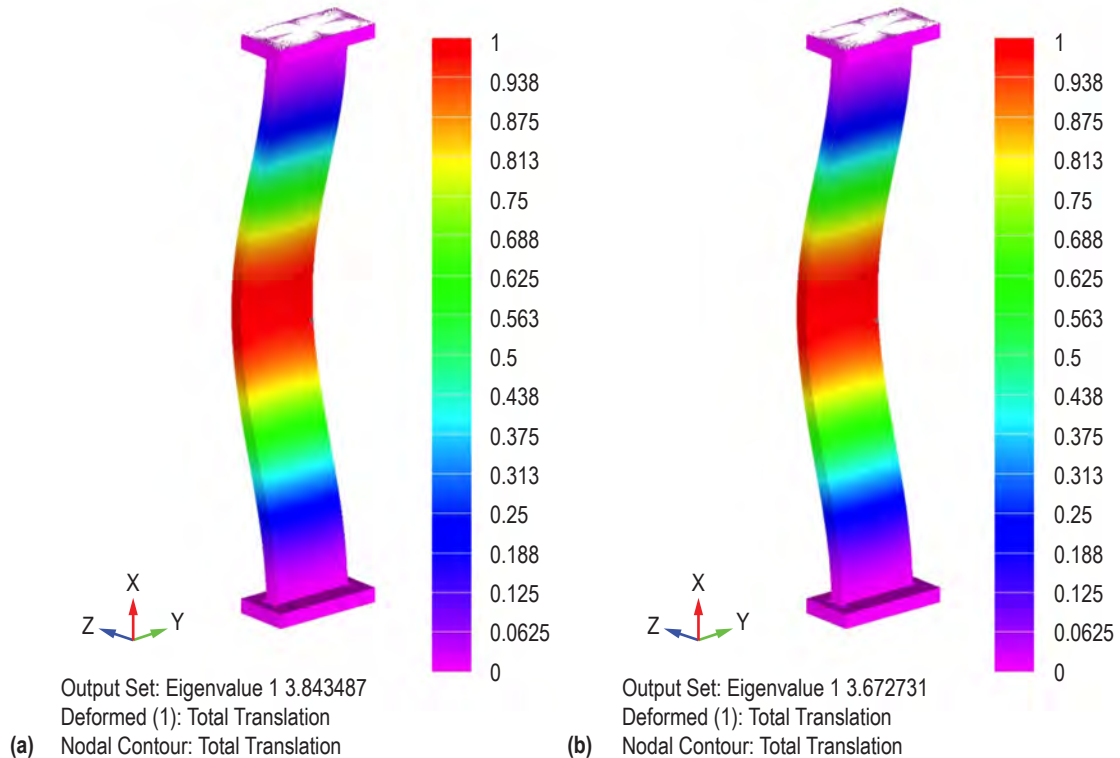


Figure 73. Buckling performance: (a) 4.5 pcf and (b) 3.1 pcf core models.

The facesheet, core, and core-fill strengths were also assessed at these buckling critical loads to ensure that the buckling will be the primary failure mechanism for these coupons. For instance, for the 4.5 pcf core, the facesheet failure index (FI), based on maximum strain failure criterion, at the buckling critical load of 38.4 kips is about 0.66. Realizing that $FI \geq 1$ indicates failure, this FI (fig. 72) provides a healthy margin against facesheet strength failure at buckling. Core and core-fill stresses are relatively low and show no risk of failure prior to buckling.

For the EWC coupons, on the other hand, the primary failure mode is facesheet failure that occurs at 85.1 kips. Failure index contour of these specimens at the ultimate load indicates an $FI = 1$ (fig. 74). It should be noted that this FI is calculated based on pristine allowables of J. Reeder's Memo, which carry some statistical basis. The actual strength value for the lamina (and facesheet) could be at a higher value.

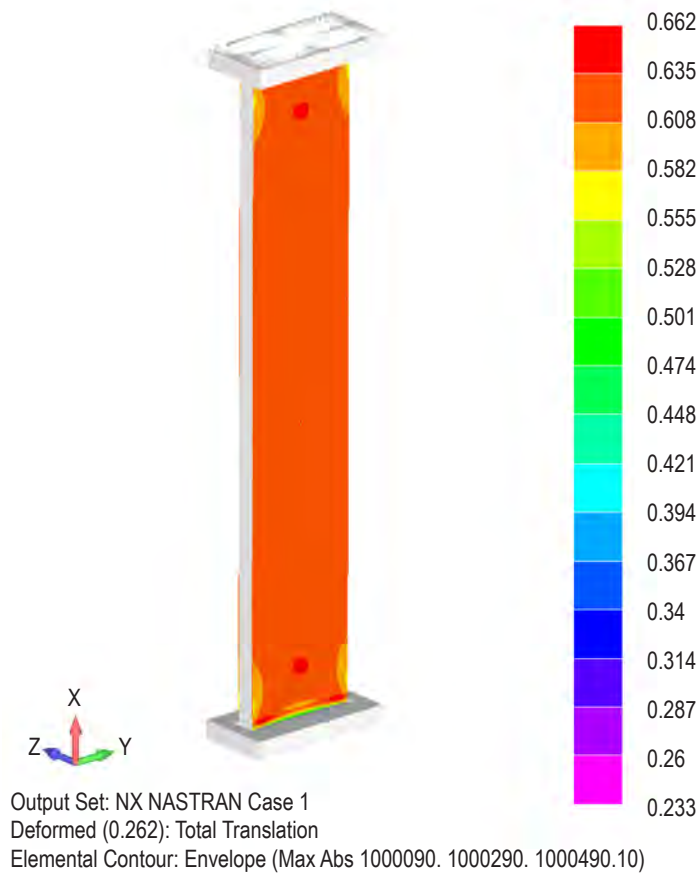


Figure 74. Facesheet failure indices at buckling.

4.2.3.3 Test Results. Test results were not available in time for publication of this Technical Memorandum.

5. MANUFACTURING

Manufacturing for the CEUS project was intended to be a NASA internal effort. Section 5 will focus on the MSFC effort to mature, develop, and procure tooling for processes specifically tailored for highly optimized thin sandwich parts. Due to the aggressive accelerated schedule, the tooling procurement was initiated well before a preliminary design cycle was complete. While from a scheduling viewpoint this appeared attractive, it presented several challenges and, ultimately, resulted in increased cost due to design changes early in the tool development.

A cure cycle effort was initiated to advance a cure cycle based on historical processes for 8-ply-thin laminates over a 3.1pcf core. It was observed early in the project that the traditional cure cycle was resulting in areas of increased porosity. Historically, this has been observed with thin laminates and low-density core during co-cure processes. A multistep cure cycle approach was adopted to closely control the flow of the film adhesive and incrementally increase the pressure to result in a decreased amount of observed porosity.

The Manufacturing section will also cover the full size panel fabrication trials that were performed using the tooling package and cure cycles. Limited mechanical tests were performed before project cancellation that indicated the processes under development would have been suitable for the full-scale fabrication effort. The team was also in the process of developing a mature concept of operations for full-scale assembly. This effort was not fully matured and was left at the conceptual design phase. Further work is needed to define the assembly requirements and tooling necessary.

5.1 Tooling Development

The CEUS barrel concept specified a segmented panel arrangement. To facilitate this design required using a $\frac{1}{8}$ OML-tooled, fiber-placement breakdown mandrel capable of withstanding 350 °F cures.

During manufacture of the tooling packages, numerous project reviews and technical coordination meetings were held to ensure functionality, schedule adherence, and cost validity. Typically, the following meetings were held for each tool:

- (1) PDR held within 1 month of contract award to review and establish tooling concepts.
- (2) Final design review of preferred design specifics and provide authority to complete tool design.
- (3) Tool design buyoffs review completed design and provide authority to begin tool fabrication.
- (4) Physical tool buyoffs review fabrication and inspection data and provide authority to ship.

5.2 Composites for Exploration Upper Stage Tooling Requirements

The CEUS tooling activities are as follows:

- (1) Facilitate the accurate creation of the CEUS within the stated tolerance range when cured at the specified 350 °F cure temperature. The concept for the CEUS Tooling Design is shown in figure 75.

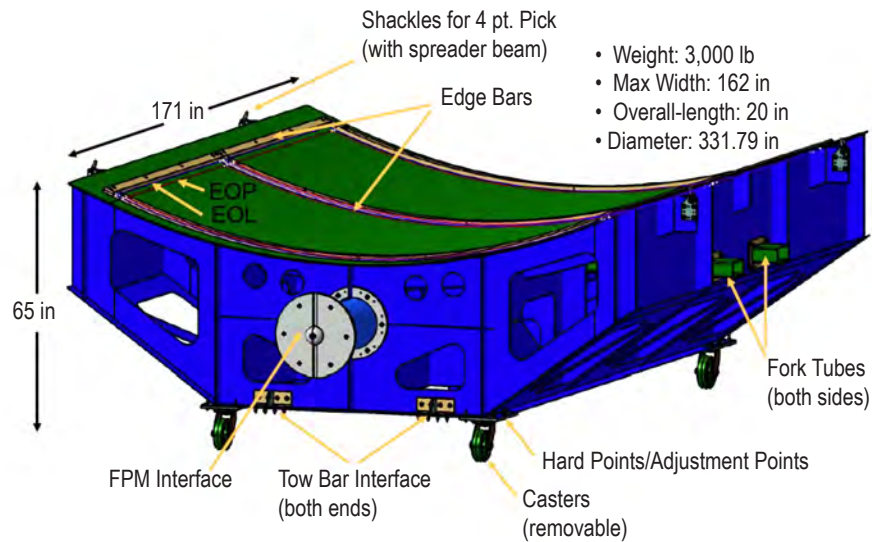


Figure 75. CEUS tooling design concept.

- (2) Meet an as-fabricated profile tolerance of ± 0.01 in. In addition to meeting the specified tolerances, the tool surface shall be smooth and fair with a surface finish of root-mean-square roughness of 32 μ in or better on all surfaces within the edge of part (EOP).
- (3) Include EOP scribble lines in layup tool.
- (4) Include part number and measured weight in identification.
- (5) Ensure tool is capable of tolerating 350 °F during cure without any mold degradation. This allows for temperature variations during the specified 350 °F cure cycle.
- (6) Design tool with capability of withstanding, at a minimum, fifty 350 °F cure cycles, each cure cycle consisting of a dwell at 350 °F for 4 hr.
- (7) Design tool with a minimum additional 12-in minimum run-out on all sides.
- (8) Ensure tool is able to fit through an 18-ft-wide door and be capable of being lifted by a 5-ton crane with a single hook.

(9) Have lifting provisions that include four host rings on the backup structure for overhead crane operations and two pair of forklift tubes (4 in×8 in×60 in minimum rectangular steel tubes), 180° apart.

(10) Adhere to the following minimum factors of safety achieved throughout the tool's life:

- 5 FS on ultimate strength.
- 3 FS of yield strength (metal parts only).

(11) Ensure tool can withstand the following transportation loads; loads are assumed to occur simultaneously in each of the three directions:

- ±2 on fore/aft g's.
- ±2 on lateral g's.
- +3, -1 on vertical g's.

(12) Provide work platform that will allow access to the tool surface while in the vertical orientation of the AFP cell rotators. Platform design shall meet OSHA (rails and toe boards and stability) requirements and be rated for 1,000 lb (load rating in pounds must be marked on platform).

(13) Construct tool surface of a carbon laminate. A polyimide topcoat to increase surface hardness and chemical resistance is required.

(14) Supply edge bars capable of fabricating two panels on the tool:

- The edge bars shall have a cross section of 3 in wide and approximately 1.25 to 1.5 in thick. (The thickness will be finalized at the design and analysis review based on the finalized government design.)
- The edge bars shall be chamfered to accommodate vacuum bagging.
- The inside edge shall be located 2 in beyond the EOP.
- Edge bars shall be divided into segments for ease of handling.
- Tooling pins shall be located and sized to support a deflection of no more than 0.020 in at 80 psi autoclave pressure at the 350 °F cure cycle.

(15) Design tool to have vacuum integrity with a maximum leak rate of $\frac{1}{4}$ in Hg in 60 min at 27 in Hg.

(16) Support tool substructure with at least four removable casters between 8- and 12-in-diameter phenolic wheels, swivel locks, and brakes.

(17) Supply three caul sheets, designed and fabricated to impart a smooth tool surface on the bag side of the part during the curing process:

- The caul sheet shall be fabricated from carbon laminate and shall be sized to approximately 0.042 in.
- The caul sheet shall be fabricated net to edge of part.
- The caul sheet shall not require indexing scribe lines.

(18) Provide a tow hole at each end of tool, with an approximate 3.5-in diameter with steel-reinforcement plate to allow for transportation with a forklift or tug, as shown in figure 76.



Figure 76. CEUS final tool.

After arriving at MSFC, the tooling surface tolerances were verified using structured light scanning. The critical surface dimensions were within the specified tolerances, as shown in figure 77.

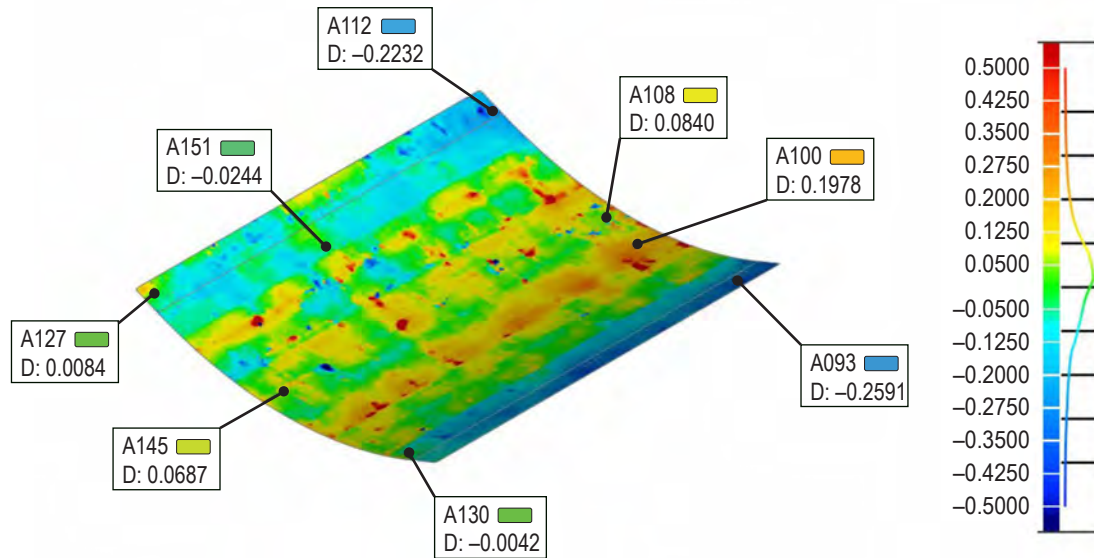


Figure 77. CEUS metrology (dimensions are in mm).

The CEUS tool was interfaced with the MSFC AFP cell (fig. 78) and located in the machine coordinate system. The trial for the CEUS tool AFP are depicted in figure 79. Programs were generated based on initial sizing. One of the major objectives of the CEUS project was to demonstrate accurate AFP over aluminum honeycomb core similar to what will be experienced at potential vendors.



Figure 78. CEUS tool installed in MSFC AFP cell.

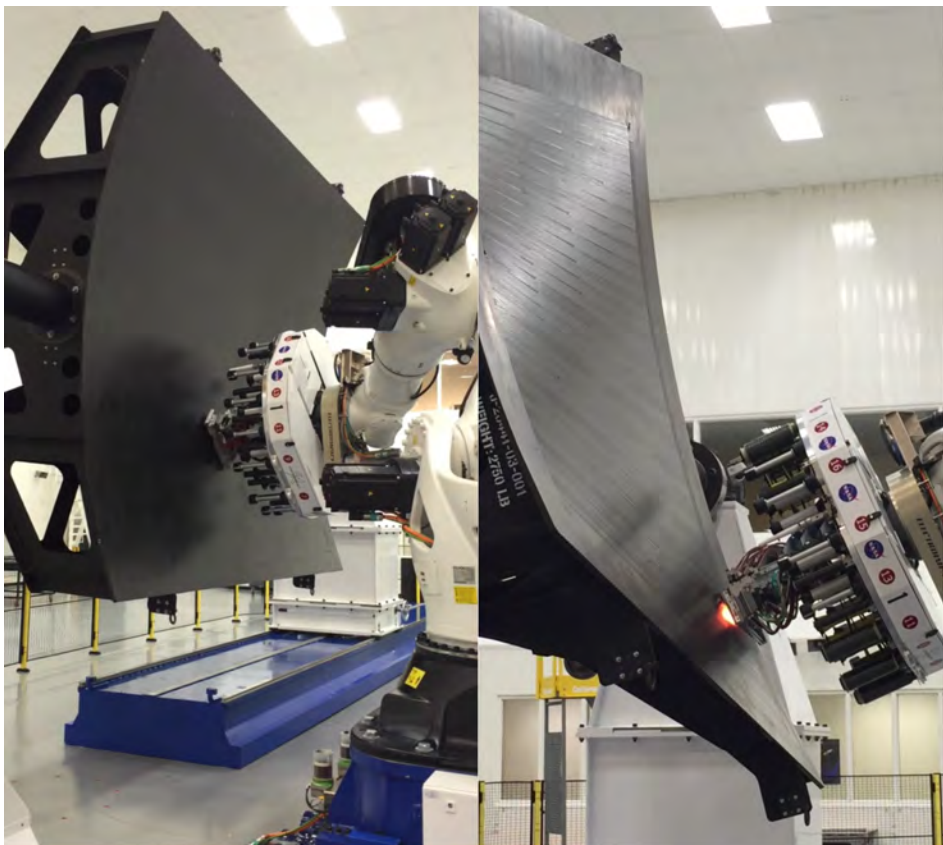


Figure 79. CEUS tool AFP trials.

5.3 Assembly Concept

This section contains the project top-level goals centered around the development of equipment, tools, and processes necessary to support the manufacturing of the CEUS large composites structures. Specifically, the following is a list of initial efforts that will focus on developing techniques needed to manufacture the CEUS:

- (1) Develop designs for tooling that support ease of manufacturing of the composites structures.
- (2) Develop designs for tooling that is configurable to accommodate multiple composite panel configurations.
- (3) Minimize operational complexity and cost. Design the tooling in such a way that frequent transfers between tools is not necessary.
- (4) Integrate tooling with the current flow of operations that NASA uses in manufacturing the composite panels. This work will be an extension of the processes that are already in place.
- (5) Begin scope of the tooling with receipt of a cured, trimmed, and machined panel. End scope of the tooling with a fully assembled interstage that has been transferred to a transporter.

The assembly tool is used during assembly of eight panels into one completed CEUS. This tool includes the following elements and capabilities, which are further refined in the CEUS Assembly Requirements document:

- Base and drive mechanisms:
 - Includes the base supports and the drive mechanism for rotating the CEUS.
 - The base supports are such that the lower edge of the aft ring are 3 to 6 ft above the floor surface, to allow personnel to have access to the aft ring during assembly operations.
 - The base has provisions for a smaller or larger barrel diameter.
- Drill station:
 - Supports drilling holes that are normal to the CEUS surface.
 - Performs match-drilling of aluminum flanges to composite panels.
 - Performs match-drilling of composite splice plates to composite panels.
 - Accommodates drilling of through-holes near the edges of each panel section.
 - Drills tower for indexing of holes in the vertical direction along the full height of the CEUS.
 - Tracks system for indexing the drill tower around the perimeter of the CEUS; limited to $\frac{1}{8}$ or $\frac{1}{4}$ of the CEUS circumference due to ability to rotate the entire assembly.
 - While in use, the towers should not restrict the ability of personnel to perform other assembly operations.
 - Drill station located such that bonding and drilling operations can occur simultaneously at two different joints (e.g., located 40 degrees from each other, or a multiple thereof).

- Bonding station:
 - Accommodate application of heat and pressure for curing joints and doublers, both sides of panel simultaneously.
 - Support pressure application up to 20 psi along entire joint height and across ~20 in of CEUS circumference at a time; pressure applied evenly along entire surface.
 - Support controllable heat application up to 250 °F (TBD) along entire joint height and across ~20 in of CEUS circumference at a time; heat applied evenly along entire surface.
 - Bonding station should be located such that bonding and drilling operations can occur simultaneously at two different joints (e.g., located 40 degrees from each other, or a multiple thereof).

- Tower sections:
 - Include provisions for precisely locating splice plates.
 - Are moveable to accommodate rotation of the CEUS assembly without interfering with other fixed assembly jig pieces.
 - Are moveable to accommodate removal of completed CEUS (if needed).
 - While in use, the towers should not restrict the ability of personnel to perform other assembly operations.

- Upper (forward) flange stiffening ring:
 - The upper stiffening ring attaches to the top of the vertical supports.
 - The upper stiffening ring includes a ring that accepts the forward flange pieces and has adjustments for locating the forward flange pieces.

- Lower stiffening ring:
 - Lower (aft) flange stiffening ring.
 - The lower stiffening ring attaches to the base and drive mechanism.
 - The lower stiffening ring receives the aft flange and has adjustments for locating the aft flange pieces.
 - The lower stiffening ring includes a rail system to allow rotation of the aft flange ring, which is itself connected to the vertical supports that are connected to the upper stiffening ring.

- Vertical supports:
 - The vertical supports interface between the lower stiffening ring and the upper stiffening ring.
 - The vertical supports include adjustments for the distance between the lower and upper stiffening rings and for the orientation of the lower and upper stiffening rings relative to one another (e.g., twist through the vertical axis).
 - Features.

- Access provisions:
 - The lower stiffening ring provides personnel access to bottom edge of the aft flange by providing 3 to 6 ft of clearance between the bottom edge of the aft flange and the facility floor.
 - Provide personnel access to top edge of the CEUS for installation of a ring.
 - Provide personnel access to inside of CEUS for section joining, etc.

- Sizing and adjustments:
 - 27.5-ft-diameter CEUS (nominal); with provisions for a minimum barrel diameter of 216 in and a maximum diameter of 330 in.
 - Approximately 13-ft-tall barrel section, including flanges, with provisions for accommodating a minimum barrel height of 60 in and a maximum height of 180 in.
 - Adjustments to bring the barrel sections into alignment for bonding and joining.
 - Interface constraints.
 - Interfacing with the facility beyond bolting equipment to the floor is not required.
 - Desire to not break the concrete floor and no concrete trenching for installation of fixture or equipment.
 - Ability to accommodate installation of a vertical separation joint is not necessary.

The assembly fixture concept and finished CEUS are pictured in figure 80.



Figure 80. Assembly fixture concept and finished CEUS.

5.4 Automated Fiber Placement Trials

Multiple large-scale composite sandwich panels were fabricated at MSFC using AFP in an effort to determine a variety of processing parameters associated with AFP and composite processing in general. The AFP parameters in question are compaction force, heater output, and feed rates. Other composite processing steps were developed, such as vacuum bagging sequences, core splice installation techniques, ply debulking frequency, and tool preparation details. The following list outlines the process developed at MSFC for fabricating large honeycomb core sandwich panels using AFP:

- (1) Tool preparation is key to allowing parts to release from the tool easily and controls, to some extent, the surface finish of the parts. It was found that, for the composite tools, tooling sealer Chemlease MPP117 only needs to be applied after the tool undergoes a reworking which would involve thorough wiping with solvents and could include light sanding. Two coats of tooling

sealer were applied, allowing 30 minutes for each coat to dry. After the tooling sealer was applied/dried, two coats of mold release, Frekote 700-NC, were applied, again allowing for 30 minutes between coats. This combination of initial tool sealer and mold release is sufficient for at least four autoclave cure cycles. After four cure cycles, two coats of NC700 should be applied. It was found that excessive use of tool sealer/mold release leaves a dull, milky finish on the composite parts. Also, only alcohol should be used to wipe the tool surface, acetone was found to be too aggressive of a solvent and required the reworking of tools.

(2) Once the tool is cleaned and prepared the first ply of composite ($\frac{1}{2}$ -in-wide IM7/8552-1 tow) was laid down using the AFP machine. It was found that the composite tape had sufficient tack to stick to the tool at ambient room temperatures without using a tackifier. For the first ply and solid laminates in general, a compaction force of 150 lb was determined to be sufficient. The heater was set to 150% for the first few plies; as the laminate becomes thicker, the heater should be reduced to 100%. As the laminate is being built, the tool/laminate starts to retain heat, and that increases the tack of the composite, which raises the tendency for tows to stick to the AFP compaction roller. A feed rate of 12,700 mm/min was used for the first ply to ensure the tows stick to the tool surface. For subsequent plies, the feed rate was increased to as much as 17,780 mm/min.

(3) After the first ply was laid, a debulk vacuum bag was installed to ensure the ply was adhered to the tool. The debulk should last for a minimum of 30 minutes. The debulk bagging scheme should follow the diagram in figure 81.

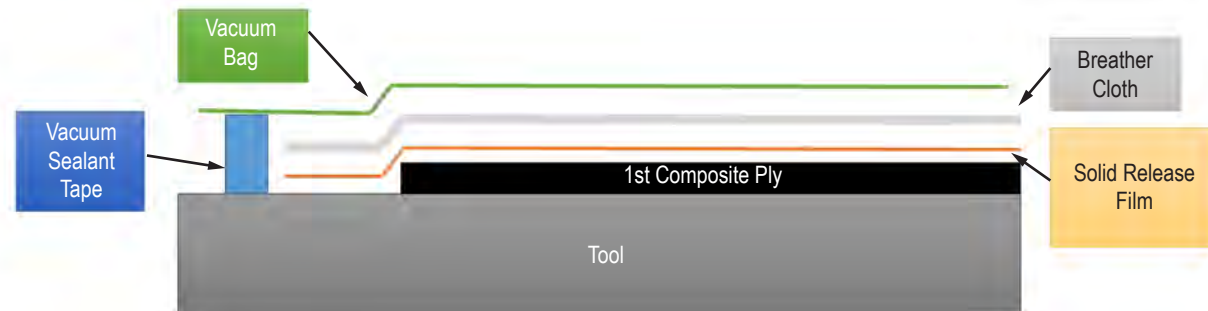


Figure 81. Debulk vacuum bag schematic.

(4) After the first ply is debulked, the vacuum bag is removed, and the remaining plies can be fiber placed again using a feed rate of up to 17,780 mm/min, 150 lb of compaction force, and a heater setting of 100%–150 %.

(5) Once the first laminate is laid (fig. 82), the structural film adhesive (FM300-2) is installed onto the composite surface (fig. 83). The film adhesive is cut to the appropriate sized patterns using an automated Geber cutting table. The joints between adjacent film adhesive pieces should be overlapping a minimum of 0.25 in with a maximum overlap of 1 in. The overlapping of the adhesive ensures complete adhesive coverage of the composite part surface, while only sacrificing a fraction of 1 lb in ‘excessive’ adhesive.

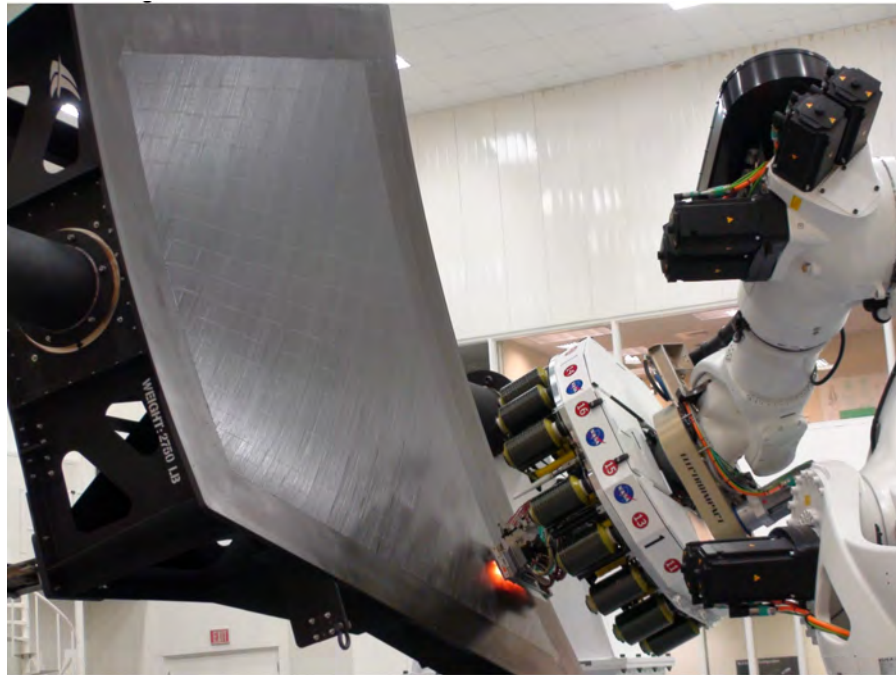


Figure 82. AFP of first skin.

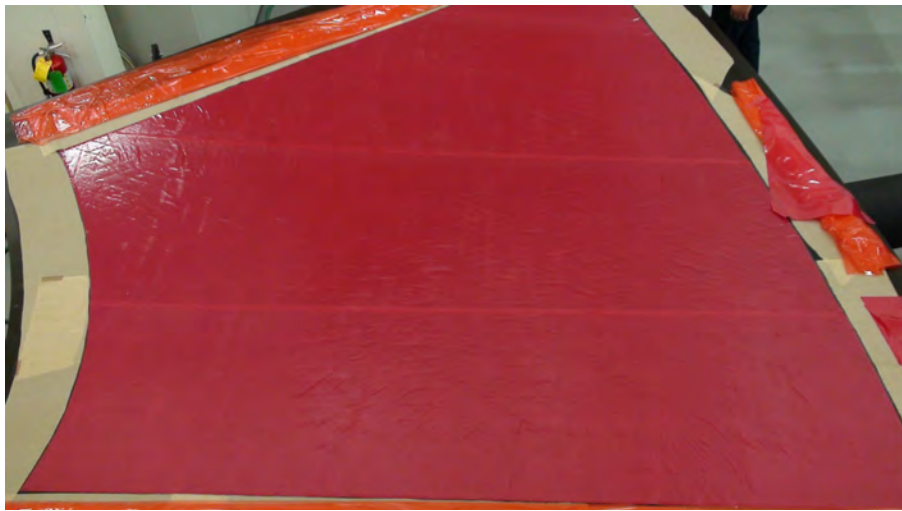


Figure 83. Film adhesive installed on first composite skin.

(6) Another debulk cycle is conducted as before to ensure the adhesive is firmly adhered to the composite skin.

(7) The next step is the installation of the honeycomb core. The aluminum honeycomb core is cut/machined to size to ensure a tight fit at all core joints. There should be no gaps more than 0.1 in between adjacent honeycomb core pieces. It was found that just routine handling very easily

damaged the light density, 3.1-pcf aluminum honeycomb core. Special attention had to be taken to ensure cells were not deformed during handling/installation. It was also observed that the light density core exhibited areas of irregular cell shapes as seen in figure 84.

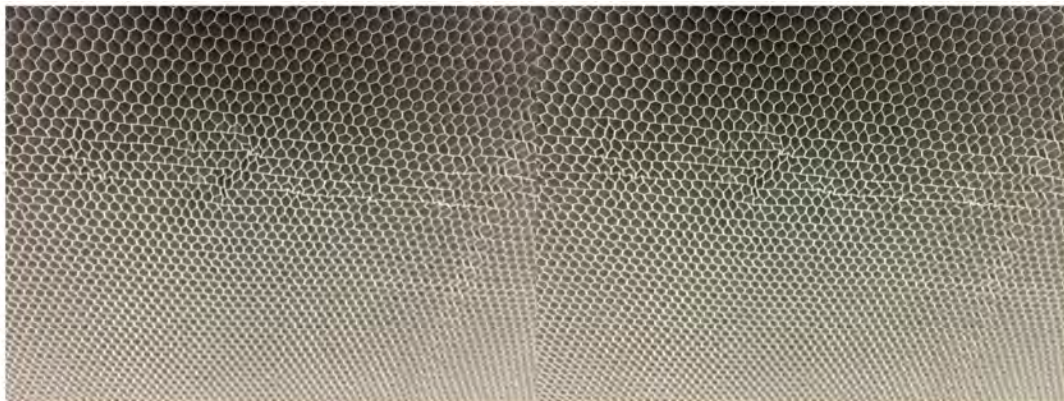


Figure 84. Honeycomb core cell irregular shapes.

(8) Next, the individual pieces of core were adhered together using a core splice adhesive. Two types of core splice adhesive were tried—a foaming core splice adhesive MA562, and a paste adhesive, EA9390. The foaming core splice adhesive was supplied in sheets $\frac{1}{2}$ in thick, and 1-in-tall strips were cut to match the height of the core. The strips of foaming core splice are kept in a freezer until right before installation to keep the tack of the material as low as possible during installation. The installation of this type of core splice was simple, quick, and clean. When installing the foaming core splice, it is beneficial to work from one edge of the tool to the other, installing a piece of core/adhesive in the same manner bricks and mortar are laid. Figure 85 shows the foaming core splice installed on the edge of the honeycomb core.

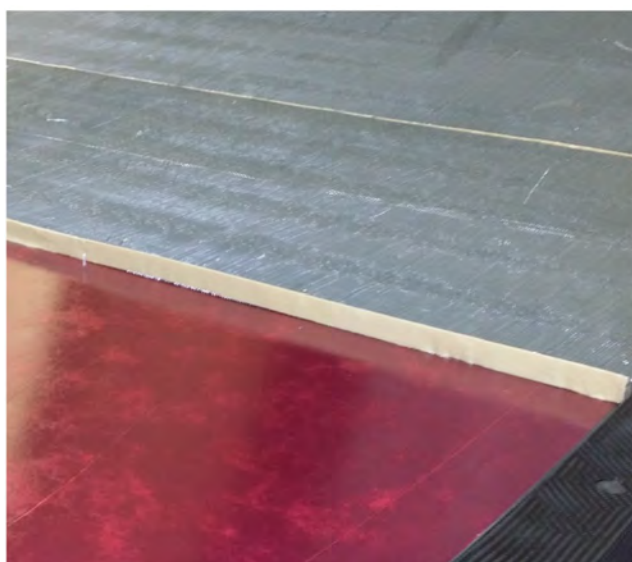


Figure 85. Foaming core splice installation.

The EA 9309 paste adhesive was also used to join pieces of honeycomb. This paste adhesive is a two-part epoxy that was in gallon cans. The adhesive had to be mixed, pushed into cartridges, and injected into core joints using a pneumatic air gun (fig. 86). The mixing of the epoxy required the use of a vacuum mixer to ensure there were no air pockets in the adhesive during injection. The vacuum mixer is a large vacuum chamber that must be cleaned between each mix. The cleaning of the mixer was found to be quite laborious, and if more adhesive is required for a particular part than the vacuum mixer can accommodate in one run, excessive time will be lost to cleaning the equipment between adhesive mixes. It is recommended that, if a paste adhesive is desired, SIMCO kits are used instead. SIMCO kits will remove the need for a vacuum mixer, saving time. The joints were covered using 2-in-wide rubber strips to press the excessive adhesive that pushed up during the injection process. A vacuum bag was installed, and the paste adhesive was allowed to set up/cure for 12 hours.



Figure 86. Paste core splice adhesive injection.

- (9) At this point, the second layer of film adhesive is installed onto the surface of the honeycomb core, in the same manner as the previous film adhesive layer, as shown in figure 87.



Figure 87. Second film adhesive layer with overlap.

(10) The film adhesive is then debulked down to the honeycomb for a minimum of 30 minutes. Before the debulking vacuum bag is installed, a core dam must be installed to prevent the crushing of the core on the edges of the panel.

(11) After removing the debulk vacuum bag, the second composite skin is fiber placed. The second skin is laid in a similar fashion to the first skin. The first ply has a lower feed rate, but in subsequent plies, the feed rate is increased. The heater output level starts at 150 % and is lowered to 100% as plies are laid. The main difference is the compaction is lowered to 50–100 lb. It was shown that no damage was induced to the honeycomb core cells from these compaction force levels as shown in figure 88.



Figure 88. View of honeycomb core after fiber placement of top skin, showing no damage.

(12) After the second skin is laid (fig. 89), the part was bagged for autoclave curing following the bagging sequence in figure 90.

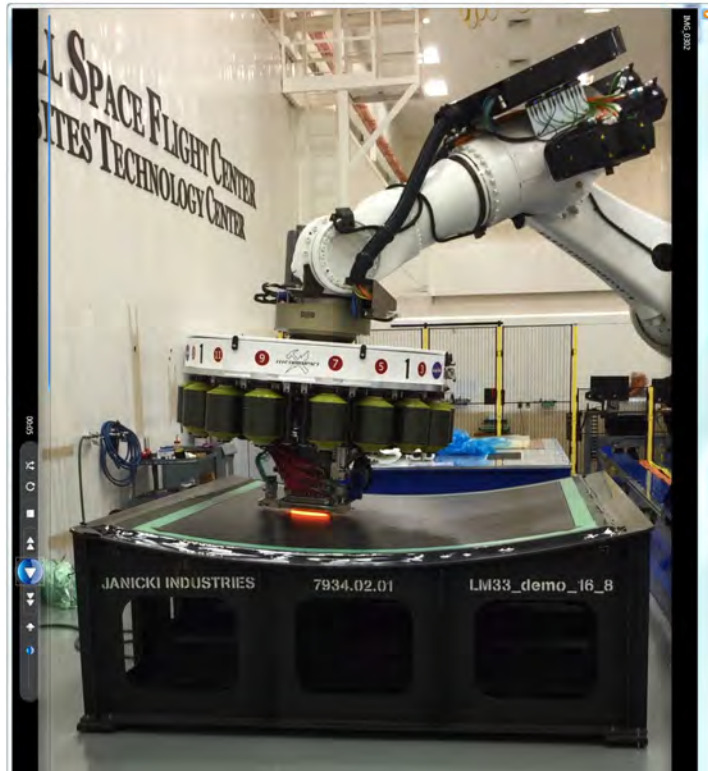


Figure 89. AFP of second skin onto surface of honeycomb core.

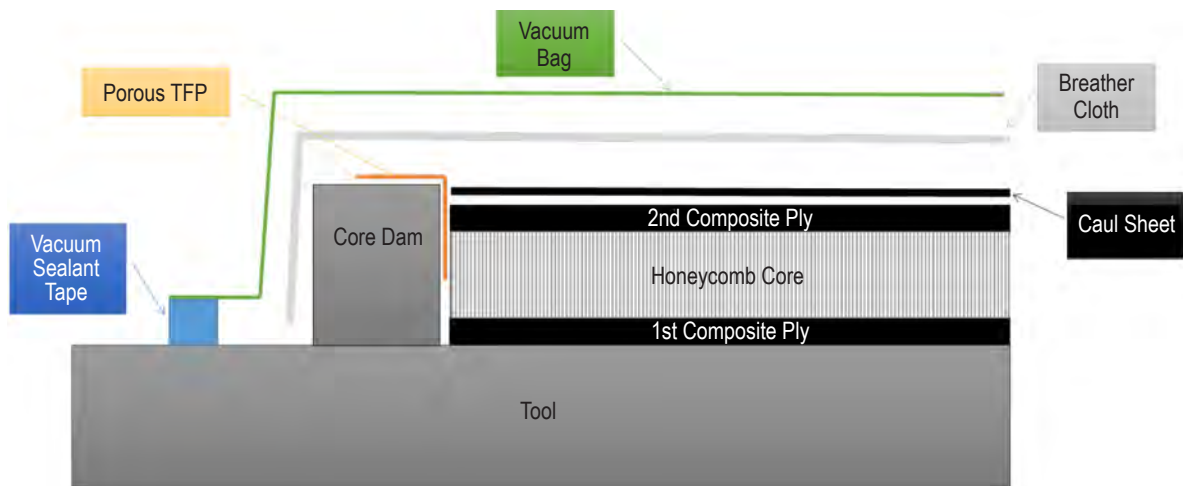


Figure 90. Autoclave cure vacuum bag.

(13) The part is then loaded into the autoclave and cured using the cure cycle in figure 91.



Figure 91. Part loaded into autoclave.

5.5 Curing

5.5.1 Scope

Optimal curing schedules are key to efficiently achieve the desired properties of the cured materials. Curing cycles determine the degree of cure of epoxy prepreg and have an important effect on the mechanical properties of the final products. Although companies manufacturing the commercial epoxy prepreg materials usually suggest curing cycles for custom applications, their curing cycles may not be the optimal ones for special applications. In order to optimize the curing cycles for epoxy prepreg used for the CEUS composite panels, it is necessary to understand the cure kinetics and characteristics of epoxy prepreg in more detail. To this end, the rheological properties of Hexcel 8552-1 prepreg and Cytec FM-300-2 film adhesive are characterized by means of dynamic mechanical analysis. This section will focus on the baseline cure cycle developed for the material systems used. All of the material had a nominal out time of 20 days. As discussed in section 2.2.4, the vilification and gelation temperature were affected with increased out-time.

5.5.2. Introduction

The flow behavior of a reacting system is closely related to the cure process. In the early cure stage, the epoxy resin is in a liquid state. Cure reaction takes place in a continuous liquid phase. In its liquid stage, the viscosity of a curing resin is influenced by two major phenomena. The first

is the increase in molecular size as cure advances, decreasing mobility, and hence increasing the viscosity. The second is the effect of the temperature on the mobility of these molecules. Resin viscosity thus depends on temperature and chemical conversion.

5.5.3. Gel Point

With the advancement of the cure process, a crosslinking reaction occurs at a critical extent of reaction. This is the onset of formation of networking and is called the gel point. At the gel point, epoxy resin changes from a liquid to a rubber state. Thus, after the gel point, the matrix can no longer flow and voids can no longer be suppressed. Although the appearance of the gelation greatly limits the fluidity of epoxy resins, it has little effect on the cure rate; so, the gelation cannot be detected by the analysis of cure rate, as is the case in the DSC. The gel time may be determined by a rheological analysis of the cure process. During a curing process under continuous sinusoidal stresses or strains, its viscoelastic characteristics change, which is reflected in the variations of rheological properties such as the storage modulus, E' ; loss modulus, E'' ; viscosity, η ; and loss tangent, $\tan \delta$. The E' is the elastic character of the epoxy prepreg and reflects the energy that can be recoverable. The E'' represents the viscous part of the epoxy prepreg and reflects loss energy by dissipation. Viscosity measures the fluidity of the epoxy resin system or, more precisely, the frequency-dependent modulus. Higher viscosity means the lower fluidity of the epoxy resin systems. The loss tangent, $\tan \delta$, equals the ratio of the loss modulus to storage modulus. It is used to evaluate the viscoelasticity of epoxy prepreg. The gel point indication for DMA is defined by a sudden rapid increase in storage modulus or the maximum in $\tan \delta$.

5.5.4 Gel Point Cure Optimization

The optimal gel point should allow for the best flow characteristics with the least amount of voiding. Flow is dependent on the part's geometry, size, and ply layup. For this reason, the optimal gel point may not be the same for every part but would use the same criteria for optimization.

5.5.5 Resin Flow

A controlled flow of the resin is desired during the initial stages of the cure. However, if pressure is increased too early during the cure, an excessive amount of resins bleeds out of the laminate layers leading to a void formation from a resin-poor region. When evaluating a cure cycle rheologically, a large drop in the storage modulus after autoclave pressure application is cause for concern. In this case, application of the full cure pressure is desired during an intermediate isothermal hold before the ramp to full cure temp at 355 °F. Thus, the isothermal hold period must be long enough and at a high enough temperature to allow for a sufficient viscosity increase. If a large drop in storage modulus is observed—half an order of magnitude or greater—during the subsequent temperature ramp to the curing temperature, the viscosity drop might induce poor resin distribution.

5.5.6 Volatile Removal

The removal of evolved vapor or air from the laminate is achieved by vacuum application during the cure, bagging schemes of the part, and the application of pressure. As temperature increases, solvent and water vapors are able to come out of the solution. If gelation occurs soon after a temperature rise without the external pressure required to suppress their formation, voids are induced into the matrix. These voids are homogeneous and spherical in nature (fig. 92).

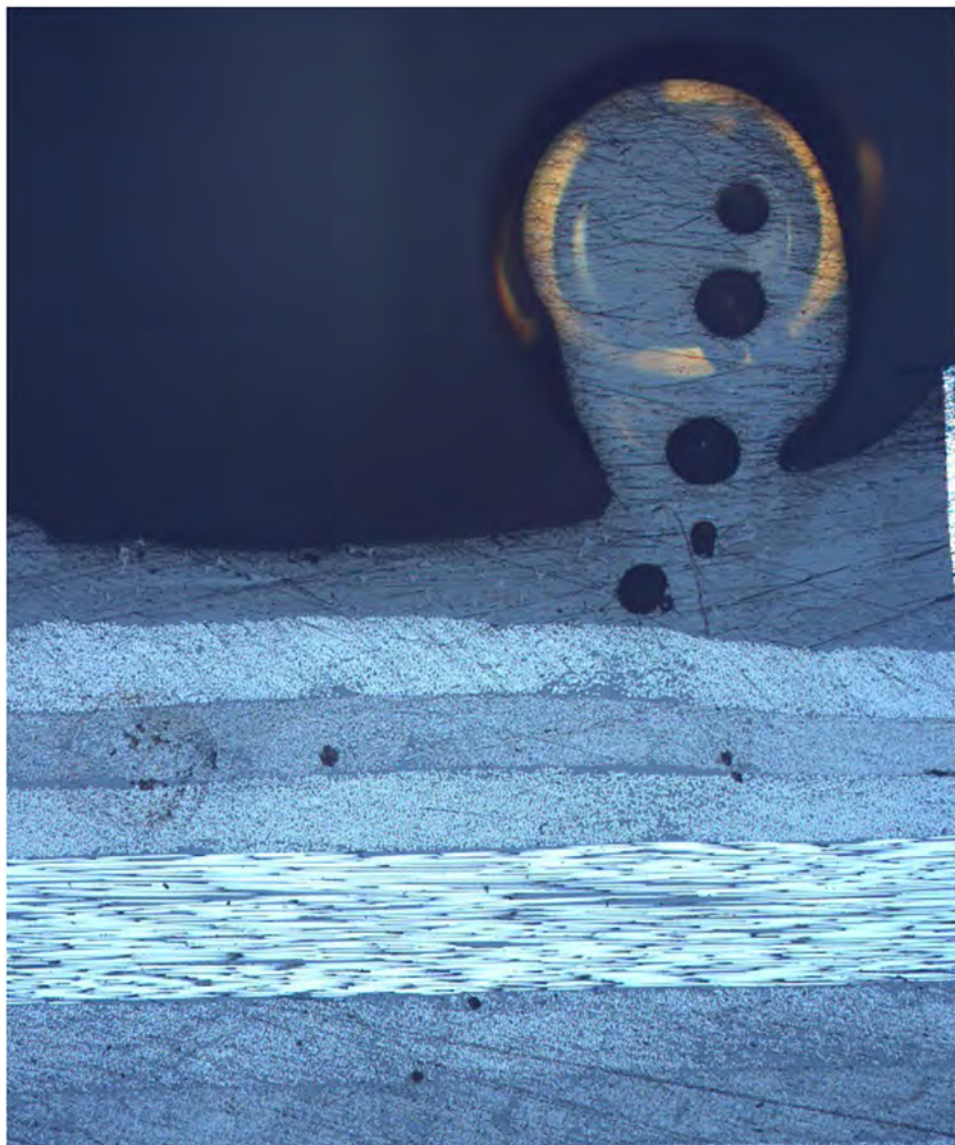


Figure 92. Voids.

A higher viscosity reduces the efficiency of removing evolved vapors as flow is reduced. To improve vapor removal efficiency, a low temperature bake-out isothermal hold period is introduced at a lower resin viscosity.

5.5.6.1 Internal Stress. The DMA is recording the resistance of fiber movement in the matrix from a given strain. After gelation, the matrix is a single molecule and the orders of magnitude increase in storage modulus from gelation is a result of this consolidation into a singular solid rather than a solution of fibers in a viscous fluid. This transition to a rubber-like state induces stress that must be relieved by the matrix.

If gelation occurs during the heating ramp, the gel network must relieve the additional thermal stress induced by the thermal gradient within the composite. This stress relief can result in void formation and, in extreme cases, delamination between plies. This effect is scalar and is amplified by poor thermal transport through the part, which may restrict higher heating rates.

During an autoclave cure process, the maximum pressure must be applied before the gel point in order to suppress the formation of voids in the matrix but also have sufficiently high enough viscosity to resist bleeding of the laminate.

In order to achieve the optimal curing conditions, the full cure pressure is applied during an isothermal holding period at an elevated temperature for a given amount of time. The higher temperature removes more volatiles and increases the viscosity of the resin before pressure application.

The time to gelation for Hexcel 8552-1 prepreg is determined using a ramp rate of 1° F/min from room temperature. Run 1 simulates a 285 °F hold for 30 minutes cure cycle used in previous work. Run 2 is a 285 °F hold until the gelation and represents the longest time until gelatin is achieved using the 285 °F hold period. Run 3 is a ramp to 355 °F with no intermediate hold period and represents the quickest time to achieve gelation using a ramp rate of 1 °F/min. Any hold period incorporated into the cure cycle will extend the amount of time required to achieve gelation but reduce the timeframe after the holding periods to bring the part to cure temperature before gelation.

As seen in the figure 93, the time to gel increased as anticipated in a roughly exponential fashion. However, gelation occurs during the ramp to the 355 °F cure temperature. Optimally, gelation of the laminate should occur after the heating ramp to reduce stress concentrations from fiber movement and rearrangement. The Run 3 DMA data indicate that even in the absence of a hold, gelation will occur during the ramp.

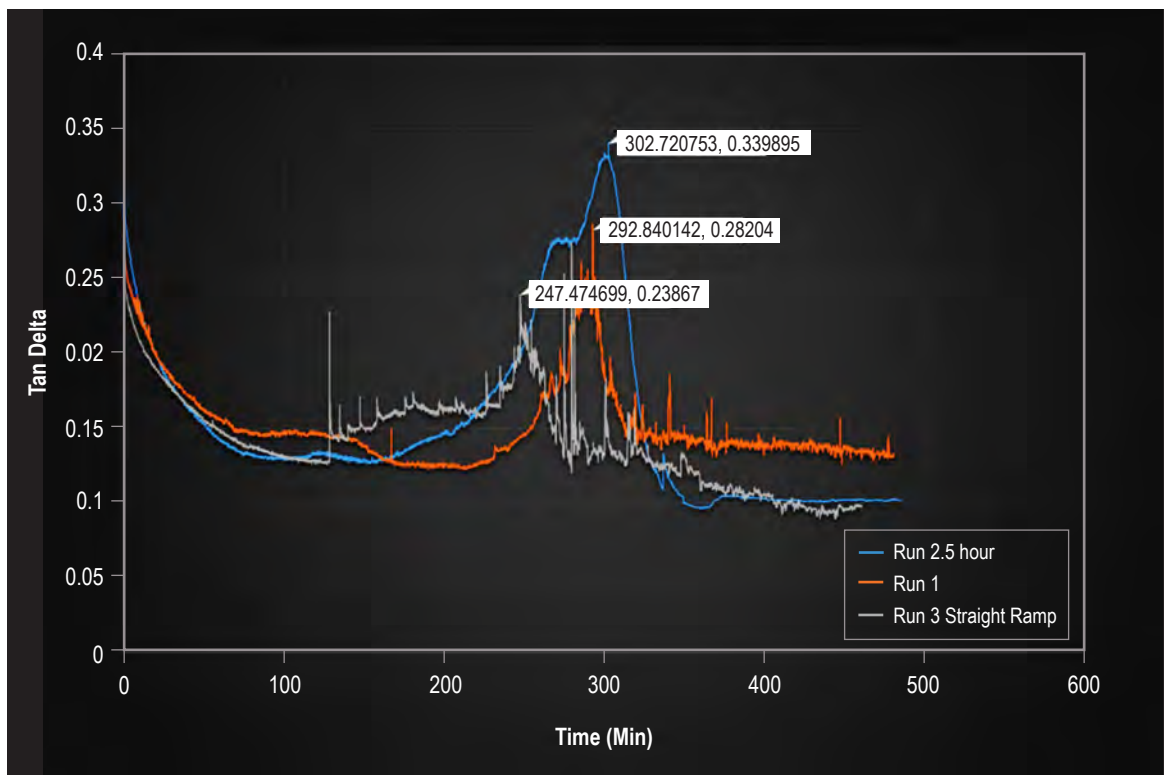


Figure 93. Tan delta peak at various 285 °F hold times.

The DMA data in figures 94 and 95 suggest that a heating rate between 2 °F/min and 5 °F/min will achieve gelation during the 355 °F hold. The selection of heating rate must also factor in the thermal lag within the part. A higher heating rate increases thermal stress induced within the part. Thus, the objective is to have the slowest heating rate that can achieve gelation during the isothermal hold at cure temperature. A 2 °F/min heating rate is the lowest heating rate, which could achieve that condition.

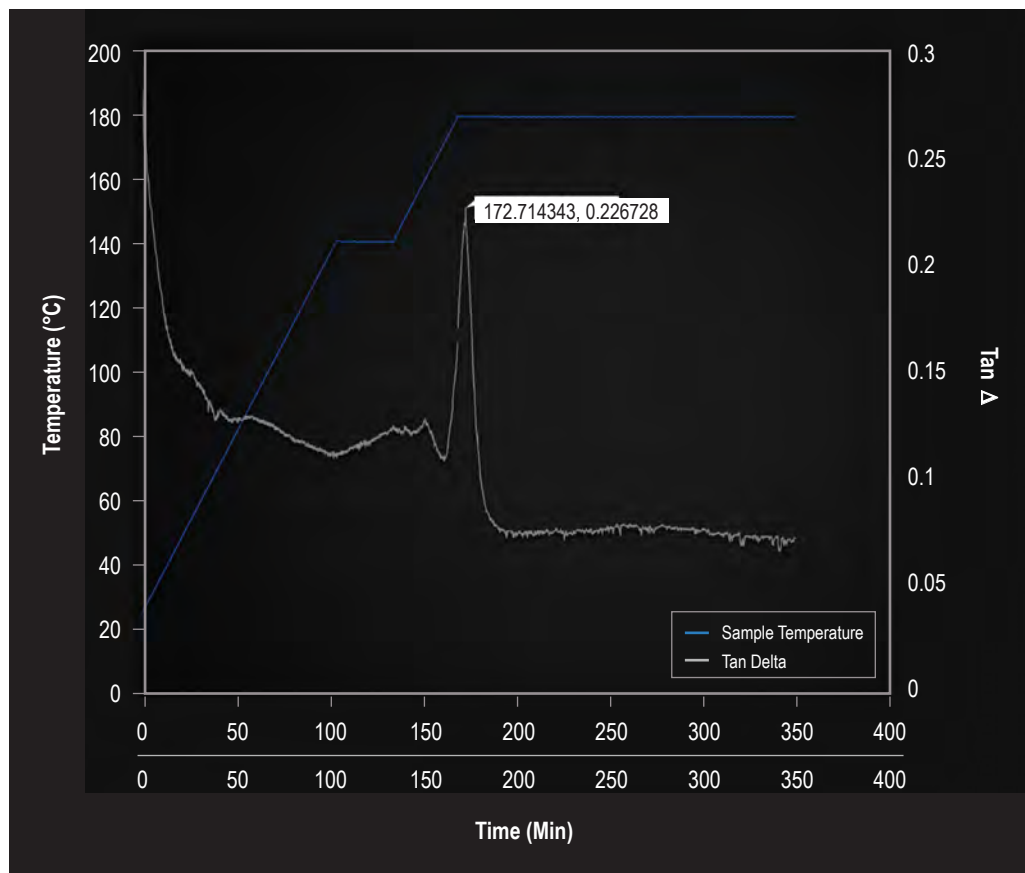


Figure 94. Ramp rate of 2 °F/min with 30-min, 285 °F hold time.

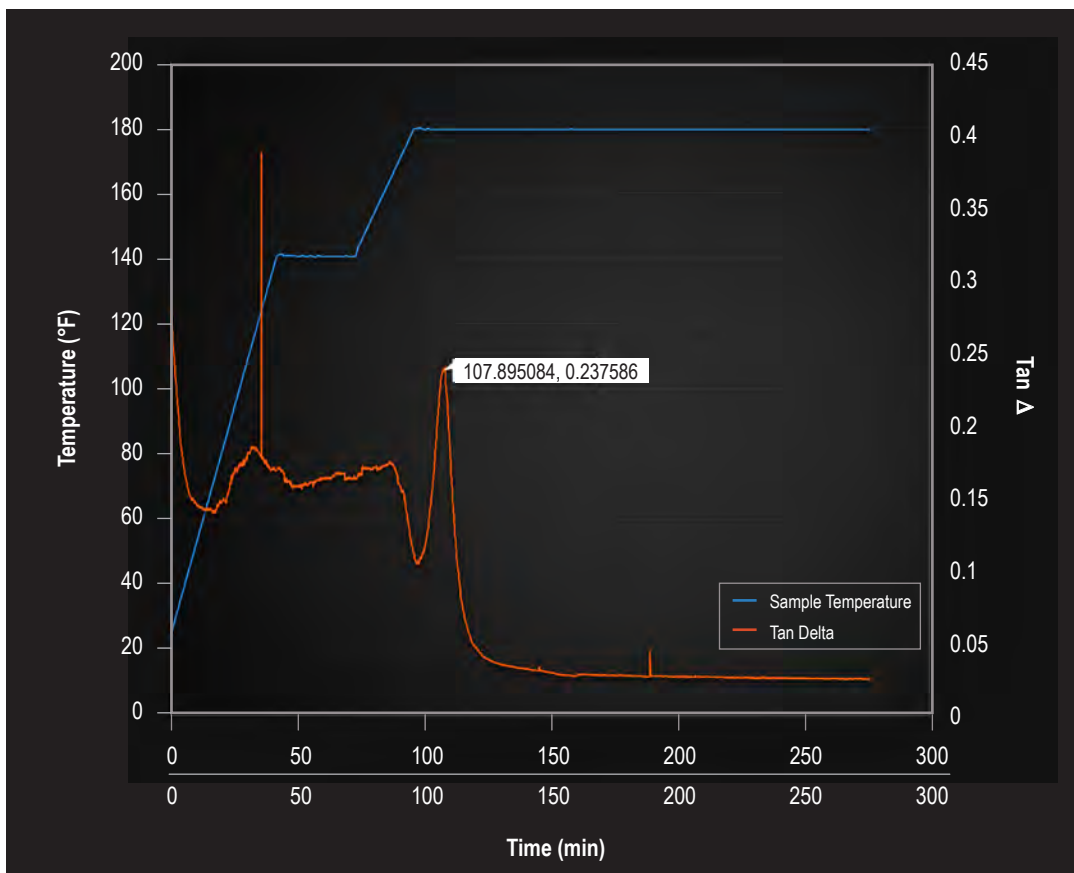


Figure 95. Ramp rate of 5 °F/min to 30-min, 285 °F/min to cure temperature.

5.5.7 Film Adhesive Considerations

5.5.7.1 Isothermal Hold at 250 °F. The CEUS composite panels are sandwich structures with composite laminate faces (Hexcel 8552-1) co-currently bonded to aluminum honeycomb core using an epoxy thermoplastic reinforce prepreg film adhesive (FM-300). The initial test panels showed evidence of resin bleeding through the film adhesive layer (fig. 96).

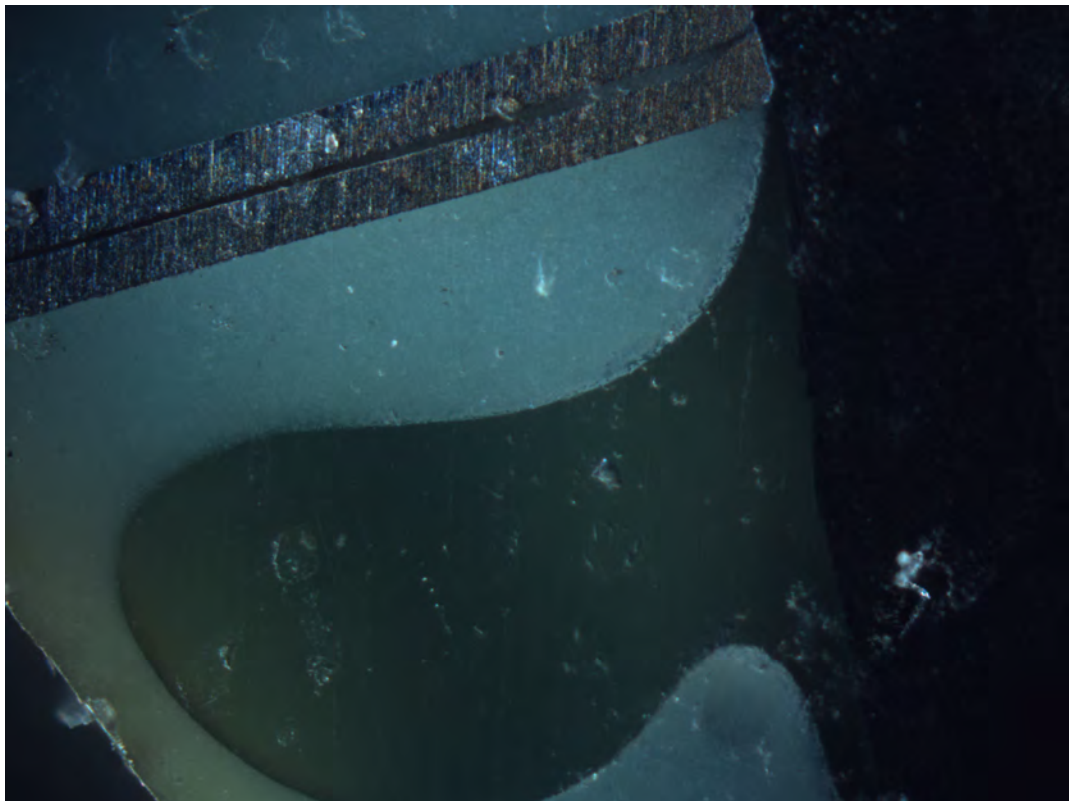


Figure 96. Micrograph of 8552-1 DDS/TGDDM resin (darker section) deforming the Cytec FM-300 film adhesive (lighter section) at core interface.

In order to control resin flow at the core interface, an elevated temperature hold period was incorporated into the cure cycle where the film adhesive can act as a barrier to resin flow into the core sections. Consequently, a lower temperate cure film adhesive, FM-300-2, was selected. FM 300-2 film adhesive is a 250 °F (121 °C) cure version of the widely used Cytec FM 300 film adhesive. The hold time and temperature were determined by the gel points indicated by the DMA data collected on the FM 300-2 adhesive.

As seen in figure 97, the gel point occurs shortly into the 250 °F hold. If the film adhesive does not achieve gelation relatively quickly into the hold period, the optimal conditions for laminate gelation and pressure application become more difficult to achieve. The gelled film adhesive can now act as a barrier layer and prevent excessive bleeding of resin into the core segment.

The second noticeable transition in figures 97 and 98 is the T_g transition occurring during the ramp to 355 °F cure temperature. Thus, the film adhesive is a gelled glass during the 250 °F hold and reverts back to the gelled rubber upon heating. This transition in the film adhesive does not significantly affect cure schedule considerations for the purpose of the present discussion, but is worth noting.

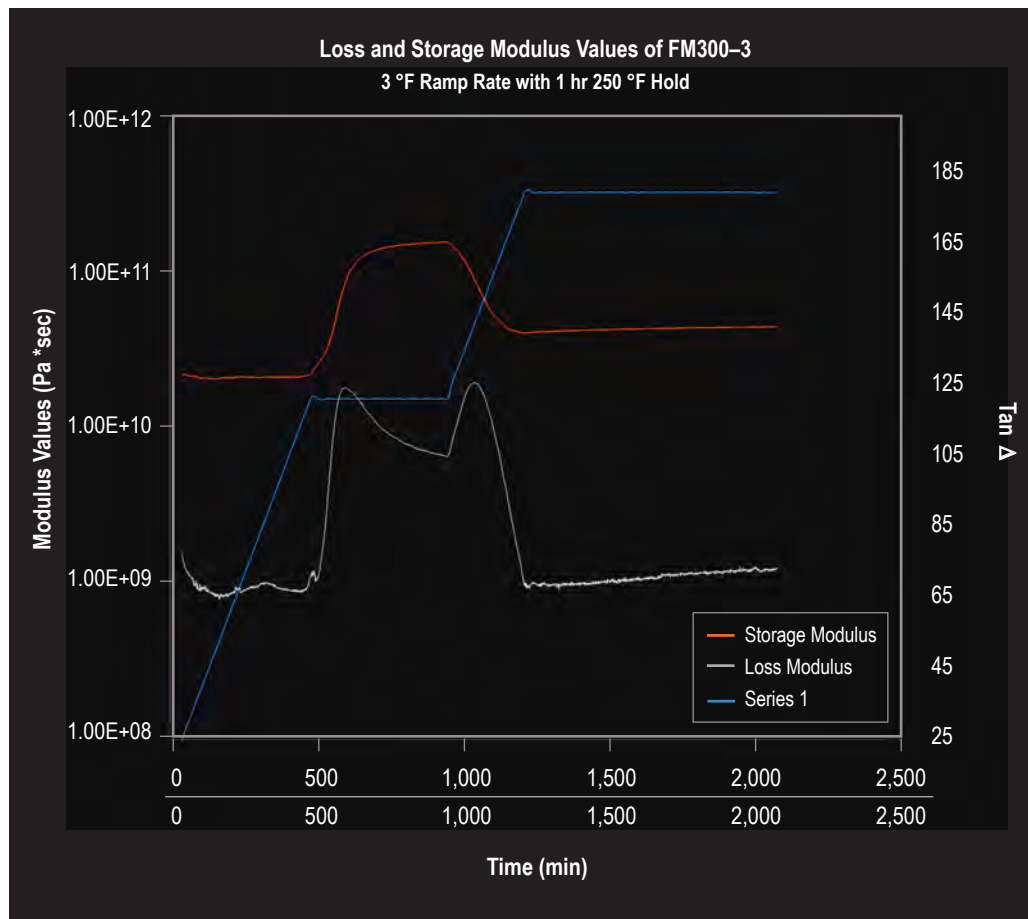


Figure 97. Loss and storage modulus values of FM300-3.

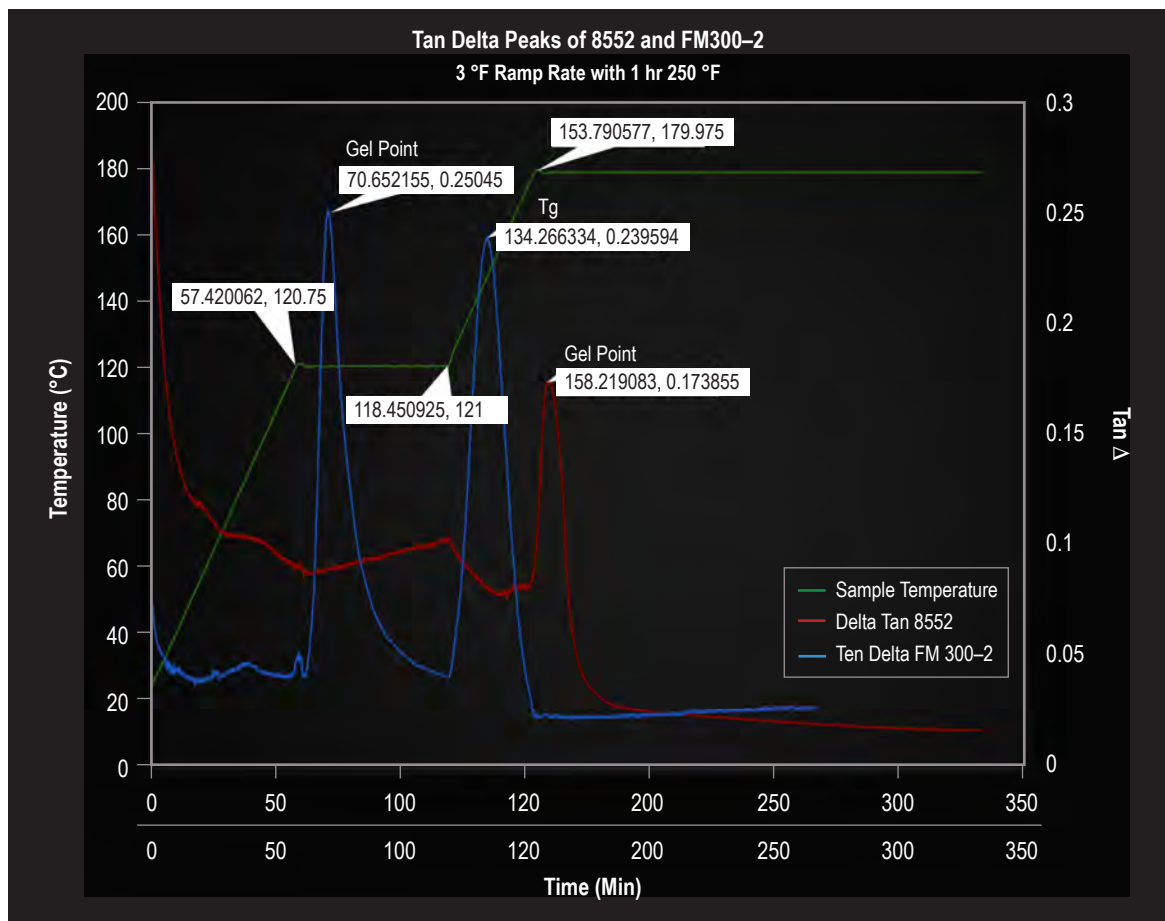


Figure 98. Combining the results of the FM300-2 film adhesive and 8552-1.

5.5.7.2 Microscopy Evaluation

Microscopic visual inspection of distributed test panel cross sections reveals no evidence of delamination or elevated porosity. All cross sections were determined to have porosity lower than 1%. Some local porosity concentrations did exist but never in excess of 1%. A slight difference in porosity morphology was observed between the developmental cure schedules. Cure cycles using the low temperature of 185 °F hold developed pores that were typically smaller, more distributed with respect to ply thickness and spherical as shown in figure 99. Figure 100 shows that larger amorphous pores were present in cure cycles not incorporating the lower temperature volatile removal hold. Figure 101 shows a void likely caused by air entrapment.

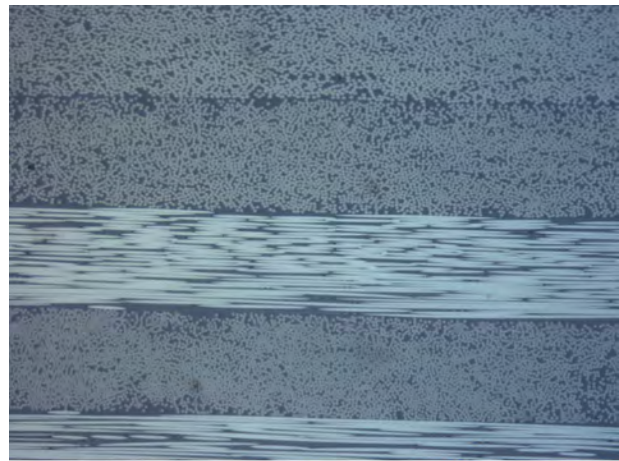


Figure 99. Clean cross section using developed cure cycle.

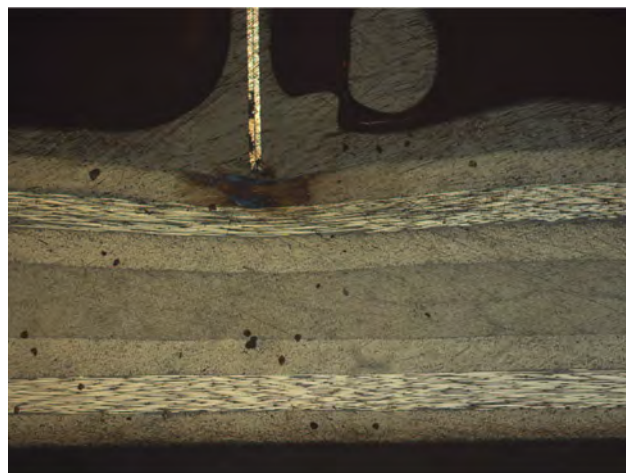


Figure 100. Typical profile of porosity using developed cure cycle.

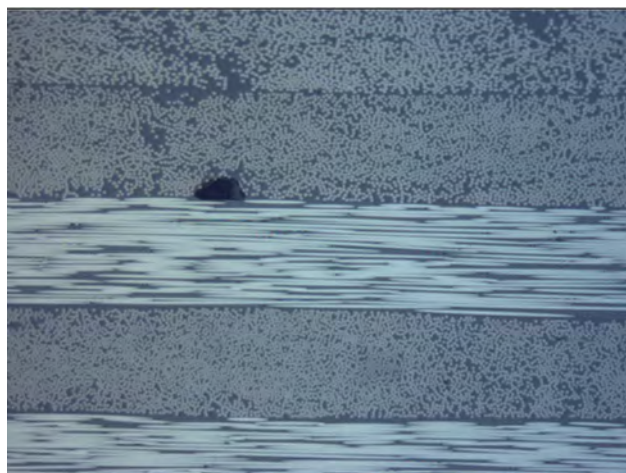


Figure 101. Example of void most likely caused from air entrainment.

This slight difference in the pore morphology suggests that the vapor phase did not coalesce and concentrate during the cure cycle, and air entrainment between plies was more efficiently removed with 185 °F debulking hold. This behavior seems preferable to the larger amorphous voids, which indicates a larger amount of stress within the composite laminate layer, as having an irregular shape indicates increased fiber rearrangement to relieve the vapor phase partial pressure contribution. Elongated regular voids occurring between ply interfaces typically indicate air entrainment.

There is no known study or data that suggests a decrease in the mechanical properties based solely on the void morphology but, larger defects typical require less energy to initiate failure modes than smaller distributed ones. Thus, the incorporation of a lower temperature volatile removal hold seems advantageous if the gel point still occurs during the isothermal cure temperature hold.

6. TEST

The USA2 STA had a two-part test plan. The first test of the STA would be to test the ultimate load in a manner to satisfy the project requirement of designing, building, and testing to conditions representative of flight conditions. The second test would be a test to failure. Both the ultimate load test and the test to failure would provide data that could be used to correlate with analytical models for validation or calibration. The SBKF team would conduct the test to failure. The SBKF study is an ongoing study aimed at developing SBKF test data and potentially lowering the conservatism from traditional design methods. The majority of the SBKF tests have been of metallic structures, so the CUSA2 STA allowed a unique opportunity to test a large composite structure to failure. For both tests, it was important to collect as much data as possible of the structure's static and dynamic displacement and strain response to loading. Options considered for data acquisition were fiber optics and digital image correlation. Strain gauges alone would not collect the fidelity of data required to validate models. There was limited experience within the project with the fiber optics technology, and in recent implementation, there had been issues collecting the data, so the preferred method of full field displacement data acquisition was digital image correlation. Digital image correlation works by covering the test article with a high contrast speckle pattern and using specialized low-speed cameras to track the movement of the speckles. The tracked movement is then translated into displacement and strain information. An example of this is shown in figure 102.

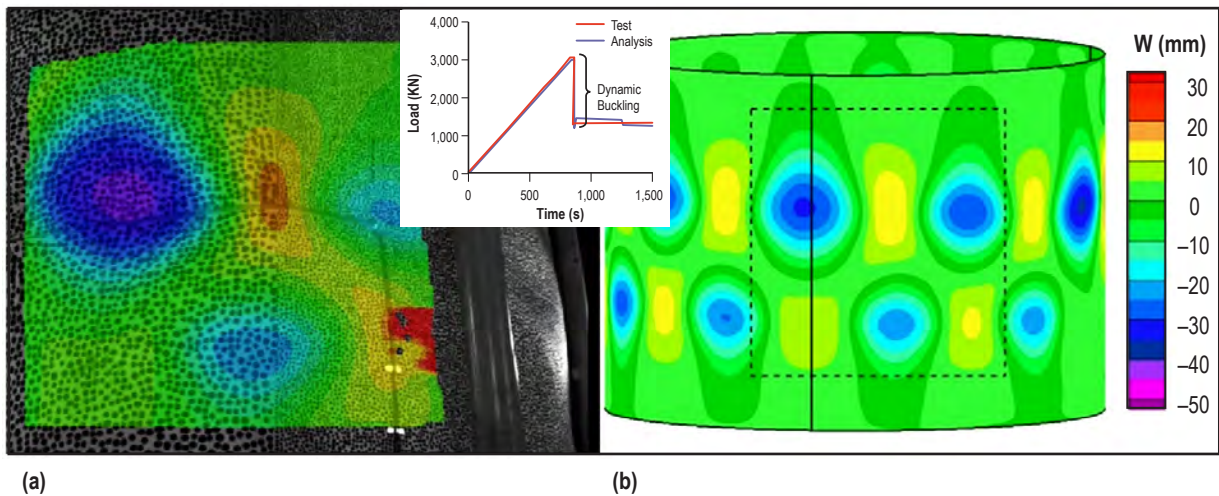


Figure 102. Example of digital image correlation data: (a) Superimposed on a barrel that has been painted with a high contrast speckle pattern compared to (b) an analytical model of predicted displacement.

The two facilities considered for the STA test were Building 4619 and Test Stand 4699. Building 4619 was the favored option because it was indoors and allowed for the use of the digital image correlation cameras. Unfortunately, this facility had limited availability because SLS hardware had the priority. The second option, Test Stand 4699, was an outdoor test stand that made the use of the digital image correlation data acquisition system difficult. Figure 103 is an illustration of test configuration in Test Stand 4699. The outdoor use of the digital image correlation cameras was an issue because of environmental concerns such as wind, temperature, and lighting. Locating the cameras inside the STA was considered an option for mitigating the environmental concerns; however, this posed the risk of damaging the expensive cameras during the test.

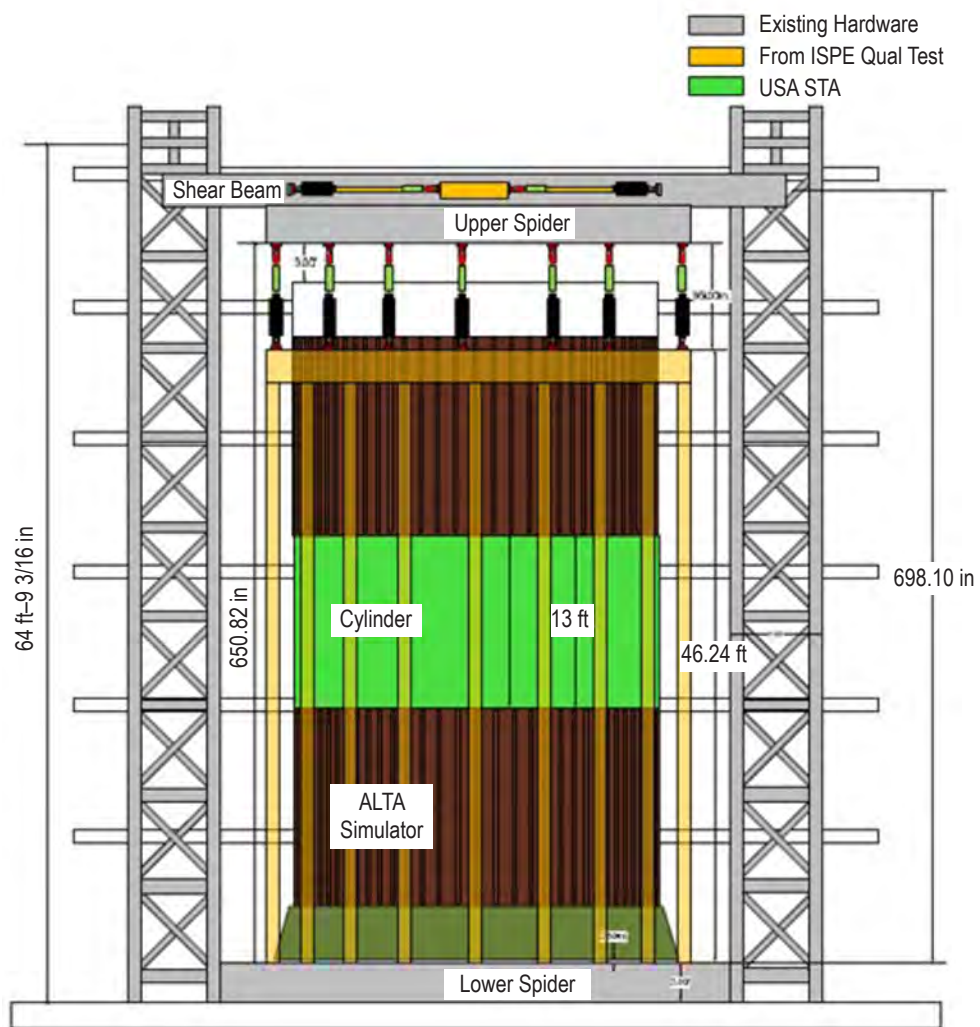


Figure 103. Test configuration in test stand 4699.

The test simulators identified for the STA test were preexisting ET simulators. The simulators had a non-symmetrical bolthole pattern from their use in the ET tests. The “Interface Definition (Sheet 1)” (figure 33) and the “Layout Drawing for the STA (Sheet 1)” (figure 35) was created to document this pattern. There was a concern that due to the factors of safety, the STA would not fail within the loads that the simulators could withstand. The ET simulators were analyzed to determine the maximum load they could safely tolerate. Contingency plans were considered for inducing failure in the test article if the maximum capacity of the simulators was predicted to be achieved prior to STA failure. The first option considered was introducing damage to the STA. This option was ruled out because, even with induced damage, there was a possibility that the STA would not fail within the limits of the simulators. Another option considered was applying a crush pressure to the test by creating a negative pressure within the STA. However, as mentioned previously, the complexity of pressurizing the test set up was a cost and schedule risk to the project, so it was decided that no burst or crush pressure loads would be tested. The contingency plan ultimately selected for failing the test article was to induce failure by applying a point load to the STA. While the STA was loaded in the axial direction, a lateral point load would be applied to the wall of the STA. This point load would be increased until the structure failed.

In addition to the STA, panel testing was also considered. A study was conducted to examine the feasibility of testing a $\frac{1}{4}$ section of the cylinder and cone – referred to as a petal (figure 32 CUSA2 STA traded assembly options). In the feasibility study the petal had a metallic vertical separation joint. There existed a concern for the petal configuration that the stiffness of the joint would prevent the composite panel sections from receiving the proper loading. Additionally, the boundary conditions for the conic section were predicted to be critical for a stability test and assessed to be unfeasible to adequately replicate. It was determined that within the scope of this project cylindrical panels would be tested, but conic panels and petal sections were not an option. A plan was made to conduct cylindrical panel testing to obtain damage tolerance data in conjunction with the large STA structural test.

7. SUMMARY

This Technical Memorandum documented the work accomplished by the NASA CEUS team from when the project received authority to proceed until the project was discontinued due to the FY 2016 NASA Appropriations Bill impacts to the STMD budget. As documented, progress was made in maturing composite technologies, as shown in figure 104.

The project completed a successful SRR, selected and procured material, developed equivalency between panels manufactured at different centers, completed a wall construction trade study and selected preferred core configuration, performed initial analysis, matured NASA AFP capability, procured large composite tool, developed fabrication and processing parameters, and developed cure process optimization. The CEUS closeout documentation and data generated during the project will be stored by the Technology Demonstration Missions (TDM) program and retained on the CEUS Project SharePoint site.



Figure 104. Progress made in composite technologies.

APPENDIX A—LESSONS LEARNED

L1 ID	Analysis, Assembly, Design, Drawings, General, Handling, Instrumentation, Manufacturing, Testing	Category	Date	Issue / Benefit	Relevance	Implementation Plan / Action items	POC	Need date	Status	Comments, Risk Closure ?
Materials	Time required to receive quote.	Description: It took on average 3 to 4 months to receive a quote from Hexcel after the initial request for that quote. Both initial quotes received included a number of various errors, including customer name, material quantities, units (ft vs lbs), and specified shipping locations.	schedule	Lessons learned: Add a minimum of 4 months to the time you would expect for a similar procurement, and carefully review the quote. Make program management aware of the issues in dealing with the large prime suppliers; considering we buy relatively small quantities.	Sandi Miller / Brian Stewart					
Materials	Preprep Specifications	Description: We ordered based on a Hexcel internal specification but we tried to include additional requirements for defects, etc.		Lesson learned: The additional requirements are non acceptable to the vendor and slow the procurement process. If NASA would like to require specifications outside the internal spec, time should be planned to essence develop a NASA spec.	Sandi Miller / Brian Stewart	I think that a NASA-wide spec for industry-standard products is imperative. Similar to Boeing's BMS, it would give us a singular product that we've once with the vendor. I think the data-spc method we've once with now really contours the vendor and somehow increases the production quality risk. We chose to use their internal spec alone, and it still took an extraordinary amount of time and they had to make the changes as the spec, also think some sort of a NASA-wide BPA (or similar) mechanism is needed for prepars. Once we pick a ready/other combination-we have effectively sole-sourced it. Then we do the same dance, JOPIC, pricing, T&Cs again and again. Except more delays, none of this extra activity really affects the outcome. At our request, LaRC Procurement				
General Procurement Requirements	Description: NASA requires a receipt for shipping as well as a shipping cost identified as a line item within a PO. Hexcel includes two issues for NASA procurement. (1) cost competitiveness, and (2) no shipping costs to verify. During both procurement processes, NASA eventually covered, but without spending weeks arguing over these points.			Lesson learned: Try to work through this upfront with NASA procurement. I thought I had, but should have emphasized that the vendors will not change their policy.	Sandi Miller / Brian Stewart	For similar reasons as the spec, also think some sort of a NASA-wide BPA (or similar) mechanism is needed for prepars. Once we pick a ready/other combination-we have effectively sole-sourced it. Then we do the same dance, JOPIC, pricing, T&Cs again and again. Except more delays, none of this extra activity really affects the outcome. At our request, LaRC Procurement				
Materials	Errors in material fabrication	Description: Hexcel quotes in lbs, but orders sent to manufacturing list quantities in ft'.		Lessons Learned: Make sure someone is on-site for at least the set-up of the prepreg run. Fortunately we were on-site and able to catch this issue early.	Sandi Miller / Brian Stewart	My concern with our 145 gram order was not just that Hexcel SLC made a bad batch, but that it left their plant in that state. Hexcel has to get their quality issues under control, I think marching up the food chain at Hexcel is the way to go for this. We should have one of our suits call one of their suits. This is supposedly our suits call one of their suits. This is supposedly				
Materials	Non-responsiveness of material vendors	Description: Both Hexcel and Cytec res are very slow to respond; it has taken upwards of a week to get a question answered, modification made, or order acknowledged.		Lesson learned: Become familiar with the chain of command. Improve up that chain with both companies when response time becomes ridiculous.	Sandi Miller / Brian Stewart	I think our order quantities may be a factor. It also could be that once we call them, they know we aren't going to anyone else - so why hurry? I think standard NASA spec, pre-arranged procurement mechanism (BPA) and a little pressure from us will help.				
Materials	Minimum number of samples needed for statistics	CEUS utilized an accelerated building block approach through application of an equivalence test matrix. CMH17 requires a minimum of 8 coupons per test for equivalence. In this project, 18 coupons were submitted per test; 8 each from panels made at GRC, LaRC, and MSFC. We were not aware that the data generated from coupons prepared at separate locations could not be pooled without a separate statistical analysis (ANOVA). In the future, a minimum of 8 coupons per location is recommended.			Sandi Miller					
Manufacturing	Phased tooling procurement too early / programmatic issue with accelerated project	Executed the tooling procurement too early in the project. There was not sufficient design and analysis performed to support the tool. We bought a best effort surface that as the project progressed was not optimal for the structure.		Tooling was long lead item, long lead schedule problem and then you need enough information to execute it.	Justin R. Jackson	[Justin] From a fabrication stand point, we leveraged what was already developed. I believe the biggest challenges were going to be in the joining and assembly which we did not get to.				
Manufacturing	Cure Cycle	Something for cure cycle development? Did we make improvements on cure cycles to improve properties (or did we get as far as strength testing? Only saw a micrograph)			Troy Mann					
Test	Tooling / Fixtures	Learned low cost tooling is a possibility?			Terry Petham					
Test	Facilities	could only test in certain buildings								
Test	Panel test size restrictions	Testing in large facilities can become cost prohibitive for a project, so generally it is a benefit to test the smallest test article capable of achieving needed test objectives. The 1-million pound machine at LaRC has an operating envelope of approximately 7' wide by 12' tall								
All	Scale Up	Many of the design, analysis, materials, and manufacturing lessons learned were not evident in the coupon, element, or subcomponent testing and only started becoming evident when building the full-scale assembly.								

CEUS Historic Lessons Learned Review, Rev. 02 Mar 2015						
Document Number	Document Name	Date	LUS #	Lesson Learned	Applicable?	Plan
n/a	Final Report of the X-33 Liquid Hydrogen Tank Test Investigation Team	May 2000	n/a	The importance of a comprehensive building-block approach to ensure mission success	yes	Utilize a building block approach. (Overall)
n/a	Final Report of the X-33 Liquid Hydrogen Tank Test Investigation Team	May 2000	n/a	The importance of communication. Communication is a two-way process. Technical information must be communicated clearly. There must be openness to receive the information properly.	yes	Do not compromise communication between requirements, design, analysis, manufacturing, test, and inspection teams. (Overall)
n/a	Final Report of the X-33 Liquid Hydrogen Tank Test Investigation Team	May 2000	n/a	Failure modes must be addressed in depth.	yes	Consider all issues; all potential failure modes to determine which ones are driving. I.e., do not make a priori assumption - all composites projects are different. (All analysis tasks)
n/a	Final Report of the X-33 Liquid Hydrogen Tank Test Investigation Team	May 2000	n/a	A risk management plan commensurate with the technical complexity must be used.	TBD	TBD
n/a	Final Report of the X-33 Liquid Hydrogen Tank Test Investigation Team	May 2000	n/a	Early expectation (at the design table) have the greatest effect on mission success.	TBD	TBD
NASA TM 4322A	NASA Preferred Reliability Practices (GD-ED-2210)	Feb. 1999	689	All of the above consideration considerations can result in a fiber composite part or component that does not satisfy design properties. 1) is unnecessarily difficult to fabricate, and 3) adds substantial program item. Item 1 may lead to an expensive redesign. Item 2 can impact cost and program schedule. Item 3 can jeopardize the entire project.	yes	Solicit and heed input from Manufacturing concerning material selection. (STA design)
NASA TM 4322A	NASA Preferred Reliability Practices (GD-ED-2205)	Feb. 1999	682	Failure to use state-of-the-art design techniques, tooling, manufacturing techniques, and automated manufacturing and inspection techniques for composite materials could result in the choice of inappropriate materials, costly scrapping, and potential failures in use. Failure to use composites in appropriate applications could result in noncompetitive products with greater complexity, weight, or damage susceptibility.	yes	Set and encourage realistic expectations for mass savings.
NASA TM 4322A	NASA Preferred Reliability Practices (PD-ED-1217)	Feb. 1999	669	Failure to adhere to proven and acceptable practices in the design, manufacture, and testing of structural laminate parts will result in acceptably high rejection rates of fabricated composite parts. This rejection rate could be due to incomplete or inaccurate inspection procedures, excessive (inadequate) porosity, surface defects, inclusions, improper dimensions, or inadequate physical, thermal, or chemical properties as revealed in nondestructive testing or in destructive coupon testing. A high rejection rate could cause delays in the vehicle assembly, testing, and checkout process, and could possibly affect the launch schedule. Increased costs of manufacture would also result from a high rejection rate.	yes	Adhere to proven and acceptable practices.
NASA TM 4322A	NASA Preferred Reliability Practices (PD-AP-1318)	Feb. 1999	819	Not performing a composite material compatibility analysis on the structural components of the structure to be used in the aerospace vehicle with unique or inefficient load paths. Without proper stress analysis, the objectives of minimum weight and a balanced design will not be met. Structural testing may also be misguided in that some components may be inadequately tested while others may be over-tested.	yes	Perform a complete and comprehensive stress analysis.
NASA TM 4322A	NASA Preferred Reliability Practices (PT-TE-1422)	Feb. 1999	765	Failure to detect cracks, flaws, and voids in aerospace materials through the proper use of ultrasonic testing and other approved nondestructive evaluation methods could result in the use of weakened structures, unlubricated propellant insulation layers, and potentially pressurized vessel failures or burst due to the use of pressure vessels without proper inspection and repair.	yes	Use appropriate NDE techniques.
NASA TM 4322A	NASA Preferred Reliability Practices (GD-ED-2201)	Feb. 1999	675	If the [external] guidelines recommended are not followed, greater numbers of fastener types, sizes, materials, and finishes may be specified or procured resulting in excessive cost. Mission performance may be also degraded due to incompatibility of materials and fasteners, or due to substandard hardware that lacks sufficient scrapping and inspection.	yes	The requirements in NASA-STD-6016 (and NASA-STD-600B, which is levied in NASA-STD-6016) are applicable to CEUS as identified in the SRD and meet the intent of many of the guidelines in this preferred reliability practice.
NASA TM 4322A	NASA Preferred Reliability Practices (PT-TE-1410)	Feb. 1999	778	Failure to understand the requirements could result in degraded science data due to excessive contamination of an instrument, or in the complete failure of a space flight mission. Noncompliance with outgassing requirements could result in non-approval of materials for space flight use. If the non-approved materials are already assembled in a flight vehicle or scientific instrument, they may have to be removed and replaced by approved materials.	yes	Consider outgassing during material selection.
n/a	LUS: "Space Charging of Composite Structures"	March 2003	1330	Surface resistance measurement of a non-homogenous composite material may not accurately measure the material's susceptibility to space charging.	TBD	TBD
n/a	LUS: "Undocumented Process Steps And Process Drift Is Root Cause For Scrap Of High Value Part", Multi-Purpose Crew Vehicle (MPCV)	May 2012	4616	During the design development and manufacturing process phase, establish configuration controlled manufacturing processes. These manufacturing processes should establish the critical steps and provide detailed instructions for the critical steps. Changes to the build process require a configuration control procedure to be followed. If a new process step is required or a new manufacturing error is used, require them to hold a process walk through of the manufacturing process to assure they understand the steps in the process, the equipment required, the condition of the equipment, and materials required. The fit of the vacuum curing bag materials is a critical parameter for the curing of a composite structural part. The perforated release film and solid release film are susceptible to having unintended holes when the materials do not lay flat. The process step of cutting the materials into gore shapes was not documented without the bagging process instructions. These steps need to be documented for any future use of these steps performed.	yes	Some level of configuration control is necessary even for one-of-a-kind builds to ensure a quality product and avoid unexpected failures.
JPL Case Number: S-2008-359-00002	LUS: "Cryogenic Tank Rupture/Close Call"	Feb. 2011	5396	The main lesson is a lack of adequate independent reviews for the test plan, procedure, and operation. The NASA and contractor test team members did not seek an outside, independent review of a test that was clearly beyond their experience and expertise. An independent review by other disciplines would have likely identified potential risks associated with the tank being pressurized to a high pressure and conclude pressure that were factors in many of the decisions made. This review would have been invaluable had procedures/requirements been followed. When testing a Composite Pressure Vessel (CPV) tank above Maximum Expected Operating Pressure (MEOP), and with limited expertise/knowledge of CPV, an abundance of caution should have been employed. The involvement of Safety and Mission Assurance functions, various NASA discipline consultations, the performance risk assessments, and the completion of various documentation, would have triggered the right questions and analyses, thereby avoiding the potential risks. Management review and insight for testing and risk analysis was inadequate.	no	The CEUS is not pressurized hardware. The CEUS team is experienced in testing similar structures.
JPL Problem/Failure Report No. 13366	Heatsield Structure #1 (Flight Spare) Handling Drop	Aug. 2008	1996	When ground handling flight hardware, even simple operations can fail without adequate procedures and training.	yes	Use trained personnel for ground handling operations. (STA manufacture and test)
n/a	LUS: "To Bond or to Bolt, That is the Question [Export Version]", OSTM/Jason 2	Nov. 2008	2038	1. Use of adhesive bonding for joining spacecraft fittings to structural components provides an opportunity for elegant design solutions, but such bonds are subject to thermal stress and may be difficult to properly inspect.	TBD	CEUS skirts have bonded fittings.
n/a	LUS: "To Bond or to Bolt, That is the Question [Export Version]", OSTM/Jason 2	Nov. 2008	2038	2. This reduced (JPL) lesson learned provides cautions regarding alternative methods of joining, such as fasteners, that may provide an additional margin of safety.	yes	Contact the office of the chief engineer at JPL to find out what the reduced lesson is.
n/a	LUS: "To Bond or to Bolt, That is the Question [Export Version]", OSTM/Jason 2	Nov. 2008	2038	3. This reduced (JPL) lesson learned discusses the benefits of alternative methods of thermal stress analysis for bonded joints.	yes	Contact the office of the chief engineer at JPL to find out what the reduced lesson is.
n/a	LUS: "To Bond or to Bolt, That is the Question [Export Version]", OSTM/Jason 2	Nov. 2008	2038	4. This reduced (JPL) lesson learned provides a material properties criterion for selecting a method for joining mechanical components that does not overstrength the hardware.	yes	Contact the office of the chief engineer at JPL to find out what the reduced lesson is.
NASA/TM-2011-217185; NESC-RP-06-019	Composite Crew Module: Primary Structure	Nov. 2011	n/a	U1.1: Small agile teams—emphasizing “in-line” work—working in parallel with, but outside the umbrella of a flight project can achieve significant results through rapid decision making. These teams can exploit unforeseen opportunities and minimize consequences through quick recovery to problems that may occur.	no	
NASA/TM-2011-217185; NESC-RP-06-019	Composite Crew Module: Primary Structure	Nov. 2011	n/a	U1.2: Engineering models predicted mass and structural response well.	yes	The tools being used by CEUS to create engineering models are the same or similar to what was used for CCM.
NASA/TM-2011-217185; NESC-RP-06-019	Composite Crew Module: Primary Structure	Nov. 2011	n/a	U1.3: Engineering models did not always predict production challenges.	no	
NASA/TM-2011-217185; NESC-RP-06-019	Composite Crew Module: Primary Structure	Nov. 2011	n/a	F-1: Many of the design, analysis, materials, and manufacturing lessons learned were not evident in the coupon, element, or subcomponent testing and only became evident when building the full-scale assembly.	yes	The CEUS project is aware that there can be scaling issues in manufacturing and analysis. The project is going to build a full-scale test article for final verification of the design and manufacturing.
NASA/TM-2011-217185; NESC-RP-06-019	Composite Crew Module: Primary Structure	Nov. 2011	n/a	F-6: Small, but focused, independent technical reviews with subject matter experts were effective for challenging assumptions and technical decisions resulting in increased innovation and a higher motivated team.	yes	TBD
NASA/TM-2011-217186; NESC-RP-06-019	Composite Crew Module: Design	Nov. 2011	n/a	F-3: Structurally connecting the internal backbone structure to the bottom of the pressure shell produced the desired load-sharing effect to ultimately save significant structural weight.	no	
NASA/TM-2011-217186; NESC-RP-06-019	Composite Crew Module: Design	Nov. 2011	n/a	F-4: Composite preform shapes are good structural design members for connecting intersecting composite panels.	yes	Consider preform shapes for connecting the panels. (Joint task)
NASA/TM-2011-217186; NESC-RP-06-019	Composite Crew Module: Design	Nov. 2011	n/a	F-8: Attaching secondary structure to composite honeycomb panels was proven to be manageable and weight-efficient.	yes	Consider this finding in trade studies as an advantage of using honeycomb. (STA design and Flight design)
NASA/TM-2011-217187; NESC-RP-06-019	Composite Crew Module: Materials and Processes	Nov. 2011	n/a	F-1: An alternative method to handle uncertainty in discontinuities is to use a single factor of safety (consistent with that for acreage), but developed element level design allowances, as opposed to material level allowances. This method handles the failure modes, variability, and uncertainty at a higher structural assembly level.	TBD	TBD
NASA/TM-2011-217187; NESC-RP-06-019	Composite Crew Module: Materials and Processes	Nov. 2011	n/a	F-2: There is a gap between many CM's design allowable and true damaged material capability (i.e., overconservatism versus compression after impact producing a 0.25-inch flaw). This gap represents a weight saving opportunity, but requires developing both performance curves (e.g., strength versus defect size) and defect Pd0 curves/studies.	TBD	TBD
NASA/TM-2011-217187; NESC-RP-06-019	Composite Crew Module: Materials and Processes	Nov. 2011	n/a	F-4: Minimum gap is partially driven by a derived permeability constraint. Decoupling leakage from structure through use of a polymeric membrane would relieve this constraint, presenting a mass savings opportunity in minimum gap size reduction.	TBD	TBD
NASA/TM-2011-217187; NESC-RP-06-019	Composite Crew Module: Materials and Processes	Nov. 2011	n/a	F-5: Large gaps are required to robustly joining solution for orthogonal joints. Specifically, their uncured flexibility accommodates large pre-cured assembly variations. Their fully interlocked waves eliminated delamination failure modes within the preform. Finally, they outperformed (strength/unit mass) conventional bonded joints for similar geometry.	yes	Consider 3D woven joints. (Joint task)
NASA/TM-2011-217187; NESC-RP-06-019	Composite Crew Module: Materials and Processes	Nov. 2011	n/a	F-6: Out-of-autoclave splicing/joining is a critical technology for enabling large launch structures without the need for large infrastructure (i.e., large autoclaves).	yes	Perform analysis and testing of splicing/joining options. (Joint task)
NASA/TM-2011-217188; NESC-RP-06-019	Composite Crew Module: Analysis	Nov. 2011	n/a	F-5: No flight structure is ever perfectly optimized. All engineering designs are a compromise to meet sometimes conflicting requirements.	no	
NASA/TM-2011-217188; NESC-RP-06-019	Composite Crew Module: Analysis	Nov. 2011	n/a	F-6: HyperSizer proved useful throughout the project, but excelled in three particular areas: 1. Early in the design, HyperSizer enabled rapid trade studies between different architectural concepts such as sandwich versus a variety of discrete stiffeners. 2. Once the architecture was selected, HyperSizer was used to analyze the light-weight structures to meet weight requirements. Weight reduction was achieved through the use of the software's integrated material selection and layout optimization tools. The manufactured layout was then used to select the best material for the structure. The manufactured layout was re-analyzed using HyperSizer to ensure that it also maintained positive MS. This process was formally incorporated into later versions of HyperSizer. 3. Once the design was released, HyperSizer was used in configuration management, ensuring that the effects of changes were tracked.	yes	Do not ignore potential sources of nonlinearity in higher-fidelity analyses. (STA and Flight design)
NASA/TM-2011-217188; NESC-RP-06-019	Composite Crew Module: Analysis	Nov. 2011	n/a	F-8: HyperSizer proved useful throughout the project, but excelled in three particular areas: 1. Early in the design, HyperSizer enabled rapid trade studies between different architectural concepts such as sandwich versus a variety of discrete stiffeners. 2. Once the architecture was selected, HyperSizer was used to analyze the light-weight structures to meet weight requirements. Weight reduction was achieved through the use of the software's integrated material selection and layout optimization tools. The manufactured layout was then used to select the best material for the structure. The manufactured layout was re-analyzed using HyperSizer to ensure that it also maintained positive MS. This process was formally incorporated into later versions of HyperSizer. 3. Once the design was released, HyperSizer was used in configuration management, ensuring that the effects of changes were tracked.	yes	HyperSizer is being used for mass trades. (Analysis tasks)

NASA/TM-2011-217188; NESC-RP-06-019	Composite Crew Module: Analysis	Nov. 2011	n/a	F-3b: A coarse grid FEM (finite element size) was sufficient to reduce drawing for manufacturing of the final design but the fine grid model (~inches element size) was constructed to better characterize the effect of pitch drops and other details within the structure. This extra detail in this model allowed for more accurately representing strains, and was especially important for the development of the backbone cap. In preparation for static test, the detail of the fine grid model generated more accurate strain predictions and allowed much faster resolution of strain issues.	yes	Use models with appropriate and sufficient levels of fidelity for the different analysis tasks. (All analysis tasks)
NASA/TM-2011-217188; NESC-RP-06-019	Composite Crew Module: Manufacturing	Nov. 2011	n/a	F-3c: Using the final hardware cure tool as part of the fabrication process development plan to do early releases provided accurate scaled feedback with coupon/element testing and allowed manufacturing lessons learned to influence the final design.	no	
NASA/TM-2011-217188; NESC-RP-06-019	Composite Crew Module: Manufacturing	Nov. 2011	n/a	F-4: Using the final hardware cure tool to perform aluminum core heat forming process eliminated the need for large limited use tooling.	TBD	TBD
NASA/TM-2011-217188; NESC-RP-06-019	Composite Crew Module: Manufacturing	Nov. 2011	n/a	F-5: Alcore SHAPEGRID offered a robust core solution for high compound curvature regions.	TBD	TBD
NASA/TM-2011-217188; NESC-RP-06-019	Composite Crew Module: Manufacturing	Nov. 2011	n/a	F-6: The multi-step cure process (i.e., cure of inner skin, cure of core to inner skin, and cure of outer skin on the core as separate, sequential cures) proved to have numerous manufacturing advantages.	yes	Consider a multi-step cure process for manufacturing of STA (STA manufacturing)
NASA/TM-2011-217188; NESC-RP-06-019	Composite Crew Module: Manufacturing	Nov. 2011	n/a	F-8: Male core tools on the CCM inner surface were selected to increase the consolidation of the IML skin to decrease porosity and increase the likelihood of low permeability skin.	TBD	TBD
NASA/TM-2011-217188; NESC-RP-06-019	Composite Crew Module: Manufacturing	Nov. 2011	n/a	F-10: FiberSIM was an invaluable software tool that facilitated the complex manufacturing of the CCM	yes	Use of FiberSIM is planned. (Manufacturing analysis)
NASA/TM-2011-217188; NESC-RP-06-019	Composite Crew Module: Manufacturing	Nov. 2011	n/a	F-11: The need for repair was caused by a variety of sources including inadvertent impact damage, failed secondary cures, and secondary mechanical fastener hole misalignment.	yes	Take special care with tooling (tethers?) to avoid impact damage. Make sure procedures for curing are followed correctly. Take special care with the placement of fastener holes; designers make sure to accommodate existing location constraints, manufacturing make sure to follow drawings. (STA design and manufacturing)
NASA/TM-2011-217188; NESC-RP-06-019	Composite Crew Module: Manufacturing	Nov. 2011	n/a	F-12: PI-preforms offer a joint configuration that has manufacturing benefits that are less sensitive to fit-up clearance, and bond line thickness	yes	Consider pi-preforms for joints. (Joint task)
NASA/TM-2011-217190; NESC-RP-06-019	Composite Crew Module: Test	Nov. 2011	n/a	F-1: Real-time monitoring of test results against analytical predictions was central to the success of the full-scale test program. This enabled the team to push the applied load progressively while minimizing the risk of catastrophic failure.	yes	Generate pre-test predictions and have analysts at stress stations during test. (STA analysis and test)
NASA/TM-2011-217190; NESC-RP-06-019	Composite Crew Module: Test	Nov. 2011	n/a	F-2: A tension test no-test was enabled using low-stretch high-strength flexible straps in combination with rollers to apply point loads. In addition to quick reconfiguration, the straps provided accurate, predictable, and repeatable load orientation and simplified the mounting of the load cylinders. A 10–12 percent frictional loss was measured when the load was rotated around a roller.	TBD	TBD
NASA/TM-2011-217190; NESC-RP-06-019	Composite Crew Module: Test	Nov. 2011	n/a	F-4: While strain gauges were the primary strain-measuring sensors for all full-scale tests, relatively newer techniques such as fiber-optic photogrammetry proved to be dependable and provided linear distribution of strain (optics). In areas of high strain gradients, these techniques were invaluable.	yes	Lobby for photogrammetry for testing of STA. (STA test)
NASA/TM-2011-217190; NESC-RP-06-019	Composite Crew Module: Test	Nov. 2011	n/a	F-5: To avoid possible interference between the painted speckled patterns and the post-test IR thermography, removable (self-adhesive paper) speckled patterns were utilized in some regions. These did not appear to affect photogrammetric measurements and the clean removal enabled improved post-test handling.	TBD	TBD
NASA/TM-2011-217190; NESC-RP-06-019	Composite Crew Module: Test	Nov. 2011	n/a	F-6: Pressurizing the CCM to failure with water instead of air preserved the mode of failure and allowed the team to carry out an effective failure analysis. Preserving the structure also offered options for further research studies.	no	
NASA/TM-2011-217190; NESC-RP-06-019	Composite Crew Module: Test	Nov. 2011	n/a	F-7: During all full-scale tests, the test team included members from all disciplines of the project. This enabled real-time decision-making and contributed to the successful and timely completion of the full-scale test.	TBD	TBD
NASA/TM-2011-217191; NESC-RP-06-019	Composite Crew Module: Nondestructive Evaluation	Nov. 2011	n/a	F-1: Woven joining technologies (i.e., PI-preform and cruxform) offer robust solutions for orthogonal joining. However, these technologies provide inspection challenges for bonding verification due to rough surface texture and complex internal fiber geometry. A custom ultrasonic probe housing was required to successfully inspect the PI-preform joint bonding on the load floor of the full-scale structure.	yes	Be mindful of inspection considerations when choosing joint construction. (Joint trade)
Internal ppt from Mark Kearney	Mark Kearney's Lessons Learned on Ares 1 Interstage	Jan. 2011	n/a	Composite testing is essential and should not be short changed	TBD	TBD
Internal ppt from Mark Kearney	Mark Kearney's Lessons Learned on Ares 1 Interstage	Jan. 2011	n/a	Testing should be completed in stages from testing/processing of basic features, through testing/processing of detailed design features, and through flight qualification testing. The schedule should be flexible since unknowns will need to be addressed.	TBD	TBD
Internal ppt from Mark Kearney	Mark Kearney's Lessons Learned on Ares 1 Interstage	Jan. 2011	n/a	Compressive testing will include risks of component failures, increase costs of design changes, and drastically compress schedules. Risk is added when activities are planned in parallel. Time should be placed in schedule for activities that feed into project decisions.	TBD	TBD
Internal ppt from Mark Kearney for EV tech luncheon	Composite Cryogenic Tank Demonstration Lessons Learned	June 2013	n/a	Flight project [should] pick materials that have 20-50 years of experience.	yes	Use conservative allowances for preliminary trade studies and design analyses. Use conservative allowances for design analysis until more accurate values obtained from testing specific to the project. If over-conservatism is a concern, select materials that are more well-characterized.
Internal ppt from Mark Kearney for EV tech luncheon	Composite Cryogenic Tank Demonstration Lessons Learned	June 2013	n/a	Requirements: Make sure all parties have agreement as to the implementation of the structural criteria.	yes	Make sure required design factors of safety and test factors are understood. Make sure NDE techniques and analysis implications (inspection limits for fracture analysis, etc.) are understood.
Internal ppt from Mark Kearney for EV tech luncheon	Composite Cryogenic Tank Demonstration Lessons Learned	June 2013	n/a	Thermal Compensation: Strain gauges are sensitive to thermal effects; use consistent gauges throughout testing or perform accurate thermal compensation. Small differences in composite lay-up between sample-size specimens and larger scale articles affect thermal compensation.	yes	Perform sufficient test planning for thermal compensation of instrumentation if needed.
Internal doc from Rob Wingate	Lessons Learned, SRB Composite Nose Cap Project, MSFC Strength Analysis Group	Dec. 1999	n/a	Material Characterization: The Strength Analysis Group should provide more insight to the project during the early stages of the material characterization process. The Strength Analysis Group should be more involved in the project during the development of the material characterization plan. The Strength Analysis Group should start doing preliminary analyses at project inception. These analyses should include all major loads, environments, and structural configurations to help determine which properties are needed. The preliminary analyses should also be used to determine which analytical techniques, finite element modeling strategies, etc. are going to be used as they may also determine what material properties are needed.	yes	Preliminary sizing studies are being performed for CEUS. Sensitivities to pristine vs. damaged properties are being explored. The stress team is communicating with the materials and testing groups concerning the damage tolerance plan and material property needed.
Internal doc from Rob Wingate	Lessons Learned, SRB Composite Nose Cap Project, MSFC Strength Analysis Group	Dec. 1999	n/a	Preliminary Analysis: The Strength Analysis Group should begin preliminary analyses at project inception using educated assumptions for material properties if necessary. By the time A basis strength allowances were available, the CNC project was well underway, with fabrication of the second prototype (P2) complete, and production of the third (final) prototype and first qualification unit scheduled to begin soon. However, the A basis allowances resulted in significant negative margins of safety in several areas of the composite shell, requiring redesigns to meet the requirements. Early in the project, the Strength Analysis Group had used jointing techniques which had much higher shear capacities than the base properties. It could be argued that the schedule was too aggressive and should have allowed more time between material characterization and production of the qualification unit. However, the Strength Analysis Group should also have worked with the Materials engineers to make educated assumptions for material properties to facilitate more accurate analyses later in the project. There was a significant amount of design iteration and rework done to develop the base properties for the materials used on other projects, etc.	yes	Preliminary sizing studies are being performed for CEUS. Sensitivities to pristine vs. damaged properties are being explored. The stress team is communicating with the materials and testing groups concerning the damage tolerance plan and material property needed.
Internal doc from Rob Wingate	Lessons Learned, SRB Composite Nose Cap Project, MSFC Strength Analysis Group	Dec. 1999	n/a	Damage Tolerance/Fracture Control: Damage tolerance of composite structures should be considered from project inception. Also, the MSFC Fracture Control Board should be consulted early in a project to gain their insight, identify any show-stoppers, and get them "on-board." A fracture control plan should be required. Damage tolerance was not addressed until well into the project and by the time the project was completed, it was determined that the damage tolerance was not being met. It is not clear why this was overlooked initially, but an informal meeting with some members of the MSFC Fracture Control Board raised the issue. The Strength Analysis Group, with support from the Materials organization, should develop a damage tolerance plan either separately or as part of the materials characterization plan or fracture control plan. This plan should begin project inception, as it may be costly due to the testing and analysis required to make any changes in the material characterization plan. After an oversight again, it is recommended that the MSFC Fracture Control Board be consulted early in a project to gain their insight, identify any show-stoppers, and get them "on-board." The Board should have been involved anyway as part of the fracture control review process, but no fracture control plan was required for the CNC. It is recommended that any future project like the CNC require a fracture control plan as well.	yes	Preliminary sizing studies are being performed for CEUS. Sensitivities to pristine vs. damaged properties are being explored. The stress team is communicating with the materials and testing groups concerning the damage tolerance plan and material property needed.
Internal doc from Rob Wingate	Lessons Learned, SRB Composite Nose Cap Project, MSFC Strength Analysis Group	Dec. 1999	n/a	Structural Verification: A Structural Verification Plan should be written, signed by the Leader of the Strength Analysis Group.	yes	TBD
Internal doc from Rob Wingate	Lessons Learned from the SRB Composite Nose Cap Project	Jan. 2000	n/a	All at the initiation of the project, a review of the preliminary requirements was conducted by the Composite Nose Cap team. Significant changes to the testing and analysis requirements were introduced throughout the design process. Based on the continuous change in testing and analysis requirements, it was identified that a formal Preliminary Design Review (PDR) should have been conducted.	yes	A Structural Requirements Review (SRR) was conducted on Feb. 13, 2015.
Internal doc from Rob Wingate	Lessons Learned from the SRB Composite Nose Cap Project	Jan. 2000	n/a	Preliminary Design Review was conducted in March, 1999. Although the review produced a good review of the material provided, the primary participants in the review were on the design team. Subsequent to the review, other representatives from MSFC and USBL became involved in the project and identified significant impacts in the areas of testing and analysis. The introduction of the additional testing and analysis provided for significant cost and schedule impacts to the project. The identification of these impacts in the project could have been avoided by a more thorough review team at the Preliminary Design Review.	yes	TBD
Internal doc from Rob Wingate	Lessons Learned from the SRB Composite Nose Cap Project	Jan. 2000	n/a	The Material Characterization Plan outlined all material level testing that would be performed in the material characterization phase of the project. Though the testing was identified in the plan, the actual testing conditions and approach were not determined until much later in the project. In several cases, there was a significant difference between the material characterization plan and the actual testing plan. The conditioning of test samples for mechanical and thermal testing in one area where it was identified that the conditioning used was significantly more conservative that the actual conditioning observed during beach exposure testing. It was also identified that all samples (including dry samples) should be weighed prior to testing to determine any moisture gain during storage.	yes	TBD
Internal doc from Rob Wingate	Lessons Learned from the SRB Composite Nose Cap Project	Jan. 2000	n/a	Design, development, test and validation (DD&T) processes historically have cost, schedule, and weight goals throughout the project. These might be minimized by taking the following approaches: (1) Lay the project out in Phases (Material Characterization, Preliminary Design/Analysis, Final Design/Analysis and Qualification). This approach would allow for periodic funding and schedule reviews prior to continuing to the next phase. (2) Partnering of projects between the contractor and NASA can provide for benefits to both parties. Conduct a trade study to determine if the project within the partnering guidelines as well as the capabilities of parties to be involved. Clearly document deliverables and required delivery dates for data that must be shared between the parties.	TBD	TBD

Internal doc from Rob Wingate	Lessons Learned from the SRB Composite Nose Cap Project	Jan. 2000	n/a	Clear management direction and support for the project should be demonstrated prior to initiating the project. Once the project is initiated, priorities should be placed to assure all schedule critical items are completed on time.	TBD	TBD
Internal doc from Rob Wingate	Lessons Learned from the SRB Composite Nose Cap Project	Jan. 2000	n/a	Changes that provide for cost or schedule impact should be addressed immediately when identified.	TBD	TBD
Internal pdf	Composite Interstage Structural Concepts for Heavy Lift Launch Vehicles; Exploration Technology Development Program Advanced Composites Technology (ACT) Structural Concepts; Lightweight Spacecraft Structures & Materials (LSSM) Project	Sep. 2011	n/a	Ensure that all penetrations and other details from the CAD model and the previous analysis model correspond.	TBD	TBD
Internal pdf	Composite Interstage Structural Concepts for Heavy Lift Launch Vehicles; Exploration Technology Development Program Advanced Composites Technology (ACT) Structural Concepts; Lightweight Spacecraft Structures & Materials (LSSM) Project	Sep. 2011	n/a	Determine the areas that will be designated as discontinuities early in the analysis process.	TBD	TBD
Internal pdf	Composite Interstage Structural Concepts for Heavy Lift Launch Vehicles; Exploration Technology Development Program Advanced Composites Technology (ACT) Structural Concepts; Lightweight Spacecraft Structures & Materials (LSSM) Project	Sep. 2011	n/a	The ring frames and longerons being modeled in the proper location had a considerable impact on the stress field around the penetrations.	TBD	TBD
Internal pdf	Composite Interstage Structural Concepts for Heavy Lift Launch Vehicles; Exploration Technology Development Program Advanced Composites Technology (ACT) Structural Concepts; Lightweight Spacecraft Structures & Materials (LSSM) Project	Sep. 2011	n/a	Any model used for a concept down select, even when using beam or bar elements, should employ offsets to obtain a better stress field.	TBD	TBD
NASA-CR-4620	Composite Chronicles: A Study of the Lessons Learned in the Development, Production, and Service of Composite Structures	Nov. 1994	n/a	The use of a basic laminate family containing 0/90/+45 plies with a minimum of 10% of the plies in each direction is well suited to most applications, generally assures fiber dominated laminate properties, and simplifies layup and inspection.	TBD	TBD
NASA-CR-4620	Composite Chronicles: A Study of the Lessons Learned in the Development, Production, and Service of Composite Structures	Nov. 1994	n/a	The number of mechanical joints should be minimized by utilizing large cocured or coldbonded subassemblies. Mechanical joints should be restricted to attachment of metal fittings and situations where assembly or access is impractical using alternative approaches.	TBD	TBD
NASA-CR-4620	Composite Chronicles: A Study of the Lessons Learned in the Development, Production, and Service of Composite Structures	Nov. 1994	n/a	Cold bonding is preferred over secondary bonding. Secondary bonding requires near perfect interface fit up.	TBD	TBD
NASA-CR-4620	Composite Chronicles: A Study of the Lessons Learned in the Development, Production, and Service of Composite Structures	Nov. 1994	n/a	Mechanically fastened joints require closer tolerance fit up. Liquid or structural shimming is usually required to assure a good fit and to avoid damage to the composite parts during assembly.	TBD	TBD
NASA-CR-4620	Composite Chronicles: A Study of the Lessons Learned in the Development, Production, and Service of Composite Structures	Nov. 1994	n/a	Dimensional tolerances are more critical in composites than in metals. Dimensional control of mating parts is important to prevent damage to parts during assembly.	TBD	TBD
NASA-CR-4620	Composite Chronicles: A Study of the Lessons Learned in the Development, Production, and Service of Composite Structures	Nov. 1994	n/a	Large, cocured assemblies reduce weight and save cost. However, the assembly requires overly complex tooling; however, the potential cost savings from low part count can be easily negated. Productability must be a key consideration in the design. Designing for producibility is generally more cost effective than optimization for weight savings.	TBD	TBD
Internal ppt from Boeing/Don Barnes	Boeing Lessons Learned: Delta IV Centerbody and Interstage, Sea Launch Fairings and Payload Attach Structures	Oct. 2007	n/a	Design structures to be simple. Minimize interfaces and less expensive to do dual testing at room temperature: (1) general knowledge of firm core material tools and thermal profiles to identify worst case; (2) Test at RT and use Environmental Correction Factor; (3) Thermally condition interfaces only if significant temperature differences are present, such as at cryogenic joints.	yes	TBD
Internal ppt from Boeing/Don Barnes	Boeing Lessons Learned: Delta IV Centerbody and Interstage, Sea Launch Fairings and Payload Attach Structures	Oct. 2007	n/a	Perform material testing as early as possible, have a good set of allowables in time for PDR. Perform testing early to prevent downstream requirements changes.	yes	TBD
Internal ppt from Boeing/Don Barnes	Boeing Lessons Learned: Delta IV Centerbody and Interstage, Sea Launch Fairings and Payload Attach Structures	Oct. 2007	n/a	For producibility, IM7/8552-2 (vs. IM7/8552) is specially formulated to run through machines better and save cost out-time. Honeycomb core 5056P has better properties and better corrosion resistance than 5952.	TBD	TBD
Internal ppt from Boeing/Don Barnes	Boeing Lessons Learned: Delta IV Centerbody and Interstage, Sea Launch Fairings and Payload Attach Structures	Oct. 2007	n/a	Develop repair procedures early.	TBD	TBD
Internal ppt from Boeing/Don Barnes	Boeing Lessons Learned: Delta IV Centerbody and Interstage, Sea Launch Fairings and Payload Attach Structures	Oct. 2007	n/a	Don't forget Secondary Structure attachment allowable testing - allowables determined analytically conservative compared to tested allowables	TBD	TBD
Internal ppt from Boeing/Don Barnes	Boeing Lessons Learned: Delta IV Centerbody and Interstage, Sea Launch Fairings and Payload Attach Structures	Oct. 2007	n/a	Identify and freeze lift point (transportation and handling) locations early to assist with GSE design.	yes	TBD
Internal ppt from Boeing/Don Barnes	Boeing Lessons Learned: Delta IV Centerbody and Interstage, Sea Launch Fairings and Payload Attach Structures	Oct. 2007	n/a	Use segmented rings for attaching to composite shell [if shell is a one-piece cylinder]. Consider placing rings against IML instead of OML for load distribution - may result in better load path and use of smooth laying surface [depending on joint configuration and tooling surface].	TBD	TBD
Internal ppt from Boeing/Don Barnes	Boeing Lessons Learned: Delta IV Centerbody and Interstage, Sea Launch Fairings and Payload Attach Structures	Oct. 2007	n/a	For one piece closeout, promotes eccentricity in lead path, can avoid ply drops on chamfered core, can avoid sharp points in core (which can be easily damaged, driving up rework).	TBD	TBD
Internal ppt from Boeing/Don Barnes	Boeing Lessons Learned: Delta IV Centerbody and Interstage, Sea Launch Fairings and Payload Attach Structures	Oct. 2007	n/a	Core mismatch criteria needs to be defined early as it potentially affects required facesheet thickness.	TBD	TBD
Internal ppt from Boeing/Don Barnes	Boeing Lessons Learned: Delta IV Centerbody and Interstage, Sea Launch Fairings and Payload Attach Structures	Oct. 2007	n/a	Use high density core rather than potting at bolted joint locations. Potting involves more touch labor, adds weight, and is rigid and does not conform to the tool surface.	TBD	TBD
Internal ppt from Boeing/Don Barnes	Boeing Lessons Learned: Delta IV Centerbody and Interstage, Sea Launch Fairings and Payload Attach Structures	Oct. 2007	n/a	Do not sculpt core for pad-ups.	TBD	TBD
Internal ppt from Boeing/Don Barnes	Boeing Lessons Learned: Delta IV Centerbody and Interstage, Sea Launch Fairings and Payload Attach Structures	Oct. 2007	n/a	Where separate doublers end up being close together or overlapping, combine doublers into a larger reinforcement. Applicable to both openings and secondary structure attachment. Also applies to areas where higher density core is needed. Combining doublers reduces the number of plies that have to be cut and letted, and also eases the creation of design and stress models.	yes	TBD
Internal ppt from Boeing/Don Barnes	Boeing Lessons Learned: Delta IV Centerbody and Interstage, Sea Launch Fairings and Payload Attach Structures	Oct. 2007	n/a	Define Access Requirements Now. Score out GSE interfaces (and stay-out zones) now, based on rough assembly drawings and experience if there are no hard requirements.	yes	TBD
Internal ppt from Boeing/Don Barnes	Boeing Lessons Learned: Delta IV Centerbody and Interstage, Sea Launch Fairings and Payload Attach Structures	Oct. 2007	n/a	Pay attention to the mass of the hardware - they help to determine what you get the most "bang for the buck" in terms of weight savings. If cost is a factor, probably more cost-effective to add the weight to the structure (productability) to pay dividends later (extensibility, reusability).	yes	TBD

APPENDIX B—MATERIALS

The test matrices in tables 27–29 were being implemented in support of the Digimat modeling effort. Fiber had been procured and resin panel procurement was in process at the time of this publication. Panels from the equivalency test program were made available to this effort, but no test coupons have been tested at the time of this publication.

Table 27. Fiber (IM7) test matrix.

Layup	Test Type and Direction	Property	No. of Batches × No. of Panels × No. of Specimens		
			Test Temperature/Moisture Condition		
			CTD	RTD	ETW
Single-filament	ASTM D3379 (withdrawn)—axial, tension	E ₁₁ , +S ₁	15	15	15
Single-filament	Tensile recoil test	-S ₁	15	15	15
Single-filament	Torsion pendulum test	G _{LT}	15	15	15

Total number of tests: 135

Table 28. Matrix (8552-1 neat resin) test matrix.

Layup/Material	Test Type and Direction	Property	No. of Batches × No. of Panels × No. of Specimens		
			Test Temperature/Moisture Condition		
			CTD	RTD	ETW
Matrix, resin	ASTM D638, tension	E, +S, nu	1×3×5	1×3×5	1×3×5
Matrix, resin	ASTM D695, compression	E, -S, nu	1×3×5	1×3×5	1×3×5
Matrix, resin	ASTM D5379, losipescu shear	G, S12	1×3×5	1×3×5	1×3×5

Total number of tests: 135

Table 29. IM7/8552-1 lamina/laminate test matrix.

Layup	Test Type and Direction	Property	No. of Batches × No. of Panels × No. of Specimen		
			Test Temperature/Moisture Condition		
			CTD	RTD	ETW
[0] ₆	ASTM D3039, tension	E ₁₁ , +S ₁ , V ₁₂	1×3×5	1×3×5	1×3×5
[0] ₁₄	ASTM D6641, compression	E _{11c} , -S ₁	1×3×5	1×3×5	1×3×5
[90] ₁₄	ASTM D3039, tension	E ₂₂ , +S ₂ , V ₁₂	1×3×5	1×3×5	1×3×5
[90] ₁₄	ASTM D6641, compression	E _{22c} , -S ₂	1×3×5	1×3×5	1×3×5
[45/-45]3s	ASTM D2344, shear	G ₁₂ , S ₁₂	1×3×5	1×3×5	1×3×5
[45/0/-45/90]s	ASTM D3039, tension	Ex or y, Fx or y	1×3×5	1×3×5	1×3×5
[45/0/-45/90]s	ASTM D6641, compression	Ex or y, Fx or y	1×3×5	1×3×5	1×3×5
[45/0/-45/90]s	ASTM D3039, tension	Ex or y, Fx or y	1×3×5	1×3×5	1×3×5
[45/0/-45/90]s	ASTM D6641, compression	Ex or y, Fx or y	1×3×5	1×3×5	1×3×5

Total number of tests: 405

B.1 8552 IM7 Unidirectional Prepreg Reports

Hexcel 8552 IM7 Unidirectional Prepreg 190 gsm and 35% RC Statistical Analysis Report for Combined NASA Samples and the Equivalent Statistical Analysis Report are found in this appendix.



WICHITA STATE
UNIVERSITY
*NATIONAL INSTITUTE
FOR AVIATION RESEARCH*

Report No: NCP-RP-2016-001 NC
Report Date: April 11th, 2016

Hexcel 8552 IM7 Unidirectional Prepreg 190 gsm & 35%RC Statistical Analysis Report for Combined NASA Samples (Glenn, Langley & Marshall)

Test Report Number: NCP-RP-2016-001 NC

Report Date: April 11, 2016

Elizabeth Clarkson
National Institute for Aviation Research
Wichita State University
Wichita, KS 67260-0093

Testing Facility:
Composites Laboratory
National Institute for Aviation Research
Wichita State University
1845 N. Fairmount
Wichita, KS 67260-0093

Test Panel Fabrication Facility:
NASA Glenn Research Center
NASA Langley Research Center
NASA Marshall Space Flight Center



WICHITA STATE
UNIVERSITY
NATIONAL INSTITUTE
FOR AVIATION RESEARCH

Report No: NCP-RP-2016-001 NC
Report Date: April 11th, 2016

Prepared by: Elizabeth Clarkson
Elizabeth Clarkson, Ph.D
Digitally signed by Elizabeth Clarkson
DN: CN=Elizabeth Clarkson, ou=CAWIFI
NWR, ou=CAWIFI, ou=CAWIFI
email=elizabethclarkson@wichita.edu, ou=CAWIFI
Date: 2016.04.11 17:02:54 -05'00'

Reviewed by: Kim Leng Poon
Kim-Leng Poon
Digitally signed by Kim Leng Poon
DN: ou=Kim Leng Poon, o=us
email=kpoon@wichita.edu,
ou=CAWIFI
Date: 2016.04.11 17:02:54 -05'00'

Approved by: Jeff Gilchrist
Jeff Gilchrist for Royal Lovingfoss
Digitally signed by Jeff
Gilchrist
Date: 2016.04.11
18:23:30 -05'00'

REVISIONS:

Rev	By	Date	Pages Revised or Added
N/C	Elizabeth Clarkson	4-11-2016	Document Initial Release

Table of Contents

1. Introduction.....	6
1.1 Symbols and Abbreviations	6
2. Background	8
2.1 Results Codes	8
2.2 Equivalency Computations	8
2.2.1 Hypothesis Testing.....	8
2.2.2 Type I and Type II errors	9
2.2.3 Cumulative Error Probability.....	9
2.2.4 Strength and Modulus Tests.....	10
2.2.5 Modified Coefficient of Variation	12
3. Equivalency Test Results.....	14
4. Individual Test Results.....	20
4.1 Longitudinal (0°) Tension (LT)	20
4.2 Quasi Isotropic (“25/50/25”) Unnotched Tension (UNT1).....	26
4.3 Quasi Isotropic “25/50/25” Open-Hole Tension 1 (OHT1).....	31
4.4 Laminate Short-Beam Strength (LSBS).....	33
4.5 Quasi Isotropic (“25/50/25”) Unnotched Compression 1 (UNC1)	35
4.6 Quasi Isotropic “25/50/25” Open-Hole Compression 1 (OHC1)	39
5. Summary of Results.....	42
5.1 Failures	43
5.2 Pass Rate	43
5.3 Probability of Failures.....	43
6. Generic Basis Values Assessment.....	45
7. References.....	49

Figures

Figure 2-1 Type I and Type II errors	9
Figure 3-1 Summary of Combined Strength means and minimums compared to their respective Equivalence limits	19
Figure 3-2 Summary of Combined Modulus means and Equivalence limits	19
Figure 4-1 Longitudinal Tension Values, Averages and Acceptance limits for CTD Condition.....	24
Figure 4-2 Longitudinal Tension Values, Averages and Acceptance limits for RTD Condition.....	24
Figure 4-3 Longitudinal Tension Values, Averages and Acceptance limits for ETW Condition.....	25
Figure 4-4 UNT1 Values, Averages and Acceptance limits for CTD Condition	29
Figure 4-5 UNT1 Values, Averages and Acceptance limits for RTD Condition	30
Figure 4-6 UNT1 Values, Averages and Acceptance limits for ETW Condition	30
Figure 4-7 OHT1 Values, Averages and Acceptance limits.....	32
Figure 4-8 Laminate Short-Beam Strength means, minimums and Acceptance limits for NASA Labs.....	34
Figure 4-9 UNC1 means, minimums and Acceptance limits for RTD Condition.....	37
Figure 4-10 UNC1 means, minimums and Acceptance limits for ETW Condition	38
Figure 4-11 OHC1 means, minimums and Acceptance limits	41
Figure 5-1 Probability of Number of Failures	44
Figure 6-1 NASA OHC1 results with NCAMP Generic Criteria and Basis values	46
Figure 6-2 NASA LT & OHT1 CTD results with NCAMP Generic Criteria and Basis values	47
Figure 6-3 NASA LT & OHT1 RTD results with NCAMP Generic Criteria and Basis values	47
Figure 6-4 NASA LT & OHT1 ETW results with NCAMP Generic Criteria and Basis values	48

Tables

Table 0-1 Test Property Abbreviations	6
Table 0-2 Environmental Conditions Abbreviations	7
Table 2-1 One-sided tolerance factors for limits on sample mean values	11
Table 2-2 One-sided tolerance factors for limits on sample minimum values	12
Table 3-1 Summary of Equivalency Test Results for NASA Combined Locations.....	15
Table 3-2 Summary of Equivalency Test Results for NASA Glenn	16
Table 3-3 Summary of Equivalency Test Results for NASA Langley	17
Table 3-4 Summary of Equivalency Test Results for NASA Marshall.....	18
Table 3-5 "% Failed" Results Scale	18
Table 4-1 Longitudinal Tension Strength Results for CTD Condition.....	20
Table 4-2 Longitudinal Tension Strength Results for RTD Condition.....	21
Table 4-3 Longitudinal Tension Strength Results for ETW Condition	21
Table 4-4 Longitudinal Tension Modulus Results for CTD Condition	21
Table 4-5 Longitudinal Tension Modulus Results for RTD Condition.....	22
Table 4-6 Longitudinal Tension Modulus Results for ETW Condition	22
Table 4-7 UNT1 Strength Results for CTD Condition.....	26
Table 4-8 UNT1 Strength Results for RTD Condition.....	27
Table 4-9 UNT1 Strength Results for ETW Condition	27
Table 4-10 UNT1 Modulus Results for CTD Condition	28
Table 4-11 UNT1 Modulus Results for RTD Condition	28
Table 4-12 UNT1 Modulus Results for ETW Condition.....	29
Table 4-13 OHT1 Strength Results for CTD	31
Table 4-14 OHT1 Strength Results for RTD	31
Table 4-15 OHT1 Strength Results for ETW	32
Table 4-16 Laminate Short-Beam Strength Results for RTD.....	33
Table 4-17 Laminate Short-Beam Strength Results for ETW	33
Table 4-18 UNC1 Strength Results for RTD.....	35
Table 4-19 UNC1 Strength Results for ETW	35
Table 4-20 UNC1 Modulus Results for RTD	36
Table 4-21 UNC1 Modulus Results for ETW	36
Table 4-22 OHC1 Strength Results For RTD Condition.....	39
Table 4-23 OHC1 Strength Results For ETW Condition	39
Table 6-1 OHC1 Generic Basis Values Acceptance Criteria and NASA test results.....	45
Table 6-2 LT Generic Basis Values Acceptance Criteria and NASA test results	46
Table 6-3 OHT1 Generic Basis Values Acceptance Criteria and NASA test results	46

1. Introduction

This report contains the equivalency test results for NASA Hexcel 8552 IM7 unidirectional material produced panels compared to the original qualification panels of the same material. The lamina and laminate material property data have been generated with a single batch of material. Panels were produced at the Glenn, Marshall and Langley research centers.

The tests on the equivalency specimens were performed at the National Institute for Aviation Research (NIAR) in Wichita, Kansas. The comparisons were performed according to CMH-17 Rev G section 8.4.1. The modified coefficient of variation (Mod CV) comparison tests were done in accordance with section 8.4.4 of CMH-17 Rev G.

The material property data for the qualification panels is published in Property Data Report CAM-RP-2009-015 Rev A. The material property data for the Integrated Composites, Inc equivalence panels is published in NCAMP Test Report CAM-RP-2012-015 N/C. Engineering basis values computed using CMH-17 methodologies were reported in NCAMP Report NCP-RP-2009-028 N/C which details the standards and methodology used for computing basis values as well as providing the B-basis values and A- and B- estimates computed from the test results for the original qualification panels. An alternative methodology, generic basis values, was developed for this material using data from multiple locations and was published in NCP-RP-2013-015 N/C.

The NCAMP shared material property database contains material property data of common usefulness to a wide range of aerospace projects. However, the data may not fulfill all the needs of a project. Specific properties, environments, laminate architecture, and loading situations that individual projects need may require additional testing.

The applicability and accuracy of this material property data, material allowables, and specifications must be evaluated on case-by-case basis by aircraft companies and certifying agencies. NIAR assumes no liability whatsoever, expressed or implied, related to the use of the material property data, material allowables and specifications.

1.1 Symbols and Abbreviations

Test Property	Abbreviation
Longitudinal Tension	LT
Unnotched Tension 1	UNT1
Unnotched Compression 1	UNC1
Laminate Short-Beam Strength	LSBS
Open-Hole Tension 1	OHT1
Open-Hole Compression 1	OHC1

Table 0-1 Test Property Abbreviations

Environmental Condition	Temperature	Abbreviation
Cold Temperature Dry	-65° F	CTD
Room Temperature Dry	70° F	RTD
Elevated Temperature Wet	250° F	ETW

Table 0-2 Environmental Conditions Abbreviations

Tests with a number immediately after the abbreviation indicate the lay-up:

1 refers to a 25/50/25 layup. This is also referred to as "Quasi-Isotropic"

2 refers to a 10/80/10 layup. This is also referred to as "Soft"

3 refers to a 40/20/40 layup. This is also referred to as "Hard"

EX: OHT1 is an Open-Hole Tension test with a 25/50/25 layup.

2. Background

Equivalence tests are performed in accordance with section 8.4.1 of CMH-17 Rev G and section 6.1 of DOT/FAA/AR-03/19, “Material Qualification and Equivalency for Polymer Matrix Composite Material Systems: Updated Procedure.”

2.1 Results Codes

Pass indicates that the test results are equivalent for that environment under both computational methods.

Fail indicates that the test results are NOT equivalent under both computational methods.

Pass with mod CV indicates the test results are equivalent under the assumption of the modified CV method that the coefficient of variation is at least 6 but the test results fail without the use of the modified CV method.

2.2 Equivalency Computations

Equivalency tests are performed to determine if the differences between test results can be reasonably explained as due to the expected random variation of the material and testing processes. If so, we can conclude the two sets of tests are from ‘equivalent’ materials.

2.2.1 Hypothesis Testing

This comparison is performed using the statistical methodology of hypothesis testing. Two mutually exclusive hypotheses are set up, termed the null (H_0) and the alternative (H_1). The null hypothesis is assumed true and must contain the equality. For equivalency testing, they are set up as follows, with M_1 and M_2 representing the two materials being compared:

$$\begin{aligned} H_0 : M_1 &= M_2 \\ H_1 : M_1 &\neq M_2 \end{aligned}$$

Samples are taken of each material and tested according to the plan. A test statistic is computed using the data from the sample tests. The probability of the actual test result is computed under the assumption of the null hypothesis. If that result is sufficiently unlikely then the null is rejected and the alternative hypothesis is accepted as true. If not, then the null hypothesis is retained as plausible.

2.2.2 Type I and Type II errors

	<i>Materials are equal</i>	<i>Materials are not equal</i>
<i>Conclude materials are equal</i>	<i>Correct Decision</i>	<i>Type II error</i>
<i>Conclude materials are not equal</i>	<i>Type I error</i>	<i>Correct Decision</i>

Figure 2-1 Type I and Type II errors

As illustrated in Figure 2-1, there are four possible outcomes: two correct conclusions and two erroneous conclusions. The two wrong conclusions are termed type I and type II errors to distinguish them. The probability of making a type I error is specified using a parameter called alpha (α), while the type II error is not easily computed or controlled. The term ‘sufficiently unlikely’ in the previous paragraph means, in more precise terminology, the probability of the computed test statistic under the assumption of the null hypothesis is less than α .

For equivalency testing of composite materials, α is set at 0.05 which corresponds to a confidence level of 95%. This means that if we reject the null and say the two materials are not equivalent with respect to a particular test, the probability that this is a correct decision is no less than 95%.

2.2.3 Cumulative Error Probability

Each characteristic (such as Longitudinal Tension strength or In-Plane Shear modulus) is tested separately. While the probability of a Type I error is the same for all tests, since many different tests are performed on a single material, each with a 5% probability of a type I error, the probability of having one or more failures in a series of tests can be much higher.

If we assume the two materials are identical, with two tests the probability of a type I error for the two tests combined is $1 - .95^2 = .0975$. For four tests, it rises to $1 - .95^4 = .1855$. For 25 tests, the probability of a type I error on 1 or more tests is $1 - .95^{25} = .7226$. With a high probability of one or more equivalence test failures due to random

chance alone, a few failed tests should be allowed and equivalence may still be presumed provided that the failures are not severe.

2.2.4 Strength and Modulus Tests

For strength test values, we are primarily concerned only if the equivalence sample shows lower strength values than the original qualification material. This is referred to as a ‘one-sided’ hypothesis test. Higher values are not considered a problem, though they may indicate a difference between the two materials. The equivalence sample mean and sample minimum values are compared against the minimum expected values for those statistics, which are computed from the qualification test result

The expected values are computed using the values listed in Table 2-1 and Table 2-2 according to the following formulas:

The mean must exceed $\bar{X} - k_n^{\text{table 2.1}} \cdot S$ where \bar{X} and S are, respectively, the mean and the standard deviation of the qualification sample.

The sample minimum must exceed $\bar{X} - k_n^{\text{table 2.2}} \cdot S$ where \bar{X} and S are, respectively, the mean and the standard deviation of the qualification sample.

If either the mean or the minimum falls below the expected minimum, the sample is considered to have failed equivalency for that characteristic and the null hypothesis is rejected. The probability of failing either the mean or the minimum test (the α level) is set at 5%.

For Modulus values, failure occurs if the equivalence sample mean is either too high or too low compared to the qualification mean. This is referred to as a ‘two-sided’ hypothesis test. A standard two-sample two-tailed t-test is used to determine if the mean from the equivalency sample is sufficiently far from the qualification sample mean to reject the null hypothesis. The probability of a type I error is set at 5%.

These tests are performed with the HYTEQ spreadsheet, which was designed to test equivalency between two materials in accordance with the requirements of CMH-17 Rev G section 8.4.1: Tests for determining equivalency between an existing database and a new dataset for the same material. Details about the methods used are documented in the references listed in Section 0.

n	One-sided tolerance factors for limits on sample mean values								
	0.25	0.1	0.05	0.025	0.01	0.005	0.0025	0.001	0.0005
2	0.6266	1.0539	1.3076	1.5266	1.7804	1.9528	2.1123	2.3076	2.4457
3	0.5421	0.8836	1.0868	1.2626	1.4666	1.6054	1.7341	1.8919	2.0035
4	0.4818	0.7744	0.9486	1.0995	1.2747	1.3941	1.5049	1.6408	1.7371
5	0.4382	0.6978	0.8525	0.9866	1.1425	1.2488	1.3475	1.4687	1.5546
6	0.4048	0.6403	0.7808	0.9026	1.0443	1.1411	1.2309	1.3413	1.4196
7	0.3782	0.5951	0.7246	0.8369	0.9678	1.0571	1.1401	1.2422	1.3145
8	0.3563	0.5583	0.6790	0.7838	0.9059	0.9893	1.0668	1.1622	1.2298
9	0.3379	0.5276	0.6411	0.7396	0.8545	0.9330	1.0061	1.0959	1.1596
10	0.3221	0.5016	0.6089	0.7022	0.8110	0.8854	0.9546	1.0397	1.1002
11	0.3084	0.4790	0.5811	0.6699	0.7735	0.8444	0.9103	0.9914	1.0490
12	0.2964	0.4593	0.5569	0.6417	0.7408	0.8086	0.8717	0.9493	1.0044
13	0.2856	0.4418	0.5354	0.6168	0.7119	0.7770	0.8376	0.9121	0.9651
14	0.2760	0.4262	0.5162	0.5946	0.6861	0.7488	0.8072	0.8790	0.9300
15	0.2673	0.4121	0.4990	0.5746	0.6630	0.7235	0.7798	0.8492	0.8985
16	0.2594	0.3994	0.4834	0.5565	0.6420	0.7006	0.7551	0.8223	0.8700
17	0.2522	0.3878	0.4692	0.5400	0.6230	0.6797	0.7326	0.7977	0.8440
18	0.2455	0.3771	0.4561	0.5250	0.6055	0.6606	0.7120	0.7753	0.8202
19	0.2394	0.3673	0.4441	0.5111	0.5894	0.6431	0.6930	0.7546	0.7984
20	0.2337	0.3582	0.4330	0.4982	0.5745	0.6268	0.6755	0.7355	0.7782
21	0.2284	0.3498	0.4227	0.4863	0.5607	0.6117	0.6593	0.7178	0.7594
22	0.2235	0.3419	0.4131	0.4752	0.5479	0.5977	0.6441	0.7013	0.7420
23	0.2188	0.3345	0.4041	0.4648	0.5359	0.5846	0.6300	0.6859	0.7257
24	0.2145	0.3276	0.3957	0.4551	0.5246	0.5723	0.6167	0.6715	0.7104
25	0.2104	0.3211	0.3878	0.4459	0.5141	0.5608	0.6043	0.6579	0.6960
26	0.2065	0.3150	0.3803	0.4373	0.5041	0.5499	0.5926	0.6451	0.6825
27	0.2028	0.3092	0.3733	0.4292	0.4947	0.5396	0.5815	0.6331	0.6698
28	0.1994	0.3038	0.3666	0.4215	0.4858	0.5299	0.5710	0.6217	0.6577
29	0.1961	0.2986	0.3603	0.4142	0.4774	0.5207	0.5611	0.6109	0.6463
30	0.1929	0.2936	0.3543	0.4073	0.4694	0.5120	0.5517	0.6006	0.6354

Table 2-1 One-sided tolerance factors for limits on sample mean values

n	α								
	0.25	0.1	0.05	0.025	0.01	0.005	0.0025	0.001	0.0005
2	1.2887	1.8167	2.1385	2.4208	2.7526	2.9805	3.1930	3.4549	3.6412
3	1.5407	2.0249	2.3239	2.5888	2.9027	3.1198	3.3232	3.5751	3.7550
4	1.6972	2.1561	2.4420	2.6965	2.9997	3.2103	3.4082	3.6541	3.8301
5	1.8106	2.2520	2.5286	2.7758	3.0715	3.2775	3.4716	3.7132	3.8864
6	1.8990	2.3272	2.5967	2.8384	3.1283	3.3309	3.5220	3.7603	3.9314
7	1.9711	2.3887	2.6527	2.8900	3.1753	3.3751	3.5638	3.7995	3.9690
8	2.0317	2.4407	2.7000	2.9337	3.2153	3.4127	3.5995	3.8331	4.0011
9	2.0838	2.4856	2.7411	2.9717	3.2500	3.4455	3.6307	3.8623	4.0292
10	2.1295	2.5250	2.7772	3.0052	3.2807	3.4745	3.6582	3.8883	4.0541
11	2.1701	2.5602	2.8094	3.0351	3.3082	3.5005	3.6830	3.9116	4.0765
12	2.2065	2.5918	2.8384	3.0621	3.3331	3.5241	3.7054	3.9328	4.0969
13	2.2395	2.6206	2.8649	3.0867	3.3558	3.5456	3.7259	3.9521	4.1155
14	2.2697	2.6469	2.8891	3.1093	3.3766	3.5653	3.7447	3.9699	4.1326
15	2.2975	2.6712	2.9115	3.1301	3.3959	3.5836	3.7622	3.9865	4.1485
16	2.3232	2.6937	2.9323	3.1495	3.4138	3.6007	3.7784	4.0019	4.1633
17	2.3471	2.7146	2.9516	3.1676	3.4306	3.6166	3.7936	4.0163	4.1772
18	2.3694	2.7342	2.9698	3.1846	3.4463	3.6315	3.8079	4.0298	4.1902
19	2.3904	2.7527	2.9868	3.2005	3.4611	3.6456	3.8214	4.0425	4.2025
20	2.4101	2.7700	3.0029	3.2156	3.4751	3.6589	3.8341	4.0546	4.2142
21	2.4287	2.7864	3.0181	3.2298	3.4883	3.6715	3.8461	4.0660	4.2252
22	2.4463	2.8020	3.0325	3.2434	3.5009	3.6835	3.8576	4.0769	4.2357
23	2.4631	2.8168	3.0463	3.2562	3.5128	3.6949	3.8685	4.0873	4.2457
24	2.4790	2.8309	3.0593	3.2685	3.5243	3.7058	3.8790	4.0972	4.2553
25	2.4941	2.8443	3.0718	3.2802	3.5352	3.7162	3.8889	4.1066	4.2644
26	2.5086	2.8572	3.0838	3.2915	3.5456	3.7262	3.8985	4.1157	4.2732
27	2.5225	2.8695	3.0953	3.3023	3.5557	3.7357	3.9077	4.1245	4.2816
28	2.5358	2.8813	3.1063	3.3126	3.5653	3.7449	3.9165	4.1328	4.2897
29	2.5486	2.8927	3.1168	3.3225	3.5746	3.7538	3.9250	4.1409	4.2975
30	2.5609	2.9036	3.1270	3.3321	3.5835	3.7623	3.9332	4.1487	4.3050

Table 2-2 One-sided tolerance factors for limits on sample minimum values

2.2.5 Modified Coefficient of Variation

A common problem with new material qualifications is that the initial specimens produced and tested do not contain all of the variability that will be encountered when the material is being produced in larger amounts over a lengthy period of time. This can result in setting basis values that are unrealistically high.

The modified Coefficient of Variation (CV) used in this report is in accordance with section 8.4.4 of CMH-17 Revision G. It is a method of adjusting the original basis values downward in anticipation of the expected additional variation. Composite materials are expected to have a CV of at least 6%. When the CV is less than 8%, a modification is made that adjusts the CV upwards.

$$\text{Modified CV} = CV^* = \begin{cases} .06 & \text{if } CV < .04 \\ \frac{CV}{2} + .04 & \text{if } .04 \leq CV < .08 \\ CV & \text{if } CV \geq .08 \end{cases} \quad \text{Equation 1}$$

This is converted to percent by multiplying by 100%.

CV^* is used to compute a modified standard deviation S^* .

$$S^* = CV^* \cdot \bar{X}$$

Equation 2

To compute the pooled standard deviation based on the modified CV:

$$S_p^* = \sqrt{\frac{\sum_{i=1}^k (n_i - 1) (CV_i^* \cdot \bar{X}_i)^2}{\sum_{i=1}^k (n_i - 1)}} \quad \text{Equation 3}$$

The A-basis and B-basis values under the assumption of the modified CV method are computed by replacing S with S^* .

When the basis values have been set using the modified CV method, we can use the modified CV to compute the equivalency test results.

3. Equivalency Test Results

The three NASA locations each had 23 different tests conducted. When combined, all tests had sufficient data for comparison purposes, but when examining individual locations only the modulus tests had sufficient data to meet the CMH-17 Rev G requirements, but the strength tests lacked sufficient data for the results to be considered conclusive. The Glenn location had six additional tests conducted for both the Low Vacuum panels and the Slow Ramp Panels. These results were evaluated separately and were not included in the combined dataset. All equivalency tests were performed with an α level of 5%.

Before the data from different locations can be combined for an equivalency test, it must be statistically tested to determine if the three locations produce similar enough product for the combined data to be considered *unstructured*, or having no significant differences between the test results from the different locations. When the data fail this test, an underlying assumption of the equivalency test is violated. The different locations will need to be evaluated individually for any property that shows differences between the locations.

The results of the equivalency comparisons are listed as ‘Pass’, ‘Fail’, or ‘Pass with Mod. CV’. ‘Pass with Mod CV’ refers to cases where the equivalency fails unless the modified coefficient of variation method is used. A minimum of eight samples from two separate panels and processing cycles is required for strength properties and a minimum of four specimens are required for modulus comparison tests. If the sample does not have an adequate number of specimens, this will be indicated with ‘Insufficient Data’ after the Pass or Fail indication. A summary of results for the combined locations is shown in Table 3-1, NASA Glenn is shown in Table 3-2, for NASA Langley in Table 3-3, and for NASA Marshall in Table 3-4.

Failures in table 3-1 through 3-5 are reported as "Failed by %". This percentage was computed by taking the ratio of the equivalency mean or minimum value to the modified CV limit for that value. Table 3-5 gives a rough scale for the relative severity of those failures.

Equivalency Test Results for NASA Glenn, Langley and Marshall Combined					
Test	Normalized Data	Property	Environmental Condition		
			CTD	RTD	ETW
Longitudinal Tension	Yes	Strength	Pass	Pass	Pass
		Modulus	Pass	Pass with Mod CV	Failed by 0.5%
Laminate Short Beam Strength	No	Strength		Pass	Pass with Mod CV
Unnotched Compression	Yes	Strength		Pass	Pass
	Yes	Modulus		Pass	* Data Not Combined
Unnotched Tension	Yes	Strength	Pass	Pass	* Data Not Combined
		Modulus	* Data Not Combined	Failed by 0.2%	Pass
Open Hole Compression	Yes	Strength		Failed by 1.6%	Failed by 5.8%
Open Hole Tension	Yes	Strength	Pass	* Data Not Combined	Pass

* Statistically significant differences between locations indicate that data should not be combined.

Table 3-1 Summary of Equivalency Test Results for NASA Combined Locations

Equivalency Test Results for Nasa Glenn M Cure Cycle with Hexcel 8552 IM7 M Cure Cycle						
Test	Normalized Data	Property	Environmental Condition			
			CTD	RTD	ETD	ETW
Longitudinal Tension	Yes	Strength	Pass Insufficient Data	Pass Insufficient Data		Pass Insufficient Data
		Modulus	Pass	Pass		Pass with Mod CV
Laminate Short Beam Strength	No	Strength		Pass Insufficient Data		Pass with Mod CV Insufficient Data
Unnotched Compression (UNC1)	Yes	Strength		Pass Insufficient Data		Pass Insufficient Data
	Yes	Modulus		Pass		Failed by 2.9%
Unnotched Tension (UNT1)	Yes	Strength	Pass Insufficient Data	Pass Insufficient Data		Pass Insufficient Data
		Modulus	Pass	Pass		Pass
Open Hole Compression (OHC1)	Yes	Strength		Failed by 1.1% Insufficient Data		Failed by 5.1% Insufficient Data
Open Hole Tension (OHT1)	Yes	Strength	Pass Insufficient Data	Pass Insufficient Data		Pass Insufficient Data

Table 3-2 Summary of Equivalency Test Results for NASA Glenn

Equivalency Test Results for NASA Langley M Cure Cycle with Hexcel 8552 IM7 M Cure Cycle						
Test	Normalized Data	Property	Environmental Condition			
			CTD	RTD	ETD	ETW
Longitudinal Tension	Yes	Strength	Pass Insufficient Data	Pass Insufficient Data		Pass Insufficient Data
		Modulus	Pass with Mod CV	Pass		Pass with Mod CV
Laminate Short Beam Strength	No	Strength		Pass Insufficient Data		Pass Insufficient Data
Unnotched Compression (UNC1)	Yes	Strength		Pass Insufficient Data		Pass Insufficient Data
	Yes	Modulus		Pass		Pass with Mod CV
Unnotched Tension (UNT1)	Yes	Strength	Pass Insufficient Data	Pass Insufficient Data		Pass Insufficient Data
		Modulus	Pass	Pass		Pass
Open Hole Compression (OHC1)	Yes	Strength		Pass with Mod CV Insufficient Data		Failed by 4.8% Insufficient Data
Open Hole Tension (OHT1)	Yes	Strength	Pass Insufficient Data	Pass Insufficient Data		Pass Insufficient Data

Table 3-3 Summary of Equivalency Test Results for NASA Langley

Equivalency Test Results for Nasa Marshall M Cure Cycle with Hexcel 8552 IM7 M Cure Cycle						
Test	Normalized Data	Property	Environmental Condition			
			CTD	RTD	ETD	ETW
Longitudinal Tension	Yes	Strength	Pass Insufficient Data	Pass Insufficient Data		Pass Insufficient Data
		Modulus	Pass with Mod CV	Pass		Pass with Mod CV
Laminate Short Beam Strength	No	Strength		Pass Insufficient Data		Failed by 0.1% Insufficient Data
Unnotched Compression (UNC1)	Yes	Strength		Pass Insufficient Data		Pass Insufficient Data
	Yes	Modulus		Pass		Pass with Mod CV
Unnotched Tension (UNT1)	Yes	Strength	Pass Insufficient Data	Pass Insufficient Data		Pass Insufficient Data
		Modulus	Pass	Pass		Pass
Open Hole Compression (OHC1)	Yes	Strength		Pass with Mod CV Insufficient Data		Failed by 1.9% Insufficient Data
Open Hole Tension (OHT1)	Yes	Strength	Pass Insufficient Data	Pass Insufficient Data		Pass Insufficient Data

Table 3-4 Summary of Equivalency Test Results for NASA Marshall

Description	Modulus	Strength
Mild Failure	% fail \leq 4%	% fail \leq 5%
Mild to Moderate Failure	4% $<$ % fail \leq 8%	5% $<$ % fail \leq 10%
Moderate Failure	8% $<$ % fail \leq 12%	10% $<$ % fail \leq 15%
Moderate to Severe Failure	12% $<$ % fail \leq 16%	15% $<$ % fail \leq 20%
Severe Failure	16% $<$ % fail \leq 20%	20% $<$ % fail \leq 25%
Extreme Failure	20% $<$ % fail	25% $<$ % fail

Table 3-5 "% Failed" Results Scale

Graphical presentations of the combined location test results are shown in Figure 3-1 and Figure 3-2. In order to show different tests on the same graphical scale, all values are plotted as a percentage of the corresponding qualification mean. Figure 3-1 shows the strength means in the upper part of the chart using left axis and the strength minimums in the lower part of the chart using the right axis. This was done to avoid overlap of the two sets of data and equivalency criteria. Figure 3-2 shows the equivalency means plotted with the upper and lower equivalency criteria.

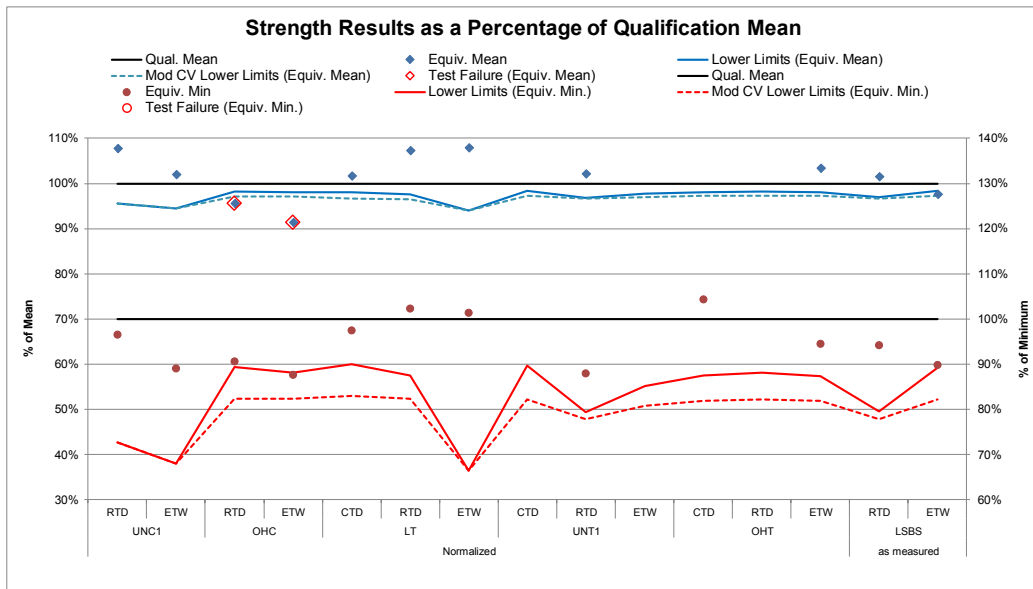


Figure 3-1 Summary of Combined Strength means and minimums compared to their respective Equivalence limits

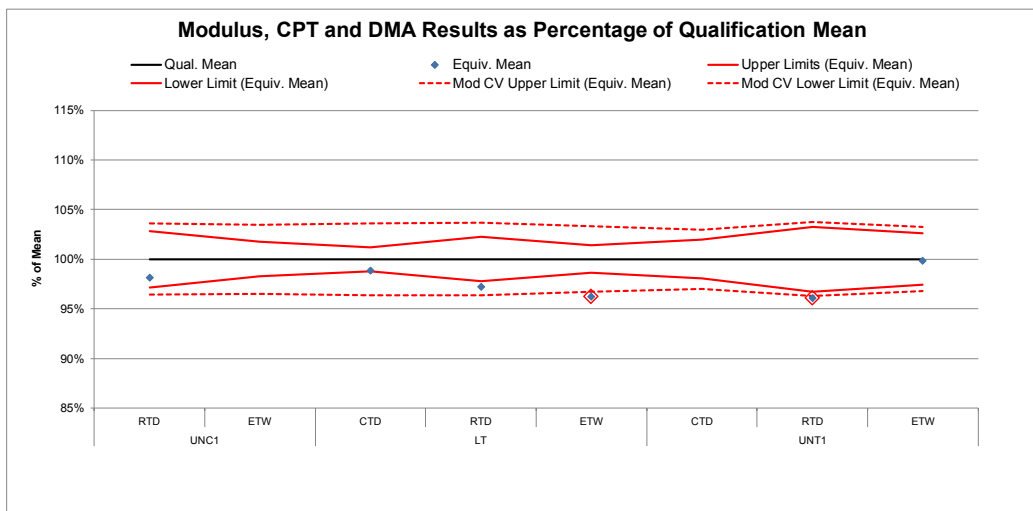


Figure 3-2 Summary of Combined Modulus means and Equivalence limits

4. Individual Test Results

4.1 Longitudinal (0°) Tension (LT)

The normalized LT data from all three locations could be combined. The combined dataset passed all equivalency tests for strength but failed equivalence for modulus in the ETW condition. All three locations failed due to the modulus values being too low. The individual locations passed with the use of the modified CV method, but the combined sample did not. This is due to the fact that larger samples have tighter acceptance limits.

Modified CV results could not be computed for the ETW strength data because that condition had a CV larger than 8%, which is not modified. However, the individual locations all passed the modulus equivalency tests with the use of the modified CV approach. There was insufficient strength data for results of the individual locations to be considered conclusive.

Statistics and analysis results are shown for the strength data CTD condition in Table 4-1, RTD condition in Table 4-2, ETW condition in Table 4-3 and for the modulus data CTD condition in Table 4-4, RTD Condition in Table 4-5 and ETW condition in Table 4-6.

Longitudinal Tension (LT) Strength CTD	Qualification Data	Glenn	Langley	Marshall	Combined
Data normalized with CPT 0.0072					
Mean Strength (ksi)	357.389	363.658	368.170	358.027	363.285
Standard Deviation	12.620	12.879	11.948	6.836	10.756
Coefficient of Variation %	3.531	3.541	3.245	1.909	2.961
Minimum	325.692	349.131	354.456	348.530	348.530
Maximum	379.970	379.884	382.683	364.778	382.683
Number of Specimens	22	4	4	4	12
RESULTS		PASS	PASS	PASS	PASS
Minimum Acceptable Equiv. Sample Mean	345.417	345.417	345.417	345.417	350.360
Minimum Acceptable Equiv. Sample Min	326.570	326.570	326.570	326.570	321.567
MOD CV RESULTS		PASS with MOD CV	PASS with MOD CV	PASS with MOD CV	PASS with MOD CV
Modified CV %		6.000			
Minimum Acceptable Equiv. Sample Mean	337.048	337.048	337.048	337.048	345.447
Minimum Acceptable Equiv. Sample Min	305.024	305.024	305.024	305.024	296.524

Table 4-1 Longitudinal Tension Strength Results for CTD Condition

Longitudinal Tension (LT) Strength RTD	Qualification Data	Glenn	Langley	Marshall	Combined
Data normalized with CPT 0.0072					
Mean Strength (ksi)	362.693	388.287	381.733	397.142	389.054
Standard Deviation	16.057	6.426	14.209	10.799	11.901
Coefficient of Variation %	4.427	1.655	3.722	2.719	3.059
Minimum	325.685	381.912	371.088	381.002	371.088
Maximum	392.322	397.057	402.585	403.821	403.821
Number of Specimens	18	4	4	4	12
RESULTS	PASS	PASS	PASS	PASS	PASS
Minimum Acceptable Equiv. Sample Mean	347.462	347.462	347.462	347.462	353.751
Minimum Acceptable Equiv. Sample Min	323.483	323.483	323.483	323.483	317.118
MOD CV RESULTS	PASS with MOD CV	PASS with MOD CV	PASS with MOD CV	PASS with MOD CV	PASS with MOD CV
Modified CV %			6.214		
Minimum Acceptable Equiv. Sample Mean	341.315	341.315	341.315	341.315	350.143
Minimum Acceptable Equiv. Sample Min	307.660	307.660	307.660	307.660	298.727

Table 4-2 Longitudinal Tension Strength Results for RTD Condition

Longitudinal Tension (LT) Strength ETW	Qualification Data	Glenn	Langley	Marshall	Combined
Data normalized with CPT					
Mean Strength (ksi)	333.504	356.367	358.081	366.531	360.005
Standard Deviation	38.823	11.526	13.232	12.901	12.462
Coefficient of Variation %	11.641	3.234	3.695	3.520	3.462
Minimum	244.533	340.091	338.169	348.106	338.169
Maximum	373.234	367.145	375.125	377.046	377.046
Number of Specimens	18	4	6	4	14
RESULTS	PASS	PASS	PASS	PASS	PASS
Minimum Acceptable Equiv. Sample Mean	296.676	303.191	296.676	296.676	313.463
Minimum Acceptable Equiv. Sample Min	238.698	232.692	238.698	238.698	221.340

Table 4-3 Longitudinal Tension Strength Results for ETW Condition

Longitudinal Tension (LT) Modulus CTD	Qualification Data	Glenn	Langley	Marshall	Combined
Data normalized with CPT 0.0072					
Mean Modulus (Msi)	22.568	22.207	22.146	22.144	22.304
Standard Deviation	0.387	0.133	0.196	0.229	0.353
Coefficient of Variation %	1.717	0.601	0.885	1.036	1.581
Minimum	21.852	22.055	21.965	21.855	21.855
Maximum	23.219	22.343	22.418	22.391	23.116
Number of Specimens	22	4	4	4	12
RESULTS	PASS	FAIL	FAIL	PASS	PASS
Passing Range for Modulus Mean	22.158 to 22.978	22.154 to 22.982	22.151 to	22.293 to 22.843	
Student's t-statistic	-1.818	-2.104	-2.100	-1.957	
p-value of Student's t-statistic	0.082	0.046	0.046	0.059	
MOD CV RESULTS	PASS with MOD CV	PASS with MOD CV	PASS with MOD CV	PASS with MOD CV	PASS with MOD CV
Modified CV%			6.000		
Passing Range for Modulus Mean	21.146 to 23.990	21.145 to 23.991	21.144 to	21.752 to 23.384	
Modified CV Student's t-statistic	-0.524	-0.612	-0.615	-0.659	
p-value of Student's t-statistic	0.605	0.546	0.545	0.515	

Table 4-4 Longitudinal Tension Modulus Results for CTD Condition

Longitudinal Tension (LT) Modulus RTD	Qualification Data	Glenn	Langley	Marshall	Combined
Data normalized with CPT 0.0072					
Mean Modulus (Msi)	22.987	22.561	22.350	22.565	22.354
Standard Deviation	0.812	0.501	0.543	0.069	0.352
Coefficient of Variation %	3.532	2.219	2.429	0.308	1.576
Minimum	20.707	22.117	21.875	22.507	21.875
Maximum	23.941	23.116	23.074	22.660	23.074
Number of Specimens	18	4	4	4	12
RESULTS	PASS	PASS	PASS	PASS	FAIL
Passing Range for Modulus Mean	22.095 to 23.878	22.090 to 23.883	22.123 to 23.85	22.475 to 23.498	
Student's t-statistic	-0.996	-1.481	-1.018	-2.535	
p-value of Student's t-statistic	0.331	0.154	0.321	0.017	
MOD CV RESULTS	PASS with MOD CV	PASS with MOD CV	PASS with MOD CV	PASS with MOD CV	
Modified CV%			6.000		
Passing Range for Modulus Mean	21.504 to 24.470	21.501 to 24.473	21.520 to	22.149 to 23.824	
Modified CV Student's t-statistic	-0.599	-0.894	-0.600	-1.548	
p-value of Student's t-statistic	0.556	0.382	0.555	0.133	

Table 4-5 Longitudinal Tension Modulus Results for RTD Condition

Longitudinal Tension (LT) Modulus ETW	Qualification Data	Glenn	Langley	Marshall	Combined
Data normalized with CPT 0.0072					
Mean Modulus (Msi)	24.001	23.249	23.160	22.847	23.096
Standard Deviation	0.557	0.393	0.367	0.203	0.354
Coefficient of Variation %	2.321	1.690	1.583	0.887	1.531
Minimum	23.222	22.787	22.693	22.652	22.652
Maximum	25.578	23.744	23.663	23.087	23.744
Number of Specimens	29	4	6	4	14
RESULTS	FAIL	FAIL	FAIL	FAIL	
Passing Range for Modulus Mean	23.410 to 24.592	23.515 to 24.487	23.421 to	23.671 to 24.33	
Student's t-statistic	-2.596	-3.521	-4.059	-5.545	
p-value of Student's t-statistic	0.014	0.001	0.0003	0.000002	
MOD CV RESULTS	PASS with MOD CV	PASS with MOD CV	PASS with MOD CV	FAIL	
Modified CV%			6.000		
Passing Range for Modulus Mean	22.506 to 25.495	22.783 to 25.218	22.510 to	23.208 to 24.794	
Modified CV Student's t-statistic	-1.026	-1.405	-1.579	-2.305	
p-value of Student's t-statistic	0.313	0.169	0.124	0.026	

Table 4-6 Longitudinal Tension Modulus Results for ETW Condition

The LT modulus data for the combined data in the RTD environment failed the equivalency test because the sample mean value (22.354) is below the lower acceptance limit (22.475). The equivalency sample mean value is 99.46% of the lower limit of acceptable values. Under the assumption of the modified CV method, the modulus data from the RTD environment passed the equivalence test.

The LT modulus data for the combined data in the ETW environment failed the equivalency test because the sample mean value (23.096) is below the lower acceptance limit (23.671). The equivalency sample mean value is 97.57% of the lower limit of acceptable values. Under the assumption of the modified CV method, it was 99.52% of the lower limit of acceptable values (23.208).

The LT modulus data for Glenn in ETW environment failed the equivalency test because the sample mean value (23.249) is below the lower acceptance limit (23.410). The equivalency sample mean value is 99.31% of the lower limit of acceptable values. Under the assumption of the modified CV method, the modulus data from the ETW environment passed the equivalence test.

The LT modulus data for Langley in the CTD environment failed the equivalency test because the sample mean value (22.146) is below the lower acceptance limit (22.154). The equivalency sample mean value is 99.96% of the lower limit of acceptable values. Under the assumption of the modified CV method, the modulus data from the CTD environment passed the equivalence test.

The LT modulus data for Langley in the ETW environment failed the equivalency test because the sample mean value (23.160) is below the lower acceptance limit (23.515). The equivalency sample mean value is 98.49% of the lower limit of acceptable values. Under the assumption of the modified CV method, the modulus data from the ETW environment passed the equivalence test.

The LT modulus data for Marshall in the CTD environment failed the equivalency test because the sample mean value (22.144) is below the lower acceptance limit (22.151). The equivalency sample mean value is 99.97% of the lower limit of acceptable values. Under the assumption of the modified CV method, the modulus data from the CTD environment passed the equivalence test.

The LT modulus data for Marshall in the ETW environment failed the equivalency test because the sample mean value (22.847) is below the lower acceptance limit (23.421). The equivalency sample mean value is 97.55% of the lower limit of acceptable values. Under the assumption of the modified CV method, the modulus data from the ETW environment passed the equivalence test.

The LT strength and modulus values and equivalency acceptance limits for the CTD condition in Figure 4-1, for the RTD condition in Figure 4-2, and for the ETW condition in Figure 4-3. The acceptance limits shown are for the individual location samples, not the combined sample which will have slightly tighter acceptance limits due to the larger sample size.

The graphs indicate that the NASA samples (all conditions) have slightly lower modulus values than the qualification sample did, but there are no obvious differences between the three locations.

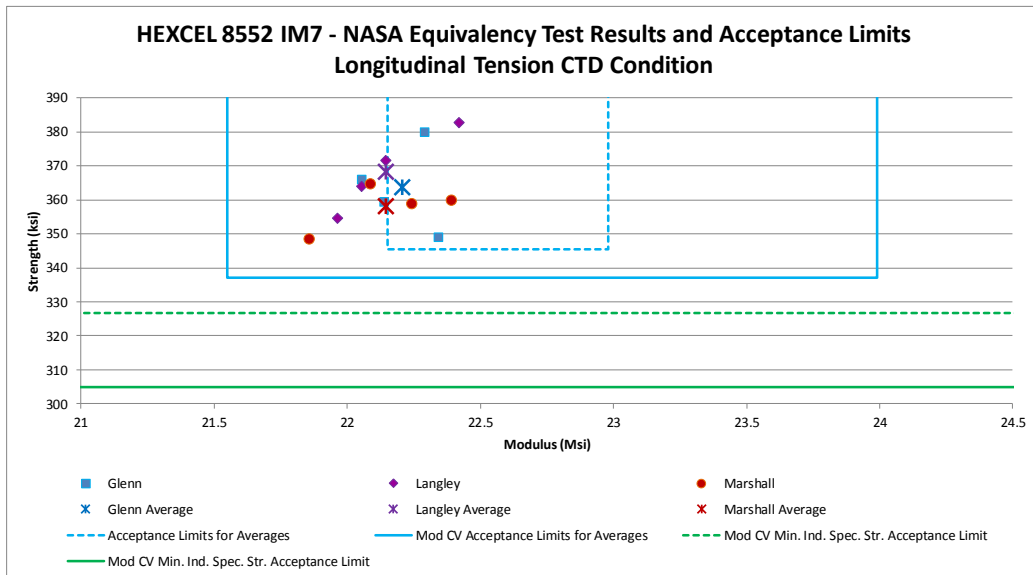


Figure 4-1 Longitudinal Tension Values, Averages and Acceptance limits for CTD Condition

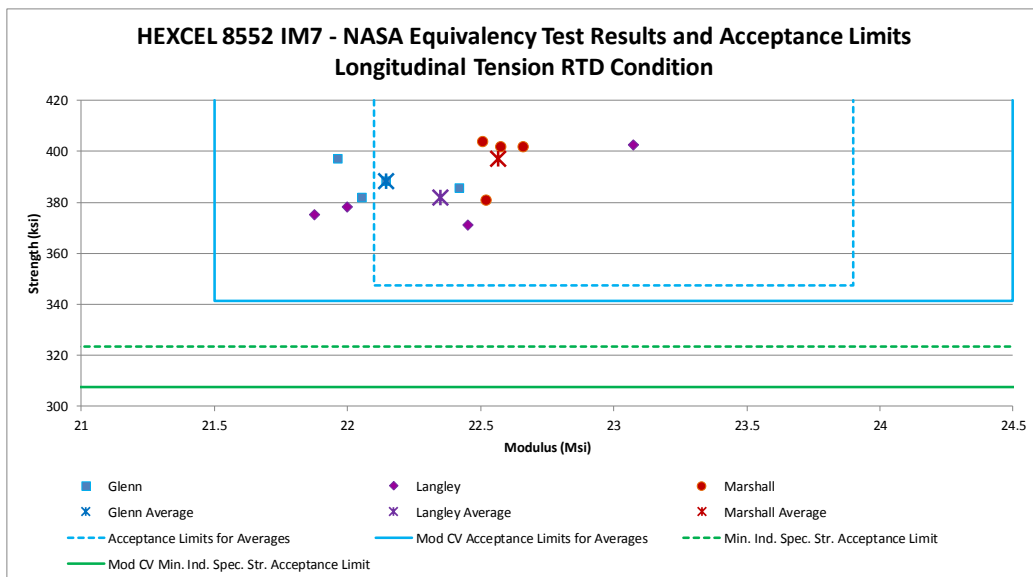


Figure 4-2 Longitudinal Tension Values, Averages and Acceptance limits for RTD Condition

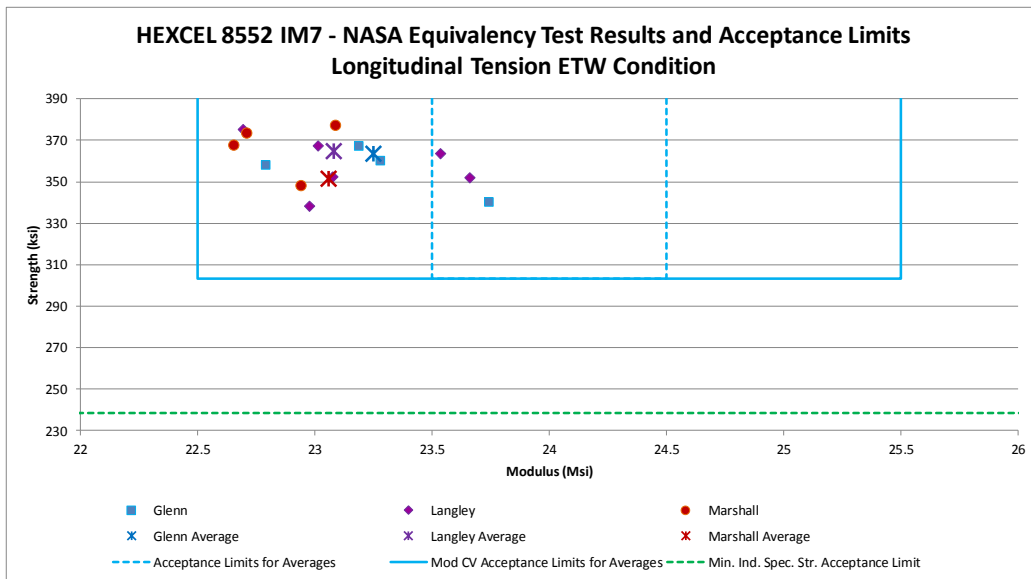


Figure 4-3 Longitudinal Tension Values, Averages and Acceptance limits for ETW Condition

4.2 Quasi Isotropic (“25/50/25”) Unnotched Tension (UNT1)

The UNT1 normalized strength data from all three locations could be combined for CTD and RTD but not the ETW condition. The UNT1 normalized modulus data from all three locations could be combined for the RTD and ETW but not the CTD condition.

The only equivalency test failure was for the combined modulus dataset in the RTD condition. This is surprising because each of the individual locations passed equivalency for this property and condition. However, they are all on the low side and the tighter acceptance criteria of the larger sample resulted in an equivalency failure for the combined sample.

Statistics and analysis results are shown for the strength data CTD condition in Table 4-7, RTD condition in Table 4-8, ETW condition in Table 4-9 and for the modulus data CTD condition in Table 4-10, RTD Condition in Table 4-11 and ETW condition in Table 4-12.

The data and acceptance limits are shown graphically for the CTD condition in Figure 4-4, the RTD condition in Figure 4-5, and the ETW condition in Figure 4-6.

Unnotched Tension (UNT1) Strength CTD	Qualification Data	Glenn	Langley	Marshall	Combined
Data normalized with CPT 0.0072					
Mean Strength (ksi)	99.348	109.862	107.068	109.487	108.806
Standard Deviation	3.442	3.298	1.502	1.747	2.526
Coefficient of Variation %	3.464	3.002	1.403	1.595	2.322
Minimum	91.601	104.504	105.336	107.820	104.504
Maximum	105.840	113.498	108.892	112.351	113.498
Number of Specimens	16	6	6	6	18
RESULTS					
PASS					
Minimum Acceptable Equiv. Sample Mean	96.660	96.660	96.660	97.778	
Minimum Acceptable Equiv. Sample Min	90.411	90.411	90.411	89.127	
MOD CV RESULTS					
PASS with MOD CV					
Modified CV %			6.000		
Minimum Acceptable Equiv. Sample Mean	94.693	94.693	94.693	97.778	
Minimum Acceptable Equiv. Sample Min	83.869	83.869	83.869	89.127	

Table 4-7 UNT1 Strength Results for CTD Condition

Unnotched Tension (UNT1) Strength RTD	Qualification Data	Glenn	Langley	Marshall	Combined
Data normalized with CPT 0.0072					
Mean Strength (ksi)	104.685	105.314	108.002	107.372	106.896
Standard Deviation	7.276	7.065	1.534	1.647	4.191
Coefficient of Variation %	6.950	6.708	1.420	1.534	3.921
Minimum	89.563	92.133	105.873	105.416	92.133
Maximum	113.712	109.828	109.469	109.930	109.930
Number of Specimens	16	6	6	6	18
RESULTS	PASS	PASS	PASS	PASS	PASS
Minimum Acceptable Equiv. Sample Mean	99.004	99.004	99.004	99.004	101.367
Minimum Acceptable Equiv. Sample Min	85.792	85.792	85.792	85.792	83.077
MOD CV RESULTS	PASS with MOD CV	PASS with MOD CV	PASS with MOD CV	PASS with MOD CV	PASS with MOD CV
Modified CV %			7.638		
Minimum Acceptable Equiv. Sample Mean	98.575	98.575	98.575	98.575	101.367
Minimum Acceptable Equiv. Sample Min	84.365	84.365	84.365	84.365	83.077

Table 4-8 UNT1 Strength Results for RTD Condition

Unnotched Tension (UNT1) Strength ETW	Qualification Data	Glenn	Langley	Marshall	Combined
Data normalized with CPT 0.0072					
Mean Strength (ksi)	112.461	108.359	116.139	110.903	111.800
Standard Deviation	5.606	3.250	2.748	2.785	4.326
Coefficient of Variation %	4.985	2.999	2.366	2.511	3.869
Minimum	101.642	103.102	112.493	107.472	103.102
Maximum	119.290	111.969	120.027	114.983	120.027
Number of Specimens	16	6	6	6	18
RESULTS	PASS	PASS	PASS	PASS	
Minimum Acceptable Equiv. Sample Mean	108.084	108.084	108.084	108.084	
Minimum Acceptable Equiv. Sample Min	97.904	97.904	97.904	97.904	
MOD CV RESULTS	PASS with MOD CV	PASS with MOD CV	PASS with MOD CV	PASS with MOD CV	
Modified CV %			6.803		
Minimum Acceptable Equiv. Sample Mean	106.760	106.760	106.760	106.760	
Minimum Acceptable Equiv. Sample Min	93.501	93.501	93.501	93.501	

**Statistical
Differences
between
Locations
preclude
combining
results**

Table 4-9 UNT1 Strength Results for ETW Condition

Unnotched Tension (UNT1) Modulus CTD	Qualification Data	Glenn	Langley	Marshall	Combined
Data normalized with CPT 0.0072					
Mean Modulus (Msi)	8.353	8.178	8.414	8.343	8.312
Standard Deviation	0.309	0.114	0.110	0.038	0.135
Coefficient of Variation %	3.696	1.398	1.307	0.455	1.622
Minimum	7.295	8.013	8.297	8.310	8.013
Maximum	8.745	8.362	8.619	8.414	8.619
Number of Specimens	16	6	6	6	18
RESULTS		PASS	PASS	PASS	
Passing Range for Modulus Mean	8.080 to 8.626	8.081 to 8.626	8.086 to 8.621		
Student's t-statistic	-1.341	0.464	-0.084		
p-value of Student's t-statistic	1.95E-01	0.6478	0.93418		
MOD CV RESULTS		PASS with MOD CV	PASS with MOD CV	PASS with MOD CV	
Modified CV%		6.000			
Passing Range for Modulus Mean	7.916 to 8.791	7.917 to 8.790	0.000		
Modified CV Student's t-statistic	-0.838	0.289	-0.052		
p-value of Student's t-statistic	0.412	0.775	0.959		

Table 4-10 UNT1 Modulus Results for CTD Condition

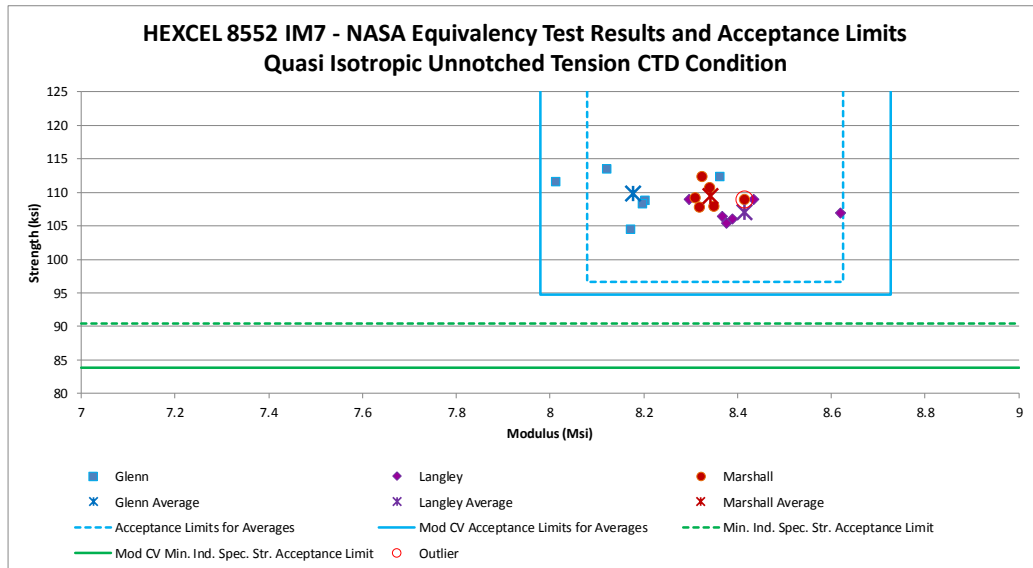
Unnotched Tension (UNT1) Modulus RTD	Qualification Data	Glenn	Langley	Marshall	Combined
Data normalized with CPT 0.0072					
Mean Modulus (Msi)	8.390	7.923	8.186	8.070	8.060
Standard Deviation	0.480	0.455	0.165	0.101	0.290
Coefficient of Variation %	5.727	5.743	2.021	1.249	3.601
Minimum	7.277	7.049	8.013	7.964	7.049
Maximum	8.984	8.394	8.494	8.223	8.494
Number of Specimens	16	6	6	6	18
RESULTS		PASS	PASS	PASS	FAIL
Passing Range for Modulus Mean	7.917 to 8.864	7.967 to 8.814	7.972 to 8.809	8.116 to 8.664	
Student's t-statistic	-2.060	-1.004	-1.598	-2.461	
p-value of Student's t-statistic	5.27E-02	0.3275	0.12583	0.0195	
MOD CV RESULTS		PASS with MOD CV	PASS with MOD CV	PASS with MOD CV	FAIL
Modified CV%		6.863			
Passing Range for Modulus Mean	7.843 to 8.938	7.885 to 8.895	7.890 to 8.891	8.077 to 8.703	
Modified CV Student's t-statistic	-1.782	-0.842	-1.336	-2.151	
p-value of Student's t-statistic	0.090	0.410	0.197	0.039	

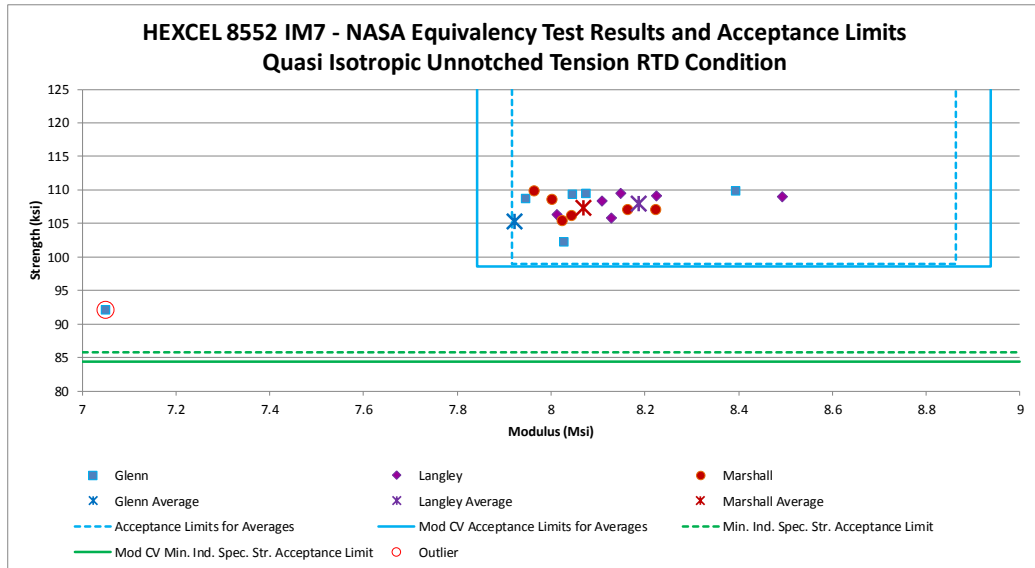
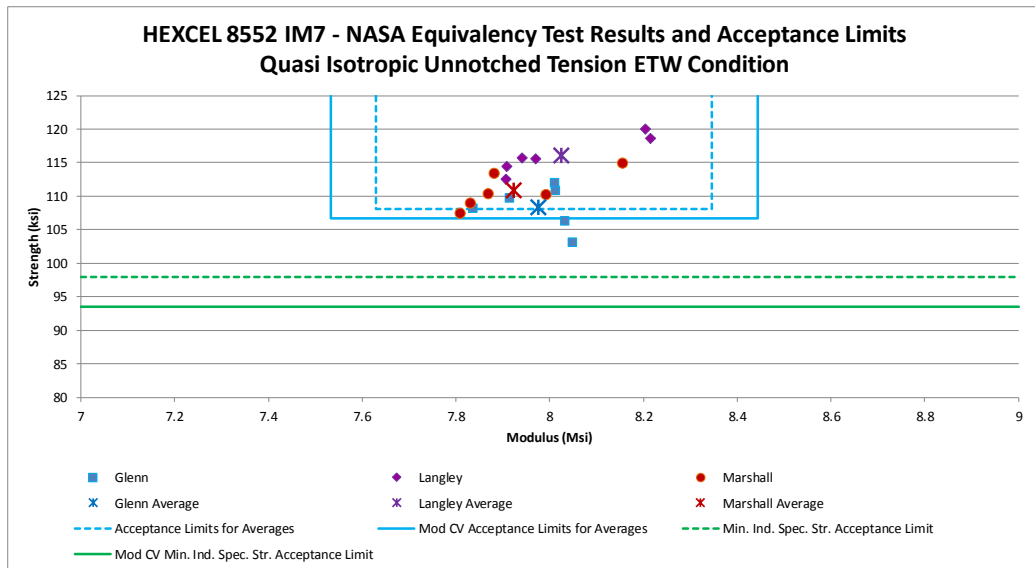
Table 4-11 UNT1 Modulus Results for RTD Condition

Unnotched Tension (UNT1) Modulus ETW	Qualification Data	Glenn	Langley	Marshall	Combined
Data normalized with CPT 0.0072					
Mean Modulus (Msi)	7.988	7.976	8.024	7.923	7.974
Standard Deviation	0.412	0.083	0.145	0.130	0.122
Coefficient of Variation %	5.162	1.038	1.811	1.641	1.536
Minimum	7.069	7.836	7.908	7.809	7.809
Maximum	8.514	8.049	8.215	8.155	8.215
Number of Specimens	17	6	6	6	18
RESULTS	PASS	PASS	PASS	PASS	PASS
Passing Range for Modulus Mean	7.630 to 8.346	7.626 to 8.35	7.627 to 8.349	7.782 to 8.195	
Student's t-statistic	-0.072	0.208	-0.374	-0.135	
p-value of Student's t-statistic	9.43E-01	0.8374	0.71188	0.89331	
MOD CV RESULTS	PASS with MOD CV	PASS with MOD CV	PASS with MOD CV	PASS with MOD CV	
Modified CV%			6.581		
Passing Range for Modulus Mean	7.533 to 8.443	7.530 to 8.447	7.531 to 8.446	7.729 to 8.247	
Modified CV Student's t-statistic	-0.057	0.164	-0.295	-0.108	
p-value of Student's t-statistic	0.955	0.871	0.771	0.915	

Table 4-12 UNT1 Modulus Results for ETW Condition

The UNT1 RTD modulus data in ETW environment failed the equivalency test because the sample mean value (8.060) is below the lower acceptance limit (8.116). The equivalency sample mean value is 99.30% of the lower limit of acceptable values. Under the assumption of the modified CV method, it was 99.78% of the lower limit of acceptable values (8.077).

**Figure 4-4 UNT1 Values, Averages and Acceptance limits for CTD Condition**

**Figure 4-5 UNT1 Values, Averages and Acceptance limits for RTD Condition****Figure 4-6 UNT1 Values, Averages and Acceptance limits for ETW Condition**

4.3 Quasi Isotropic “25/50/25” Open-Hole Tension 1 (OHT1)

The OHT1 normalized strength data from all three locations could be combined for CTD and ETW but not the RTD condition. There were no equivalency test failures for the OHT1 data, either for the individual locations or the combined dataset.

Statistics and analysis results are shown for the strength data CTD condition in Table 4-13, RTD condition in Table 4-14, ETW condition in Table 4-15. The data and acceptance limits are shown graphically for all condition in Figure 4-7.

Open Hole Tension (OHT1) Strength CTD	Qualification Data	Glenn	Langley	Marshall	Combined
Data normalized with CPT 0.0072					
Mean Strength (ksi)	57.754	64.584	63.564	62.631	63.593
Standard Deviation	2.433	1.471	1.756	1.352	1.660
Coefficient of Variation %	4.213	2.277	2.763	2.159	2.610
Minimum	53.645	63.046	61.618	60.242	60.242
Maximum	62.524	66.763	66.570	64.241	66.763
Number of Specimens	19	6	6	6	18
RESULTS		PASS	PASS	PASS	PASS
Minimum Acceptable Equiv. Sample Mean		55.855	55.855	55.855	56.645
Minimum Acceptable Equiv. Sample Min		51.436	51.436	51.436	50.528
MOD CV RESULTS		PASS with MOD CV	PASS with MOD CV	PASS with MOD CV	PASS with MOD CV
Modified CV %			6.106		
Minimum Acceptable Equiv. Sample Mean		55.001	55.001	55.001	56.146
Minimum Acceptable Equiv. Sample Min		48.597	48.597	48.597	47.281

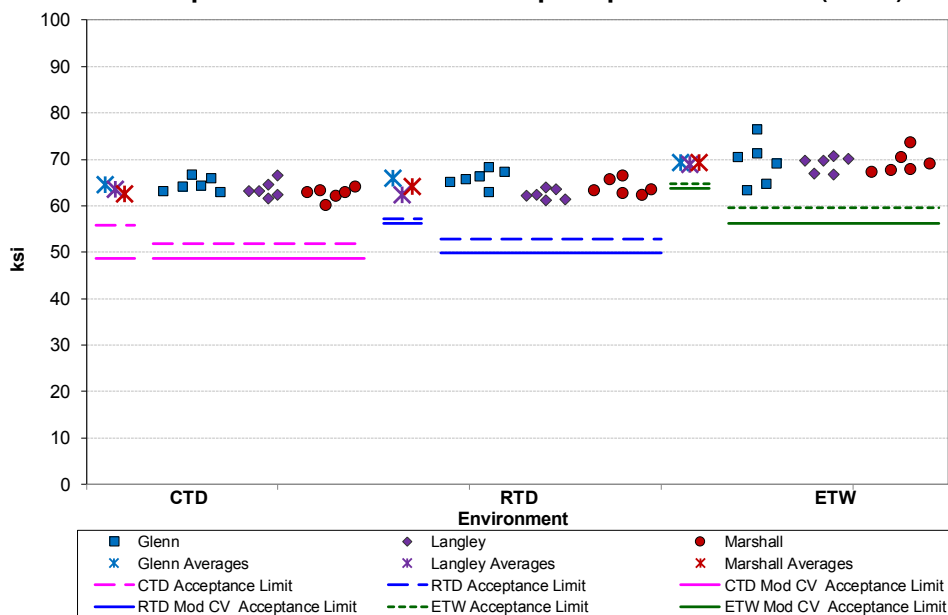
Table 4-13 OHT1 Strength Results for CTD

Open Hole Tension (OHT1) Strength RTD	Qualification Data	Glenn	Langley	Marshall	Combined
Data normalized with CPT 0.0072					
Mean Strength (ksi)	59.003	65.988	62.410	64.072	64.156
Standard Deviation	2.350	1.846	1.117	1.697	2.117
Coefficient of Variation %	3.982	2.798	1.789	2.649	3.299
Minimum	54.120	62.985	61.142	62.276	61.142
Maximum	64.610	68.375	63.946	66.602	68.375
Number of Specimens	19	6	6	6	18
RESULTS		PASS	PASS	PASS	
Minimum Acceptable Equiv. Sample Mean		57.169	57.169	57.169	
Minimum Acceptable Equiv. Sample Min		52.902	52.902	52.902	
MOD CV RESULTS		PASS with MOD CV	PASS with MOD CV	PASS with MOD CV	
Modified CV %			6.000		
Minimum Acceptable Equiv. Sample Mean		56.239	56.239	56.239	
Minimum Acceptable Equiv. Sample Min		49.811	49.811	49.811	

Statistical
Differences
between
Locations
preclude
combining
results

Table 4-14 OHT1 Strength Results for RTD

Open Hole Tension (OHT1) Strength ETW	Qualification Data	Glenn	Langley	Marshall	Combined
Data normalized with CPT 0.0072					
Mean Strength (ksi)	66.966	69.241	68.990	69.356	69.196
Standard Deviation	2.850	4.799	1.680	2.368	3.046
Coefficient of Variation %	4.255	6.931	2.436	3.414	4.402
Minimum	62.154	63.279	66.791	67.399	63.279
Maximum	72.587	76.500	70.669	73.603	76.500
Number of Specimens	20	6	6	6	18
RESULTS	PASS	PASS	PASS	PASS	PASS
Minimum Acceptable Equiv. Sample Mean	64.742	64.742	64.742	64.742	65.667
Minimum Acceptable Equiv. Sample Min	59.567	59.567	59.567	59.567	58.504
MOD CV RESULTS	PASS with MOD CV				
Modified CV %			6.128		
Minimum Acceptable Equiv. Sample Mean	63.763	63.763	66.791	66.791	65.095
Minimum Acceptable Equiv. Sample Min	56.311	56.311	56.311	56.311	54.780

Table 4-15 OHT1 Strength Results for ETW**HEXCEL 8552 IM7 - NASA Equivalency Test Results and Acceptance Limits Quasi Isotropic Open Hole Tenion(OHT1)****Figure 4-7 OHT1 Values, Averages and Acceptance limits**

4.4 Laminate Short-Beam Strength (LSBS)

The Laminate Short-Beam Strength data is not normalized. The LSBS data from all three locations could be combined. The combined data passed all equivalency tests, although the ETW data required the use of the modified CV approach. The individual locations all passed the equivalency tests for the RTD condition, but Glenn and Marshall failed the ETW equivalency tests. Glenn passed for the ETW condition with the use of the modified CV approach but Marshall did not. However, there was insufficient strength data for results of the individual locations to be considered conclusive.

Statistics and analysis results are shown for the RTD condition in Table 4-5 and for the ETW condition in Table 4-6.

Laminate Short Beam Strength (LSBS) RTD	Qualification Data	Glenn	Langley	Marshall	Combined
Data as measured (not normalized)					
Mean Strength (ksi)	12.129	12.446	12.033	12.399	12.301
Standard Deviation	0.831	0.398	0.466	0.474	0.459
Coefficient of Variation %	6.851	3.199	3.871	3.822	3.732
Minimum	9.550	11.987	11.423	11.687	11.423
Maximum	12.983	13.109	12.548	12.892	13.109
Number of Specimens	21	7	6	6	19
RESULTS		PASS	PASS	PASS	PASS
Minimum Acceptable Equiv. Sample Mean	11.527	11.480	11.480	11.760	
Minimum Acceptable Equiv. Sample Min	9.925	9.971	9.971	9.647	
MOD CV RESULTS		PASS with MOD CV			
Modified CV %			7.425		
Minimum Acceptable Equiv. Sample Mean	11.476	11.426	11.426	11.729	
Minimum Acceptable Equiv. Sample Min	9.740	9.790	9.790	9.439	

Table 4-16 Laminate Short-Beam Strength Results for RTD

Laminate Short Beam Strength (LSBS) ETW	Qualification Data	Glenn	Langley	Marshall	Combined
Data as measured (not normalized)					
Mean Strength (ksi)	6.991	6.840	6.959	6.658	6.819
Standard Deviation	0.255	0.276	0.162	0.210	0.244
Coefficient of Variation %	3.646	4.040	2.325	3.149	3.573
Minimum	6.635	6.296	6.696	6.277	6.277
Maximum	7.699	7.050	7.150	6.850	7.150
Number of Specimens	19	6	6	6	18
RESULTS		FAIL	PASS	FAIL	FAIL
Minimum Acceptable Equiv. Sample Mean	6.792	6.792	6.792	6.874	
Minimum Acceptable Equiv. Sample Min	6.329	6.329	6.329	6.234	
MOD CV RESULTS		PASS with MOD CV	PASS with MOD CV	FAIL	PASS with MOD CV
Modified CV %			6.000		
Minimum Acceptable Equiv. Sample Mean	6.663	6.663	6.663	6.799	
Minimum Acceptable Equiv. Sample Min	5.901	5.901	5.901	5.745	

Table 4-17 Laminate Short-Beam Strength Results for ETW

The LSBS data for the combined data in the ETW environment failed equivalence due sample minimum being too low. The equivalency minimum value is (6.819) is 99.19% of

the lowest acceptable minimum value (6.874). Under the assumption of the modified CV method, the ETW environment passed the equivalence test.

The LSBS data for Glenn in the ETW environment failed equivalence due sample minimum being too low. The equivalency minimum value is (6.296) is 99.48% of the lowest acceptable minimum value (6.329). Under the assumption of the modified CV method, the ETW environment passed the equivalence test.

The LSBS data for Marshall in the ETW environment failed equivalence due to both the sample mean and sample minimum being too low. The equivalency sample mean (6.658) is 98.03% of the minimum acceptable mean value (6.792). The equivalency sample minimum (6.277) is 99.19% of the lowest acceptable minimum value (6.329). Under the assumption of the modified CV method, the equivalency sample mean is 99.92% of the lowest acceptable mean value (6.663). The equivalency sample minimum passed the test.

The LSBS strength means, individual specimen results and acceptance limits are shown for all labs in Figure 4-8.

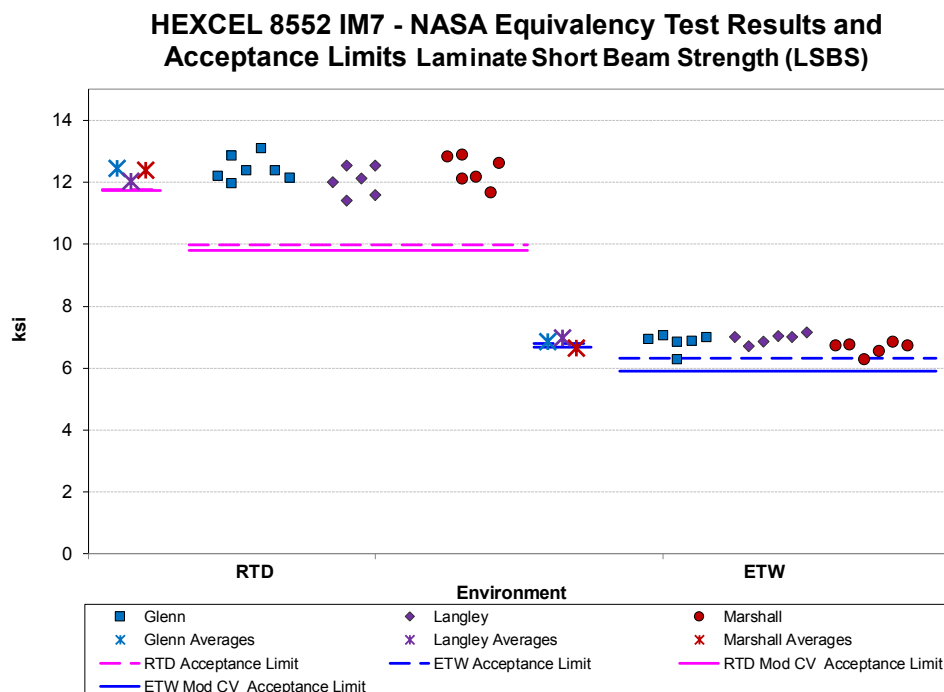


Figure 4-8 Laminate Short-Beam Strength means, minimums and Acceptance limits for NASA Labs

4.5 Quasi Isotropic (“25/50/25”) Unnotched Compression 1 (UNC1)

The UNC1 data from all three locations could be combined for strength properties and modulus for the RTD condition, but there were statistically significant differences between the locations for modulus values in the ETW condition. The combined dataset passed the equivalency tests for strength and for the modulus RTD condition.

The three locations all failed equivalency tests for modulus in the ETW condition due to the modulus values being too high. Although the Langley and Marshall locations were able to pass equivalency with the use of the modified CV approach, Glenn was not. In fact, all of the modulus values from Glenn for the ETW condition fell above the upper acceptance limit.

Modified CV results could not be computed for the strength data because both conditions had a CV larger than 8%, which is not modified.

Statistics and analysis results are shown for strength RTD condition in Table 4-18, and for strength in the ETW condition in Table 4-19, for the modulus RTD condition in Table 4-20, and for modulus in the ETW condition in Table 4-21.

Unnotched Compression (UNC1) Strength RTD	Qualification Data	Glenn	Langley	Marshall	Combined
Data normalized with CPT 0.0072					
Mean Strength (ksi)	87.045	94.483	92.219	94.951	92.389
Standard Deviation	8.111	7.341	2.075	3.160	4.733
Coefficient of Variation %	9.318	7.769	2.250	3.328	5.123
Minimum	68.065	84.038	88.961	91.952	80.740
Maximum	97.037	100.706	94.741	98.458	100.706
Number of Specimens	16	4	6	6	24
RESULTS	PASS	PASS	PASS	PASS	PASS
Minimum Acceptable Equiv. Sample Mean	79.351	80.712	80.712	83.836	
Minimum Acceptable Equiv. Sample Min	67.239	65.984	65.984	62.232	

Table 4-18 UNC1 Strength Results for RTD

Unnotched Compression (UNC1) Strength ETW	Qualification Data	Glenn	Langley	Marshall	Combined
Data normalized with CPT 0.0072					
Mean Strength (ksi)	57.675	60.488	56.413	60.336	57.701
Standard Deviation	6.355	7.683	4.257	1.674	4.967
Coefficient of Variation %	11.019	12.702	7.546	2.774	8.608
Minimum	48.716	54.063	51.380	58.131	48.189
Maximum	72.226	69.852	63.319	62.169	69.852
Number of Specimens	30	4	6	5	24
RESULTS	PASS	PASS	PASS	PASS	PASS
Minimum Acceptable Equiv. Sample Mean	51.647	52.713	52.257	55.161	
Minimum Acceptable Equiv. Sample Min	42.155	41.172	41.605	38.232	

Table 4-19 UNC1 Strength Results for ETW

Unnotched Compression (UNC1) Modulus RTD	Qualification Data	Glenn	Langley	Marshall	Combined
Data normalized with CPT 0.0072					
Mean Modulus (Msi)	7.857	7.955	7.597	7.662	7.711
Standard Deviation	0.373	0.360	0.099	0.035	0.227
Coefficient of Variation %	4.749	4.526	1.307	0.451	1.801
Minimum	6.890	7.445	7.474	7.636	6.852
Maximum	8.407	8.274	7.706	7.714	7.344
Number of Specimens	16	4	6	6	16
RESULTS	PASS	PASS	PASS	PASS	PASS
Passing Range for Modulus Mean	7.421 to 8.293	7.531 to 8.183	7.534 to 8.18	7.634 to 8.08	
Student's t-statistic	0.473	-1.661	-1.256	-1.337	
p-value of Student's t-statistic	0.642	0.112	0.223	0.191	
MOD CV RESULTS	PASS with MOD CV	PASS with MOD CV	PASS with MOD CV	PASS with MOD CV	
Modified CV%		6.374			
Passing Range for Modulus Mean	7.293 to 8.421	7.421 to 8.293	7.424 to 8.290	7.576 to 8.138	
Modified CV Student's t-statistic	0.365	-1.244	-0.937	-1.062	
p-value of Student's t-statistic	0.719	0.228	0.360	0.297	

Table 4-20 UNC1 Modulus Results for RTD

Unnotched Compression (UNC1) Modulus ETW	Qualification Data	Glenn	Langley	Marshall	Combined
Data normalized with CPT 0.0072					
Mean Modulus (Msi)	7.126	7.806	7.375	7.464	7.519
Standard Deviation	0.128	0.123	0.058	0.090	0.201
Coefficient of Variation %	1.801	1.582	0.783	1.206	2.666
Minimum	6.852	7.621	7.296	7.353	7.296
Maximum	7.344	7.878	7.443	7.578	7.878
Number of Specimens	16	4	6	5	15
RESULTS	FAIL	FAIL	FAIL	FAIL	
Passing Range for Modulus Mean	6.977 to 7.276	7.012 to 7.241	6.996 to 7.256		
Student's t-statistic	9.528	4.528	5.429		
p-value of Student's t-statistic	1.87E-08	0.0002	0.00003		
MOD CV RESULTS	FAIL	PASS with MOD CV	PASS with MOD CV		
Modified CV%		6.000			
Passing Range for Modulus Mean	6.664 to 7.589	6.755 to 7.497	0.000		
Modified CV Student's t-statistic	3.088	1.400	1.723		
p-value of Student's t-statistic	0.006	0.177	0.101		

Statistical
Differences
between
Locations
preclude
combining
results

Table 4-21 UNC1 Modulus Results for ETW

The UNC1 modulus data for the Glenn ETW environment failed equivalence due to the sample mean being too high. The equivalency sample mean (7.806) is 107.28% of the maximum acceptable mean value (7.276). Under the assumption of the modified CV method, the equivalency sample mean is 102.85% of the highest acceptable mean value (7.589).

The UNC1 modulus data for the Langley ETW environment failed equivalence due to sample mean being too high. The equivalency sample mean (7.375) is 101.85% of the

maximum acceptable mean value (7.241). Under the assumption of the modified CV method, the equivalency sample mean passed the test.

The UNC1 modulus data for the Marshall ETW environment failed equivalence due to sample mean being too high. The equivalency sample mean (7.464) is 102.86% of the maximum acceptable mean value (7.256). Under the assumption of the modified CV method, the equivalency sample mean passed the test.

The UNC1 strength and modulus values and equivalency acceptance limits for the RTD condition in Figure 4-9, and for the ETW condition in Figure 4-10. The acceptance limits shown are for the individual location samples, not the combined sample which will have slightly tighter acceptance limits due to the larger sample size.

The graphs indicate that the Glenn Lab samples have higher modulus values than the other two locations, although the differences are not statistically significant for the RTD condition.

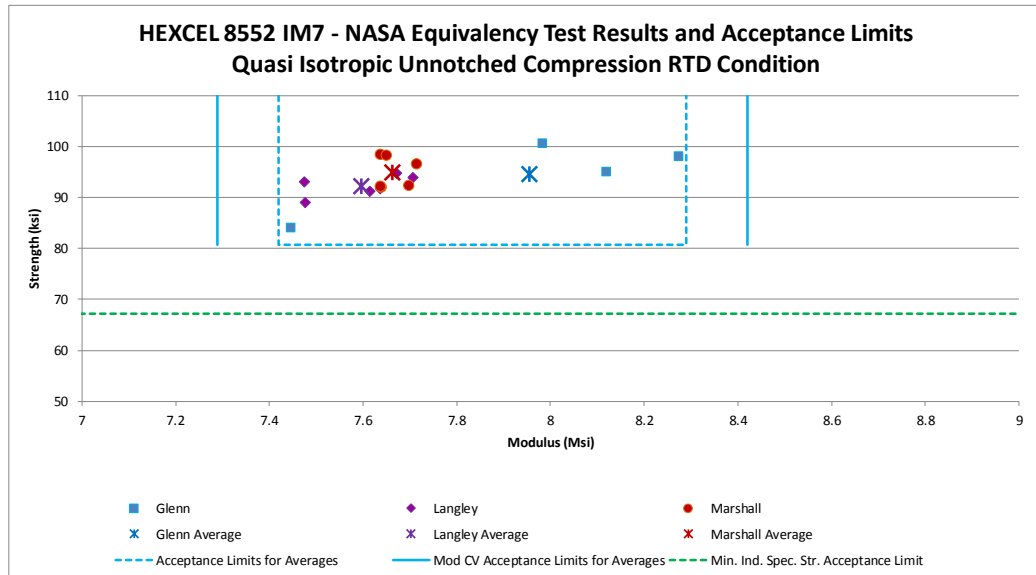


Figure 4-9 UNC1 means, minimums and Acceptance limits for RTD Condition

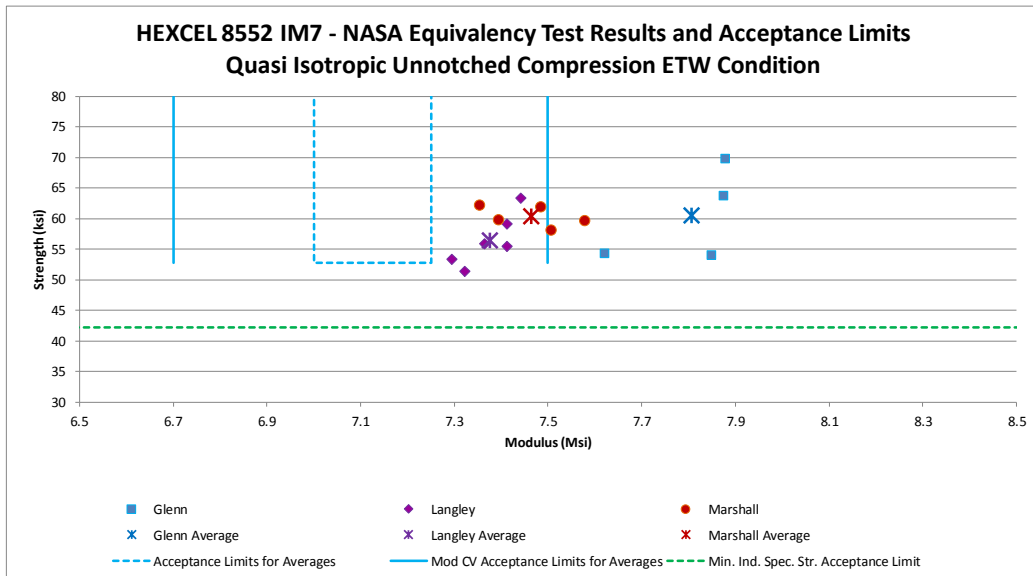


Figure 4-10 UNC1 means, minimums and Acceptance limits for ETW Condition

4.6 Quasi Isotropic “25/50/25” Open-Hole Compression 1 (OHC1)

The OHC1 normalized strength data from all three locations could be combined for both the RTD and ETW conditions. The combined datasets for OHC1 normalized strength data failed equivalency tests for the both RTD and ETW conditions. This was not surprising given that all three locations failed equivalency for both conditions, although the Langley and Marshall locations passed for the RTD condition with the use of the modified CV method.

Statistics and analysis results are shown for strength RTD condition in Table 4-22, and for strength in the ETW condition in Table 4-23.

The OHC1 strength means, individual specimen results and acceptance limits are shown for all labs in Figure 4-11.

Open Hole Compression (OHC1) Strength RTD	Qualification Data	Glenn	Langley	Marshall	Combined
Data normalized with CPT 0.0072					
Mean Strength (ksi)	49.083	45.792	47.082	47.503	46.918
Standard Deviation	1.793	0.973	1.379	1.193	1.335
Coefficient of Variation %	3.653	2.124	2.928	2.512	2.846
Minimum	43.909	44.449	46.004	45.898	44.449
Maximum	50.993	46.741	49.699	49.343	49.699
Number of Specimens	19	4	6	6	16
RESULTS	FAIL	FAIL	FAIL	FAIL	FAIL
Minimum Acceptable Equiv. Sample Mean	47.383	47.683	47.683	48.217	
Minimum Acceptable Equiv. Sample Min	44.705	44.428	44.428	43.826	
MOD CV RESULTS	FAIL	PASS with MOD CV	PASS with MOD CV	FAIL	FAIL
Modified CV %	6.000	6.000	6.000	6.000	6.000
Minimum Acceptable Equiv. Sample Mean	46.290	46.784	46.784	47.660	
Minimum Acceptable Equiv. Sample Min	41.892	41.436	41.436	40.448	

Table 4-22 OHC1 Strength Results For RTD Condition

Open Hole Compression (OHC1) Strength ETW	Qualification Data	Glenn	Langley	Marshall	Combined
Data normalized with CPT 0.0072					
Mean Strength (ksi)	35.515	31.767	32.214	33.186	32.467
Standard Deviation	1.445	0.444	0.766	0.910	0.935
Coefficient of Variation %	4.069	1.397	2.377	2.743	2.879
Minimum	33.080	31.130	31.638	31.785	31.130
Maximum	38.956	32.157	33.633	34.367	34.367
Number of Specimens	19	4	6	6	16
RESULTS	FAIL	FAIL	FAIL	FAIL	FAIL
Minimum Acceptable Equiv. Sample Mean	34.144	34.387	34.387	34.817	
Minimum Acceptable Equiv. Sample Min	31.986	31.763	31.763	31.278	
MOD CV RESULTS	FAIL	FAIL	FAIL	FAIL	FAIL
Modified CV %		6.034			
Minimum Acceptable Equiv. Sample Mean	33.482	33.842	33.842	34.479	
Minimum Acceptable Equiv. Sample Min	30.282	29.950	29.950	29.231	

Table 4-23 OHC1 Strength Results For ETW Condition

The OHC1 combined strength data for the RTD environment failed equivalence due to sample mean being too low. The equivalency sample mean (46.918) is 97.31% of the minimum acceptable mean value (48.217). The equivalency sample minimum passed the test. Under the assumption of the modified CV method, the equivalency sample mean is 98.44% of the lowest acceptable mean value (47.660).

The OHC1 combined strength data for the ETW environment failed equivalence due to both the sample mean and sample minimum being too low. The equivalency sample mean (32.467) is 93.25% of the minimum acceptable mean value (34.817). The equivalency sample minimum (31.130) is 99.53% of the lowest acceptable minimum value (31.278). Under the assumption of the modified CV method, the equivalency sample mean is 94.16% of the lowest acceptable mean value (34.479). The equivalency sample minimum passed the test.

The Glenn OHC1 strength data for the RTD environment failed equivalence due to both the sample mean and sample minimum being too low. The equivalency sample mean (45.792) is 96.64% of the minimum acceptable mean value (47.383). The equivalency sample minimum (44.449) is 99.43% of the lowest acceptable minimum value (44.705). Under the assumption of the modified CV method, the equivalency sample mean is 98.93% of the lowest acceptable mean value (46.29). The equivalency sample minimum passed the test.

The Glenn OHC1 strength data for the ETW environment failed equivalence due to both the sample mean and sample minimum being too low. The equivalency sample mean (31.767) is 93.04% of the minimum acceptable mean value (34.144). The equivalency sample minimum (31.130) is 97.32% of the lowest acceptable minimum value (31.986). Under the assumption of the modified CV method, the equivalency sample mean is 94.88% of the lowest acceptable mean value (33.482). The equivalency sample minimum passed the test.

The Langley OHC1 strength data for the RTD environment failed equivalence due to sample mean being too low. The equivalency sample mean (47.082) is 98.74% of the minimum acceptable mean value (47.683). Under the assumption of the modified CV method, the equivalency sample mean passed the test.

The Langley OHC1 strength data for the ETW environment failed equivalence due to both the sample mean and sample minimum being too low. The equivalency sample mean (32.214) is 93.68% of the minimum acceptable mean value (34.387). The equivalency sample minimum (31.638) is 99.61% of the lowest acceptable minimum value (31.763). Under the assumption of the modified CV method, the equivalency sample mean is 95.19% of the lowest acceptable mean value (33.842). The equivalency sample minimum passed the test.

The Marshall OHC1 strength data for the RTD environment failed equivalence due to sample mean being too low. The equivalency sample mean (47.503) is 99.62% of the

minimum acceptable mean value (47.683). Under the assumption of the modified CV method, the equivalency sample mean passed the test.

The Marshall OHC1 strength data for the ETW environment failed equivalence due to sample mean being too low. The equivalency sample mean (33.186) is 96.51% of the minimum acceptable mean value (34.387). Under the assumption of the modified CV method, the equivalency sample mean is 98.06% of the lowest acceptable mean value (33.842).

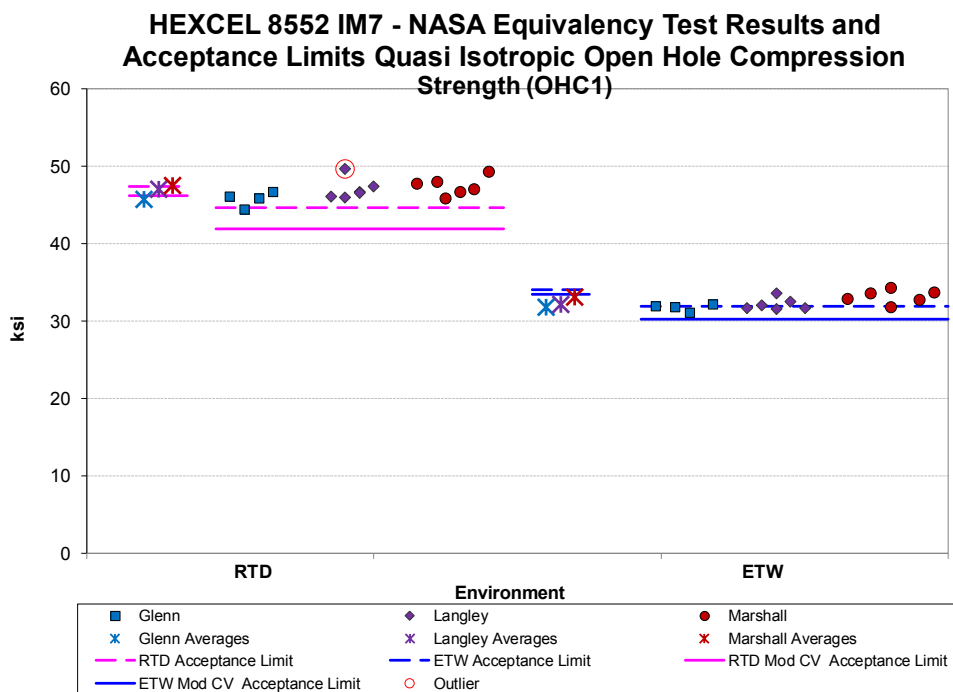


Figure 4-11 OHC1 means, minimums and Acceptance limits

5. Summary of Results

All the equivalency comparisons are conducted with Type I error probability (α) of 5% in accordance with FAA/DOT/AR-03/19 report and CMH-17 Rev G section 8.4.1. It is common to obtain a few or even several failures in a typical equivalency program involving multiple independent property comparisons. In theory, if the equivalency dataset is truly identical to the qualification dataset, we expect to obtain approximately 5% failures. Since the equivalency test panels were fabricated by a different company, the test panel quality is expected to differ at least marginally; so, we expect to obtain slightly higher failure rates than 5% because the equivalency dataset may not be truly identical to the qualification dataset. However, a failure rate that is significantly higher than 5% is an indication that equivalency should not be assumed and some retesting is justified.

In addition to the frequency of failures, the severity of the failures (i.e. how far away from the pass/fail threshold) and any pattern of failures should be taken into account when making a determination of overall equivalency. Severity of failure can be determined using the graphs accompanying the individual test results. Whether or not a pattern of failures exists is a subjective evaluation to be made by the original equipment manufacturer or certifying agency. The question of how close is close enough is often difficult to answer, and may depend on specific application and purpose of equivalency. NIAR does not make a judgment regarding the overall equivalence; the following information is provided to aid the original equipment manufacturer or certifying agency in making that judgment.

The following computations are based on the assumption that the tests are independent. While the tests are all conducted independently, measurements for strength and modulus are made from a single specimen. Modulus measurements are generally considered to be independent of the strength measurements.

However the computations can be considered conservative. If the tests are not independent and a failure in IPS 0.2% offset strength is correlated with a failure in IPS 5% strain strength, the probability of both failures occurring together should be higher than predicted with the assumption of independence, thus leading to a conservative overall judgment about the material.

5.1 Failures

The three NASA locations each had 23 different tests conducted but only the modulus tests (8) had sufficient data to meet the CMH-17 Rev G requirements for the individual locations. All strength tests lack sufficient data for the results to be considered conclusive. When the data from the three locations was combined, there was sufficient data for conclusive results for all tests.

Using the modified CV method and examining the tests with sufficient data, the combined dataset had four failures. The main problem area is the compression test results. The OHT1 strength data failed equivalency for both conditions tested.

1. Combined – OHT1 Strength RTD condition failed by 1.6%
2. Combined – OHT1 Strength ETW condition failed by 5.8%
3. Combined – LT modulus ETW condition failed by 0.5%
4. Combined – UNT1 modulus RTD condition failed by 0.2%

5.2 Pass Rate

The combined NASA dataset had four failures out of a 19 tests for a pass rate of 78.95% for NASA overall. If the equivalency samples came from a material with identical properties to the original qualification material and all tests were independent of all other tests, the expected pass rate would be 95%. This equates to 0.95 failures out of 19 tests.

5.3 Probability of Failures

If the equivalency sample came from a material with characteristics identical to the original qualification material and all tests were independent of all other tests, the chance of having four or more failures out of 19 tests is 1.32%.

If the equivalency sample came from a material with characteristics identical to the original qualification material and all tests were independent of all other tests, the chance of having one or more failures is 26.49%, two or more failures is 3.28% and three or more failures is 0.22%.

Figure 5-1 illustrates the probability of getting one or more failures, two or more failures, etc. for a set of 19 independent tests. If the two materials were equivalent, the probability of getting four or more failures is less than 5%. This means that the material could be considered as “not equivalent” with a 95% level of confidence if there were four or more failures out of 19 independent tests.

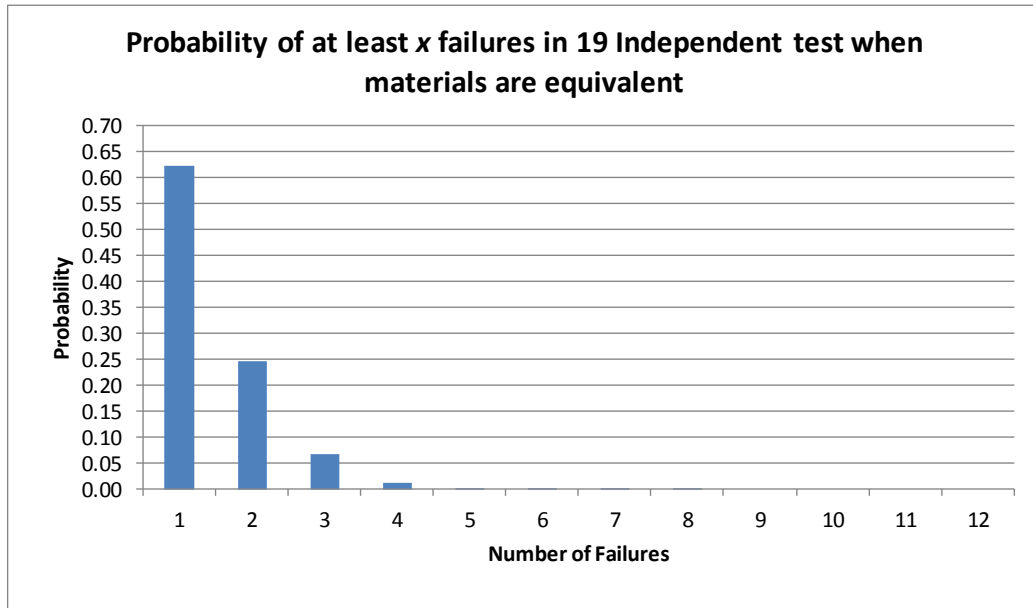


Figure 5-1 Probability of Number of Failures

6. Generic Basis Values Assessment

This material, HEXCEL 8552 IM7, has been used to compute generic basis values, a method designed to take account of the variability introduced by different locations using the same material and methodology. This methods and results were documented in NCAMP Report NCP-RP-2013-015 N/C.

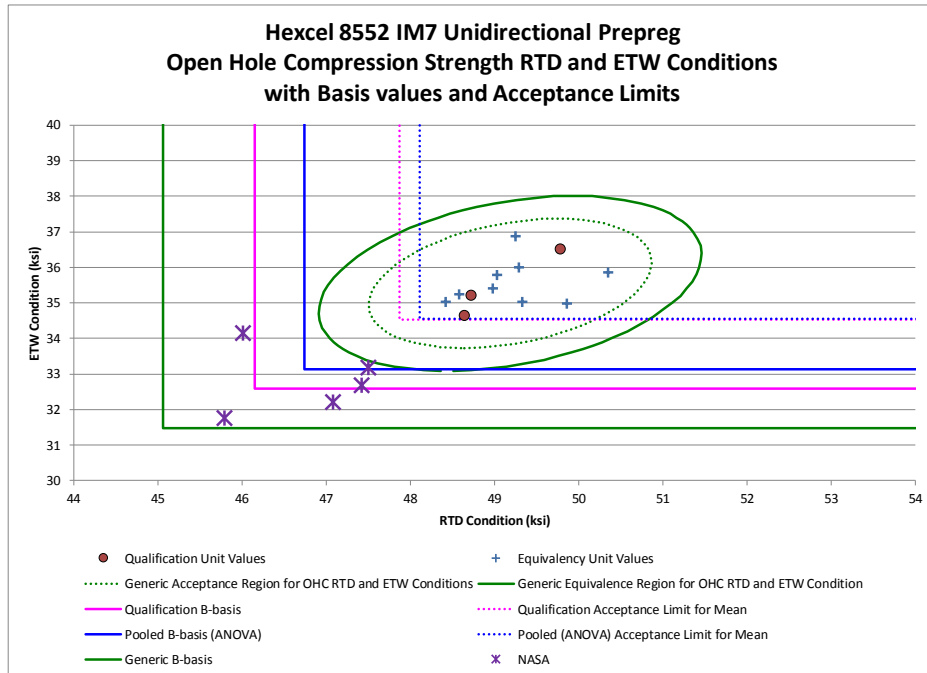
Generic basis values are lower, with lower acceptance criteria, than those computed using the CMH-17 methodology. To determine if a location is able to use these basis values, test results are compared to acceptance criteria for the mean (must be greater than acceptance limit) and standard deviation (must be less than acceptance limit). The sample size of 4 strength specimens is sufficient for this approach. LSBS and Quasi-Isotropic Unnotched tests were not included in the generic basis values analysis, so they cannot be included here.

Since the NASA samples passed the tension strength tests, they also pass the generic acceptance criteria for those tests. Open Hole compression tests results were lower for the NASA samples than the other NCAMP samples of this material. The NASA Glenn Low Vacuum and Slow Ramp tests results were included in the analysis of compression results. The results were similar to the other three NASA samples.

The Generic B-basis values, acceptance criteria and NASA results are given in Table 6-1 for OHC1 tests, in Table 6-2 for LT tests and in Table 6-3 for OHT1 tests. The NASA results are shown graphically along with the complete NCAMP database of HEXCEL 8552 IM7 results for comparison purposes. The results for OHC1 are in Figure 6-1, for LT and OHT1 CTD in Figure 6-2, for LT and OHT1 RTD in Figure 6-3 and for LT and OHT1 ETW results in Figure 6-4.

	OHC1 RTD		OHC1 ETW	
	Mean	Std. Dev.	Mean	Std. Dev.
Generic Acceptance Limit	47.505	2.8052	33.722	2.5744
Glenn	45.792	0.973	31.767	0.444
Glenn: Low Vacuum	47.416	1.575	32.678	1.193
Glenn: Slow Ramp	46.011	1.461	34.148	1.626
Langley	47.082	1.379	32.678	0.766
Marshall	47.503	1.193	33.186	0.910

Table 6-1 OHC1 Generic Basis Values Acceptance Criteria and NASA test results

**Figure 6-1 NASA OHC1 results with NCAMP Generic Criteria and Basis values**

	LT CTD		LT RTD		LT ETW	
	Mean	Std. Dev.	Mean	Std. Dev.	Mean	Std. Dev.
Generic Acceptance Limit	285.24	30.05	294.68	42.21	254.31	45.92
Glenn	363.66	12.88	388.29	6.43	356.37	11.53
Langley	368.17	11.95	381.73	14.21	358.08	13.23
Marshall	358.03	6.84	397.14	10.80	366.51	12.90

Table 6-2 LT Generic Basis Values Acceptance Criteria and NASA test results

	OHT1 CTD		OHT1 RTD		OHT1 ETW	
	Mean	Std. Dev.	Mean	Std. Dev.	Mean	Std. Dev.
Generic Acceptance Limit	43.81	4.11	49.59	3.83	59.35	3.84
Glenn	64.58	1.47	65.99	1.85	69.24	4.80
Langley	63.56	1.76	62.41	1.12	68.99	1.68
Marshall	62.63	1.35	64.16	1.70	69.36	2.37

Table 6-3 OHT1 Generic Basis Values Acceptance Criteria and NASA test results

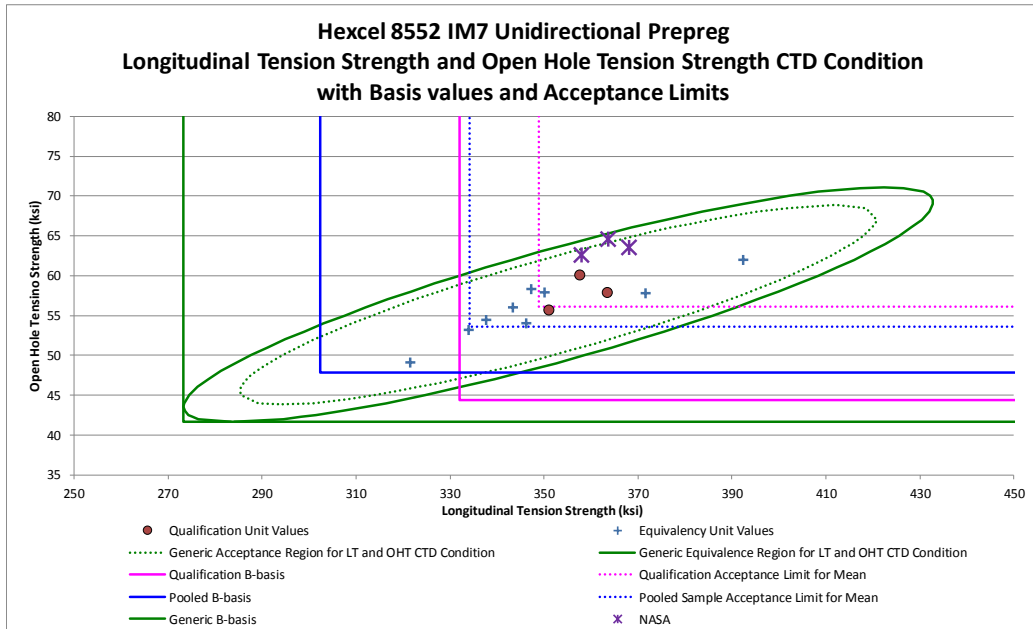


Figure 6-2 NASA LT & OHT1 CTD results with NCAMP Generic Criteria and Basis values

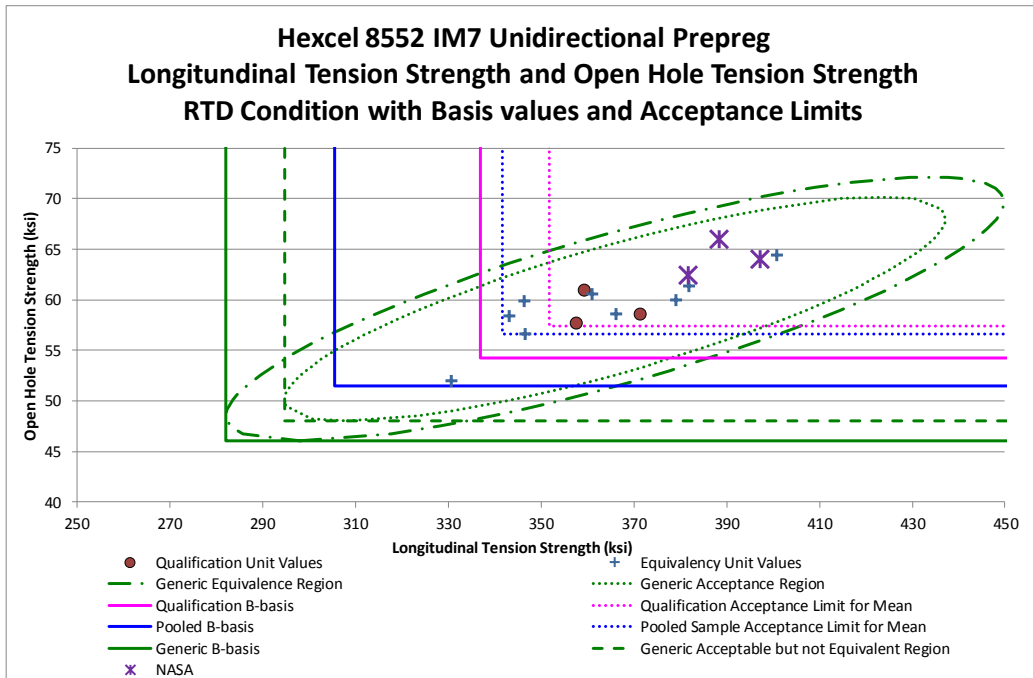


Figure 6-3 NASA LT & OHT1 RTD results with NCAMP Generic Criteria and Basis values

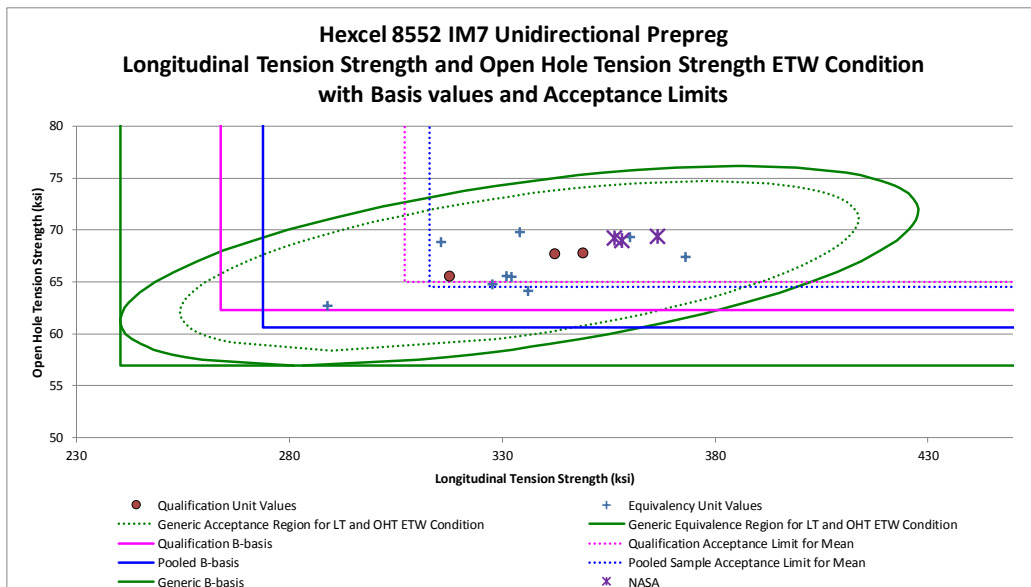


Figure 6-4 NASA LT & OHT1 ETW results with NCAMP Generic Criteria and Basis values

7. References

1. CMH-17 Rev G, Volume 1, 2012. SAE International, 400 Commonwealth Drive, Warrendale, PA 15096
2. John Tomblin, Yeow C. Ng, and K. Suresh Raju, "*Material Qualification and Equivalency for polymer Matrix Composite Material Systems: Updated Procedure*", National Technical Information Service (NTIS), Springfield, Virginia 22161
3. Vangel, Mark, "Lot Acceptance and Compliance Testing Using the Sample Mean and an Extremum", *Technometrics*, Vol 44, NO. 3, August 2002, pp. 242-249



WICHITA STATE
UNIVERSITY
*NATIONAL INSTITUTE
FOR AVIATION RESEARCH*

Report No: CAM-RP-2016-007 NC
Report Date: February 23, 2016

**Hexcel 8552 IM7 Unidirectional Prepreg
190 gsm & 35%RC
Equivalency Statistical Analysis Report
NASA (Glenn, Langley & Marshall)**

Test Report Number: CAM-RP-2016-007 NC

Report Date: February 23, 2016

Kim-Leng Poon
National Institute for Aviation Research
Wichita State University
Wichita, KS 67260-0093

Testing Facility:
Composites Laboratory
National Institute for Aviation Research
Wichita State University
1845 N. Fairmount
Wichita, KS 67260-0093

Test Panel Fabrication Facility:
NASA Glenn Research Center
NASA Langley Research Center
NASA Marshall Space Flight Center



WICHITA STATE
UNIVERSITY
NATIONAL INSTITUTE
FOR AVIATION RESEARCH

Report No: CAM-RP-2016-007 NC
Report Date: February 23, 2016

Prepared by: 
Kim-Leng Poon

Reviewed by: Elizabeth Clarkson, Ph.D
Elizabeth Clarkson, Ph.D

Digitally signed by Elizabeth Clarkson
DN: cn=Elizabeth Clarkson, o=NCAMP/
NIAR, ou=NCAMPNIAR,
email=b.clarkson@niar.wichita.edu, c=US
Date: 2016.02.23 10:10:55 -06'00'

Approved by: 
Royal Lovingfoss

REVISIONS:

Rev	By	Date	Pages Revised or Added
N/C	Kim-Leng Poon		Document Initial Release

Table of Contents

Introduction.....	6
1.1 Symbols and Abbreviations	6
2. Background	8
2.1 Results Codes	8
2.2 Equivalency Computations	8
2.2.1 Hypothesis Testing.....	8
2.2.2 Type I and Type II errors	9
2.2.3 Cumulative Error Probability.....	9
2.2.4 Strength and Modulus Tests.....	10
2.2.5 Modified Coefficient of Variation	12
3. Equivalency Test Results.....	14
3.1 Longitudinal (0°) Tension (LT) For NASA Glenn	18
3.2 Longitudinal (0°) Tension (LT) For NASA Langley	20
3.3 Longitudinal (0°) Tension (LT) For NASA Marshall.....	22
3.4 Laminate Short-Beam Strength (LSBS) for NASA Glenn	24
3.5 Laminate Short-Beam Strength (LSBS) for NASA Langley	26
3.6 Laminate Short-Beam Strength (LSBS) for NASA Marshall	27
3.7 “25/50/25” Unnotched Compression 1 (UNC1) for NASA Glenn Baseline	29
3.8 “25/50/25” Unnotched Compression 1 (UNC1) for NASA Glenn Low Vacuum Panel	31
3.9 “25/50/25” Unnotched Compression 1 (UNC1) for NASA Glenn Slow Ramp Panel	33
3.10 “25/50/25” Unnotched Compression 1 (UNC1) for NASA Langley	35
3.11 “25/50/25” Unnotched Compression 1 (UNC1) for NASA Marshall.....	37
3.12 “25/50/25” Unnotched Tension 1 (UNT1) for NASA Glenn.....	39
3.13 “25/50/25” Unnotched Tension 1 (UNT1) for NASA Langley	41
3.14 “25/50/25” Unnotched Tension 1 (UNT1) for NASA Marshall	43
3.15 “25/50/25” Open-Hole Compression 1 (OHC1) for NASA Glenn	45
3.16 “25/50/25” Open-Hole Compression 1 (OHC1) for NASA Glenn Low Vacuum Panel	47
3.17 “25/50/25” Open-Hole Compression 1 (OHC1) for NASA Glenn Slow Ramp Panel	49
3.18 “25/50/25” Open-Hole Compression 1 (OHC1) for NASA Langley	51
3.19 “25/50/25” Open-Hole Compression 1 (OHC1) for NASA Marshall.....	53
3.20 “25/50/25” Open-Hole Tension 1 (OHT1) for NASA Glenn.....	55
3.21 “25/50/25” Open-Hole Tension 1 (OHT1) for NASA Langley	56
3.22 “25/50/25” Open-Hole Tension 1 (OHT1) for NASA Marshall	57
4. Summary of Results.....	58
4.1 Failures	59
4.2 Pass Rate	59
4.3 Probability of Failures	59
5. References.....	60

Figures

Figure 2-1 Type I and Type II errors	9
Figure 3-1 Longitudinal Tension means, minimums and Equivalence limits for NASA Glenn.....	19
Figure 3-2 Longitudinal Tension means, minimums and Equivalence limits for NASA Langley	21
Figure 3-3 Longitudinal Tension means, minimums and Equivalence limits for NASA Marshall	23
Figure 3-4 Laminate Short-Beam Strength means, minimums and Equivalence limits for NASA Glenn.....	25
Figure 3-5 Laminate Short-Beam Strength means, minimums and Equivalence limits for NASA Langley.....	26
Figure 3-6 Laminate Short-Beam Strength means, minimums and Equivalence limits for NASA Marshall	28
Figure 3-7 UNC1 means, minimums and Equivalence limits for NASA Glenn Baseline	30
Figure 3-8 UNC1 means, minimums and Equivalence limits for NASA Glenn Low Vacuum Panels.....	32
Figure 3-9 UNC1 means, minimums and Equivalence limits for NASA Glenn Slow Ramp Panels.....	34
Figure 3-10 UNC1 means, minimums and Equivalence limits for NASA Langley.....	36
Figure 3-11 UNC1 means, minimums and Equivalence limits for NASA Marshall.....	38
Figure 3-12 UNT1 means, minimums and Equivalence limits for NASA Glenn	40
Figure 3-13 UNT1 means, minimums and Equivalence limits for NASA Langley	42
Figure 3-14 UNT1 means, minimums and Equivalence limits for NASA Marshall.....	44
Figure 3-15 Open-Hole Compression 1 means, minimums and Equivalence limits for NASA Glenn.....	46
Figure 3-16 Open-Hole Compression 1 means, minimums and Equivalence limits for NASA Glenn Low Vacuum Panel	48
Figure 3-17 Open-Hole Compression 1 means, minimums and Equivalence limits for NASA Glenn Slow Ramp Panel	50
Figure 3-18 Open-Hole Compression 1 means, minimums and Equivalence limits for NASA Langley.....	52
Figure 3-19 Open-Hole Compression 1 means, minimums and Equivalence limits for NASA Marshall	54
Figure 3-20 Open-Hole Tension 1 means, minimums and Equivalence limits for NASA Glenn.....	55
Figure 3-21 Open-Hole Tension 1 means, minimums and Equivalence limits for NASA Langley	56
Figure 3-22 Open-Hole Tension 1 means, minimums and Equivalence limits for NASA Marshall	57
Figure 5-1 Probability of Number of Failures	60

Tables

Table 0-1 Test Property Abbreviations.....	6
Table 0-2 Environmental Conditions Abbreviations	7
Table 2-1 One-sided tolerance factors for limits on sample mean values	11
Table 2-2 One-sided tolerance factors for limits on sample minimum values	12
Table 3-1 Summary of Equivalency Test Results for NASA Glenn	15
Table 3-2 Summary of Equivalency Test Results for Low Vacuum Panels.....	15
Table 3-3 Summary of Equivalency Test Results for Slow Ramp Panels.....	16
Table 3-4 Summary of Equivalency Test Results for NASA Langley	16
Table 3-5 Summary of Equivalency Test Results for NASA Marshall.....	17
Table 3-6 "% Failed" Results Scale	17
Table 3-5 Longitudinal Tension Strength Results for (NASA Glenn)	18
Table 3-6 Longitudinal Tension Modulus Results for (NASA Glenn)	18
Table 3-7 Longitudinal Tension Strength Results for (NASA Langley).....	20
Table 3-8 Longitudinal Tension Modulus Results for (NASA Langley)	20
Table 3-9 Longitudinal Tension Strength Results for (NASA Marshall).....	22
Table 3-10 Longitudinal Tension Modulus Results for (NASA Marshall)	22
Table 3-11 Laminate Short-Beam Strength Results for (NASA Glenn)	24
Table 3-12 Laminate Short-Beam Strength Results for (NASA Langley).....	26
Table 3-13 Laminate Short-Beam Strength Results for (NASA Marshall)	27
Table 3-14 Unnotched Compression 1 Results for (NASA Glenn Baseline).....	29
Table 3-15 Unnotched Compression 1 Modulus Results for (NASA Glenn Baseline)....	29
Table 3-16 Unnotched Compression 1 Results for (NASA Glenn Low Vacuum).....	31
Table 3-17 Unnotched Compression 1 Modulus Results for	31
Table 3-18 Unnotched Compression 1 Results for (NASA Glenn Slow Ramp).....	33
Table 3-19 Unnotched Compression 1 Modulus Results for	33
Table 3-20 Unnotched Compression 1 Results for (NASA Langley)	35
Table 3-21 Unnotched Compression 1 Modulus Results for	35
Table 3-22 Unnotched Compression 1 Results for (NASA Marshall)	37
Table 3-23 Unnotched Compression 1 Modulus Results for (NASA Marshall)	37
Table 3-24 Unnotched Tension 1 Results for (NASA Glenn).....	39
Table 3-25 Unnotched Tension 1 Modulus Results for	39
Table 3-26 Unnotched Tension 1 Results for (NASA Langley).....	41
Table 3-27 Unnotched Tension 1 Modulus Results for (NASA Langley)	41
Table 3-28 Unnotched Tension 1 Results for (NASA Marshall)	43
Table 3-29 Unnotched Tension 1 Modulus Results for (NASA Marshall)	43
Table 3-30 Open-Hole Compression 1 Strength Results For NASA Glenn.....	45
Table 3-31 Open-Hole Compression 1 Strength Results For NASA Glenn Low Vacuum	47
Table 3-32 Open-Hole Compression 1 Strength Results For NASA Glenn Slow Ramp.	49
Table 3-33 Open-Hole Tension 1 Strength Results For NASA Langley.....	51
Table 3-34 Open-Hole Tension 1 Strength Results For NASA Marshall	53
Table 3-35 Open-Hole Tension 1 Strength Results for NASA Glenn	55
Table 3-36 Open-Hole Tension 1 Strength Results for NASA Langley	56
Table 3-37 Open-Hole Tension 1 Strength Results for NASA Marshall	57

Introduction

This report contains the equivalency test results for NASA Hexcel 8552 IM7 unidirectional material produced panels compared to the original qualification panels of the same material. The lamina and laminate material property data have been generated with a single batch of material.

The tests on the equivalency specimens were performed at the National Institute for Aviation Research (NIAR) in Wichita, Kansas. The comparisons were performed according to CMH-17 Rev G section 8.4.1. The modified coefficient of variation (Mod CV) comparison tests were done in accordance with section 8.4.4 of CMH-17 Rev G.

The material property data for the qualification panels is published in Property Data Report CAM-RP-2009-015 Rev A. The material property data for the Integrated Composites, Inc equivalence panels is published in NCAMP Test Report CAM-RP-2012-015 N/C. Engineering basis values were reported in NCAMP Report NCP-RP-2009-028 N/C which details the standards and methodology used for computing basis values as well as providing the B-basis values and A- and B- estimates computed from the test results for the original qualification panels.

The NCAMP shared material property database contains material property data of common usefulness to a wide range of aerospace projects. However, the data may not fulfill all the needs of a project. Specific properties, environments, laminate architecture, and loading situations that individual projects need may require additional testing.

The applicability and accuracy of this material property data, material allowables, and specifications must be evaluated on case-by-case basis by aircraft companies and certifying agencies. NIAR assumes no liability whatsoever, expressed or implied, related to the use of the material property data, material allowables and specifications.

1.1 Symbols and Abbreviations

Test Property	Abbreviation
Longitudinal Tension	LT
Unnotched Tension 1	UNT1
Unnotched Compression 1	UNC1
Laminate Short-Beam Strength	LSBS
Open-Hole Tension 1	OHT1
Open-Hole Compression 1	OHC1

Table 0-1 Test Property Abbreviations

Environmental Condition	Temperature	Abbreviation
Cold Temperature Dry	-65° F	CTD
Room Temperature Dry	70° F	RTD
Elevated Temperature Wet	250° F	ETW

Table 0-2 Environmental Conditions Abbreviations

Tests with a number immediately after the abbreviation indicate the lay-up:

1 refers to a 25/50/25 layup. This is also referred to as "Quasi-Isotropic"

2 refers to a 10/80/10 layup. This is also referred to as "Soft"

3 refers to a 40/20/40 layup. This is also referred to as "Hard"

EX: OHT1 is an Open-Hole Tension test with a 25/50/25 layup.

2. Background

Equivalence tests are performed in accordance with section 8.4.1 of CMH-17 Rev G and section 6.1 of DOT/FAA/AR-03/19, “Material Qualification and Equivalency for Polymer Matrix Composite Material Systems: Updated Procedure.”

2.1 Results Codes

Pass indicates that the test results are equivalent for that environment under both computational methods.

Fail indicates that the test results are NOT equivalent under both computational methods.

Pass with mod CV indicates the test results are equivalent under the assumption of the modified CV method that the coefficient of variation is at least 6 but the test results fail without the use of the modified CV method.

2.2 Equivalency Computations

Equivalency tests are performed to determine if the differences between test results can be reasonably explained as due to the expected random variation of the material and testing processes. If so, we can conclude the two sets of tests are from ‘equivalent’ materials.

2.2.1 Hypothesis Testing

This comparison is performed using the statistical methodology of hypothesis testing. Two mutually exclusive hypotheses are set up, termed the null (H_0) and the alternative (H_1). The null hypothesis is assumed true and must contain the equality. For equivalency testing, they are set up as follows, with M_1 and M_2 representing the two materials being compared:

$$\begin{aligned} H_0 &: M_1 = M_2 \\ H_1 &: M_1 \neq M_2 \end{aligned}$$

Samples are taken of each material and tested according to the plan. A test statistic is computed using the data from the sample tests. The probability of the actual test result is computed under the assumption of the null hypothesis. If that result is sufficiently unlikely then the null is rejected and the alternative hypothesis is accepted as true. If not, then the null hypothesis is retained as plausible.

2.2.2 Type I and Type II errors

	<i>Materials are equal</i>	<i>Materials are not equal</i>
<i>Conclude materials are equal</i>	<i>Correct Decision</i>	<i>Type II error</i>
<i>Conclude materials are not equal</i>	<i>Type I error</i>	<i>Correct Decision</i>

Figure 2-1 Type I and Type II errors

As illustrated in Figure 2-1, there are four possible outcomes: two correct conclusions and two erroneous conclusions. The two wrong conclusions are termed type I and type II errors to distinguish them. The probability of making a type I error is specified using a parameter called alpha (α), while the type II error is not easily computed or controlled. The term ‘sufficiently unlikely’ in the previous paragraph means, in more precise terminology, the probability of the computed test statistic under the assumption of the null hypothesis is less than α .

For equivalency testing of composite materials, α is set at 0.05 which corresponds to a confidence level of 95%. This means that if we reject the null and say the two materials are not equivalent with respect to a particular test, the probability that this is a correct decision is no less than 95%.

2.2.3 Cumulative Error Probability

Each characteristic (such as Longitudinal Tension strength or In-Plane Shear modulus) is tested separately. While the probability of a Type I error is the same for all tests, since many different tests are performed on a single material, each with a 5% probability of a type I error, the probability of having one or more failures in a series of tests can be much higher.

If we assume the two materials are identical, with two tests the probability of a type I error for the two tests combined is $1 - .95^2 = .0975$. For four tests, it rises to $1 - .95^4 = .1855$. For 25 tests, the probability of a type I error on 1 or more tests is $1 - .95^{25} = .7226$. With a high probability of one or more equivalence test failures due to random

chance alone, a few failed tests should be allowed and equivalence may still be presumed provided that the failures are not severe.

2.2.4 Strength and Modulus Tests

For strength test values, we are primarily concerned only if the equivalence sample shows lower strength values than the original qualification material. This is referred to as a ‘one-sided’ hypothesis test. Higher values are not considered a problem, though they may indicate a difference between the two materials. The equivalence sample mean and sample minimum values are compared against the minimum expected values for those statistics, which are computed from the qualification test result

The expected values are computed using the values listed in Table 2-1 and Table 2-2 according to the following formulas:

The mean must exceed $\bar{X} - k_n^{\text{table 2.1}} \cdot S$ where \bar{X} and S are, respectively, the mean and the standard deviation of the qualification sample.

The sample minimum must exceed $\bar{X} - k_n^{\text{table 2.2}} \cdot S$ where \bar{X} and S are, respectively, the mean and the standard deviation of the qualification sample.

If either the mean or the minimum falls below the expected minimum, the sample is considered to have failed equivalency for that characteristic and the null hypothesis is rejected. The probability of failing either the mean or the minimum test (the α level) is set at 5%.

For Modulus values, failure occurs if the equivalence sample mean is either too high or too low compared to the qualification mean. This is referred to as a ‘two-sided’ hypothesis test. A standard two-sample two-tailed t-test is used to determine if the mean from the equivalency sample is sufficiently far from the qualification sample mean to reject the null hypothesis. The probability of a type I error is set at 5%.

These tests are performed with the HYTEQ spreadsheet, which was designed to test equivalency between two materials in accordance with the requirements of CMH-17 Rev G section 8.4.1: Tests for determining equivalency between an existing database and a new dataset for the same material. Details about the methods used are documented in the references listed in Section 0.

n	One-sided tolerance factors for limits on sample mean values								
	α								
	0.25	0.1	0.05	0.025	0.01	0.005	0.0025	0.001	0.0005
2	0.6266	1.0539	1.3076	1.5266	1.7804	1.9528	2.1123	2.3076	2.4457
3	0.5421	0.8836	1.0868	1.2626	1.4666	1.6054	1.7341	1.8919	2.0035
4	0.4818	0.7744	0.9486	1.0995	1.2747	1.3941	1.5049	1.6408	1.7371
5	0.4382	0.6978	0.8525	0.9866	1.1425	1.2488	1.3475	1.4687	1.5546
6	0.4048	0.6403	0.7808	0.9026	1.0443	1.1411	1.2309	1.3413	1.4196
7	0.3782	0.5951	0.7246	0.8369	0.9678	1.0571	1.1401	1.2422	1.3145
8	0.3563	0.5583	0.6790	0.7838	0.9059	0.9893	1.0668	1.1622	1.2298
9	0.3379	0.5276	0.6411	0.7396	0.8545	0.9330	1.0061	1.0959	1.1596
10	0.3221	0.5016	0.6089	0.7022	0.8110	0.8854	0.9546	1.0397	1.1002
11	0.3084	0.4790	0.5811	0.6699	0.7735	0.8444	0.9103	0.9914	1.0490
12	0.2964	0.4593	0.5569	0.6417	0.7408	0.8086	0.8717	0.9493	1.0044
13	0.2856	0.4418	0.5354	0.6168	0.7119	0.7770	0.8376	0.9121	0.9651
14	0.2760	0.4262	0.5162	0.5946	0.6861	0.7488	0.8072	0.8790	0.9300
15	0.2673	0.4121	0.4990	0.5746	0.6630	0.7235	0.7798	0.8492	0.8985
16	0.2594	0.3994	0.4834	0.5565	0.6420	0.7006	0.7551	0.8223	0.8700
17	0.2522	0.3878	0.4692	0.5400	0.6230	0.6797	0.7326	0.7977	0.8440
18	0.2455	0.3771	0.4561	0.5250	0.6055	0.6606	0.7120	0.7753	0.8202
19	0.2394	0.3673	0.4441	0.5111	0.5894	0.6431	0.6930	0.7546	0.7984
20	0.2337	0.3582	0.4330	0.4982	0.5745	0.6268	0.6755	0.7355	0.7782
21	0.2284	0.3498	0.4227	0.4863	0.5607	0.6117	0.6593	0.7178	0.7594
22	0.2235	0.3419	0.4131	0.4752	0.5479	0.5977	0.6441	0.7013	0.7420
23	0.2188	0.3345	0.4041	0.4648	0.5359	0.5846	0.6300	0.6859	0.7257
24	0.2145	0.3276	0.3957	0.4551	0.5246	0.5723	0.6167	0.6715	0.7104
25	0.2104	0.3211	0.3878	0.4459	0.5141	0.5608	0.6043	0.6579	0.6960
26	0.2065	0.3150	0.3803	0.4373	0.5041	0.5499	0.5926	0.6451	0.6825
27	0.2028	0.3092	0.3733	0.4292	0.4947	0.5396	0.5815	0.6331	0.6698
28	0.1994	0.3038	0.3666	0.4215	0.4858	0.5299	0.5710	0.6217	0.6577
29	0.1961	0.2986	0.3603	0.4142	0.4774	0.5207	0.5611	0.6109	0.6463
30	0.1929	0.2936	0.3543	0.4073	0.4694	0.5120	0.5517	0.6006	0.6354

Table 2-1 One-sided tolerance factors for limits on sample mean values

n	One-sided tolerance factors for limits on sample minimum values								
	α								
	0.25	0.1	0.05	0.025	0.01	0.005	0.0025	0.001	0.0005
2	1.2887	1.8167	2.1385	2.4208	2.7526	2.9805	3.1930	3.4549	3.6412
3	1.5407	2.0249	2.3239	2.5888	2.9027	3.1198	3.3232	3.5751	3.7550
4	1.6972	2.1561	2.4420	2.6965	2.9997	3.2103	3.4082	3.6541	3.8301
5	1.8106	2.2520	2.5286	2.7758	3.0715	3.2775	3.4716	3.7132	3.8864
6	1.8990	2.3272	2.5967	2.8384	3.1283	3.3309	3.5220	3.7603	3.9314
7	1.9711	2.3887	2.6527	2.8900	3.1753	3.3751	3.5638	3.7995	3.9690
8	2.0317	2.4407	2.7000	2.9337	3.2153	3.4127	3.5995	3.8331	4.0011
9	2.0838	2.4856	2.7411	2.9717	3.2500	3.4455	3.6307	3.8623	4.0292
10	2.1295	2.5250	2.7772	3.0052	3.2807	3.4745	3.6582	3.8883	4.0541
11	2.1701	2.5602	2.8094	3.0351	3.3082	3.5005	3.6830	3.9116	4.0765
12	2.2065	2.5918	2.8384	3.0621	3.3331	3.5241	3.7054	3.9328	4.0969
13	2.2395	2.6206	2.8649	3.0867	3.3558	3.5456	3.7259	3.9521	4.1155
14	2.2697	2.6469	2.8891	3.1093	3.3766	3.5653	3.7447	3.9699	4.1326
15	2.2975	2.6712	2.9115	3.1301	3.3959	3.5836	3.7622	3.9865	4.1485
16	2.3232	2.6937	2.9323	3.1495	3.4138	3.6007	3.7784	4.0019	4.1633
17	2.3471	2.7146	2.9516	3.1676	3.4306	3.6166	3.7936	4.0163	4.1772
18	2.3694	2.7342	2.9698	3.1846	3.4463	3.6315	3.8079	4.0298	4.1902
19	2.3904	2.7527	2.9868	3.2005	3.4611	3.6456	3.8214	4.0425	4.2025
20	2.4101	2.7700	3.0029	3.2156	3.4751	3.6589	3.8341	4.0546	4.2142
21	2.4287	2.7864	3.0181	3.2298	3.4883	3.6715	3.8461	4.0660	4.2252
22	2.4463	2.8020	3.0325	3.2434	3.5009	3.6835	3.8576	4.0769	4.2357
23	2.4631	2.8168	3.0463	3.2562	3.5128	3.6949	3.8685	4.0873	4.2457
24	2.4790	2.8309	3.0593	3.2685	3.5243	3.7058	3.8790	4.0972	4.2553
25	2.4941	2.8443	3.0718	3.2802	3.5352	3.7162	3.8889	4.1066	4.2644
26	2.5086	2.8572	3.0838	3.2915	3.5456	3.7262	3.8985	4.1157	4.2732
27	2.5225	2.8695	3.0953	3.3023	3.5557	3.7357	3.9077	4.1245	4.2816
28	2.5358	2.8813	3.1063	3.3126	3.5653	3.7449	3.9165	4.1328	4.2897
29	2.5486	2.8927	3.1168	3.3225	3.5746	3.7538	3.9250	4.1409	4.2975
30	2.5609	2.9036	3.1270	3.3321	3.5835	3.7623	3.9332	4.1487	4.3050

Table 2-2 One-sided tolerance factors for limits on sample minimum values

2.2.5 Modified Coefficient of Variation

A common problem with new material qualifications is that the initial specimens produced and tested do not contain all of the variability that will be encountered when the material is being produced in larger amounts over a lengthy period of time. This can result in setting basis values that are unrealistically high.

The modified Coefficient of Variation (CV) used in this report is in accordance with section 8.4.4 of CMH-17 Revision G. It is a method of adjusting the original basis values downward in anticipation of the expected additional variation. Composite materials are expected to have a CV of at least 6%. When the CV is less than 8%, a modification is made that adjusts the CV upwards.

$$\text{Modified CV} = CV^* = \begin{cases} .06 & \text{if } CV < .04 \\ \frac{CV}{2} + .04 & \text{if } .04 \leq CV < .08 \\ CV & \text{if } CV \geq .08 \end{cases} \quad \text{Equation 1}$$

This is converted to percent by multiplying by 100%.

CV^* is used to compute a modified standard deviation S^* .

$$S^* = CV^* \cdot \bar{X}$$

Equation 2

To compute the pooled standard deviation based on the modified CV:

$$S_p^* = \sqrt{\frac{\sum_{i=1}^k ((n_i - 1)(CV_i^* \cdot \bar{X}_i)^2)}{\sum_{i=1}^k (n_i - 1)}}$$

Equation 3

The A-basis and B-basis values under the assumption of the modified CV method are computed by replacing S with S^* .

When the basis values have been set using the modified CV method, we can use the modified CV to compute the equivalency test results.

3. Equivalency Test Results

The three NASA locations each had 24 different tests conducted. Only the modulus tests had sufficient data to meet the CMH-17 Rev G requirements, all strength tests lack sufficient data for the results to be considered conclusive. The Glenn location had six additional tests conducted for both the Low Vacuum panels and the Slow Ramp Panels. All tests were performed with an α level of 5%.

The results of the equivalency comparisons are listed as 'Pass', 'Fail', or 'Pass with Mod. CV'. 'Pass with Mod CV' refers to cases where the equivalency fails unless the modified coefficient of variation method is used. A minimum of eight samples from two separate panels and processing cycles is required for strength properties and a minimum of four specimens are required for modulus comparison tests. If the sample does not have an adequate number of specimens, this will be indicated with 'Insufficient Data' after the Pass or Fail indication. A summary of results for NASA Glenn is shown in Table 3-1, for the Low Vacuum panels in Table 3-2, for the Slow Ramp Panels in Table 3-3, for NASA Langley in Table 3-4, and for NASA Marshall in Table 3-5.

Failures in table 3-1 through 3-5 are reported as "Failed by %". This percentage was computed by taking the ratio of the equivalency mean or minimum value to the modified CV limit for that value. Table 3-6 gives a rough scale for the relative severity of those failures.

Equivalency Test Results for Nasa Glenn M Cure Cycle with Hexcel 8552 IM7 M Cure Cycle						
Test	Normalized Data	Property	Environmental Condition			
			CTD	RTD	ETD	ETW
Longitudinal Tension	Yes	Strength	Pass Insufficient Data	Pass Insufficient Data		Pass Insufficient Data
		Modulus	Pass	Pass		Pass with Mod CV
Laminate Short Beam Strength	No	Strength		Pass Insufficient Data		Pass with Mod CV Insufficient Data
Unnotched Compression (UNC1)	Yes	Strength		Pass Insufficient Data		Pass Insufficient Data
	Yes	Modulus		Pass		Failed by 2.9%
Unnotched Tension (UNT1)	Yes	Strength	Pass Insufficient Data	Pass Insufficient Data		Pass Insufficient Data
		Modulus	Pass	Pass		Pass
Open Hole Compression (OHC1)	Yes	Strength		Failed by 1.1% Insufficient Data		Failed by 5.1% Insufficient Data
Open Hole Tension (OHT1)	Yes	Strength	Pass Insufficient Data	Pass Insufficient Data		Pass Insufficient Data

Table 3-1 Summary of Equivalency Test Results for NASA Glenn**NASA Glenn Low Vacuum Panels for UNC1 & OHC1**

Unnotched Compression (UNC1)	Yes	Strength		Pass Insufficient Data		Pass Insufficient Data
	Yes	Modulus		Pass		Pass with Mod CV
Open Hole Compression (OHC1)	Yes	Strength		Pass Insufficient Data		Failed by 2.4% Insufficient Data

Table 3-2 Summary of Equivalency Test Results for Low Vacuum Panels

NASA Glenn Slow Ramp Panels for UNC1 & OHC1

Unnotched Compression (UNC1)	Yes	Strength		Pass Insufficient Data		Pass Insufficient Data
	Yes	Modulus		Pass		Pass with Mod CV
Open Hole Compression (OHC1)	Yes	Strength		Failed by 0.6% Insufficient Data		Pass Insufficient Data

Table 3-3 Summary of Equivalency Test Results for Slow Ramp Panels

Equivalency Test Results for NASA Langley M Cure Cycle with Hexcel 8552 IM7 M Cure Cycle						
Test	Normalized Data	Property	Environmental Condition			
			CTD	RTD	ETD	ETW
Longitudinal Tension	Yes	Strength	Pass Insufficient Data	Pass Insufficient Data		Pass Insufficient Data
		Modulus	Pass with Mod CV	Pass		Pass with Mod CV
Laminate Short Beam Strength	No	Strength		Pass Insufficient Data		Pass Insufficient Data
Unnotched Compression (UNC1)	Yes	Strength		Pass Insufficient Data		Pass Insufficient Data
	Yes	Modulus		Pass		Pass with Mod CV
Unnotched Tension (UNT1)	Yes	Strength	Pass Insufficient Data	Pass Insufficient Data		Pass Insufficient Data
		Modulus	Pass	Pass		Pass
Open Hole Compression (OHC1)	Yes	Strength		Pass with Mod CV Insufficient Data		Failed by 4.8% Insufficient Data
Open Hole Tension (OHT1)	Yes	Strength	Pass Insufficient Data	Pass Insufficient Data		Pass Insufficient Data

Table 3-4 Summary of Equivalency Test Results for NASA Langley

Equivalency Test Results for Nasa Marshall M Cure Cycle with Hexcel 8552 IM7 M Cure Cycle						
Test	Normalized Data	Property	Environmental Condition			
			CTD	RTD	ETD	ETW
Longitudinal Tension	Yes	Strength	Pass Insufficient Data	Pass Insufficient Data		Pass Insufficient Data
		Modulus	Pass with Mod CV	Pass		Pass with Mod CV
Laminate Short Beam Strength	No	Strength		Pass Insufficient Data		Failed by 0.1% Insufficient Data
Unnotched Compression (UNC1)	Yes	Strength		Pass Insufficient Data		Pass Insufficient Data
	Yes	Modulus		Pass		Pass with Mod CV
Unnotched Tension (UNT1)	Yes	Strength	Pass Insufficient Data	Pass Insufficient Data		Pass Insufficient Data
		Modulus	Pass	Pass		Pass
Open Hole Compression (OHC1)	Yes	Strength		Pass with Mod CV Insufficient Data		Failed by 1.9% Insufficient Data
Open Hole Tension (OHT1)	Yes	Strength	Pass Insufficient Data	Pass Insufficient Data		Pass Insufficient Data

Table 3-5 Summary of Equivalency Test Results for NASA Marshall

Description	Modulus	Strength
Mild Failure	% fail \leq 4%	% fail \leq 5%
Mild to Moderate Failure	4% $<$ % fail \leq 8%	5% $<$ % fail \leq 10%
Moderate Failure	8% $<$ % fail \leq 12%	10% $<$ % fail \leq 15%
Moderate to Severe Failure	12% $<$ % fail \leq 16%	15% $<$ % fail \leq 20%
Severe Failure	16% $<$ % fail \leq 20%	20% $<$ % fail \leq 25%
Extreme Failure	20% $<$ % fail	25% $<$ % fail

Table 3-6 "% Failed" Results Scale

3.1 Longitudinal (0°) Tension (LT) For NASA Glenn

The LT normalized data passed equivalency tests for both strength and modulus. The ETW Modulus data passed only with the use of modified coefficient of variation approach. Statistics and analysis results are shown for the strength data in Table 3-7 and for the modulus data in Table 3-8.

Longitudinal Tension (LT) Strength	CTD		RTD		ETW	
	Qual.	Equiv.	Qual.	Equiv.	Qual.	Equiv.
Data normalized with CPT 0.0072	Insufficient Data		Insufficient Data		Insufficient Data	
Mean Strength (ksi)	357.389	363.658	362.693	388.287	333.504	356.367
Standard Deviation	12.620	12.879	16.057	6.426	38.823	11.526
Coefficient of Variation %	3.531	3.541	4.427	1.655	11.641	3.234
Minimum	325.692	349.131	325.685	381.912	244.533	340.091
Maximum	379.970	379.884	392.322	397.057	373.234	367.145
Number of Specimens	22	4	18	4	18	4
RESULTS	PASS		PASS		PASS	
Minimum Acceptable Equiv. Sample Mean	345.417		347.462		296.676	
Minimum Acceptable Equiv. Sample Min	326.570		323.483		238.698	
MOD CV RESULTS	PASS with MOD CV		PASS with MOD CV		PASS with MOD CV	
Modified CV %	6.00		6.21		11.64	
Minimum Acceptable Equiv. Sample Mean	337.048		341.315		296.676	
Minimum Acceptable Equiv. Sample Min	305.024		307.660		238.698	

Table 3-7 Longitudinal Tension Strength Results for (NASA Glenn)

Longitudinal Tension (LT) Modulus	CTD		RTD		ETW	
	Qual.	Equiv.	Qual.	Equiv.	Qual.	Equiv.
Data normalized with CPT 0.0072	Insufficient Data		Insufficient Data		Insufficient Data	
Mean Modulus (Ms) ⁱ	22.568	22.207	22.987	22.561	24.001	23.249
Standard Deviation	0.387	0.133	0.812	0.501	0.557	0.393
Coefficient of Variation %	1.717	0.601	3.532	2.219	2.321	1.690
Minimum	21.852	22.055	20.707	22.117	23.222	22.787
Maximum	23.219	22.343	23.941	23.116	25.578	23.744
Number of Specimens	22	4	18	4	29	4
RESULTS	PASS		PASS		FAIL	
Passing Range for Modulus Mean	22.158 to 22.978		22.095 to 23.878		23.410 to 24.592	
Student's t-statistic	-1.818		-0.996		-2.596	
p-value of Student's t-statistic	0.082		0.331		0.014	
MOD CV RESULTS	PASS with MOD CV		PASS with MOD CV		PASS with MOD CV	
Modified CV %	6.00		6.00		6.00	
Passing Range for Modulus Mean	21.146 to 23.990		21.504 to 24.470		22.506 to 25.495	
Modified CV Student's t-statistic	-0.524		-0.599		-1.026	
p-value of Student's t-statistic	0.605		0.556		0.313	

Table 3-8 Longitudinal Tension Modulus Results for (NASA Glenn)

The LT modulus data for the ETW environment failed the equivalency test because the sample mean value (23.249) is below the lower acceptance limit (23.410). The equivalency sample mean value is 99.31% of the lower limit of acceptable values. Under the assumption of the modified CV method, the modulus data from the ETW environment passed the equivalence test.

Figure 3-1 illustrates the 0° Tension strength means and minimum values and the modulus means for the qualification sample and the equivalency sample. The limits for equivalency samples are shown as error bars with the qualification data. The longer, lighter colored error bars are for the modified CV computations.

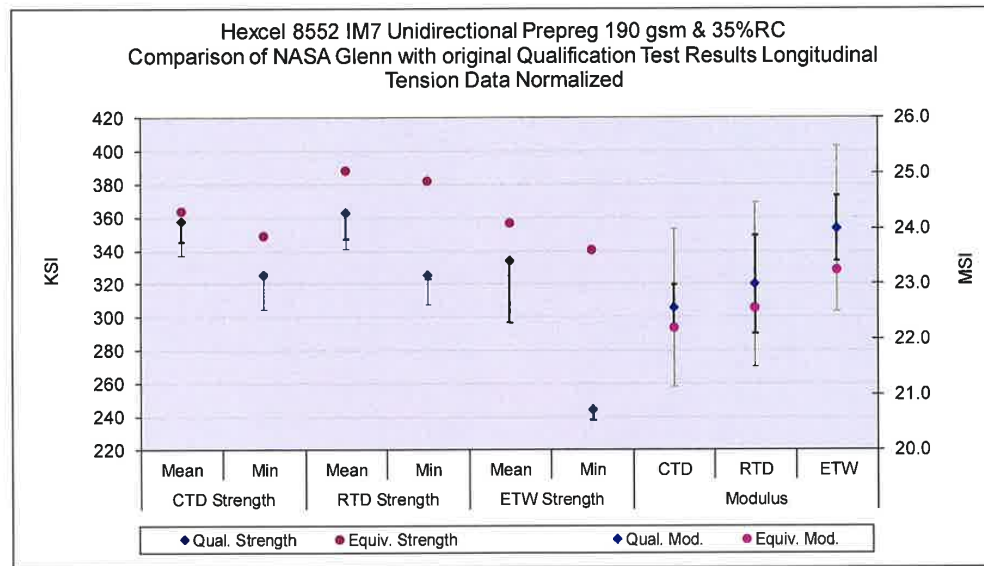


Figure 3-1 Longitudinal Tension means, minimums and Equivalence limits for NASA Glenn

3.2 Longitudinal (0°) Tension (LT) For NASA Langley

The LT normalized data passed equivalency tests for both strength and modulus. The CTD & ETW Modulus data passed only with the use of modified coefficient of variation approach. Statistics and analysis results are shown for the strength data in Table 3-7 and for the modulus data in Table 3-8

Longitudinal Tension (LT) Strength	CTD		RTD		ETW	
	Qual.	Equiv.	Qual.	Equiv.	Qual.	Equiv.
Data normalized with CPT 0.0072	Insufficient Data		Insufficient Data		Insufficient Data	
Mean Strength (ksi)	357.389	368.170	362.693	381.733	333.504	358.081
Standard Deviation	12.620	11.948	16.057	14.209	38.823	13.232
Coefficient of Variation %	3.531	3.245	4.427	3.722	11.641	3.695
Minimum	325.692	354.456	325.685	371.088	244.533	338.169
Maximum	379.970	382.683	392.322	402.585	373.234	375.125
Number of Specimens	22	4	18	4	18	6
RESULTS	PASS		PASS		PASS	
Minimum Acceptable Equiv. Sample Mean	345.417		347.462		303.191	
Minimum Acceptable Equiv. Sample Min	326.570		323.483		232.692	
MOD CV RESULTS	PASS with MOD CV		PASS with MOD CV		PASS with MOD CV	
Modified CV %	6.00		6.21		11.64	
Minimum Acceptable Equiv. Sample Mean	337.048		341.315		303.191	
Minimum Acceptable Equiv. Sample Min	305.024		307.660		232.692	

Table 3-9 Longitudinal Tension Strength Results for (NASA Langley)

Longitudinal Tension (LT) Modulus	CTD		RTD		ETW	
	Qual.	Equiv.	Qual.	Equiv.	Qual.	Equiv.
Data normalized with CPT 0.0072	FAIL		PASS		FAIL	
Mean Modulus (Msi)	22.568	22.146	22.987	22.350	24.001	23.160
Standard Deviation	0.387	0.196	0.812	0.543	0.557	0.367
Coefficient of Variation %	1.717	0.885	3.532	2.429	2.321	1.583
Minimum	21.852	21.965	20.707	21.875	23.222	22.693
Maximum	23.219	22.418	23.941	23.074	25.578	23.663
Number of Specimens	22	4	18	4	29	6
RESULTS	FAIL		PASS		FAIL	
Passing Range for Modulus Mean	22.154 to 22.982		22.090 to 23.883		23.515 to 24.487	
Student's t-statistic	-2.104		-1.481		-3.521	
p-value of Student's t-statistic	0.046		0.154		0.001	
MOD CV RESULTS	PASS with MOD CV		PASS with MOD CV		PASS with MOD CV	
Modified CV%	6.00		6.00		6.00	
Passing Range for Modulus Mean	21.145 to 23.991		21.501 to 24.473		22.783 to 25.218	
Modified CV Student's t-statistic	-0.612		-0.894		-1.405	
p-value of Student's t-statistic	0.546		0.382		0.169	

Table 3-10 Longitudinal Tension Modulus Results for (NASA Langley)

The LT modulus data for the CTD environment failed the equivalency test because the sample mean value (22.146) is below the lower acceptance limit (22.154). The equivalency sample mean value is 99.96% of the lower limit of acceptable values. Under the assumption of the modified CV method, the modulus data from the CTD environment passed the equivalence test.

The LT modulus data for the ETW environment failed the equivalency test because the sample mean value (23.160) is below the lower acceptance limit (23.515). The

equivalency sample mean value is 98.49% of the lower limit of acceptable values. Under the assumption of the modified CV method, the modulus data from the ETW environment passed the equivalence test.

Figure 3-2 illustrates the 0° Tension strength means and minimum values and the modulus means for the qualification sample and the equivalency sample. The limits for equivalency samples are shown as error bars with the qualification data. The longer, lighter colored error bars are for the modified CV computations.

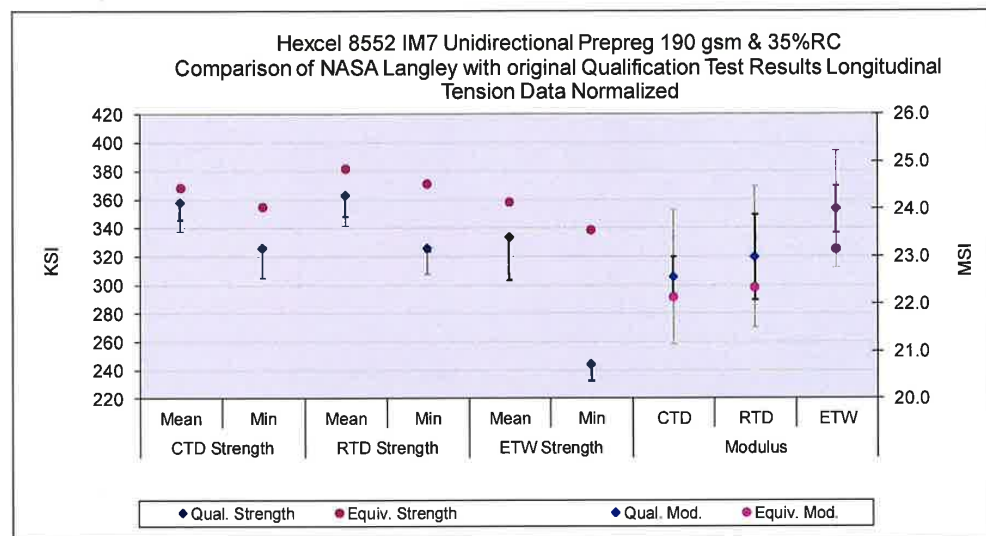


Figure 3-2 Longitudinal Tension means, minimums and Equivalence limits for NASA Langley

3.3 Longitudinal (0°) Tension (LT) For NASA Marshall

The LT normalized data passed equivalency tests for both strength and modulus. The CTD & ETW Modulus data passed only with the use of modified coefficient of variation approach. Statistics and analysis results are shown for the strength data in Table 3-7 and for the modulus data in Table 3-8

Longitudinal Tension (LT) Strength	CTD		RTD		ETW	
	Qual.	Equiv.	Qual.	Equiv.	Qual.	Equiv.
Data normalized with CPT 0.0072	Insufficient Data		Insufficient Data		Insufficient Data	
Mean Strength (ksi)	357.389	358.027	362.693	397.142	333.504	366.531
Standard Deviation	12.620	6.836	16.057	10.799	38.823	12.901
Coefficient of Variation %	3.531	1.909	4.427	2.719	11.641	3.520
Minimum	325.692	348.530	325.685	381.002	244.533	348.106
Maximum	379.970	364.778	392.322	403.821	373.234	377.046
Number of Specimens	22	4	18	4	18	4
RESULTS	PASS		PASS		PASS	
Minimum Acceptable Equiv. Sample Mean	345.417		347.462		296.676	
Minimum Acceptable Equiv. Sample Min	326.570		323.483		238.698	
MOD CV RESULTS	PASS with MOD CV		PASS with MOD CV		PASS with MOD CV	
Modified CV %	6.00		6.21		11.64	
Minimum Acceptable Equiv. Sample Mean	337.048		341.315		296.676	
Minimum Acceptable Equiv. Sample Min	305.024		307.660		238.698	

Table 3-11 Longitudinal Tension Strength Results for (NASA Marshall)

Longitudinal Tension (LT) Modulus	CTD		RTD		ETW	
	Qual.	Equiv.	Qual.	Equiv.	Qual.	Equiv.
Data normalized with CPT 0.0072	FAIL		PASS		FAIL	
Mean Modulus (Msi)	22.568	22.144	22.987	22.565	24.001	22.847
Standard Deviation	0.387	0.229	0.812	0.069	0.557	0.203
Coefficient of Variation %	1.717	1.036	3.532	0.308	2.321	0.887
Minimum	21.852	21.855	20.707	22.507	23.222	22.652
Maximum	23.219	22.391	23.941	22.660	25.578	23.087
Number of Specimens	22	4	18	4	29	4
RESULTS	FAIL		PASS		FAIL	
Passing Range for Modulus Mean	22.151 to 22.985		22.123 to 23.850		23.421 to 24.581	
Student's t-statistic	-2.100		-1.018		-4.059	
p-value of Student's t-statistic	0.046		0.321		0.000	
MOD CV RESULTS	PASS with MOD CV		PASS with MOD CV		PASS with MOD CV	
Modified CV%	6.00		6.00		6.00	
Passing Range for Modulus Mean	21.144 to 23.992		21.520 to 24.453		22.510 to 25.491	
Modified CV Student's t-statistic	-0.615		-0.600		-1.579	
p-value of Student's t-statistic	0.545		0.555		0.124	

Table 3-12 Longitudinal Tension Modulus Results for (NASA Marshall)

The LT modulus data for the CTD environment failed the equivalency test because the sample mean value (22.144) is below the lower acceptance limit (22.151). The equivalency sample mean value is 99.97% of the lower limit of acceptable values. Under the assumption of the modified CV method, the modulus data from the CTD environment passed the equivalence test.

The LT modulus data for the ETW environment failed the equivalency test because the sample mean value (22.847) is below the lower acceptance limit (23.421). The

equivalency sample mean value is 97.55% of the lower limit of acceptable values. Under the assumption of the modified CV method, the modulus data from the ETW environment passed the equivalence test.

Figure 3-1 illustrates the 0° Tension strength means and minimum values and the modulus means for the qualification sample and the equivalency sample. The limits for equivalency samples are shown as error bars with the qualification data. The longer, lighter colored error bars are for the modified CV computations.

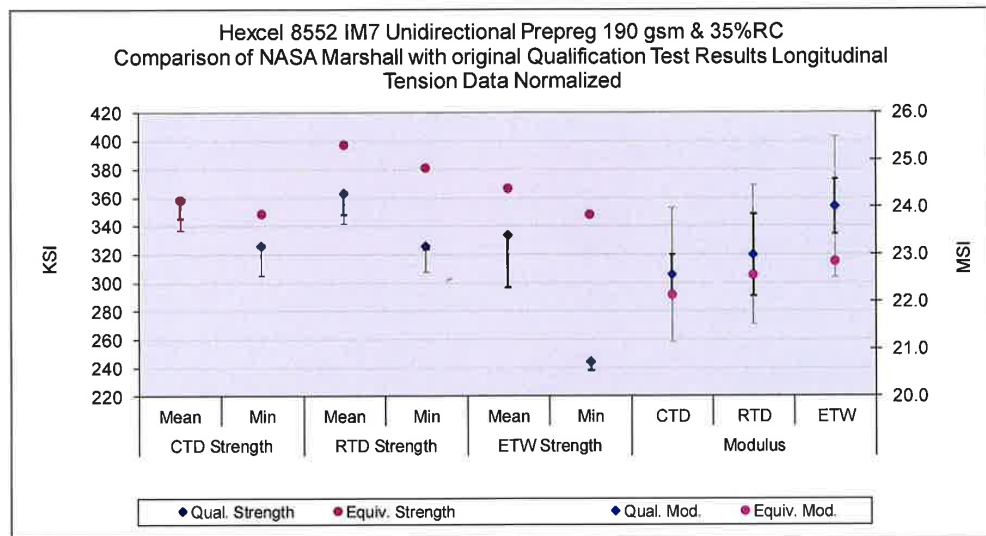


Figure 3-3 Longitudinal Tension means, minimums and Equivalence limits for NASA Marshall

3.4 Laminate Short-Beam Strength (LSBS) for NASA Glenn

The Laminate Short-Beam Strength data is not normalized. The laminate Short-Beam Strength data passed all equivalency tests. However the ETW data passed only with the use of modified coefficient of variation approach. Statistics and analysis results for the LSBS data are shown in Table 3-11

Laminate Short Beam Strength (LSBS)	RTD		ETW	
	Qual.	Equiv.	Qual.	Equiv.
Mean Strength (ksi)	Insufficient	12.129	12.446	6.991
Standard Deviation		0.831	0.398	0.255
Coefficient of Variation %	6.851	3.199	3.646	4.040
Minimum	9.550	11.987	6.635	6.296
Maximum	12.983	13.109	7.699	7.050
Number of Specimens	21	7	19	6
RESULTS	PASS		FAIL	
Minimum Acceptable Equiv. Sample Mean	11.527		6.792	
Minimum Acceptable Equiv. Sample Min	9.925		6.329	
MOD CV RESULTS	PASS with MOD CV		PASS with MOD CV	
Modified CV %	7.43		6.00	
Minimum Acceptable Equiv. Sample Mean	11.476		6.663	
Minimum Acceptable Equiv. Sample Min	9.740		5.901	

Table 3-13 Laminate Short-Beam Strength Results for (NASA Glenn)

The LSBS data for the ETW environment failed equivalence due sample minimum being too low. The equivalency minimum value is (6.296) is 99.48% of the lowest acceptable minimum value (6.329). Under the assumption of the modified CV method, the ETW environment passed the equivalence test.

Figure 3-4 illustrates the Laminate Short-Beam Strength means and minimum values for the qualification sample and the equivalency sample. The limits for equivalency samples are shown as error bars with the qualification data. The longer, lighter colored error bars are for the modified CV computations.

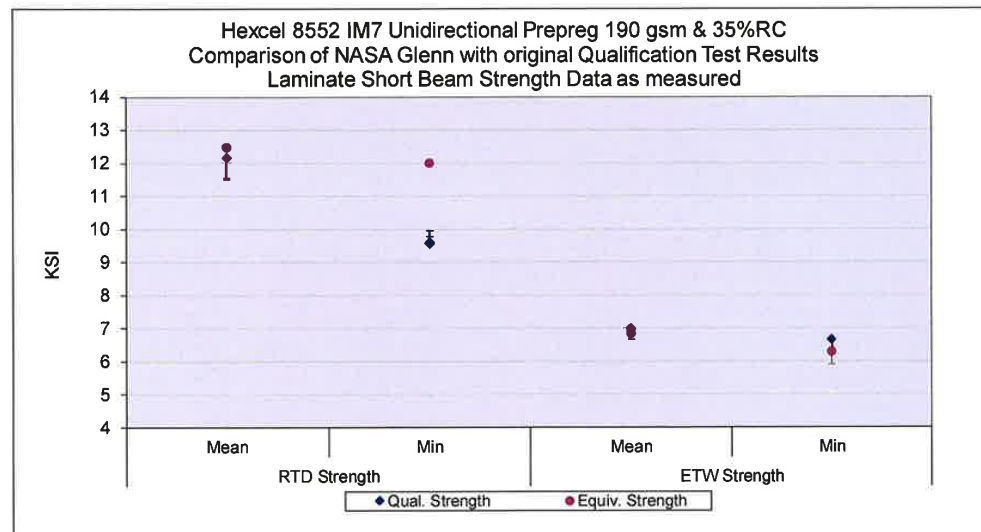


Figure 3-4 Laminate Short-Beam Strength means, minimums and Equivalence limits for NASA Glenn

3.5 Laminate Short-Beam Strength (LSBS) for NASA Langley

The Laminate Short-Beam Strength data is not normalized. The laminate Short-Beam Strength data passed all equivalency tests. Statistics and analysis results for the LSBS data are shown in Table 3-12

Laminate Short Beam Strength (LSBS)	RTD		ETW	
	Qual.	Equiv.	Qual.	Equiv.
Insufficient Data		Insufficient Data		
Mean Strength (ksi)	12.129	12.033	6.991	6.959
Standard Deviation	0.831	0.466	0.255	0.162
Coefficient of Variation %	6.851	3.871	3.646	2.325
Minimum	9.550	11.423	6.635	6.696
Maximum	12.983	12.548	7.699	7.150
Number of Specimens	21	6	19	6
RESULTS		PASS		PASS
Minimum Acceptable Equiv. Sample Mean	11.480		6.792	
Minimum Acceptable Equiv. Sample Min	9.971		6.329	
MOD CV RESULTS		PASS with MOD CV		PASS with MOD CV
Modified CV %	7.43		6.00	
Minimum Acceptable Equiv. Sample Mean	11.426		6.663	
Minimum Acceptable Equiv. Sample Min	9.790		5.901	

Table 3-14 Laminate Short-Beam Strength Results for (NASA Langley)

Figure 3-5 illustrates the Laminate Short-Beam Strength means and minimum values for the qualification sample and the equivalency sample. The limits for equivalency samples are shown as error bars with the qualification data. The longer, lighter colored error bars are for the modified CV computations.

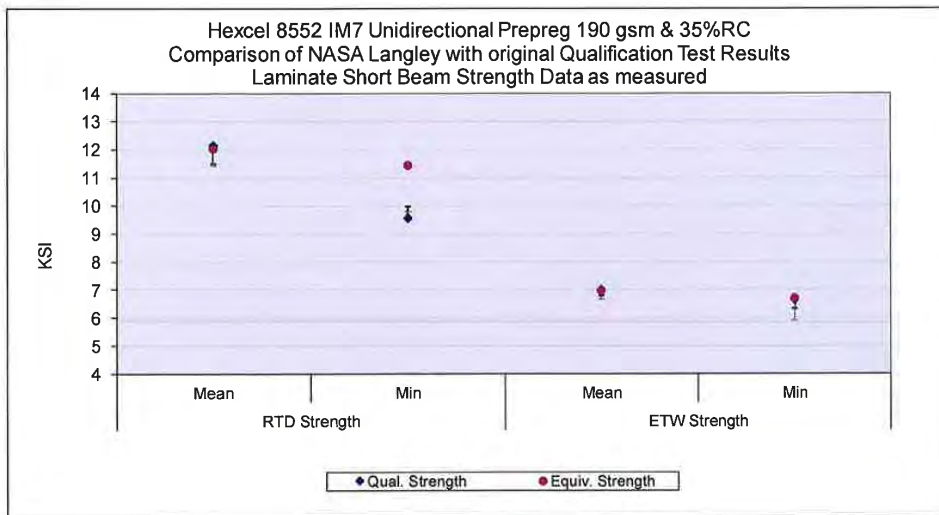


Figure 3-5 Laminate Short-Beam Strength means, minimums and Equivalence limits for NASA Langley

3.6 Laminate Short-Beam Strength (LSBS) for NASA Marshall

The Laminate Short-Beam Strength data is not normalized. The laminate Short-Beam Strength data passed RTD equivalency test. But it has failed the ETW condition. Statistics and analysis results for the LSBS data are shown in Table 3-13.

Laminate Short Beam Strength (LSBS)	RTD		ETW	
	Qual.	Equiv.	Qual.	Equiv.
	Insufficient Data		Insufficient Data	
Mean Strength (ksi)	12.129	12.399	6.991	6.658
Standard Deviation	0.831	0.474	0.255	0.210
Coefficient of Variation %	6.851	3.822	3.646	3.149
Minimum	9.550	11.687	6.635	6.277
Maximum	12.983	12.892	7.699	6.850
Number of Specimens	21	6	19	6
RESULTS	PASS		FAIL	
Minimum Acceptable Equiv. Sample Mean	11.480		6.792	
Minimum Acceptable Equiv. Sample Min	9.971		6.329	
MOD CV RESULTS	PASS with MOD CV		FAIL	
Modified CV %	7.43		6.00	
Minimum Acceptable Equiv. Sample Mean	11.426		6.663	
Minimum Acceptable Equiv. Sample Min	9.790		5.901	

Table 3-15 Laminate Short-Beam Strength Results for (NASA Marshall)

The laminate Short-Beam Strength data for the ETW environment failed equivalence due to both the sample mean and sample minimum being too low. The equivalency sample mean (6.658) is 98.03% of the minimum acceptable mean value (6.792). The equivalency sample minimum (6.277) is 99.19% of the lowest acceptable minimum value (6.392). Under the assumption of the modified CV method, the equivalency sample mean is 99.92% of the lowest acceptable mean value (6.663). The equivalency sample minimum passed the test.

Figure 3-4 illustrates the Laminate Short-Beam Strength means and minimum values for the qualification sample and the equivalency sample. The limits for equivalency samples are shown as error bars with the qualification data. The longer, lighter colored error bars are for the modified CV computations.

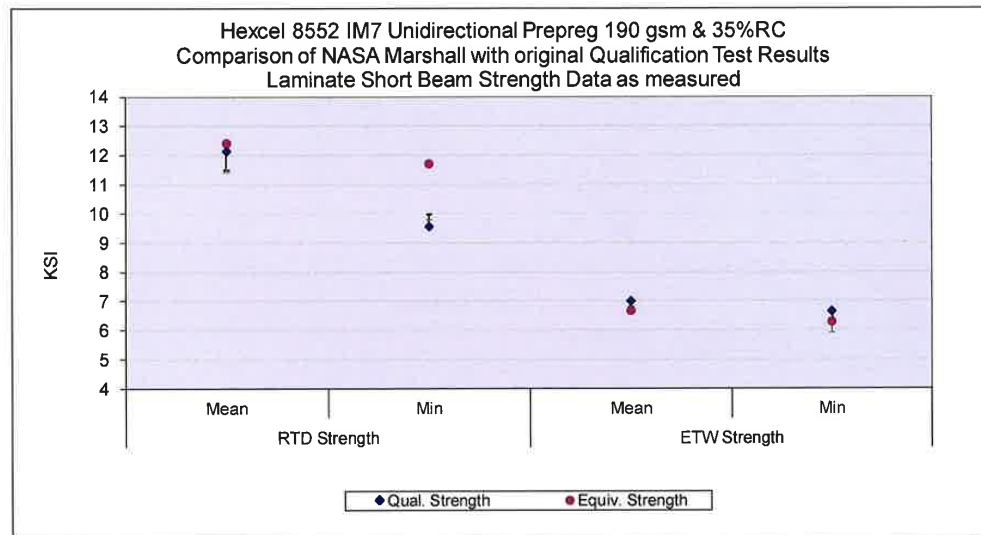


Figure 3-6 Laminate Short-Beam Strength means, minimums and Equivalence limits for NASA Marshall

3.7 “25/50/25” Unnotched Compression 1 (UNC1) for NASA Glenn Baseline

The UNC1 normalized data passed equivalency tests for strength and CTD modulus. The ETW Modulus failed the equivalency test. The modified CV method could not be used with the strength properties due to the qualification CV of both tested conditions being greater than 8%. Statistics and analysis results are shown for the strength data in Table 3-7 and for the modulus data in Table 3-8.

Unnotched Compression (UNC1) Strength	RTD		ETW	
	Qual.	Equiv.	Qual.	Equiv.
Data normalized with CPT 0.0072	Insufficient Data		Insufficient Data	
Mean Strength (ksi)	87.045	94.483	57.675	60.488
Standard Deviation	8.111	7.341	6.355	7.683
Coefficient of Variation %	9.318	7.769	11.019	12.702
Minimum	68.065	84.038	48.716	54.063
Maximum	97.037	100.706	72.226	69.852
Number of Specimens	16	4	30	4
RESULTS	PASS		PASS	
Minimum Acceptable Equiv. Sample Mean	79.351		51.647	
Minimum Acceptable Equiv. Sample Min	67.239		42.155	

Table 3-16 Unnotched Compression 1 Results for (NASA Glenn Baseline)

Unnotched Compression (UNC1) Modulus	RTD		ETW	
	Qual.	Equiv.	Qual.	Equiv.
Data normalized with CPT 0.0072				
Mean Modulus (Msi)	7.857	7.955	7.126	7.806
Standard Deviation	0.373	0.360	0.128	0.123
Coefficient of Variation %	4.749	4.526	1.801	1.582
Minimum	6.890	7.445	6.852	7.621
Maximum	8.407	8.274	7.344	7.878
Number of Specimens	16	4	16	4
RESULTS	PASS		FAIL	
Passing Range for Modulus Mean	7.421 to 8.293		6.977 to 7.276	
Student's t-statistic	0.473		9.528	
p-value of Student's t-statistic	0.642		1.87E-08	
MOD CV RESULTS	PASS with MOD CV		FAIL	
Modified CV%	6.37		6.00	
Passing Range for Modulus Mean	7.293 to 8.421		6.664 to 7.589	
Modified CV Student's t-statistic	0.365		3.088	
p-value of Student's t-statistic	0.719		0.006	

Table 3-17 Unnotched Compression 1 Modulus Results for (NASA Glenn Baseline)

The UNC1 modulus data for the ETW environment failed equivalence due to the sample mean being too high. The equivalency sample mean (7.806) is 107.28% of the maximum acceptable mean value (7.276). Under the assumption of the modified CV method, the equivalency sample mean is 102.85% of the highest acceptable mean value (7.589).

Figure 3-1 illustrates the UNC1 strength means and minimum values and the modulus means for the qualification sample and the equivalency sample. The limits for equivalency samples are shown as error bars with the qualification data. The longer, lighter colored error bars are for the modified CV computations.

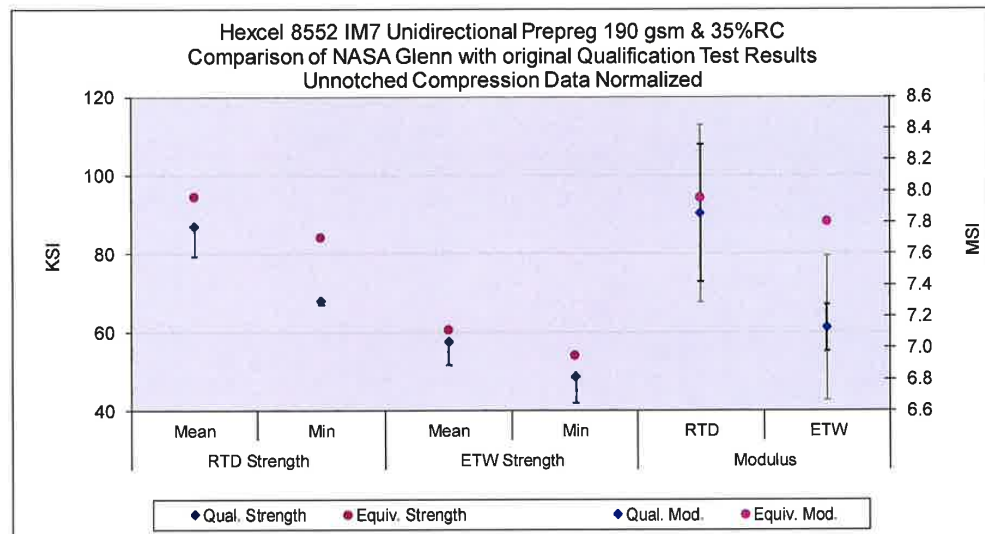


Figure 3-7 UNC1 means, minimums and Equivalence limits for NASA Glenn Baseline

3.8 “25/50/25” Unnotched Compression 1 (UNC1) for NASA Glenn Low Vacuum Panel

The UNC1 normalized data passed equivalency tests for strength. The ETW Modulus failed the equivalency test. The modified CV method could not be used with the strength properties due to the qualification CV of both tested conditions being greater than 8%. Statistics and analysis results are shown for the strength data in Table 3-7 and for the modulus data in Table 3-8.

Unnotched Compression (UNC1) Strength	RTD		ETW	
	Qual.	Equiv.	Qual.	Equiv.
Data normalized with CPT 0.0072	Insufficient Data		Insufficient Data	
Mean Strength (ksi)	87.045	87.860	57.675	54.486
Standard Deviation	8.111	4.972	6.355	5.895
Coefficient of Variation %	9.318	5.659	11.019	10.820
Minimum	68.065	80.740	48.716	48.189
Maximum	97.037	92.323	72.226	61.040
Number of Specimens	16	4	30	5
RESULTS	PASS		PASS	
Minimum Acceptable Equiv. Sample Mean	79.351		52.257	
Minimum Acceptable Equiv. Sample Min	67.239		41.605	

Table 3-18 Unnotched Compression 1 Results for (NASA Glenn Low Vacuum)

Unnotched Compression (UNC1) Modulus	RTD		ETW	
	Qual.	Equiv.	Qual.	Equiv.
Data normalized with CPT 0.0072				
Mean Modulus (Msi)	7.857	7.748	7.126	7.558
Standard Deviation	0.373	0.117	0.128	0.138
Coefficient of Variation %	4.749	1.504	1.801	1.825
Minimum	6.890	7.635	6.852	7.359
Maximum	8.407	7.904	7.344	7.668
Number of Specimens	16	4	16	4
RESULTS	PASS		FAIL	
Passing Range for Modulus Mean	7.453 to 8.261		6.974 to 7.279	
Student's t-statistic	-0.567		5.938	
p-value of Student's t-statistic	0.577		0.00001	
MOD CV RESULTS	PASS with MOD CV		PASS with MOD CV	
Modified CV%	6.37		6.00	
Passing Range for Modulus Mean	7.317 to 8.397		6.663 to 7.589	
Modified CV Student's t-statistic	-0.425		1.957	
p-value of Student's t-statistic	0.676		0.066	

Table 3-19 Unnotched Compression 1 Modulus Results for (NASA Glenn Low Vacuum)

The UNC1 modulus data for the ETW environment failed equivalence due to sample mean being too high. The equivalency sample mean (7.558) is 103.83% of the maximum acceptable mean value (7.279). Under the assumption of the modified CV method, the equivalency sample mean passed the test.

Figure 3-1 illustrates the UNC1 strength means and minimum values and the modulus means for the qualification sample and the equivalency sample. The limits for equivalency samples are shown as error bars with the qualification data. The longer, lighter colored error bars are for the modified CV computations.

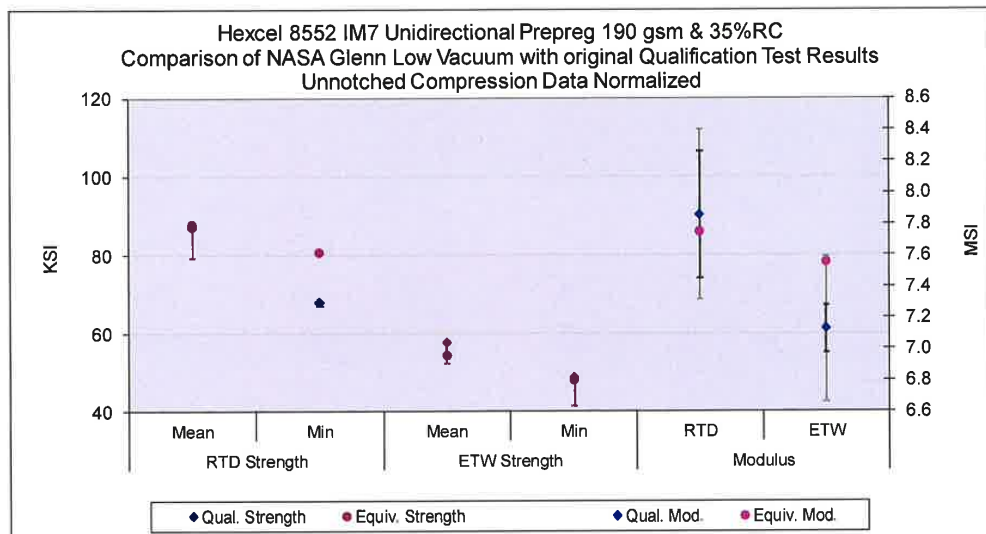


Figure 3-8 UNC1 means, minimums and Equivalence limits for NASA Glenn Low Vacuum Panels

3.9 “25/50/25” Unnotched Compression 1 (UNC1) for NASA Glenn Slow Ramp Panel

The UNC1 normalized data passed equivalency tests for strength. The ETW Modulus failed the equivalency test. The modified CV method could not be used with the strength properties due to the qualification CV of both tested conditions being greater than 8%. Statistics and analysis results are shown for the strength data in Table 3-7 and for the modulus data in Table 3-8.

Unnotched Compression (UNC1) Strength	RTD		ETW	
	Qual.	Equiv.	Qual.	Equiv.
Data normalized with CPT 0.0072	Insufficient Data		Insufficient Data	
Mean Strength (ksi)	87.045	91.234	57.675	57.568
Standard Deviation	8.111	4.600	6.355	2.703
Coefficient of Variation %	9.318	5.042	11.019	4.696
Minimum	68.065	86.020	48.716	55.077
Maximum	97.037	95.786	72.226	60.357
Number of Specimens	16	4	30	4
RESULTS	PASS		PASS	
Minimum Acceptable Equiv. Sample Mean	79.351		51.647	
Minimum Acceptable Equiv. Sample Min	67.239		42.155	

Table 3-20 Unnotched Compression 1 Results for (NASA Glenn Slow Ramp)

Unnotched Compression (UNC1) Modulus	RTD		ETW	
	Qual.	Equiv.	Qual.	Equiv.
Data normalized with CPT 0.0072				
Mean Modulus (Msi)	7.857	7.853	7.126	7.576
Standard Deviation	0.373	0.095	0.128	0.092
Coefficient of Variation %	4.749	1.214	1.801	1.215
Minimum	6.890	7.740	6.852	7.490
Maximum	8.407	7.955	7.344	7.699
Number of Specimens	16	4	16	4
RESULTS	PASS		FAIL	
Passing Range for Modulus Mean	7.454 to 8.260		6.982 to 7.271	
Student's t-statistic	-0.018		6.533	
p-value of Student's t-statistic	0.986		0.000004	
MOD CV RESULTS	PASS with MOD CV		PASS with MOD CV	
Modified CV%	6.37		6.00	
Passing Range for Modulus Mean	7.318 to 8.396		6.666 to 7.587	
Modified CV Student's t-statistic	-0.014		2.050	
p-value of Student's t-statistic	0.989		0.055	

Table 3-21 Unnotched Compression 1 Modulus Results for (NASA Glenn Slow Ramp)

The UNC1 modulus data for the ETW environment failed equivalence due to sample mean being too high. The equivalency sample mean (7.576) is 104.19% of the maximum acceptable mean value (7.271). Under the assumption of the modified CV method, the equivalency sample mean passed the test.

Figure 3-1 illustrates the UNC1 strength means and minimum values and the modulus means for the qualification sample and the equivalency sample. The limits for equivalency samples are shown as error bars with the qualification data. The longer, lighter colored error bars are for the modified CV computations.

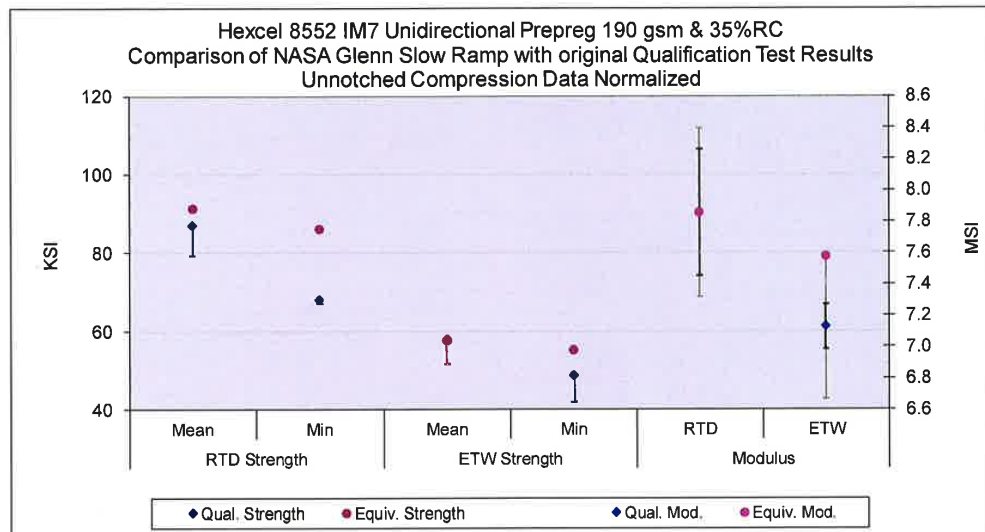


Figure 3-9 UNC1 means, minimums and Equivalence limits for NASA Glenn Slow Ramp Panels

3.10 “25/50/25” Unnotched Compression 1 (UNC1) for NASA Langley

The UNC1 normalized data passed equivalency tests for strength. The ETW Modulus failed the equivalency test. The modified CV method could not be used with the strength properties due to the qualification CV of both tested conditions being greater than 8%. Statistics and analysis results are shown for the strength data in Table 3-7 and for the modulus data in Table 3-8.

Unnotched Compression (UNC1) Strength	RTD		ETW	
	Qual.	Equiv.	Qual.	Equiv.
Data normalized with CPT 0.0072	Insufficient Data		Insufficient Data	
Mean Strength (ksi)	87.045	92.219	57.675	56.413
Standard Deviation	8.111	2.075	6.355	4.257
Coefficient of Variation %	9.318	2.250	11.019	7.546
Minimum	68.065	88.961	48.716	51.380
Maximum	97.037	94.741	72.226	63.319
Number of Specimens	16	6	30	6
RESULTS	PASS		PASS	
Minimum Acceptable Equiv. Sample Mean	80.712		52.713	
Minimum Acceptable Equiv. Sample Min	65.984		41.172	

Table 3-22 Unnotched Compression 1 Results for (NASA Langley)

Unnotched Compression (UNC1) Modulus	RTD		ETW	
	Qual.	Equiv.	Qual.	Equiv.
Data normalized with CPT 0.0072				
Mean Modulus (Msi)	7.857	7.597	7.126	7.375
Standard Deviation	0.373	0.099	0.128	0.058
Coefficient of Variation %	4.749	1.307	1.801	0.783
Minimum	6.890	7.474	6.852	7.296
Maximum	8.407	7.706	7.344	7.443
Number of Specimens	16	6	16	6
RESULTS	PASS		FAIL	
Passing Range for Modulus Mean	7.531 to 8.183		7.012 to 7.241	
Student's t-statistic	-1.661		4.528	
p-value of Student's t-statistic	0.112		0.0002	
MOD CV RESULTS	PASS with MOD CV		PASS with MOD CV	
Modified CV%	6.37		6.00	
Passing Range for Modulus Mean	7.421 to 8.293		6.755 to 7.497	
Modified CV Student's t-statistic	-1.244		1.400	
p-value of Student's t-statistic	0.228		0.177	

Table 3-23 Unnotched Compression 1 Modulus Results for (NASA Langley)

The UNC1 modulus data for the ETW environment failed equivalence due to sample mean being too high. The equivalency sample mean (7.375) is 101.85% of the maximum acceptable mean value (7.241). Under the assumption of the modified CV method, the equivalency sample mean passed the test.

Figure 3-10 illustrates the UNC1 strength means and minimum values and the modulus means for the qualification sample and the equivalency sample. The limits for equivalency samples are shown as error bars with the qualification data. The longer, lighter colored error bars are for the modified CV computations.

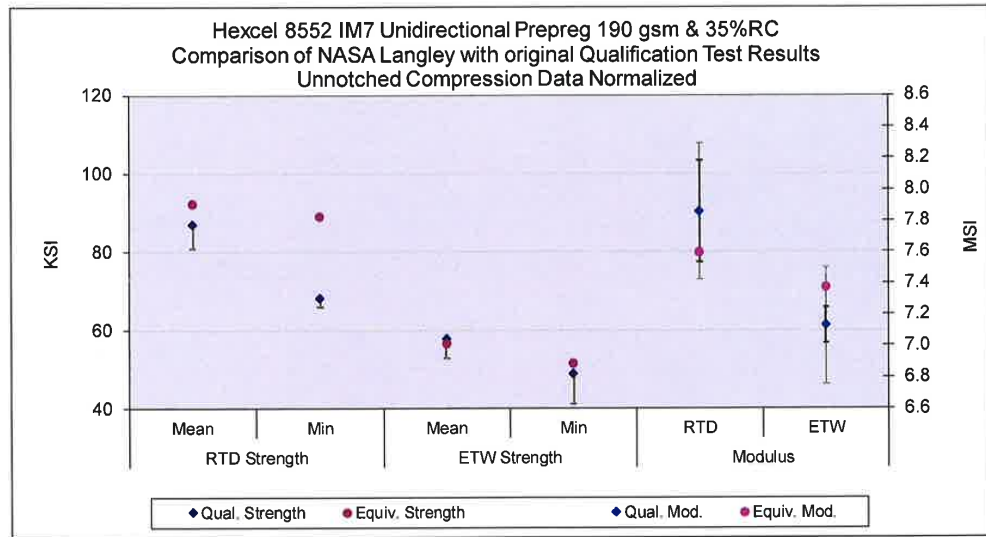


Figure 3-10 UNC1 means, minimums and Equivalence limits for NASA Langley

3.11 “25/50/25” Unnotched Compression 1 (UNC1) for NASA Marshall

The UNC1 normalized data passed equivalency tests for strength. The ETW Modulus failed the equivalency test. The modified CV method could not be used with the strength properties due to the qualification CV of both tested conditions being greater than 8%. Statistics and analysis results are shown for the strength data in Table 3-7 and for the modulus data in Table 3-8.

Unnotched Compression (UNC1) Strength	RTD		ETW	
	Qual.	Equiv.	Qual.	Equiv.
Data normalized with CPT 0.0072	Insufficient Data		Insufficient Data	
Mean Strength (ksi)	87.045	94.951	57.675	60.336
Standard Deviation	8.111	3.160	6.355	1.674
Coefficient of Variation %	9.318	3.328	11.019	2.774
Minimum	68.065	91.952	48.716	58.131
Maximum	97.037	98.458	72.226	62.169
Number of Specimens	16	6	30	5
RESULTS	PASS		PASS	
Minimum Acceptable Equiv. Sample Mean	80.712		52.257	
Minimum Acceptable Equiv. Sample Min	65.984		41.605	

Table 3-24 Unnotched Compression 1 Results for (NASA Marshall)

Unnotched Compression (UNC1) Modulus	RTD		ETW	
	Qual.	Equiv.	Qual.	Equiv.
Data normalized with CPT 0.0072	Insufficient Data		Insufficient Data	
Mean Modulus (Msi)	7.857	7.662	7.126	7.464
Standard Deviation	0.373	0.035	0.128	0.090
Coefficient of Variation %	4.749	0.451	1.801	1.206
Minimum	6.890	7.636	6.852	7.353
Maximum	8.407	7.714	7.344	7.578
Number of Specimens	16	6	16	5
RESULTS	PASS		FAIL	
Passing Range for Modulus Mean	7.534 to 8.180		6.996 to 7.256	
Student's t-statistic	-1.256		5.429	
p-value of Student's t-statistic	0.223		0.00003	
MOD CV RESULTS	PASS with MOD CV		PASS with MOD CV	
Modified CV%	6.37		6.00	
Passing Range for Modulus Mean	7.424 to 8.290		6.717 to 7.536	
Modified CV Student's t-statistic	-0.937		1.723	
p-value of Student's t-statistic	0.360		0.101	

Table 3-25 Unnotched Compression 1 Modulus Results for (NASA Marshall)

The UNC1 modulus data for the ETW environment failed equivalence due to sample mean being too high. The equivalency sample mean (7.464) is 102.86% of the maximum acceptable mean value (7.256). Under the assumption of the modified CV method, the equivalency sample mean passed the test.

Figure 3-1 illustrates the UNC1 strength means and minimum values and the modulus means for the qualification sample and the equivalency sample. The limits for equivalency samples are shown as error bars with the qualification data. The longer, lighter colored error bars are for the modified CV computations.

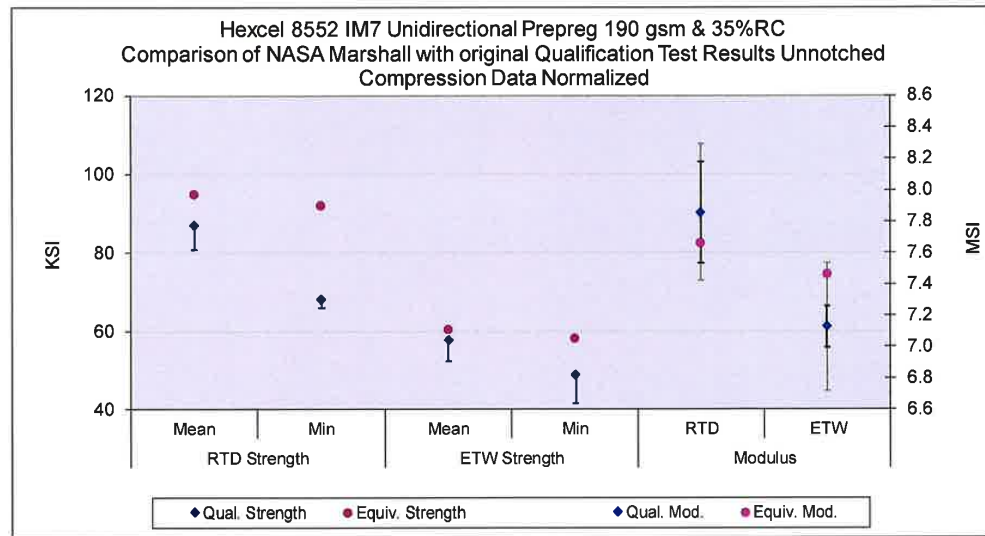


Figure 3-11 UNC1 means, minimums and Equivalence limits for NASA Marshall

3.12 “25/50/25” Unnotched Tension 1 (UNT1) for NASA Glenn

The UNT1 normalized data passed equivalency tests for both strength and modulus. Statistics and analysis results are shown for the strength data in Table 3-7 and for the modulus data in Table 3-8.

Unnotched Tension (UNT1) Strength	CTD		RTD		ETW	
	Qual.	Equiv.	Qual.	Equiv.	Qual.	Equiv.
Data normalized with CPT 0.0072						
Mean Strength (ksi)	99.348	109.862	104.685	105.314	112.461	108.359
Standard Deviation	3.442	3.298	7.276	7.065	5.606	3.250
Coefficient of Variation %	3.464	3.002	6.950	6.708	4.985	2.999
Minimum	91.601	104.504	89.563	92.133	101.642	103.102
Maximum	105.840	113.498	113.712	109.828	119.290	111.969
Number of Specimens	16	6	16	6	16	6
RESULTS	PASS		PASS		PASS	
Minimum Acceptable Equiv. Sample Mean	96.660		99.004		108.084	
Minimum Acceptable Equiv. Sample Min	90.411		85.792		97.904	
MOD CV RESULTS	PASS with MOD CV		PASS with MOD CV		PASS with MOD CV	
Modified CV %	6.00		7.48		6.49	
Minimum Acceptable Equiv. Sample Mean	94.693		98.575		106.760	
Minimum Acceptable Equiv. Sample Min	83.869		84.365		93.501	

Table 3-26 Unnotched Tension 1 Results for (NASA Glenn)

Unnotched Tension (UNT1) Modulus	CTD		RTD		ETW	
	Qual.	Equiv.	Qual.	Equiv.	Qual.	Equiv.
Data normalized with CPT 0.0072						
Mean Modulus (Msi)	8.353	8.178	8.390	7.923	7.988	7.976
Standard Deviation	0.309	0.114	0.480	0.455	0.412	0.083
Coefficient of Variation %	3.696	1.398	5.727	5.743	5.162	1.038
Minimum	7.295	8.013	7.277	7.049	7.069	7.836
Maximum	8.745	8.362	8.984	8.394	8.514	8.049
Number of Specimens	16	6	16	6	17	6
RESULTS	PASS		PASS		PASS	
Passing Range for Modulus Mean	8.080 to 8.626		7.917 to 8.864		7.630 to 8.346	
Student's t-statistic	-1.341		-2.060		-0.072	
p-value of Student's t-statistic	0.195		0.053		0.943	
MOD CV RESULTS	PASS with MOD CV		PASS with MOD CV		PASS with MOD CV	
Modified CV%	6.00		6.86		6.58	
Passing Range for Modulus Mean	7.916 to 8.791		7.843 to 8.938		7.533 to 8.443	
Modified CV Student's t-statistic	-0.838		-1.782		-0.057	
p-value of Student's t-statistic	0.412		0.090		0.955	

Table 3-27 Unnotched Tension 1 Modulus Results for (NASA Glenn)

Figure 3-1 illustrates the UNT1 strength means and minimum values and the modulus means for the qualification sample and the equivalency sample. The limits for equivalency samples are shown as error bars with the qualification data. The longer, lighter colored error bars are for the modified CV computations.

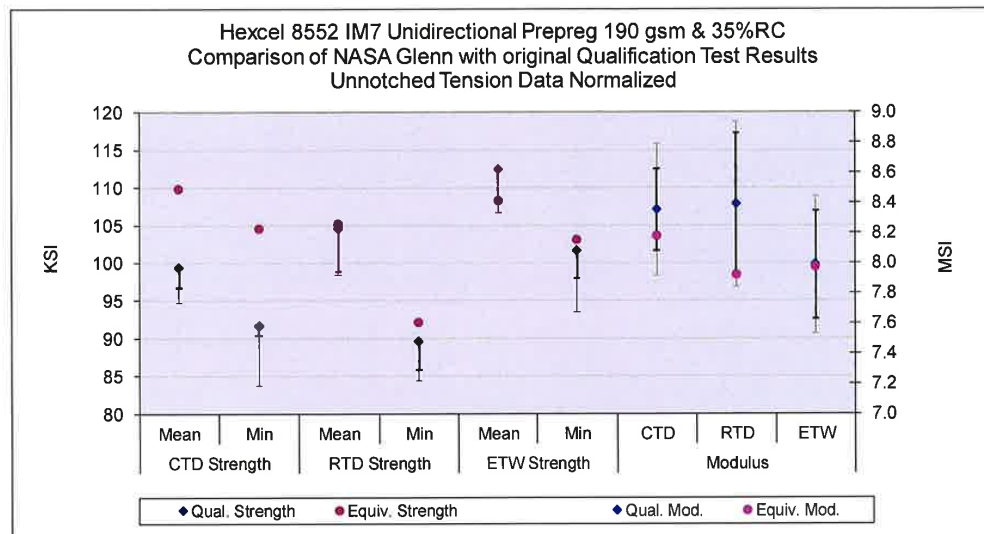


Figure 3-12 UNT1 means, minimums and Equivalence limits for NASA Glenn

3.13 “25/50/25” Unnotched Tension 1 (UNT1) for NASA Langley

The UNT1 normalized data passed equivalency tests for both strength and modulus. Statistics and analysis results are shown for the strength data in Table 3-7 and for the modulus data in Table 3-8.

Unnotched Tension (UNT1) Strength	CTD		RTD		ETW	
	Qual.	Equiv.	Qual.	Equiv.	Qual.	Equiv.
Data normalized with CPT 0.0072						
Mean Strength (ksi)	99.348	107.068	104.685	108.002	112.461	116.139
Standard Deviation	3.442	1.502	7.276	1.534	5.606	2.748
Coefficient of Variation %	3.464	1.403	6.950	1.420	4.985	2.366
Minimum	91.601	105.336	89.563	105.873	101.642	112.493
Maximum	105.840	108.892	113.712	109.469	119.290	120.027
Number of Specimens	16	6	16	6	16	6
RESULTS	PASS		PASS		PASS	
Minimum Acceptable Equiv. Sample Mean	96.660		99.004		108.084	
Minimum Acceptable Equiv. Sample Min	90.411		85.792		97.904	
MOD CV RESULTS	PASS with MOD CV		PASS with MOD CV		PASS with MOD CV	
Modified CV %	6.00		7.48		6.49	
Minimum Acceptable Equiv. Sample Mean	94.693		98.575		106.760	
Minimum Acceptable Equiv. Sample Min	83.869		84.365		93.501	

Table 3-28 Unnotched Tension 1 Results for (NASA Langley)

Unnotched Tension (UNT1) Modulus	CTD		RTD		ETW	
	Qual.	Equiv.	Qual.	Equiv.	Qual.	Equiv.
Data normalized with CPT 0.0072						
Mean Modulus (Msi)	8.353	8.414	8.390	8.186	7.988	8.024
Standard Deviation	0.309	0.110	0.480	0.165	0.412	0.145
Coefficient of Variation %	3.696	1.307	5.727	2.021	5.162	1.811
Minimum	7.295	8.297	7.277	8.013	7.069	7.908
Maximum	8.745	8.619	8.984	8.494	8.514	8.215
Number of Specimens	16	6	16	6	17	6
RESULTS	PASS		PASS		PASS	
Passing Range for Modulus Mean	8.081 to 8.626		7.967 to 8.814		7.626 to 8.350	
Student's t-statistic	0.464		-1.004		0.208	
p-value of Student's t-statistic	0.648		0.327		0.837	
MOD CV RESULTS	PASS with MOD CV		PASS with MOD CV		PASS with MOD CV	
Modified CV %	6.00		6.86		6.58	
Passing Range for Modulus Mean	7.917 to 8.790		7.885 to 8.895		7.530 to 8.447	
Modified CV Student's t-statistic	0.289		-0.842		0.164	
p-value of Student's t-statistic	0.775		0.410		0.871	

Table 3-29 Unnotched Tension 1 Modulus Results for (NASA Langley)

Figure 3-1 illustrates the UNT1 strength means and minimum values and the modulus means for the qualification sample and the equivalency sample. The limits for equivalency samples are shown as error bars with the qualification data. The longer, lighter colored error bars are for the modified CV computations.

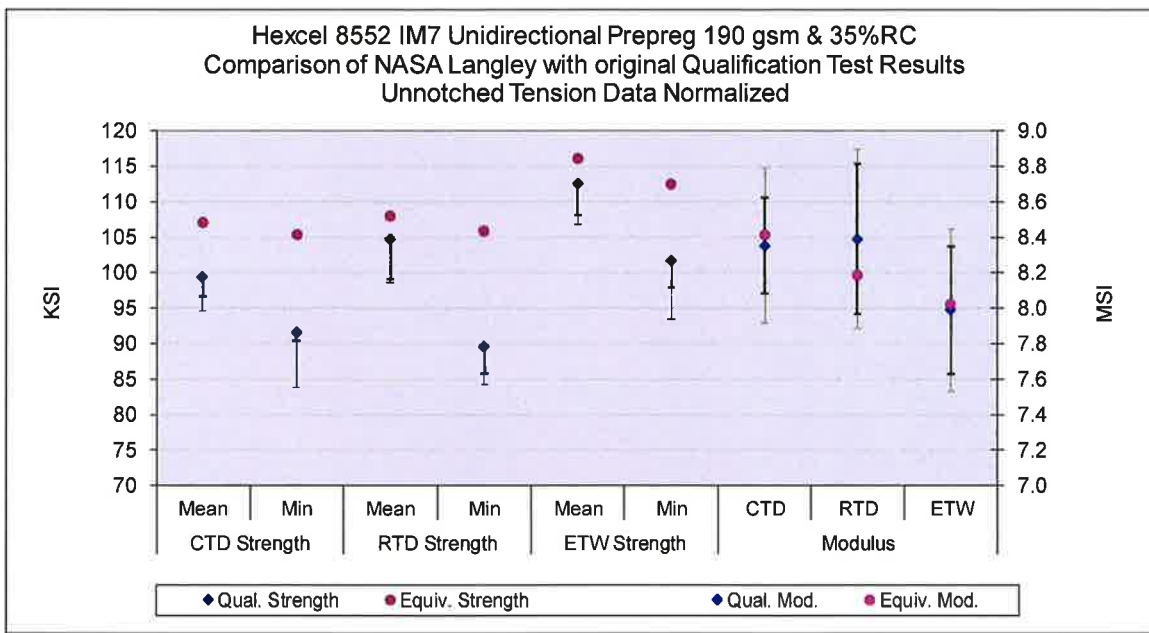


Figure 3-13 UNT1 means, minimums and Equivalence limits for NASA Langley

3.14 “25/50/25” Unnotched Tension 1 (UNT1) for NASA Marshall

The UNT1 normalized data passed equivalency tests for both strength and modulus. Statistics and analysis results are shown for the strength data in Table 3-28 and for the modulus data in Table 3-29.

Unnotched Tension (UNT1) Strength	CTD		RTD		ETW	
	Qual.	Equiv.	Qual.	Equiv.	Qual.	Equiv.
Data normalized with CPT 0.0072						
Mean Strength (ksi)	99.348	109.487	104.685	107.372	112.461	110.903
Standard Deviation	3.442	1.747	7.276	1.647	5.606	2.785
Coefficient of Variation %	3.464	1.595	6.950	1.534	4.985	2.511
Minimum	91.601	107.820	89.563	105.416	101.642	107.472
Maximum	105.840	112.351	113.712	109.930	119.290	114.983
Number of Specimens	16	6	16	6	16	6
RESULTS	PASS		PASS		PASS	
Minimum Acceptable Equiv. Sample Mean	96.660		99.004		108.084	
Minimum Acceptable Equiv. Sample Min	90.411		85.792		97.904	
MOD CV RESULTS	PASS with MOD CV		PASS with MOD CV		PASS with MOD CV	
Modified CV %	6.00		7.48		6.49	
Minimum Acceptable Equiv. Sample Mean	94.693		98.575		106.760	
Minimum Acceptable Equiv. Sample Min	83.869		84.365		93.501	

Table 3-30 Unnotched Tension 1 Results for (NASA Marshall)

Unnotched Tension (UNT1) Modulus	CTD		RTD		ETW	
	Qual.	Equiv.	Qual.	Equiv.	Qual.	Equiv.
Data normalized with CPT 0.0072						
Mean Modulus (Msi)	8.353	8.343	8.390	8.070	7.988	7.923
Standard Deviation	0.309	0.038	0.480	0.101	0.412	0.130
Coefficient of Variation %	3.696	0.455	5.727	1.249	5.162	1.641
Minimum	7.295	8.310	7.277	7.964	7.069	7.809
Maximum	8.745	8.414	8.984	8.223	8.514	8.155
Number of Specimens	16	6	16	6	17	6
RESULTS	PASS		PASS		PASS	
Passing Range for Modulus Mean	8.086 to 8.621		7.972 to 8.809		7.627 to 8.349	
Student's t-statistic	-0.084		-1.598		-0.374	
p-value of Student's t-statistic	0.934		0.126		0.712	
MOD CV RESULTS	PASS with MOD CV		PASS with MOD CV		PASS with MOD CV	
Modified CV%	6.00		6.86		6.58	
Passing Range for Modulus Mean	7.920 to 8.787		7.890 to 8.891		7.531 to 8.446	
Modified CV Student's t-statistic	-0.052		-1.336		-0.295	
p-value of Student's t-statistic	0.959		0.197		0.771	

Table 3-31 Unnotched Tension 1 Modulus Results for (NASA Marshall)

Figure 3-14 illustrates the UNT1 strength means and minimum values and the modulus means for the qualification sample and the equivalency sample. The limits for equivalency samples are shown as error bars with the qualification data. The longer, lighter colored error bars are for the modified CV computations.

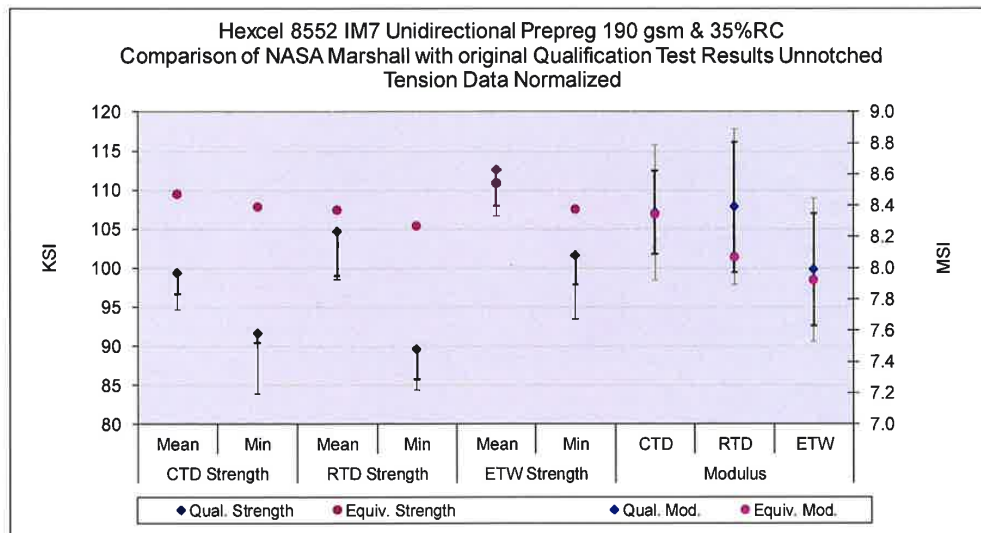


Figure 3-14 UNT1 means, minimums and Equivalence limits for NASA Marshall

3.15 “25/50/25” Open-Hole Compression 1 (OHC1) for NASA Glenn

The Open-Hole Compression normalized strength data failed equivalency tests for both RTD and ETW conditions. Statistics and analysis results for the OHC1 strength data are shown in Table 3-30.

Open Hole Compression (OHC1) Strength	RTD		ETW	
	Qual.	Equiv.	Qual.	Equiv.
Data normalized with CPT 0.0072	Insufficient Data		Insufficient Data	
Mean Strength (ksi)	49.083	45.792	35.515	31.767
Standard Deviation	1.793	0.973	1.445	0.444
Coefficient of Variation %	3.653	2.124	4.069	1.397
Minimum	43.909	44.449	33.080	31.130
Maximum	50.993	46.741	38.956	32.157
Number of Specimens	19	4	19	4
RESULTS	FAIL		FAIL	
Minimum Acceptable Equiv. Sample Mean	47.383		34.144	
Minimum Acceptable Equiv. Sample Min	44.705		31.986	
MOD CV RESULTS	FAIL		FAIL	
Modified CV %	6.00		6.03	
Minimum Acceptable Equiv. Sample Mean	46.290		33.482	
Minimum Acceptable Equiv. Sample Min	41.892		30.282	

Table 3-32 Open-Hole Compression 1 Strength Results For NASA Glenn

The OHC1 strength data for the RTD environment failed equivalence due to both the sample mean and sample minimum being too low. The equivalency sample mean (45.792) is 96.64% of the minimum acceptable mean value (47.383). The equivalency sample minimum (44.449) is 99.43% of the lowest acceptable minimum value (44.705). Under the assumption of the modified CV method, the equivalency sample mean is 98.93% of the lowest acceptable mean value (46.29). The equivalency sample minimum passed the test.

The OHC1 strength data for the ETW environment failed equivalence due to both the sample mean and sample minimum being too low. The equivalency sample mean (31.767) is 93.04% of the minimum acceptable mean value (34.144). The equivalency sample minimum (31.130) is 97.32% of the lowest acceptable minimum value (31.986). Under the assumption of the modified CV method, the equivalency sample mean is 94.88% of the lowest acceptable mean value (33.482). The equivalency sample minimum passed the test.

Figure 3-15 illustrates the Open-Hole Compression strength means and minimum values for the qualification sample and the equivalency sample. The limits for equivalency samples are shown as error bars with the qualification data. The longer, lighter colored error bars are for the modified CV computations.

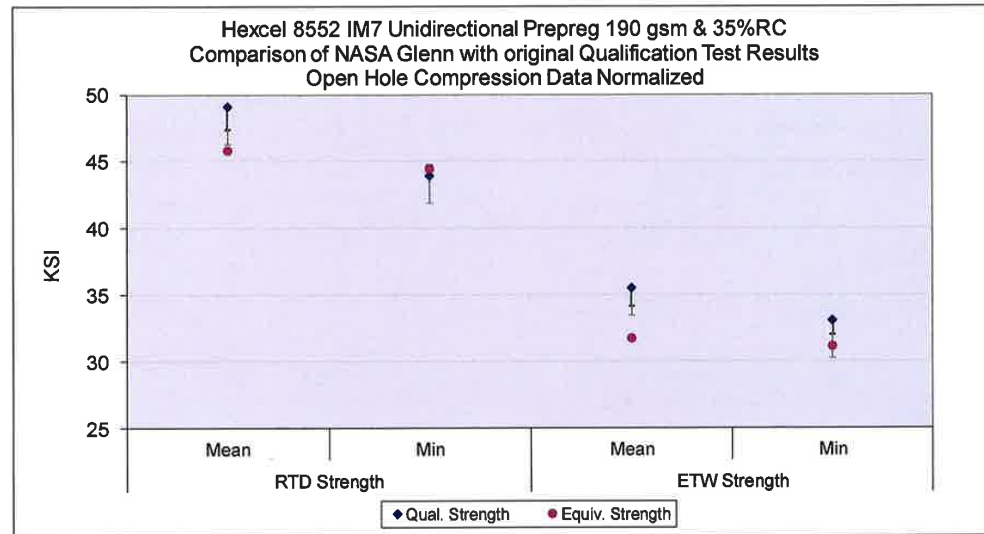


Figure 3-15 Open-Hole Compression 1 means, minimums and Equivalence limits for NASA Glenn

3.16 “25/50/25” Open-Hole Compression 1 (OHC1) for NASA Glenn Low Vacuum Panel

The Open-Hole Compression normalized strength data pass equivalency tests for RTD. But failed equivalency test for ETW condition. Statistics and analysis results for the OHC1 strength data are shown in Table 3-31.

Open Hole Compression (OHC1) Strength	RTD		ETW	
	Qual.	Equiv.	Qual.	Equiv.
Data normalized with CPT 0.0072	Insufficient Data		Insufficient Data	
Mean Strength (ksi)	49.083	47.416	35.515	32.678
Standard Deviation	1.793	1.575	1.445	1.193
Coefficient of Variation %	3.653	3.321	4.069	3.651
Minimum	43.909	45.880	33.080	31.078
Maximum	50.993	49.600	38.956	33.922
Number of Specimens	19	4	19	4
RESULTS	PASS		FAIL	
Minimum Acceptable Equiv. Sample Mean	47.383		34.144	
Minimum Acceptable Equiv. Sample Min	44.705		31.986	
MOD CV RESULTS	PASS with MOD CV		FAIL	
Modified CV %	6.00		6.03	
Minimum Acceptable Equiv. Sample Mean	46.290		33.482	
Minimum Acceptable Equiv. Sample Min	41.892		30.282	

Table 3-33 Open-Hole Compression 1 Strength Results For NASA Glenn Low Vacuum

The OHC strength data for the ETW environment failed equivalence due to both the sample mean and sample minimum being too low. The equivalency sample mean (32.678) is 95.71% of the minimum acceptable mean value (34.144). The equivalency sample minimum (31.078) is 97.16% of the lowest acceptable minimum value (31.986). Under the assumption of the modified CV method, the equivalency sample mean is 97.60% of the lowest acceptable mean value (33.482). The equivalency sample minimum passed the test.

Figure 3-16 illustrates the Open-Hole Compression strength means and minimum values for the qualification sample and the equivalency sample. The limits for equivalency samples are shown as error bars with the qualification data. The longer, lighter colored error bars are for the modified CV computations.

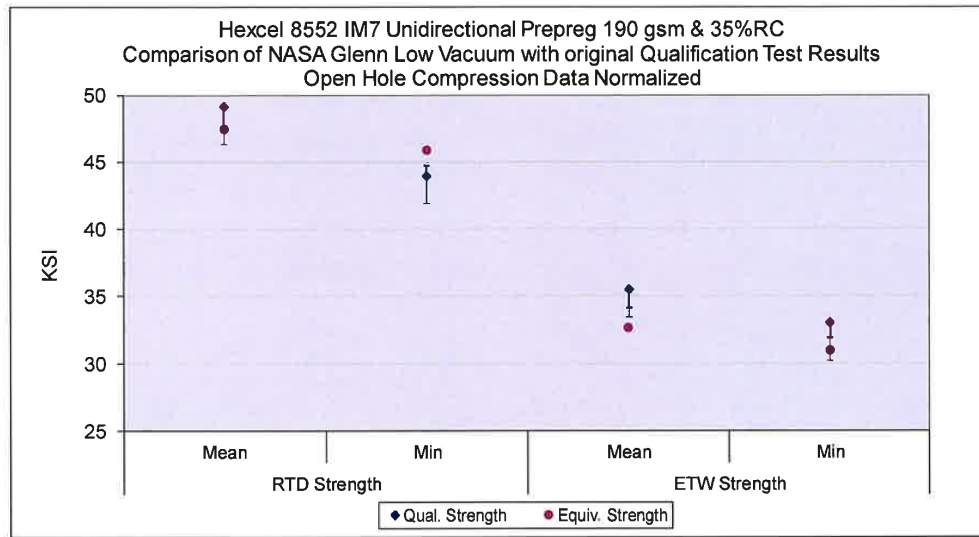


Figure 3-16 Open-Hole Compression 1 means, minimums and Equivalence limits for NASA Glenn Low Vacuum Panel

3.17 “25/50/25” Open-Hole Compression 1 (OHC1) for NASA Glenn Slow Ramp Panel

The Open-Hole Compression normalized strength data pass equivalency tests for ETW. But failed equivalency test for RTD condition. Statistics and analysis results for the OHC1 strength data are shown in Table 3-32.

Open Hole Compression (OHC1) Strength	RTD		ETW	
	Qual.	Equiv.	Qual.	Equiv.
Data normalized with CPT 0.0072	Insufficient Data		Insufficient Data	
Mean Strength (ksi)	49.083	46.011	35.515	34.148
Standard Deviation	1.793	1.461	1.445	1.626
Coefficient of Variation %	3.653	3.175	4.069	4.760
Minimum	43.909	44.425	33.080	32.183
Maximum	50.993	47.398	38.956	36.097
Number of Specimens	19	4	19	4
RESULTS	FAIL		PASS	
Minimum Acceptable Equiv. Sample Mean	47.383		34.144	
Minimum Acceptable Equiv. Sample Min	44.705		31.986	
MOD CV RESULTS	FAIL		PASS with MOD CV	
Modified CV %	6.00		6.03	
Minimum Acceptable Equiv. Sample Mean	46.290		33.482	
Minimum Acceptable Equiv. Sample Min	41.892		30.282	

Table 3-34 Open-Hole Compression 1 Strength Results For NASA Glenn Slow Ramp

The OHC strength data for the ETW environment failed equivalence due to both the sample mean and sample minimum being too low. The equivalency sample mean (46.011) is 97.10% of the minimum acceptable mean value (47.383). The equivalency sample minimum (44.425) is 99.37% of the lowest acceptable minimum value (44.705). Under the assumption of the modified CV method, the equivalency sample mean is 99.40% of the lowest acceptable mean value (46.290). The equivalency sample minimum passed the test.

Figure 3-17 illustrates the Open-Hole Compression strength means and minimum values for the qualification sample and the equivalency sample. The limits for equivalency samples are shown as error bars with the qualification data. The longer, lighter colored error bars are for the modified CV computations.

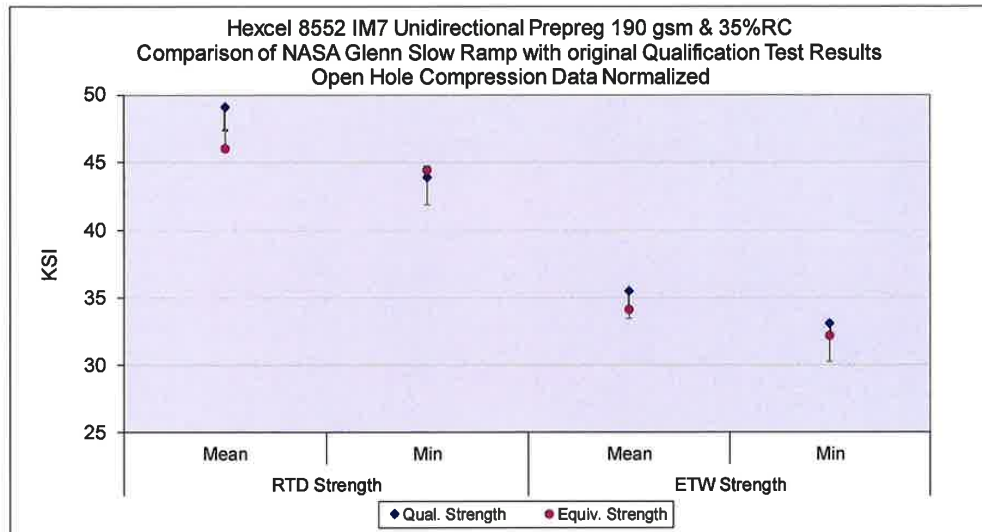


Figure 3-17 Open-Hole Compression 1 means, minimums and Equivalence limits for NASA Glenn Slow Ramp Panel

3.18 “25/50/25” Open-Hole Compression 1 (OHC1) for NASA Langley

The Open-Hole Compression normalized strength data failed equivalency tests for both RTD and ETW conditions. However the RTD data passed with the use of modified coefficient of variation approach. The Statistics and analysis results for the OHC1 strength data are shown in Table 3-33.

Open Hole Compression (OHC1) Strength	RTD		ETW	
	Qual.	Equiv.	Qual.	Equiv.
Data normalized with CPT 0.0072	Insufficient Data		Insufficient Data	
Mean Strength (ksi)	49.083	47.082	35.515	32.214
Standard Deviation	1.793	1.379	1.445	0.766
Coefficient of Variation %	3.653	2.928	4.069	2.377
Minimum	43.909	46.004	33.080	31.638
Maximum	50.993	49.699	38.956	33.633
Number of Specimens	19	6	19	6
RESULTS	FAIL		FAIL	
Minimum Acceptable Equiv. Sample Mean	47.683		34.387	
Minimum Acceptable Equiv. Sample Min	44.428		31.763	
MOD CV RESULTS	PASS with MOD CV		FAIL	
Modified CV %	6.00		6.03	
Minimum Acceptable Equiv. Sample Mean	46.784		33.842	
Minimum Acceptable Equiv. Sample Min	41.436		29.950	

Table 3-35 Open-Hole Tension 1 Strength Results For NASA Langley

The OHC strength data for the RTD environment failed equivalence due to sample mean being too low. The equivalency sample mean (47.082) is 98.74% of the minimum acceptable mean value (47.683). Under the assumption of the modified CV method, the equivalency sample mean passed the test.

The OHC strength data for the ETW environment failed equivalence due to both the sample mean and sample minimum being too low. The equivalency sample mean (32.214) is 93.68% of the minimum acceptable mean value (34.387). The equivalency sample minimum (31.638) is 99.61% of the lowest acceptable minimum value (31.763). Under the assumption of the modified CV method, the equivalency sample mean is 95.19% of the lowest acceptable mean value (33.842). The equivalency sample minimum passed the test.

Figure 3-18 illustrates the Open-Hole Compression strength means and minimum values for the qualification sample and the equivalency sample. The limits for equivalency samples are shown as error bars with the qualification data. The longer, lighter colored error bars are for the modified CV computations.

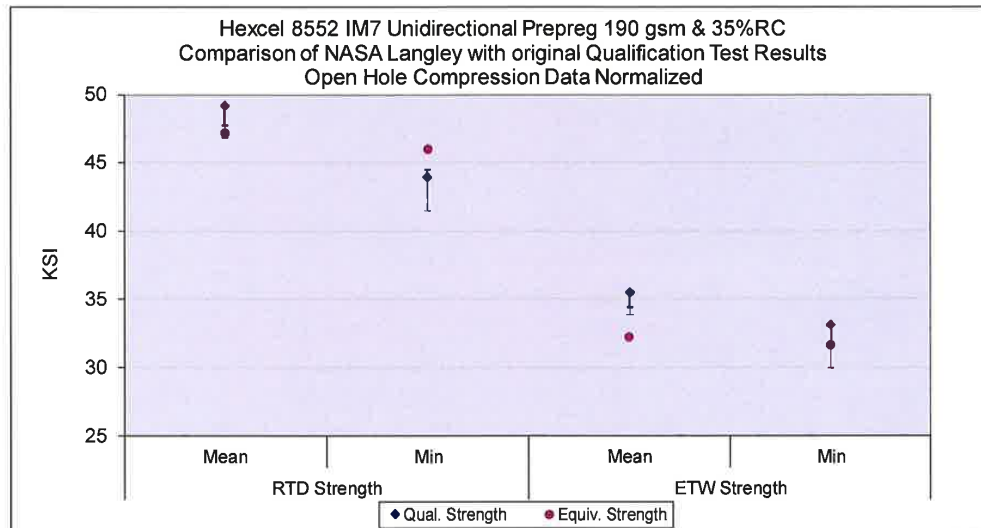


Figure 3-18 Open-Hole Compression 1 means, minimums and Equivalence limits for NASA Langley

3.19 “25/50/25” Open-Hole Compression 1 (OHC1) for NASA Marshall

The Open-Hole Compression normalized strength data failed equivalency tests for the both RTD and ETW conditions. The Statistics and analysis results for the OHC1 strength data are shown in Table 3-34.

Open Hole Compression (OHC1) Strength	RTD		ETW	
	Qual.	Equiv.	Qual.	Equiv.
Data normalized with CPT 0.0072	Insufficient Data		Insufficient Data	
Mean Strength (ksi)	49.083	47.503	35.515	33.186
Standard Deviation	1.793	1.193	1.445	0.910
Coefficient of Variation %	3.653	2.512	4.069	2.743
Minimum	43.909	45.898	33.080	31.785
Maximum	50.993	49.343	38.956	34.367
Number of Specimens	19	6	19	6
RESULTS	FAIL		FAIL	
Minimum Acceptable Equiv. Sample Mean	47.683		34.387	
Minimum Acceptable Equiv. Sample Min	44.428		31.763	
MOD CV RESULTS	PASS with MOD CV		FAIL	
Modified CV %	6.00		6.03	
Minimum Acceptable Equiv. Sample Mean	46.784		33.842	
Minimum Acceptable Equiv. Sample Min	41.436		29.950	

Table 3-36 Open-Hole Tension 1 Strength Results For NASA Marshall

The OHC strength data for the RTD environment failed equivalence due to sample mean being too low. The equivalency sample mean (47.503) is 99.62% of the minimum acceptable mean value (47.683). Under the assumption of the modified CV method, the equivalency sample mean passed the test.

The OHC strength data for the ETW environment failed equivalence due to sample mean being too low. The equivalency sample mean (33.186) is 96.51% of the minimum acceptable mean value (34.387). Under the assumption of the modified CV method, the equivalency sample mean is 98.06% of the lowest acceptable mean value (33.842).

Figure 3-19 illustrates the Open-Hole Compression strength means and minimum values for the qualification sample and the equivalency sample. The limits for equivalency samples are shown as error bars with the qualification data. The longer, lighter colored error bars are for the modified CV computations.

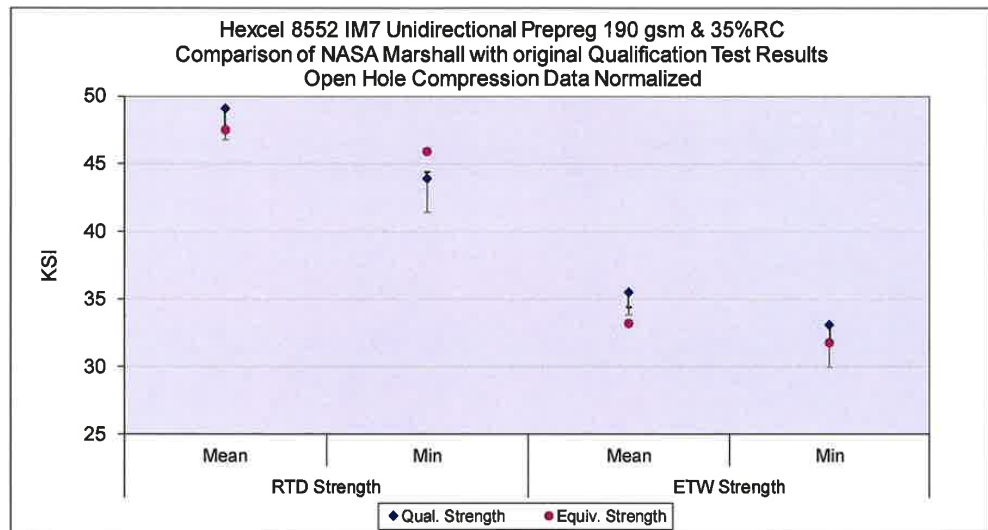


Figure 3-19 Open-Hole Compression 1 means, minimums and Equivalence limits for NASA Marshall

3.20 “25/50/25” Open-Hole Tension 1 (OHT1) for NASA Glenn

The Open-Hole Tension normalized strength data passed equivalency tests for all test conditions. Statistics and analysis results for the OHT1 strength data are shown in Table 3-35.

Open Hole Tension (OHT1) Strength	CTD		RTD		ETW	
	Qual.	Equiv.	Qual.	Equiv.	Qual.	Equiv.
Data normalized with CPT 0.0072	Insufficient Data		Insufficient Data		Insufficient Data	
Mean Strength (ksi)	57.754	64.584	59.003	65.988	66.966	69.241
Standard Deviation	2.433	1.471	2.350	1.846	2.850	4.799
Coefficient of Variation %	4.213	2.277	3.982	2.798	4.255	6.931
Minimum	53.645	63.046	54.120	62.985	62.154	63.279
Maximum	62.524	66.763	64.610	68.375	72.587	76.500
Number of Specimens	19	6	19	6	20	6
RESULTS	PASS		PASS		PASS	
Minimum Acceptable Equiv. Sample Mean	55.855		57.169		64.742	
Minimum Acceptable Equiv. Sample Min	51.436		52.902		59.567	
MOD CV RESULTS	PASS with MOD CV		PASS with MOD CV		PASS with MOD CV	
Modified CV %	6.11		6.00		6.13	
Minimum Acceptable Equiv. Sample Mean	55.001		56.239		63.763	
Minimum Acceptable Equiv. Sample Min	48.597		49.811		56.311	

Table 3-37 Open-Hole Tension 1 Strength Results for NASA Glenn

Figure 3-20 illustrates the Open-Hole Tension strength means and minimum values for the qualification sample and the equivalency sample. The limits for equivalency samples are shown as error bars with the qualification data. The longer, lighter colored error bars are for the modified CV computations.

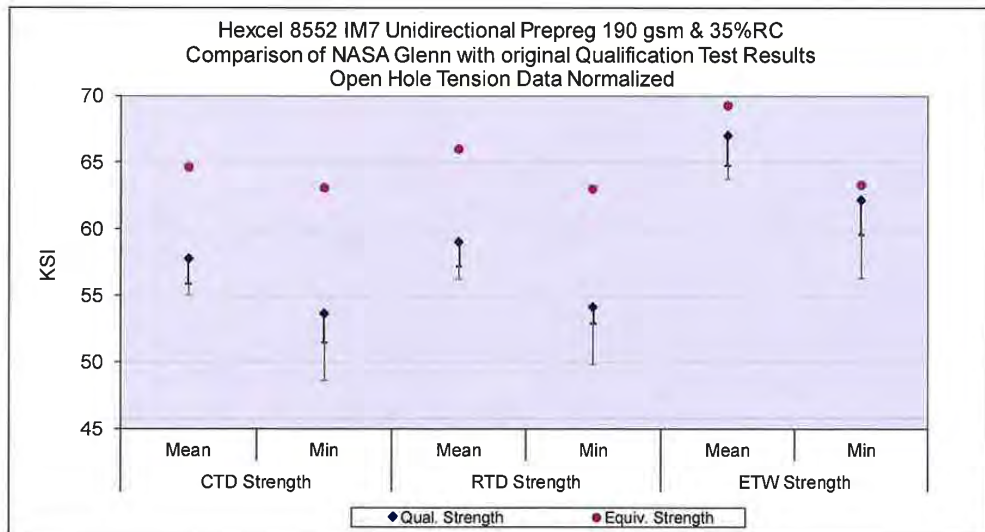


Figure 3-20 Open-Hole Tension 1 means, minimums and Equivalence limits for NASA Glenn

3.21 “25/50/25” Open-Hole Tension 1 (OHT1) for NASA Langley

The Open-Hole Tension normalized strength data passed equivalency tests for all test conditions. Statistics and analysis results for the OHT1 strength data are shown in Table 3-36.

Open Hole Tension (OHT1) Strength	CTD		RTD		ETW	
	Qual.	Equiv.	Qual.	Equiv.	Qual.	Equiv.
Data normalized with CPT 0.0072						
Mean Strength (ksi)	57.754	63.564	59.003	62.410	66.966	68.990
Standard Deviation	2.433	1.756	2.350	1.117	2.850	1.680
Coefficient of Variation %	4.213	2.763	3.982	1.789	4.255	2.436
Minimum	53.645	61.618	54.120	61.142	62.154	66.791
Maximum	62.524	66.570	64.610	63.946	72.587	70.669
Number of Specimens	19	6	19	6	20	6
RESULTS						
Minimum Acceptable Equiv. Sample Mean	PASS		PASS		PASS	
Minimum Acceptable Equiv. Sample Min	55.855		57.169		64.742	
MOD CV RESULTS						
Modified CV %	PASS with MOD CV		PASS with MOD CV		PASS with MOD CV	
Minimum Acceptable Equiv. Sample Mean	6.11		6.00		6.13	
Minimum Acceptable Equiv. Sample Min	55.001		56.239		63.763	
Minimum Acceptable Equiv. Sample Max	48.597		49.811		56.311	

Table 3-38 Open-Hole Tension 1 Strength Results for NASA Langley

Figure 3-21 illustrates the Open-Hole Tension strength means and minimum values for the qualification sample and the equivalency sample. The limits for equivalency samples are shown as error bars with the qualification data. The longer, lighter colored error bars are for the modified CV computations.

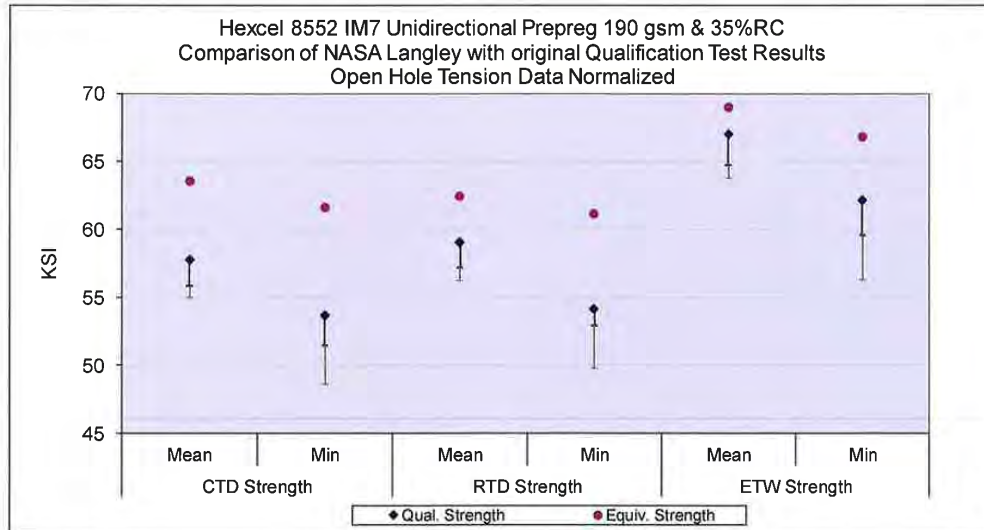


Figure 3-21 Open-Hole Tension 1 means, minimums and Equivalence limits for NASA Langley

3.22 “25/50/25” Open-Hole Tension 1 (OHT1) for NASA Marshall

The Open-Hole Tension normalized strength data passed equivalency tests for all test conditions. Statistics and analysis results for the OHT1 strength data are shown in Table 3-37.

Open Hole Tension (OHT1) Strength	CTD		RTD		ETW	
	Qual.	Equiv.	Qual.	Equiv.	Qual.	Equiv.
Data normalized with CPT 0.0072						
Mean Strength (ksi)	57.754	62.631	59.003	64.072	66.966	69.356
Standard Deviation	2.433	1.352	2.350	1.697	2.850	2.368
Coefficient of Variation %	4.213	2.159	3.982	2.649	4.255	3.414
Minimum	53.645	60.242	54.120	62.276	62.154	67.399
Maximum	62.524	64.241	64.610	66.602	72.587	73.603
Number of Specimens	19	6	19	6	20	6
RESULTS		PASS		PASS		PASS
Minimum Acceptable Equiv. Sample Mean	55.855		57.169		64.742	
Minimum Acceptable Equiv. Sample Min	51.436		52.902		59.567	
MOD CV RESULTS		PASS with MOD CV		PASS with MOD CV		PASS with MOD CV
Modified CV %	6.11		6.00		6.13	
Minimum Acceptable Equiv. Sample Mean	55.001		56.239		63.763	
Minimum Acceptable Equiv. Sample Min	48.597		49.811		56.311	

Table 3-39 Open-Hole Tension 1 Strength Results for NASA Marshall

Figure 3-22 illustrates the Open-Hole Tension strength means and minimum values for the qualification sample and the equivalency sample. The limits for equivalency samples are shown as error bars with the qualification data. The longer, lighter colored error bars are for the modified CV computations.

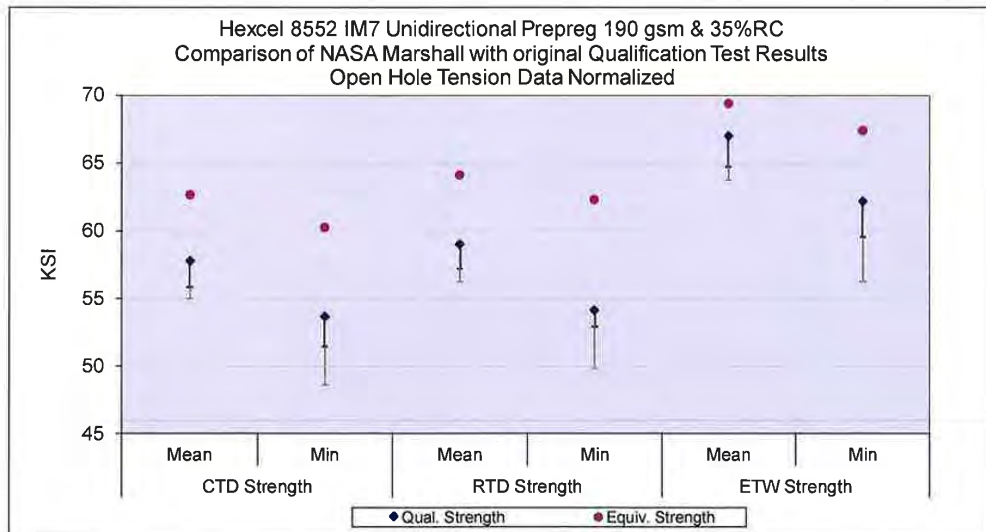


Figure 3-22 Open-Hole Tension 1 means, minimums and Equivalence limits for NASA Marshall

4. Summary of Results

All the equivalency comparisons are conducted with Type I error probability (α) of 5% in accordance with FAA/DOT/AR-03/19 report and CMH-17 Rev G section 8.4.1. It is common to obtain a few or even several failures in a typical equivalency program involving multiple independent property comparisons. In theory, if the equivalency dataset is truly identical to the qualification dataset, we expect to obtain approximately 5% failures. Since the equivalency test panels were fabricated by a different company, the test panel quality is expected to differ at least marginally; so, we expect to obtain slightly higher failure rates than 5% because the equivalency dataset may not be truly identical to the qualification dataset. However, a failure rate that is significantly higher than 5% is an indication that equivalency should not be assumed and some retesting is justified.

In addition to the frequency of failures, the severity of the failures (i.e. how far away from the pass/fail threshold) and any pattern of failures should be taken into account when making a determination of overall equivalency. Severity of failure can be determined using the graphs accompanying the individual test results. Whether or not a pattern of failures exists is a subjective evaluation to be made by the original equipment manufacturer or certifying agency. The question of how close is close enough is often difficult to answer, and may depend on specific application and purpose of equivalency. NIAR does not make a judgment regarding the overall equivalence; the following information is provided to aid the original equipment manufacturer or certifying agency in making that judgment.

The following computations are based on the assumption that the tests are independent. While the tests are all conducted independently, measurements for strength and modulus are made from a single specimen. Modulus measurements are generally considered to be independent of the strength measurements.

However the computations can be considered conservative. If the tests are not independent and a failure in IPS 0.2% offset strength is correlated with a failure in IPS 5% strain strength, the probability of both failures occurring together should be higher than predicted with the assumption of independence, thus leading to a conservative overall judgment about the material.

4.1 Failures

The three NASA locations each had 24 different tests conducted. Only the modulus tests had sufficient data to meet the CMH-17 Rev G requirements, all strength tests lack sufficient data for the results to be considered conclusive. The Glenn location had six additional tests conducted for both the Low Vacuum panels and the Slow Ramp Panels.

Using the modified CV method, there were three failures at the Glenn location, two at Marshall and one at Langley. The Low Vacuum and the Slow Ramp panels had one failure each. Out of these eight failures, six were for the OHC1 property.

1. Glenn – UNC1 modulus ETW condition failed by 2.9%
2. Marshall – LSBS ETW condition failed by 0.1%
3. Glenn – OHT1 RTD condition failed by 1.1%
4. Glenn – OHT1 ETW condition failed by 5.1%
5. Glenn – Slow Ramp Panels – OHT1 RTD condition failed by 0.6%
6. Glenn – Low Vacuum Panels – OHT1 ETW condition failed by 2.4%
7. Marshall – OHT1 RTD condition failed by 1.9%
8. Langley – OHT1 ETW condition failed by 4.8%

4.2 Pass Rate

One failure out of 6 tests give both the Low Vacuum and Slow Ramp Panels a pass rate of 83.33%. One failure out of 24 tests gives Langley a pass rate of 95.83% for these tests. Two failures out of 24 tests give Marshall a pass rate of 91.67% for these tests. Three failures out of 24 tests give Glenn a pass rate of 87.50% for these tests. If the equivalency samples came from a material with identical properties to the original qualification material and all tests were independent of all other tests, the expected pass rate would be 95%. This equates to 1.2 failures out of 24 tests or 0.3 failures in six.

4.3 Probability of Failures

If the equivalency sample came from a material with characteristics identical to the original qualification material and all tests were independent of all other tests, the chance of having one or more failures is 26.49%, two or more failures is 3.28% and three or more failures is 0.22%. Figure 4-1 illustrates the probability of getting one or more failures, two or more failures, etc. for a set of 24 independent tests. If the two materials were equivalent, the probability of getting two or more failures is less than 5%. This means that the material could be considered as “not equivalent” with a 95% level of confidence if there were two or more failures out of 24 independent tests.

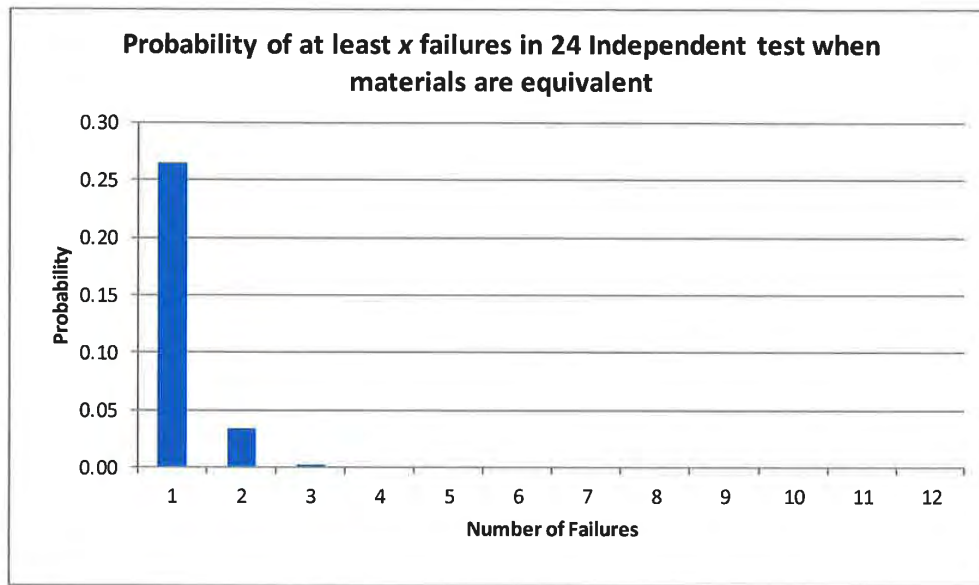


Figure 4-1 Probability of Number of Failures

5. References

1. CMH-17 Rev G, Volume 1, 2012. SAE International, 400 Commonwealth Drive, Warrendale, PA 15096
2. John Tomblin, Yeow C. Ng, and K. Suresh Raju, "Material Qualification and Equivalency for polymer Matrix Composite Material Systems: Updated Procedure", National Technical Information Service (NTIS), Springfield, Virginia 22161
3. Vangel, Mark, "Lot Acceptance and Compliance Testing Using the Sample Mean and an Extremum", Technometrics, Vol 44, NO. 3, August 2002, pp. 242-249

APPENDIX C—TECHNOLOGY READINESS LEVEL ASSESSMENT

The CEUS project team assessed the TRL and, in the case of manufacturing, the manufacturing readiness assessment (MRL) of 8.4-m-diameter composite dry structures based on the limited accomplishments of the project. Table 30 reflects the results of that assessment. Overall, there are several individual technology areas in the TRL 3–5 range within structures and manufacturing that need to be matured to enable the overall composites capability for future space vehicles.

Table 30. Assessment of TRL/MRL of 8.4-m-diameter composites technologies.

Historically	Today
Human-rated composites	Prior experience up to 3.6 m diameter TRL not ratable for 8.4 m composites
8.4-m-diameter forward and aft skirts	Improved design/analysis/manufacturability experience TRL 4
Automated manufacturing	Advancement in low-cost tooling to support larger diameter (8.4 m) segmented construction MRL 5–6
OOA joints	Designed/analyzed OOA joints at 8.4 m diameter TRL 3
Design database	Utilized existing material database on CEUS and demonstrated equivalency TRL 8

Several months prior to the beginning of the CEUS project, an MSFC-LaRC-GRC team examined the perceived impediments to the utilization of composites in flight structures within the Agency. Table 31 is a quick look at where the CEUS project team believes we are in addressing some of those impediments. Composites are already being used in flight structures at dimensions of up to 5 m diameter, and are ready for the next large step in technology maturation and infusion into an 8.4-m, human-rated flight hardware path.

Table 31. Assessment of composite technologies versus perceived impediment.

Perceived Impediment (2013)	Status Today
Affordability means limiting risk by using what we already know (heritage hardware).	CEUS would have demonstrated design/analysis/manufacturing/test of new hardware with minimal risk. Considerable work remains to mature the technology.
'Composites' means funding costly materials development programs.	CEUS utilized existing database for an established material with process modifications—much less cost and risk.
NASA design and certification standards are driving a 'stacking of conservatism' that is limiting the performance gains offered by composite structures. (Does not allow for an affordable approach.)	Standards are tailorabile. An aggressive program can take advantage of such tailoring and reduce cost and schedule while increasing performance.
Composites will mean developing costly new manufacturing processes and tooling and negate the advantages of common tooling.	CEUS developed low-cost tooling and utilized existing facilities to keep infrastructure costs low.
Meeting the damage tolerance requirements for composites will introduce significant technical/schedule/cost risks.	CEUS developed designs to account for damage; utilized damage-based material properties to significantly reduce risks.

APPENDIX D—DESIGN DATA SHEETS AND DRAWINGS

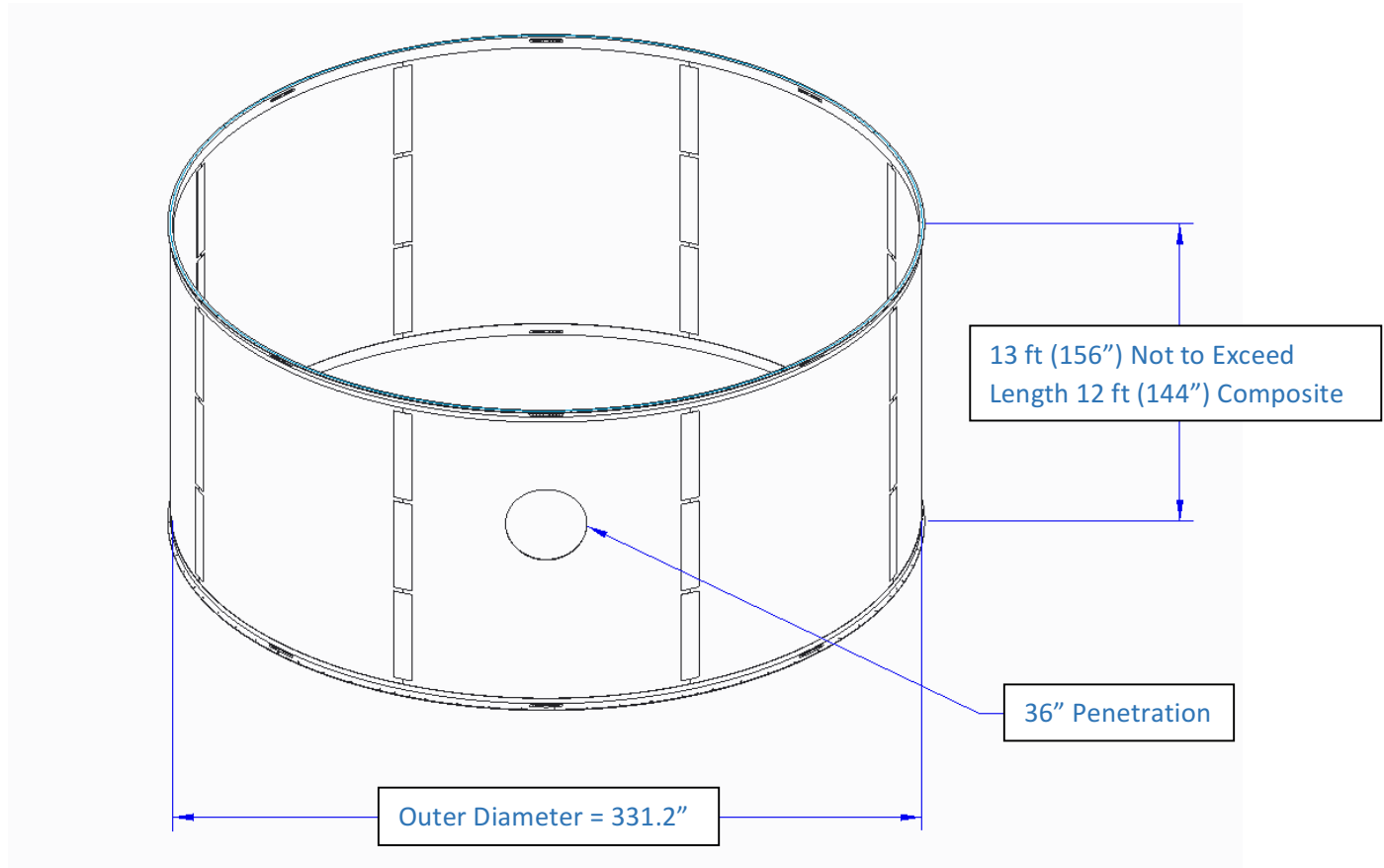
Design data sheets for the STA and Pathfinder and two drawings for the STA are given in this appendix.

Composites Technology for Exploration (CTE) Structural Test Article

Design Data Sheet

INTENT: This document will provide specific design criteria for the CTE STA geometry, loads, and overall description. Analysis guidance for composites will be documented in Composites for Exploration Upper Stage – CEUS Structural Analysis Ground Rules and Assumptions.

Layout



Construction:

- 8 sandwich composite panels to be joined with out-of-autoclave, out-of-oven vertical joints.
- Metallic end rings mechanically attached to the existing simulators with existing bolt pattern.

Manufacturing:

- Use automated fiber placement machine to lay up face sheets.
- Autoclave curing of the facesheets.
- Assembly fixture to support out-of-autoclave, out-of-oven vertical joints.

Materials

Composite:

- Intermediate modulus/toughened epoxy skins

Adhesive:

- Epoxy

Potting:

- Epoxy Liquid shim between the metal fitting and the composite surface

Core:

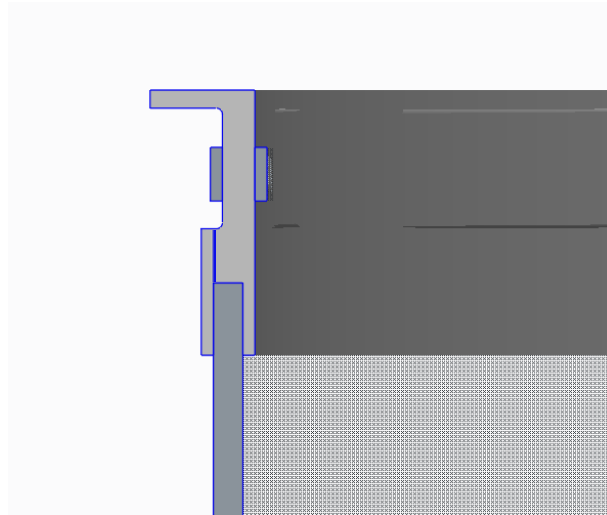
- Aluminum honeycomb core
- Higher density composite inserts (plugs) to reinforce base and lifting points

End Rings:

- Separable Clevis design
- Aluminum
- Joined by aluminum splice plates

Vertical Joints:

- TBD



End Rings, Fwd and Aft
(Notional)

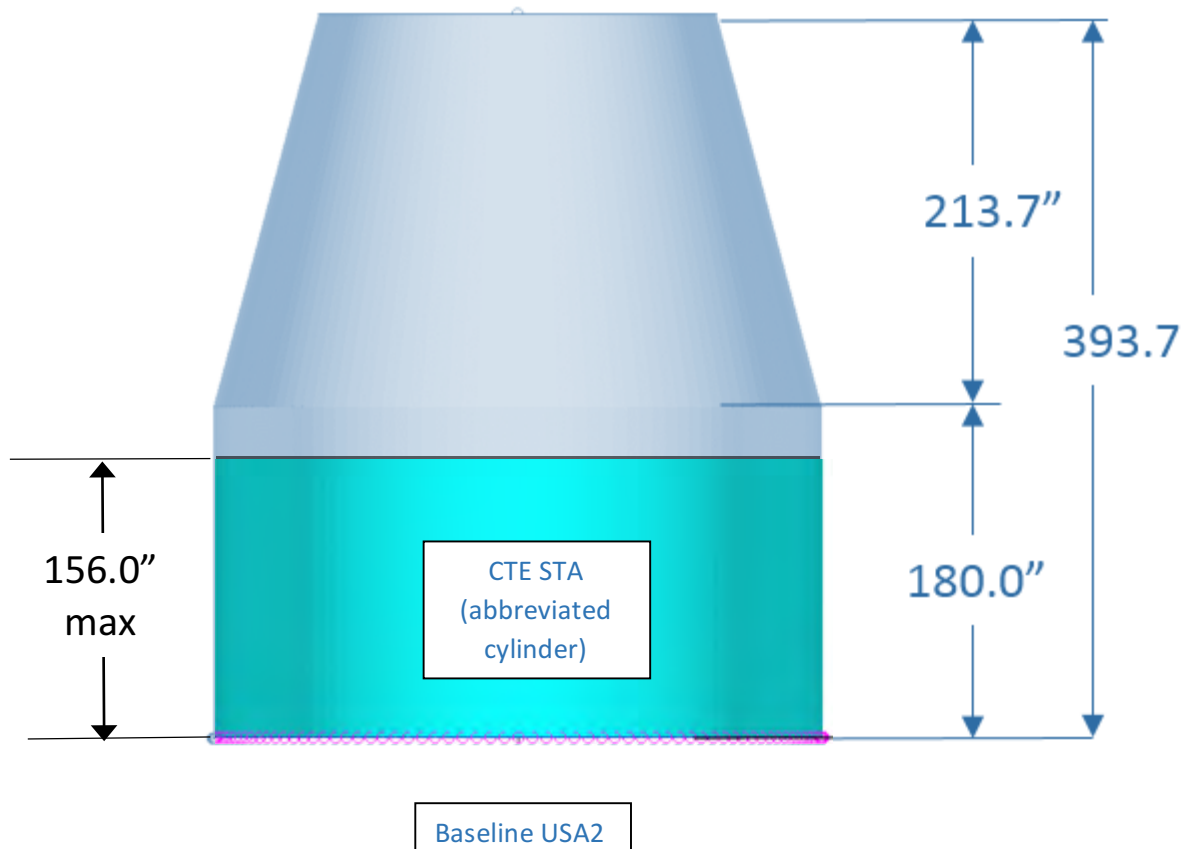
Vehicle Line Loads

Coupled loads analysis: EV31 DAC0 Block 1B Cargo and Crew Configurations.

Requirement to test to a representative flight load case. Bin 5 was chosen for the STA to facilitate using the existing External Tank test simulators without structural modification.

Compression for Ascent Bin 5

	P (lb)	M (in-lb)	V (lb)
Cylinder fwd	ITAR Information Removed	ITAR Information Removed	ITAR Information Removed
Cylinder aft	ITAR Information Removed	ITAR Information Removed	ITAR Information Removed



Venting Pressures (Cylinder):

- Burst Pressure: 0 psi
- Crush Pressure: 0 psi

Knockdown Factor (KDF):

- Discrepancies between analytically and empirically derived buckling load capability are due in part to the differences between idealized model geometry and the physical structure. "Knockdown factors" (correlation coefficients) are used to adjust predicted values to account for these differences. Typical knockdown factors for thin-walled circular cylinders are listed in NASA SP-8007, Buckling of Thin-Walled Circular Cylinders.

Design Details to Accommodate:

- STA will include one 36" penetration positioned at least 1D from top of panel.
- Handling Provisions needed for EM

Temperature: Ambient

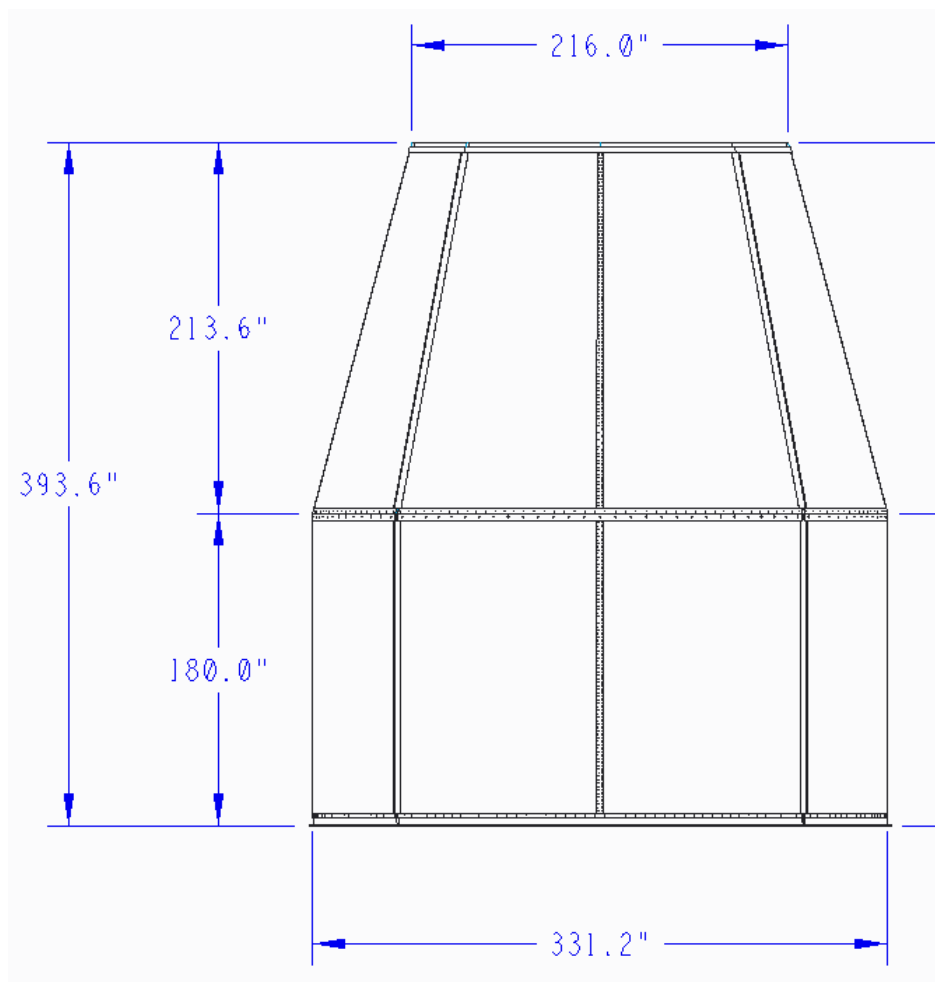
Design details above and overall geometry will be documented in layout drawing (SMDB-CTE-0003).

**Composites Technologies for Exploration (CTE) Pathfinder
Design Data Sheet**

INTENT: This document will provide specific design criteria for the CTE Pathfinder geometry, loads, and overall description. Analysis guidance for composites will be documented in Composites for Exploration Upper Stage – CEUS Structural Analysis Ground Rules and Assumptions.

Layout

Per SPIE Baseline:

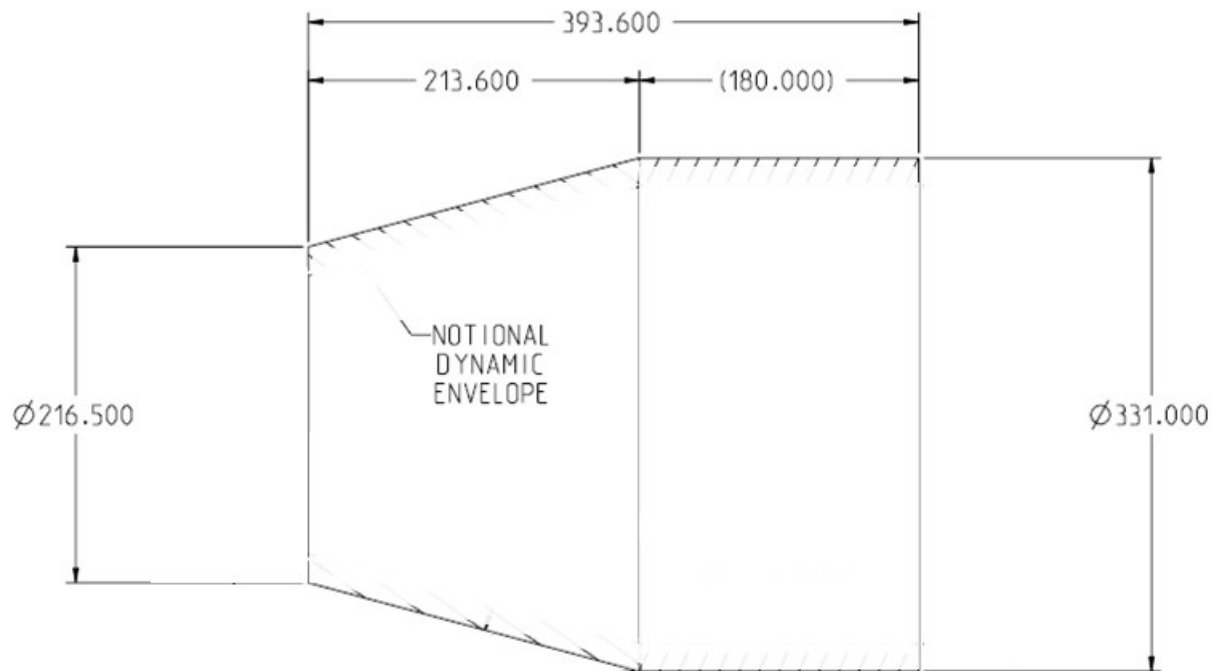


Construction:

- Honeycomb or foam sandwich composite panels.
- Vertical separation joints and horizontal separation joints.
- Metallic clevis type end rings joined by splice plates

Notional Dynamic Envelope (Keep-out Zone):

- From drawing 150601MRA002, USA2-1000-OML



Trade Studies

Multiple trade studies conducted to explore different configurations:

- Geometry Study:

Two Part: Cone
and Cylinder



Alternate Geometry



- Metallic Acreage vs. Composite Acreage Study
- Core Material Study: Aluminum Honeycomb or Foam
- Core Density Study
- Knockdown Factor Study
- Vertical Separation Joint Study
- Discontinuity Factor Sensitivity Study



Vehicle Line Loads

Coupled loads analysis: EV31 DAC0 Block 1B Cargo and Crew Configurations.

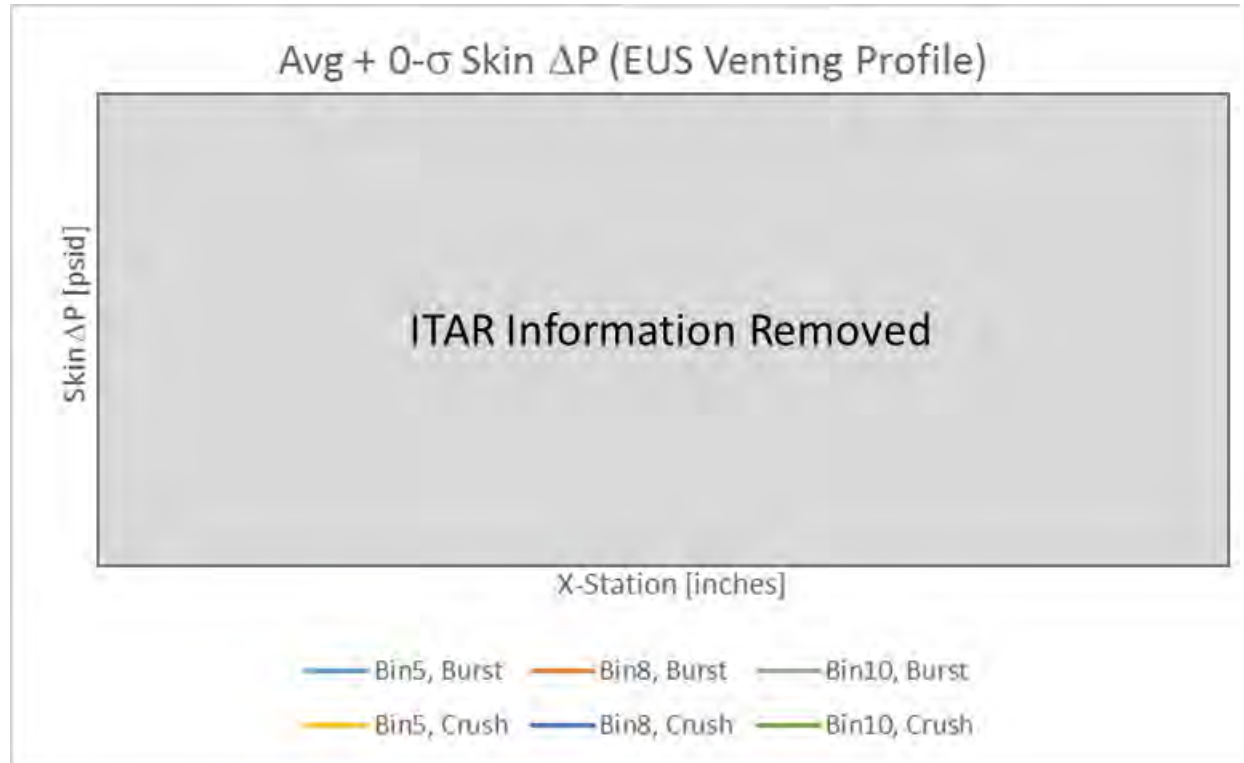
Consider DAC0 to be the final verification loads cycle for the Pathfinder design.

	Lift-off			Ascent					
	LO.BU	LO.IG (axial compression)	LO.IG (axial tension)	LO.SD	Bin 5	Bin 8	Bin 10	Bin 12	Presep
Cone fwd									
P (lb)									
M (in-lb)									
V (lb)									
Cone/cyl intfc									
P (lb)									
M (in-lb)									
V (lb)									
Cyl aft									
P (lb)									
M (in-lb)									
V (lb)									

ITAR Information Removed

Venting Pressures

ΔP_{skin} Results by Bin (Enveloped Qmax, Qmin):



Mach Bin Definitions:

Bin	Min. Mach	Max Mach
5	0.8	1.2
8	1.4	2.1
10	3.2	3.7
12	3.7	4

Knockdown Factor (KDF):

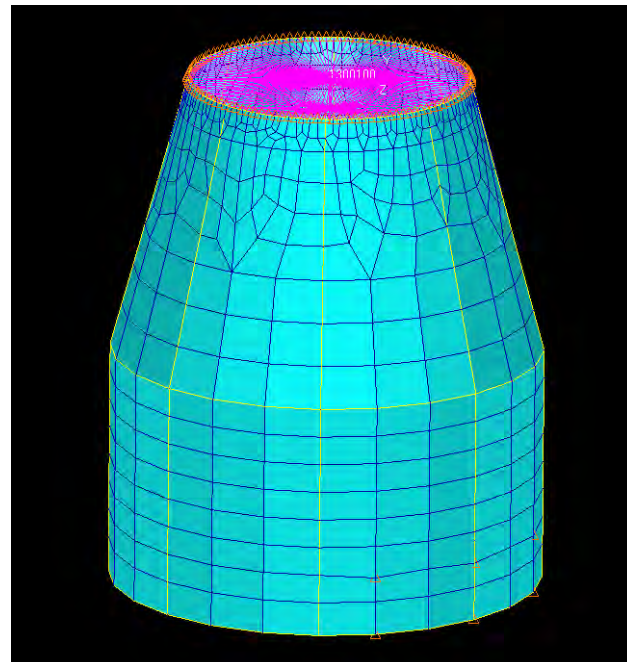
- Discrepancies between analytically and empirically derived buckling load capability are due in part to the differences between idealized model geometry and the physical structure. “Knockdown factors” (correlation coefficients) are used to adjust predicted values to account for these differences.
- Typical knockdown factors are listed in NASA SP-8007, Buckling of Thin-Walled Circular Cylinders, NASA SP-8019 Buckling of Thin-Walled Truncated Cones, and NASA SP-8032 Buckling of Thin-Walled Doubly Curved Shells

Stiffness Requirement:

- From DAC1 MSFC Loads model

Free Free Mode #	Frequency (Hz)
1	Removed
2	Removed
3	Removed
4	Removed
5	Removed
6	Removed
7	Removed
8	Removed
9	Removed
10	Removed

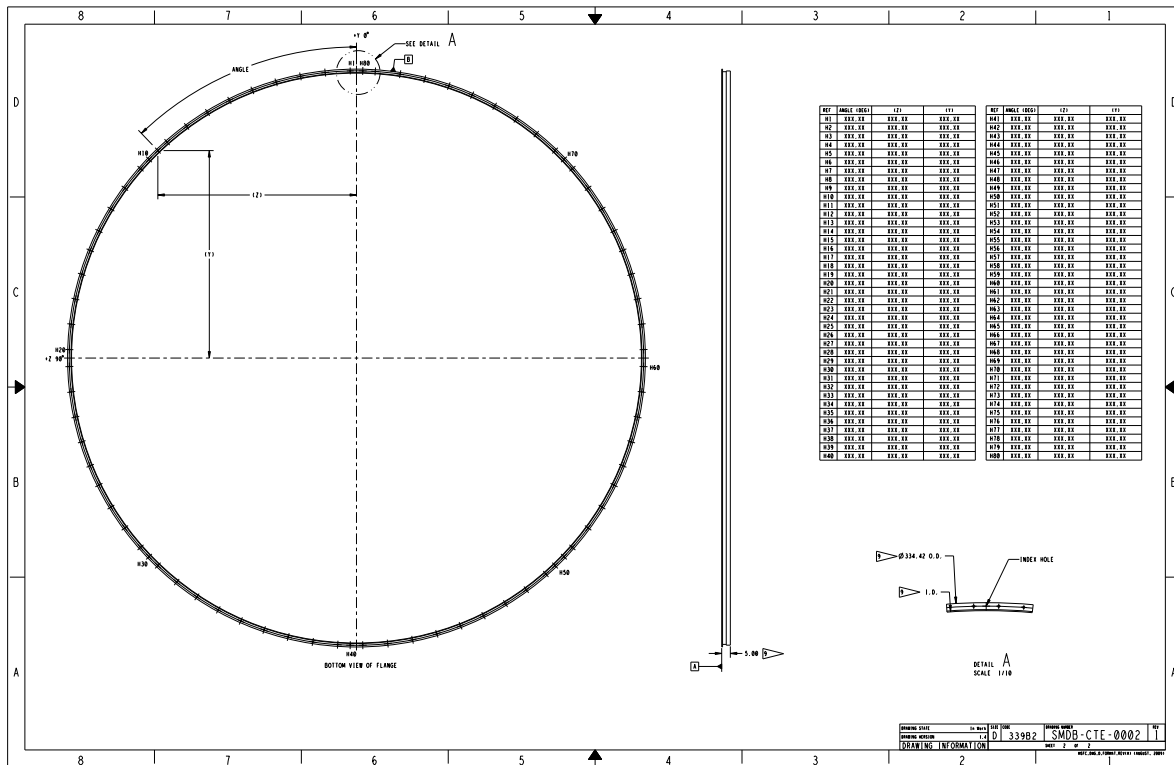
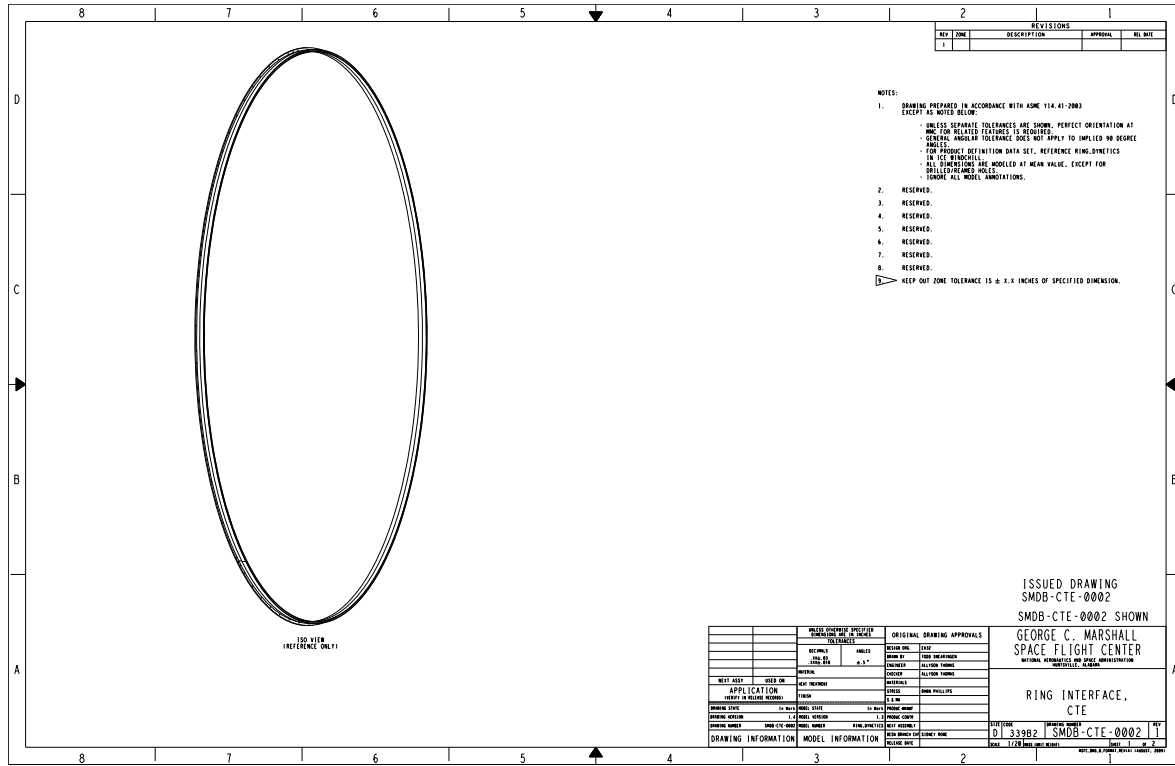
Mass (lbm)	
Removed	
Stiffness (lb/in)	
Axial	Removed
Shear 1	Removed
Shear 2	Removed

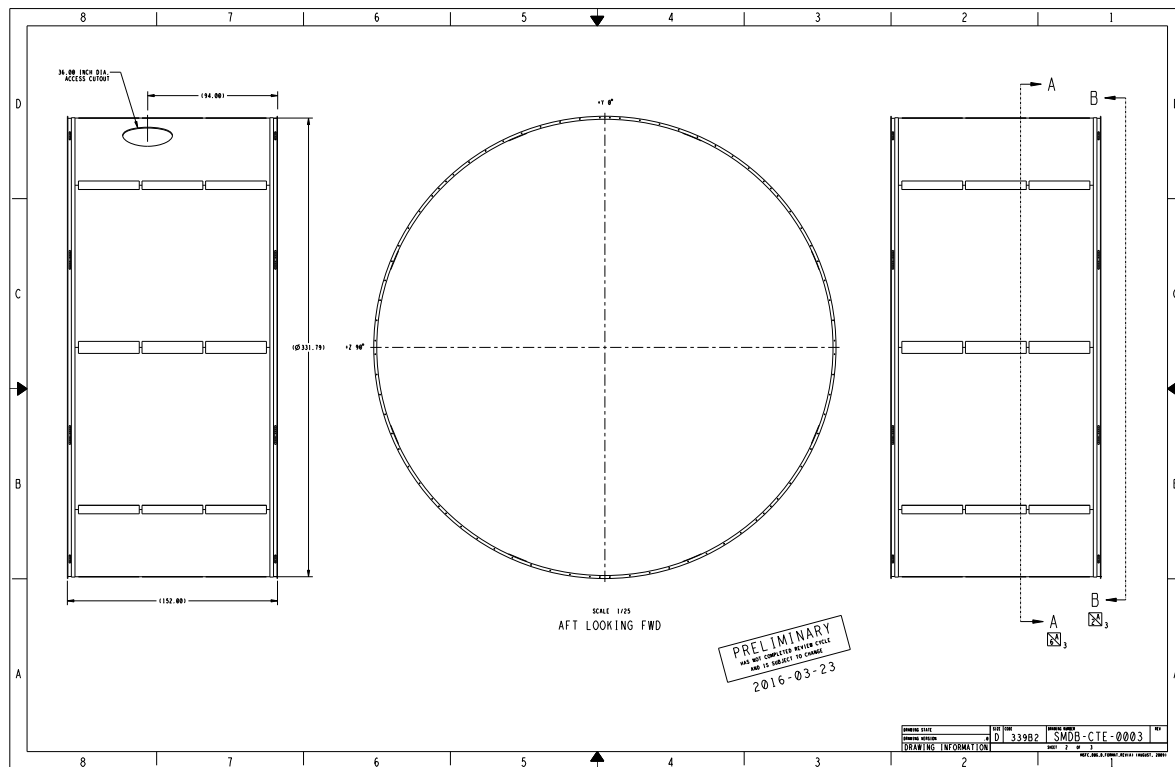
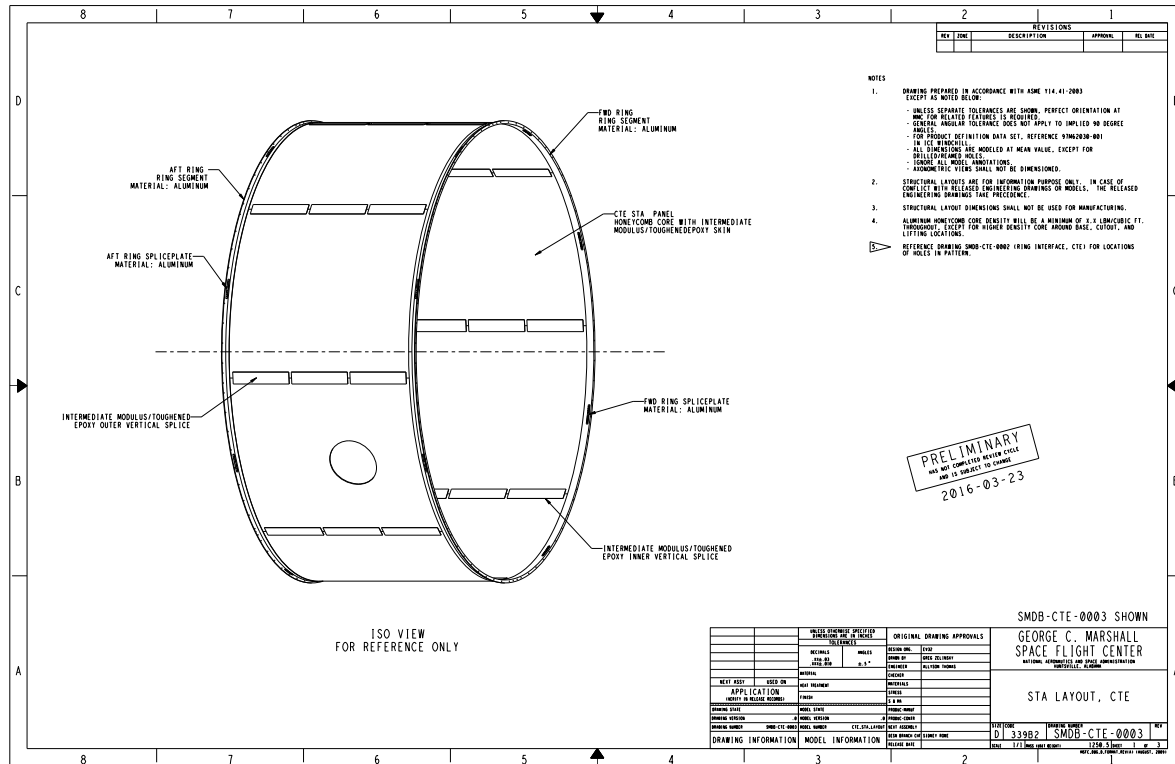


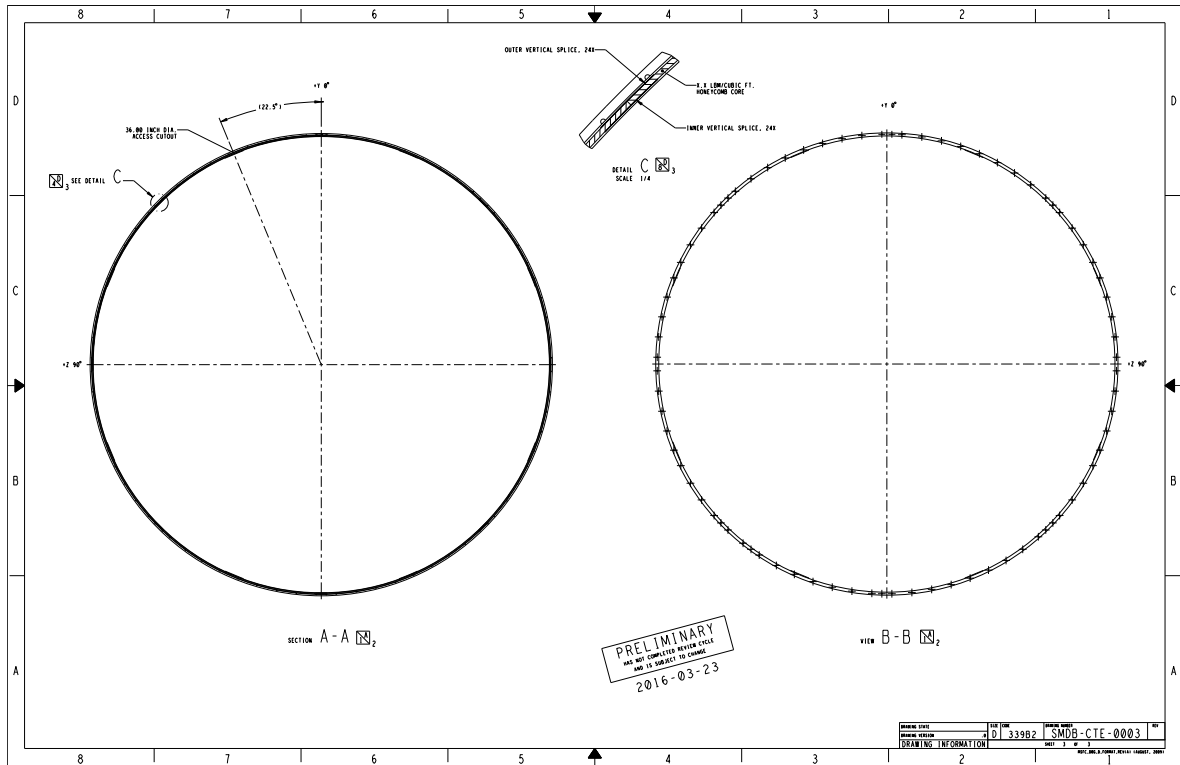
Temperature:

- Transient temperature profiles will be developed for hot/cold pre-launch DSNE terrestrial environments (e.g., roll-out, on-pad, tanking) as well as ascent aero-thermodynamic environments.
 - Initial case will assume no TPS
 - Aero-thermal heating data not currently available for USA2 in the Block 1B DAC-0 database, will coordinate with EV33 for reasonable aero-heating assumptions for preliminary assessment
 - Initial results May 1, 2016

ENGINEER_SMDB-CTE-0002.pdf







APPENDIX E—MANUFACTURING

Appendix E contains the Thermographic Inspection Report.

Thermographic Inspection Report

Work Order 2016-0063

Prepared For

James Walker
NASA MSFC
James.L.Walker@nasa.gov
(256) 961-1784

Prepared By

Scott Ragasa
METTS
Scott.Ragasa@nasa.gov
(256) 544-3935

Specimen Information

Project	CEUS
Serial Number	CEUS_001A, _001B, _006
Surface Preparation	None
Special Handling	None

Inspection Equipment

Infrared Camera	FLIR SC6000
Lens	25 mm
Heating Method	Flash Lamps
Hood Configuration	Small FOV

Inspection Settings

Capture Software	EchoTherm 8
Image Size	640 x 512
Capture Frequency	30 Hz
Capture Duration	9.2 seconds
Flash Duration	30 milliseconds
Flash Delay	0 milliseconds
Flash Frame	10
TSR Skip Frames	1

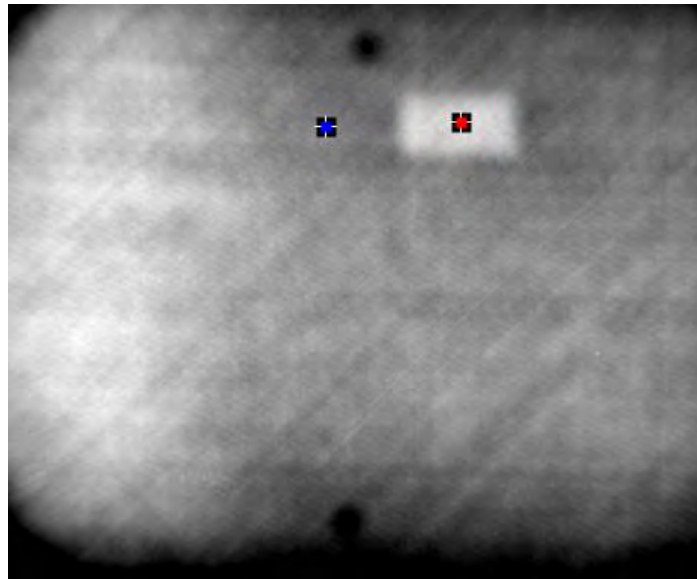
February 19, 2016

WR: 2016-0063

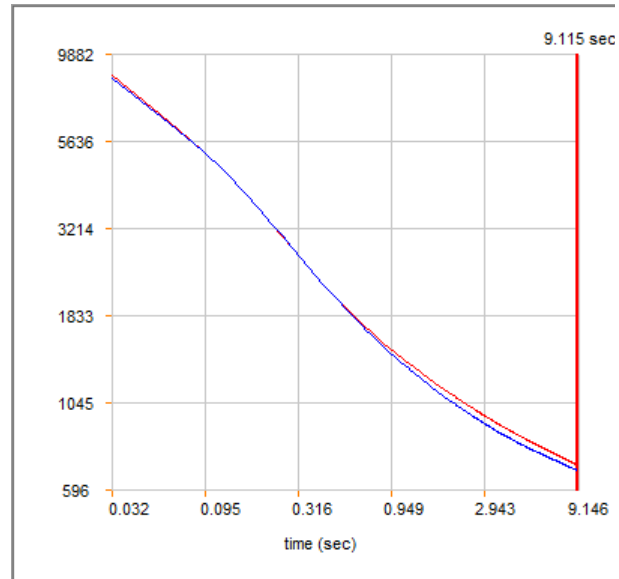
Revision A

Remarks

- A thermography inspection was performed to determine if there were any initial defects in the set of panels prior to mechanical testing.
- Due to the low emissivity of the panel surfaces, only derivative processing of the images was used.
- One indication was found in panel CEUS_006, Front, Location J02.

CEUS_006 – Front – Location J02

Raw, Frame 100, ROI Adjusted



T-t Plot

The logarithmic time versus temperature plot shows the area of interest (red) deviates slightly from the background (blue).

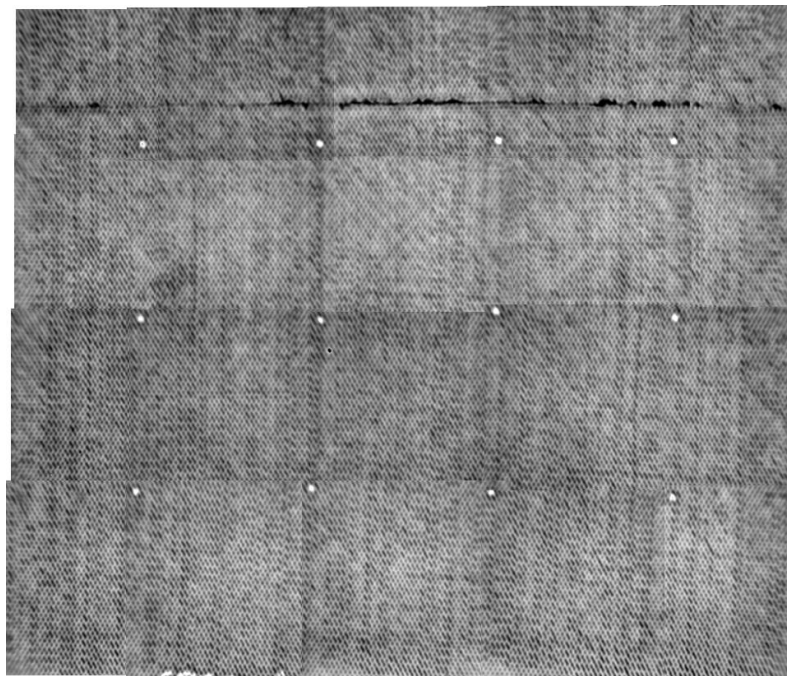
The regular shape suggests it is likely FOD – tape or backing material.

February 19, 2016

WR: 2016-0063

Revision A

Panel CEUS_001A – Front



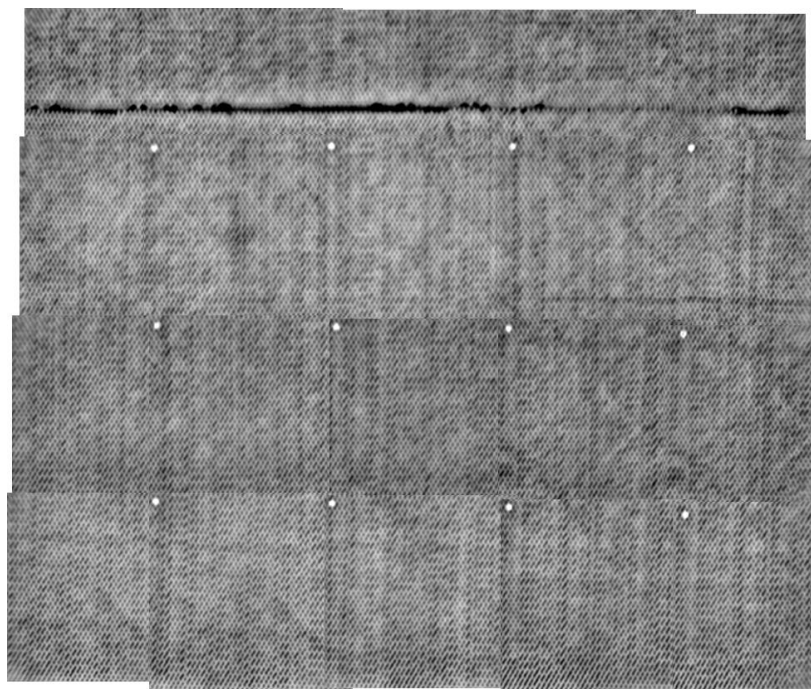
First Derivative, Frame 50

February 19, 2016

WR: 2016-0063

Revision A

Panel CEUS_001A – Back

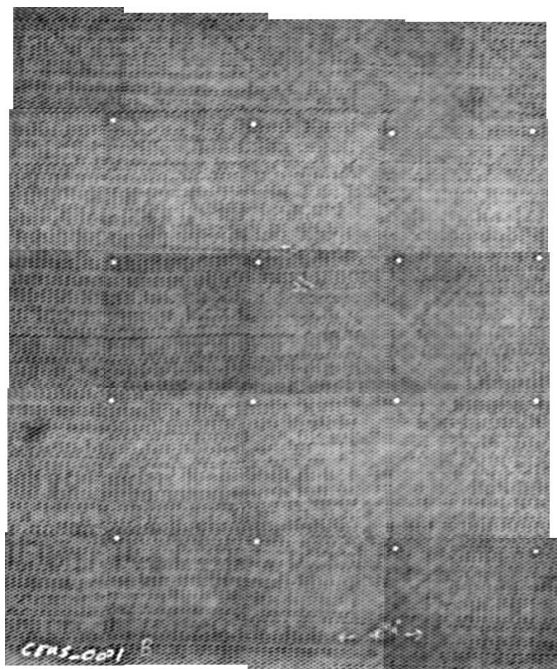


February 19, 2016

WR: 2016-0063

Revision A

Panel CEUS_001B – Front



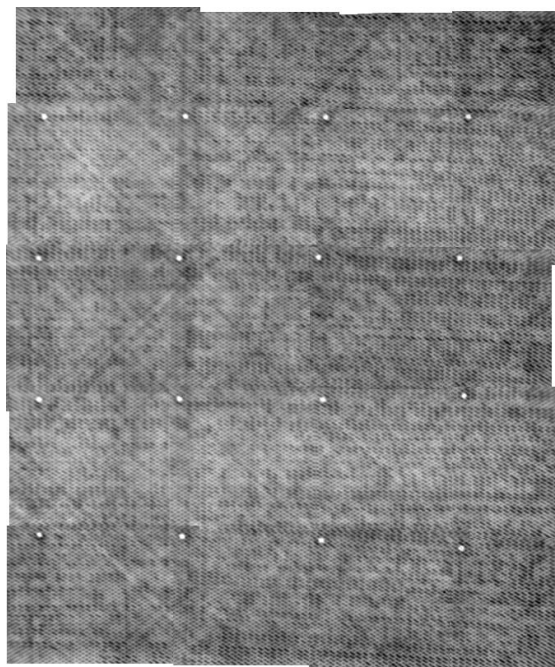
First Derivative, Frame 50

February 19, 2016

WR: 2016-0063

Revision A

Panel CEUS_001B – Back

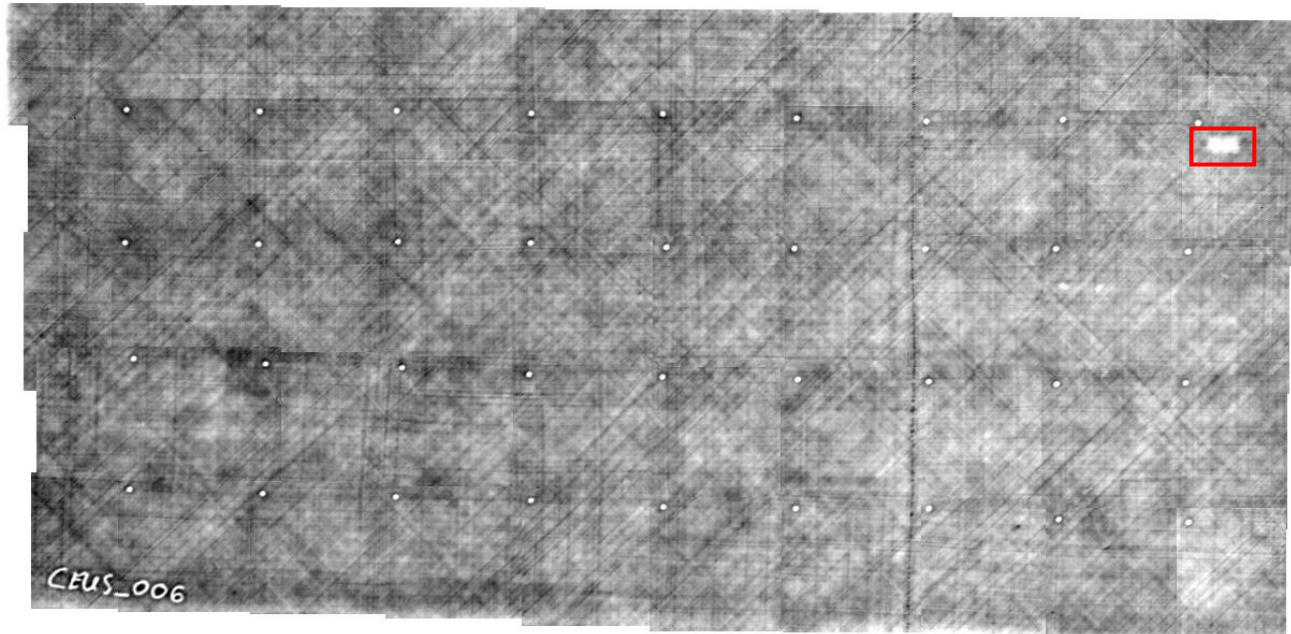


February 19, 2016

WR: 2016-0063

Revision A

Panel CEUS_006 – Front



First Derivative, Frame 50

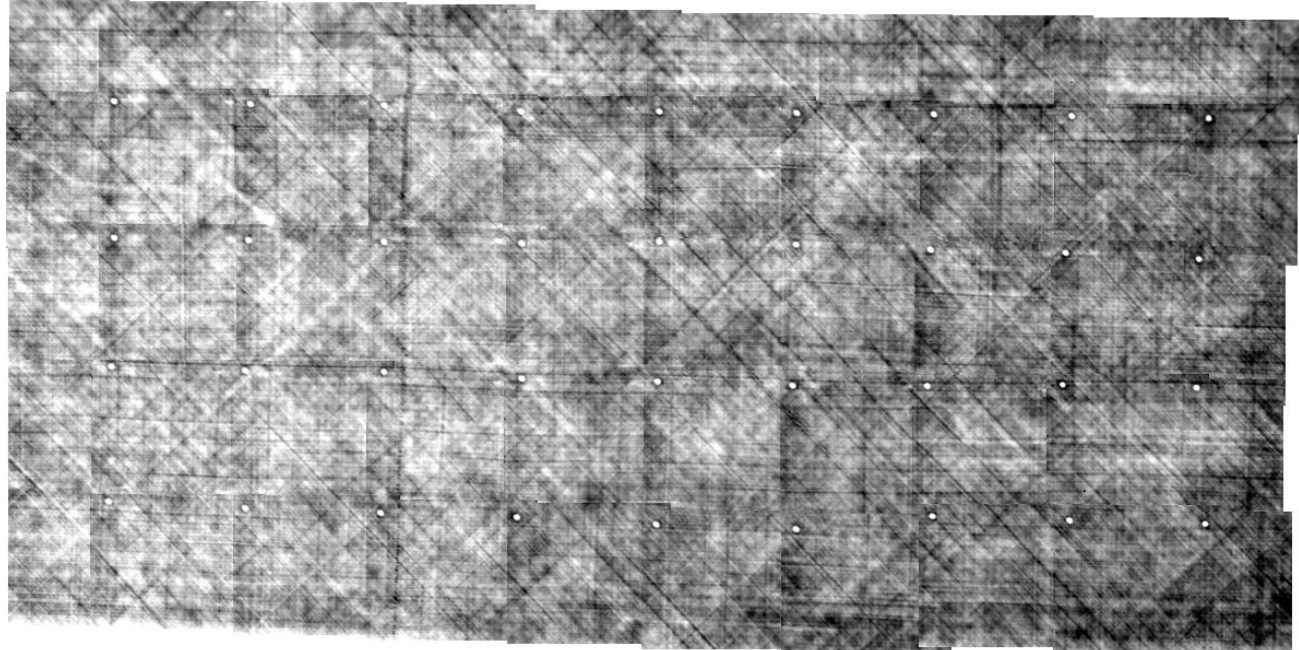
Page 8 of 9

February 19, 2016

WR: 2016-0063

Revision A

Panel CEUS 006 – Back



Page 9 of 9

REFERENCES

1. NASA MPR 7120.1, Rev. G, “MSFC Engineering and Program/Project Management Requirements,” August 26, 2014.
2. NASA-STD-5019, “Fracture Control Requirements for Spaceflight Hardware,” NASA, Washington, DC, 44 pp., 2008.
3. MSFC-RQMT-3479, “Fracture Control Requirements for Composite and Bonded Vehicle and Payload Structures,” NASA Marshall Space Flight Center, Huntsville, AL, 50 pp., June 2006.
4. Clarkson, E.: “Hexcel 8552 IM7 Unidirectional Prepreg 190 gsm and 35% RC Qualification Statistical Analysis Report,” NCP-RP-2009-028, Rev N/C, National Institute for Aviation Research, Wichita State University, Wichita, pp. 104, January 2011.
5. CMH-17, Rev. G, “Polymer Matrix Composites: Guidelines for Characterization of Structural Materials,” SAE International, Warrendale, PA, 711 pp., 2012.
6. Ng, Y.; and Tomblin, J.: “Fabrication of NMS 128 Qualification, Equivalency, and Acceptance Test Panels (for Hexcel 8552 and 8552S prepgs),” National Institute for Aviation Research, NCAMP Process Specification, NPS 81228, Rev. B, 2011.
7. Wu, K.C.; Stewart, B.K.; and Martin, R.A.: “ISAAC—A Testbed for Advanced Composite Research,” Paper presented at The American Society for Composites 29th Annual Technical Conference, San Diego, CA, September 8–10, 2014.
8. Jeffries, K.A.: “Enhanced Robotic Automated Fiber Placement with Accurate Robot Technology and Modular Fiber Placement Head,” *SAE Int. J. Aerosp.*, Vol. 6, No. 2, doi: 10.4271/2013-01-2290, September 17, 2013.
9. Krivanek, T.M.; and Yount, B.C.: “Composite Payload Fairing Structural Architecture Assessment and Selection,” Technical Report E-18094, NASA Glenn Research Center, Cleveland, OH, 15 pp., May 2012.
10. NASA-STD-6016, “Standard Materials and Processes Requirement for Spacecraft,” Johnson Space Center, Houston, TX, September 25, 2009.

11. Pineda, E.J.; Myers, D.E.; Bednarcyk, B.A.; and Krivanek, T.M.: “A Numerical Study on the Effect of Facesheet-Core Disbonds on the Buckling Load of Curved Honeycomb Sandwich Panels,” Paper presented at the American Society for Composites 30th Technical Conference, Lansing, MI, September 28–30, 2015.
12. Rinker, M.K.; Krueger, R.; and Ratcliffe, J.: “Analysis of an Aircraft Honeycomb Sandwich Panel with Circular Face Sheet/Core Disbond Subjected to Ground-Air Pressurization,” NASA/CR—2013-217974, NASA Langley Research Center, Hampton, VA, 32 pp., March 2013.
13. Glaessgen, E.H.; Reeder, J.R.; Sleight, D.W.; et al.: “Debonding Failure of Sandwich-Composite Cryogenic Fuel Tank with Internal Core Pressure,” *Journal of Spacecraft and Rockets*, Vol. 42, No. 4, pp. 613–627, 2005.
14. Ratcliffe, J.: “Sizing Single Cantilever Beam Specimens for Characterizing Facesheet/Core Peel Debonding in Sandwich Structure,” ICSS 9, G. Ravichandran, Editor, 9th International Conference on Sandwich Structures, Pasadena, CA, June 14–16, 2010, 13 pp., 2011.
15. Reeder, J.R.; Song, K.; Chunchu, P.B.; and Ambur, D.R.: “Postbuckling and Growth of Delaminations in Composite Plates Subjected to Axial Compression,” Paper presented at the 43rd AIAA/ASME/ASCE/AHS Structures, Structural Dynamics, and Materials Conference, Denver, CO, April 22–25, 2002.
16. Ural, A.Z.; Zehnder, A.T.; and Ingraffea, A.R.: “Fracture Mechanics Approach to Facesheet Delamination in Honeycomb: Measurement of Energy Release Rate of the Adhesive Bond,” *Engineering Fracture Mechanics*, Vol. 70, Issue 1, pp. 93–103, 2003.
17. Turon, A.D.; Davila, C.G.; Camanho, P.P.; and Costa, J.: “An Engineering Solution for Solving Mesh Size Effects in the Simulation of Delamination Using Cohesive Zone Models,” *Engineering Fracture Mechanics*, Vol. 74, pp. 1665–1682, 2007.
18. Krueger, R.: “A Summary of Benchmark Examples to Assess the Performance of Quasi-Static Delamination Propagation Prediction Capabilities in Finite Element Codes,” *Journal of Composite Materials*, Vol. 49, pp. 3297–3316, November 2015.
19. Thévenin, R.: “Airbus Composite Structures: Perspectives on Safe Maintenance Practice,” Paper Presented at the Commercial Aircraft Committee Meeting and Related Industry/FAA/EASA Workshop, Amsterdam, 43 pp., May 7–11, 2007.

REPORT DOCUMENTATION PAGE				Form Approved OMB No. 0704-0188	
<p>The public reporting burden for this collection of information is estimated to average 1 hour per response, including the time for reviewing instructions, searching existing data sources, gathering and maintaining the data needed, and completing and reviewing the collection of information. Send comments regarding this burden estimate or any other aspect of this collection of information, including suggestions for reducing this burden, to Department of Defense, Washington Headquarters Services, Directorate for Information Operation and Reports (0704-0188), 1215 Jefferson Davis Highway, Suite 1204, Arlington, VA 22202-4302. Respondents should be aware that notwithstanding any other provision of law, no person shall be subject to any penalty for failing to comply with a collection of information if it does not display a currently valid OMB control number.</p> <p>PLEASE DO NOT RETURN YOUR FORM TO THE ABOVE ADDRESS.</p>					
1. REPORT DATE (DD-MM-YYYY) 01-12-2016		2. REPORT TYPE Technical Memorandum		3. DATES COVERED (From - To)	
4. TITLE AND SUBTITLE Composites for Exploration Upper Stage				5a. CONTRACT NUMBER	
				5b. GRANT NUMBER	
				5c. PROGRAM ELEMENT NUMBER	
6. AUTHOR(S) J.C. Fikes, J.R. Jackson, S.W. Richardson, A.D. Thomas, T.O. Mann,* and S.G. Miller**				5d. PROJECT NUMBER	
				5e. TASK NUMBER	
				5f. WORK UNIT NUMBER	
7. PERFORMING ORGANIZATION NAME(S) AND ADDRESS(ES) George C. Marshall Space Flight Center Huntsville, AL 35812				8. PERFORMING ORGANIZATION REPORT NUMBER	M-1422
9. SPONSORING/MONITORING AGENCY NAME(S) AND ADDRESS(ES) National Aeronautics and Space Administration Washington, DC 20546-0001				10. SPONSORING/MONITOR'S ACRONYM(S) NASA	
				11. SPONSORING/MONITORING REPORT NUMBER	NASA/TM—2016-219433
12. DISTRIBUTION/AVAILABILITY STATEMENT Unclassified-Unlimited Subject Category 39 Availability: NASA STI Information Desk (757-864-9658)					
13. SUPPLEMENTARY NOTES Prepared by the Technology Development and Transfer Office, Science and Technology Office *Langley Research Center, **Glenn Research Center					
14. ABSTRACT The primary objective of the Composites for Exploration Upper Stage project was to mature the technology readiness of composite dry structures at diameters that are suitable for Space Launch System (SLS) Exploration Upper Stage and other in-space applications. SLS studies have shown that composites provide important programmatic enhancements, including increased capability and accelerated expansion of exploration and science mission objectives. Reducing the weight and cost of these structures will provide a significant benefit, perhaps even an enabling benefit, to an upper stage. This initiative was a cooperative effort between the Space Technology Mission Directorate and the Human Exploration and Operations Mission Directorate, including multiple NASA Centers.					
15. SUBJECT TERMS exploration, Upper Stage, Ares, Space Launch System					
16. SECURITY CLASSIFICATION OF: a. REPORT U b. ABSTRACT U c. THIS PAGE U			17. LIMITATION OF ABSTRACT UU	18. NUMBER OF PAGES 294	19a. NAME OF RESPONSIBLE PERSON STI Help Desk at email: help@sti.nasa.gov
					19b. TELEPHONE NUMBER (Include area code) STI Help Desk at: 757-864-9658

National Aeronautics and

Space Administration

IS02

George C. Marshall Space Flight Center

Huntsville, Alabama 35812